Regulation of p42/44 Mitogen-activated Protein Kinase by G-protein Coupled Receptors.

A THESIS PRESENTED FOR

THE DEGREE OF

DOCTOR OF PHILOSOPHY

BY

ANDREW ROBERT BURT

DIVISION OF BIOCHEMISTRY AND MOLECULAR BIOLOGY

INSTITUTE OF BIOMEDICAL AND LIFE SCIENCES

UNIVERSITY OF GLASGOW

February 1997

ProQuest LLC.
789 East Eisenhower Parkway
P.O. Box 1346
Ann Arbor, MI 48106 – 1346

Abstract

The cascade linking growth factor receptors and G-protein coupled receptors (GPCRs) to the regulation of p42/44 mitogen-activated protein kinase ($p42/44^{MAPK}$) has been described in some detail and involves numerous steps of phosphorylation and protein-protein interaction. There is a remarkable degree of similarity in the pathways initiated by these two receptor families, although some degree of cell/receptor specificity exists. In this study, the regulation of $p42/44^{MAPK}$ by the α_{2A} adrenoceptor and the δ opioid receptor following transfection into Rat1 fibroblasts to different receptor densities was quantitatively measured and compared to the regulation by endogenous G-protein (lysophosphatidic acid: LPA) and tyrosine kinase (epidermal growth factor: EGF) coupled receptors.

The wild type α_{2A} adrenoceptor was expressed at a high (clone TAGWT 17: 5600 fmol/mg protein) and low density (clone TAGWT 3: 460 fmol/mg protein) which permitted greater G-protein activation in clone TAGWT 17 cells as measured by agonist (UK14304)-mediated stimulation of high affinity GTPase activity and cholera toxin-catalysed [^{32}P]ADP-ribosylation of G_i-like proteins. Greater maximal activity and lower half-maximal agonist concentrations (EC_{50} values) were determined for clone TAGWT 17. The greater signalling ability was also determined at the level of inhibition of adenylyl cyclase. Previous studies had demonstrated the activation of $p42/44^{MAPK}$ by the α_{2A} adrenoceptor. UK14304 treatment of cells of both these clones phosphorylated a significant proportion of $p44^{MAPK}$, demonstrating that there was no requirement for high level expression to observe this coupling. This response was dose-dependent with TAGWT 3 clone displaying a 10-fold greater EC_{50} value than clone TAGWT 17.

An Asn^{79} mutation of the α_{2A} adrenoceptor (Asp^{79} changed to Asn) substantially reduced the G-protein coupling efficiency of the receptor, previously demonstrated as a complete or partial loss of signalling capacity. This mutant receptor expressed in

fibroblasts (clone ASN79 4 : 3000 fmol/mg protein; ASN79 9: 4300 fmol/mg protein) demonstrated an attenuated, but not eliminated, ability to stimulate G-protein activation, inhibit adenylyl cyclase and phosphorylate p42/44^{MAPK}. This indicated that the coupling efficiency to the MAPK cascade was not exceptionally poor, as even a severely limited G-protein activation substantially stimulated this pathway. However, the time course of phosphorylation of p44^{MAPK} was significantly more delayed and transient which would indicate that the kinetics of this regulation is dependent on the level of stimulation of the G-protein-coupled pathway.

The δ opioid receptor was also expressed to a low (clone DOE : 170 fmol/mg protein) and high density (clone D2 : 6400 fmol/mg protein), and the ability of this receptor to regulate G_i-like proteins (as determined by agonist (DADLE: [D-Ala^2, D-Leu^5] enkephalin)-mediated stimulation of high affinity GTPase activity, [^{35}S]GTPγS binding and cholera toxin-catalysed [^{32}P]ADP-ribosylation) again correlated with the receptor level in the two clones: higher maximal activities and lower EC_{50} values were determined for clone D2. DADLE-mediated adenylyl cyclase inhibition and phospholipase D activation was also greater in clone D2. Consistent with the similarities of signalling capacity of the α_{2A} adrenoceptor, DADLE treatment phosphorylated and activated p42^{MAPK} and p44^{MAPK} via G_i-proteins in both of these clones. This result added another GPCR to the list which can regulate p42/44^{MAPK} and again demonstrated that there was no requirement for receptor overexpression. Activation by DADLE was dose-dependent and a 40 fold higher concentration of DADLE was required for half-maximal activation in clone DOE compared with clone D2. This difference was much more pronounced than that detected at the level of G-protein activation and indicated the presence of a large receptor and stimulated G-protein reserve for the activation of p42/44^{MAPK} in both clone D2 and DOE, although the magnitude of this reserve was greater in clone D2. These DADLE-mediated concentration-response curves also demonstrated that the activation of p42/44^{MAPK} was co-operative in nature for both clones (indicated by Hill coefficients greater than 1.0), suggesting that there may be more

than one input point into the p42/44^{MAPK} cascade for the δ opioid receptor. This co-operativity was not observed for the response to UK14304 in clone TAGWT3 or 17 or to LPA in any clone, demonstrating that this is not a universal feature of GPCRs.

The time course of DADLE-mediated activation of p42/44^{MAPK} followed a similar pattern in both opioid receptor expressing clones, however, the activation was significantly more sustained in clone D2. The time course of activation in clone D2 was more delayed and more transient with lower concentrations of DADLE. This confirms that the time course of activation is dependent on the level of G-protein stimulation.

These conclusions were confirmed by the ability of ligands with a range of intrinsic activities at this receptor to phosphorylate p44^{MAPK}. Even ligands which displayed very limited intrinsic activity in GTPase activity measurements significantly phosphorylated p44^{MAPK} in clone D2, although the time course was more delayed and transient than with a full agonist. Only the more efficacious ligands stimulated phosphorylation of p44^{MAPK} in clone DOE, and again they displayed a more delayed and transient time course than for DADLE.

The influence of other signalling pathways and kinases on the regulation of p42/44^{MAPK} phosphorylation by both the α_{2A} adrenoceptor and δ opioid receptor was also examined. Both of these responses were sensitive to inhibition by cAMP elevating agents and may suggest a secondary input into the MAPK cascade. The lack of any significant effect of butan-1-ol or chelerythrine pretreatment indicated that phospholipase D and protein kinase C were not involved in the DADLE-medated phosphorylation of p44^{MAPK} in clone D2. Similarly, genistein displayed no inhibitory effect on the activation of p44^{MAPK} by either of these GPCRs. However, tyrphostin AG1478 and wortmannin attenuated the response to DADLE in clone DOE, although the higher level of receptor expression in clone D2 permitted this inhibition to be overcome. This would appear to indicate that the EGF

receptor kinase and the phosphatidylinositol 3-kinase are involved in the pathway initiated by the δ opioid receptor leading to the phosphorylation of $p44^{MAPK}$.

Contents

List of Figures

List of Tables

Abbreviations

The abbreviations used in this thesis are as set out in "Instructions to Authors" Biochemical Journal (1985) 225, 1-26 with the following additions:

ADP	Adenosine 5'-diphosphate
ANF	Atrial natriuretic factor
App(NH)p	Adenylyl 5'-imidodiphosphate
ATP	Adenosine 5'-triphosphate
βARK	β-adrenergic receptor kinase
βARKct	β-adrenergic receptor kinase C-terminus
B_{max}	Maximal binding capacity
BSA	Bovine serum albumin
cAMP	Adenosine 3',5'-cyclic monophosphate
CPM	Counts per minute
DADLE	[D-Ala^2, D-Leu^5] enkephalin
DAG	sn-1,2-diacylglycerol
DMSO	Dimethyl sulphoxide
DPM	Disintegrations per minute
DTT	Dithiothreitol
EC_{50}	Median effective dose
ECL	Enhanced chemiluminescence
E.coli	*Escherichia coli*
EDTA	Ethylenediaminetetraacetic acid
EGF	Epidermal growth factor
EGFR	Epidermal growth factor receptor
EGTA	Ethylene glycol-bis(β-aminoethyl ether)- N,N,N',N'-tetraacetic acid
ERK	Extracellular regulated kinase
ET-1	Endothelin-1
FGF	Fibroblast growth factor

DMEM	Dulbecco's modified Eagle's medium
GAP	GTPase activating protein
GDP	Guanosine 5'-diphosphate
GEF	Guanine nucleotide exchange factor
GPCR	G-protein coupled receptor
G-protein	Guanine nucleotide binding protein
Grb2	Growth factor receptor binding protein 2
GRK	G-protein receptor kinase
GTP	Guanosine 5'-triphosphate
GTPγS	Guanosine 5'-O-(3-thiotriphosphate)
HEPES	4-(2-Hydroxyethyl)-1-piperazine-N'-2-ethanesulphonic acid
IP_3	D-*myo*-inositol 1,4,5-trisphosphate
IGF-1	Insulin-like growth factor-1
IRS-1	Insulin receptor substrate-1
JNK/SAPK	c-Jun N-terminal kinase/stress activated protein kinase
Kd	Equilibrium dissociation constant
kDa	Kilodaltons
LPA	Lysophosphatidic acid
MAPK	Mitogen-activated protein kinase
MBP	Myelin basic protein
MEK	MAPK or ERK kinase
MEKK	MEK kinase
MKP-1	MAPK phosphatase-1
MOPS	4-Morpholinepropanesulphonic acid
mSos	Mammalian Son of sevenless
NAD	Nicotinamide adenine dinucleotide
NGF	Nerve growth factor
NP40	Nonidet P-40
$p70^{s6k}$	p70 ribosomal S6 kinase

PAF	Platelet activating factor
PBS	Phosphate buffered saline
PDGF	Platelet derived growth factor
PEG8000	Polyethylene glycol 8000
PH	Pleckstrin homology
PI3-kinase	Phosphatidylinositol 3-kinase
PI-PLC	Phosphatidylinositol-specific phospholipase C
PKA	Protein kinase A
PKC	Protein kinase C
PLC	Phospholipase C
PLD	Phospholipase D
PP2A	Protein phosphatase 2A
$PI(3,4,5)P_3$	Phosphatidylinositol 3,4,5-trisphosphate
PYK2	Protein tyrosine kinase 2
SDS	Sodium dodecyl sulphate
SEK	SAPK kinase
SEM	Standard error of the mean
SH2	Src homology 2
SH3	Src homology 3
Shc	Src homology/collagen
TEMED	N,N,N',N'-tetramethylethylenediamine
Tris	Tris(hydroxymethyl)aminomethane

Acknowledgements

I would like to thank Prof. Charles Fewson and Prof. Gordon Lindsay, the heads of IBLS and the Division of Biochemistry and Molecular Biology, for the opportunity to work in this department and to the BBSRC for my studentship. Many thanks to Prof. Graeme Milligan, my supervisor, for his advice, encouragement and support and the opportunity to work in his lab. I would also like to thank Dr. Neil Anderson and his lab for their help and advice.

Thanks to the past and present members of Lab A20 for all their help, friendship and useful discussions. Thanks especially to Craig Carr for his patience, training and his unique methods of calculation and, with Dr. Ian Mullaney, for their collaboration on parts of this work and the use of their data. I am also grateful to Dr. Moira Wilson for her help and advice.

Thank you, Mum and Dad, for your support and love over all my years and also to my big brothers, Graeme and Alasdair, and my wee sister, Magdalene, for their friendship and laughter. Finally, to my wife, Lorna, whose encouragement, understanding and love is beyond measure, my heartfelt thanks and love.

Chapter 1: Introduction

Chapter 1: Introduction

The problem of how cells convey a signal from the binding of an extracellular ligand to an intracellular effect is central to modern biology. In this field, an increasing amount of attention is being given to intracellular signalling pathways which transduce signals which regulate cellular growth and differentiation. Of these pathways, those stimulated by growth factors acting on tyrosine kinase-linked receptors were historically the first to be discovered and much of the early information about these pathways arose from studies on these systems. Many of the early signalling events leading to mitogenesis have been discovered and found to involve numerous kinases and protein-protein interactions. Receptors which make use of the heterotrimeric guanine nucleotide-binding proteins (G-proteins) to transduce their signals were also found to stimulate mitogenesis. The similarities and differences between the signalling pathways initiated by these two categories of receptors has been an area of intense study in recent years.

These studies have discovered the importance of an increasingly large and complex family of enzymes involved in mitogenic pathways: the mitogen-activated protein kinase (MAPK) family. The work which is described in this thesis is focused on the regulation of a subset of this family, namely p42 and p44 mitogen-activated protein kinase ($p42^{MAPK}$ and $p44^{MAPK}$) by receptors which couple to the G_i family of G-proteins.

1.1 G-protein coupled receptors

Many external signals such as hormones, neurotransmitters, light, and odorants produce their effects by interacting with transmembrane receptors which transduce the extracellular signals to effector molecules in the interior of the cells by means of heterotrimeric G-proteins. Many of these receptors (the G-protein coupled receptors - GPCRs) have been cloned and sequenced and found to share common structural features (which are explained in more detail in Dohlman *et al.*, 1991). Hydropathy plots suggested that GPCRs contained seven hydrophobic, membrane spanning regions and all

receptors of this family are believed to fit this model with an extracellular amino-terminus and an intracellular carboxy-terminus. The transmembrane spanning regions are thought to be composed of α helices based on structural similarities with bacteriorhodopsin. The agonist binding region has been determined in many of the receptors to be formed at least in part by the transmembrane region of the receptor. An important feature is that antagonists often display a distinctly different binding site from the naturally occurring agonists.

Site-directed mutagenesis, deletions and chimeric receptor studies have been performed in order to identify regions of the receptor which are important for coupling to their G-proteins (Dohlman *et al.*, 1991; Exton, 1996). It is thought that the important regions for this function are the carboxy-terminal end of the third intracellular loop and the proximal part of the cytoplasmic tail as well as part of the second intracellular loop. However, this work has not been able to determine specific amino acid sequences required for coupling to selective G-proteins and thus it appears that the overall three-dimensional structure of the cytoplasmic parts of the receptor is the important determinant for G-protein coupling.

GPCRs are post-translationally modified. These modifications may include extracellular N-linked glycosylation on the amino-terminal region which might contribute to determining proper distribution of the receptor and intracellular lipid modification which takes the form of palmitoylation at a cysteine or cysteines in the carboxy-terminal region. This palmitoylation may be dynamic and regulated by receptor activation and through intercalation with the membrane bilayer may create a fourth cytoplasmic loop which may play various roles in different receptors such as membrane anchorage, regulation of desensitisation or G-protein interaction (Milligan *et al.*, 1995).

Prolonged stimulation of a cell often results in reduced responsiveness to subsequent challenge with the same stimulus in a rapid process termed desensitisation. For many GPCRs this process is rapid and involves serine/threonine phosphorylation of the

receptors by second messenger-regulated kinases such as protein kinase A (PKA) and protein kinase C (PKC) and by G-protein receptor kinases (GRKs) . PKA is involved in heterologous desensitisation which may occur in response to elevated cAMP levels in the cell and leads to the modification of any receptor with an appropriate target site. The GRKs are involved in homologous desensitisation occurring only at high levels of agonist and their action is dependent on agonist binding to the receptor. The GRKs are apparently synergistically activated by $G_{\beta\gamma}$ and by the agonist-bound receptor (see later) and the phosphorylation permits the binding of a second factor (an arrestin) which uncouples the receptor from its G-protein (Dohlman *et al.*, 1991). A longer-term process is that of down-regulation which is characterised by a reduction in the total number of receptors present in the cell and this occurs over several hours.

1.2 Heterotrimeric G-proteins

The large family of heterotrimeric G-proteins plays an important role in transducing signals at the cell surface to effector proteins within the cell in all eukaryotic organisms (Hepler and Gilman, 1992; Neer, 1995; Rens-Domiano and Hamm, 1995). These proteins are heterotrimeric, being composed of three distinct subunits: α, β and γ. The α subunit family is composed of over 20 members with approximate molecular masses ranging between 39 and 52 kDa. The α subunits contain a single high affinity binding site for guanine nucleotides (GDP and GTP) and have intrinsic GTPase activity. G-proteins have been defined by the identity of the α subunit which they contain. There are now five known mammalian β subunits of approximate 36 kDa and ten γ subunits of 6-9 kDa. β and γ subunits are tightly complexed and function as a unit. The structures of these subunits have been extensively studied (see Neer, 1995; Rens-Domiano and Hamm, 1995; Gudermann *et al.*, 1996; Exton 1996 for reviews) and recently crystal structures of heterotrimeric G-proteins have been described which have revealed the guanine nucleotide-dependent interaction of the α and $\beta\gamma$ subunits which regulates their interaction with receptor and effector molecules (Wall *et al.*, 1995; Lambright *et al.*, 1996).

Although all three subunits lack any sequence which would obviously traverse a lipid bilayer, the heterotrimer is bound to the plasma membrane. The isoprenylation of the carboxy-terminus of the γ subunit appears to be essential for the plasma membrane association of the βγ complex, as well as for interaction with effectors and G_α subunits (Clapham and Neer, 1993). The role of lipid modification of the α subunit is currently the subject of much investigation. Members of the $G_{i\alpha}$ class (see below) have been shown to be co-translationally myristoylated at their amino-terminal glycine and this may play a role in membrane association and interaction with $G_{\beta\gamma}$. Members of all the classes of G_α have been shown to be palmitoylated in a post-translational modification which is dynamic and appears to be regulated by their activation (Milligan *et al.*, 1995). The role of the palmitoylation of these proteins is still somewhat controversial but may include some contribution to plasma membrane localisation as well as subunit and G-protein-receptor coupling.

The GDP bound form of α is tightly bound to βγ and is inactive, whereas the GTP bound form is dissociated from βγ which permits the α and the βγ subunits to regulate effector proteins. The intrinsic GTPase of α switches off this activity and allows reassociation with βγ to occur. Receptors regulate this cycle of activation and deactivation of the G-proteins by inducing a conformational change which causes GDP dissociation from the inactive G-protein complex (Figure 1.1).

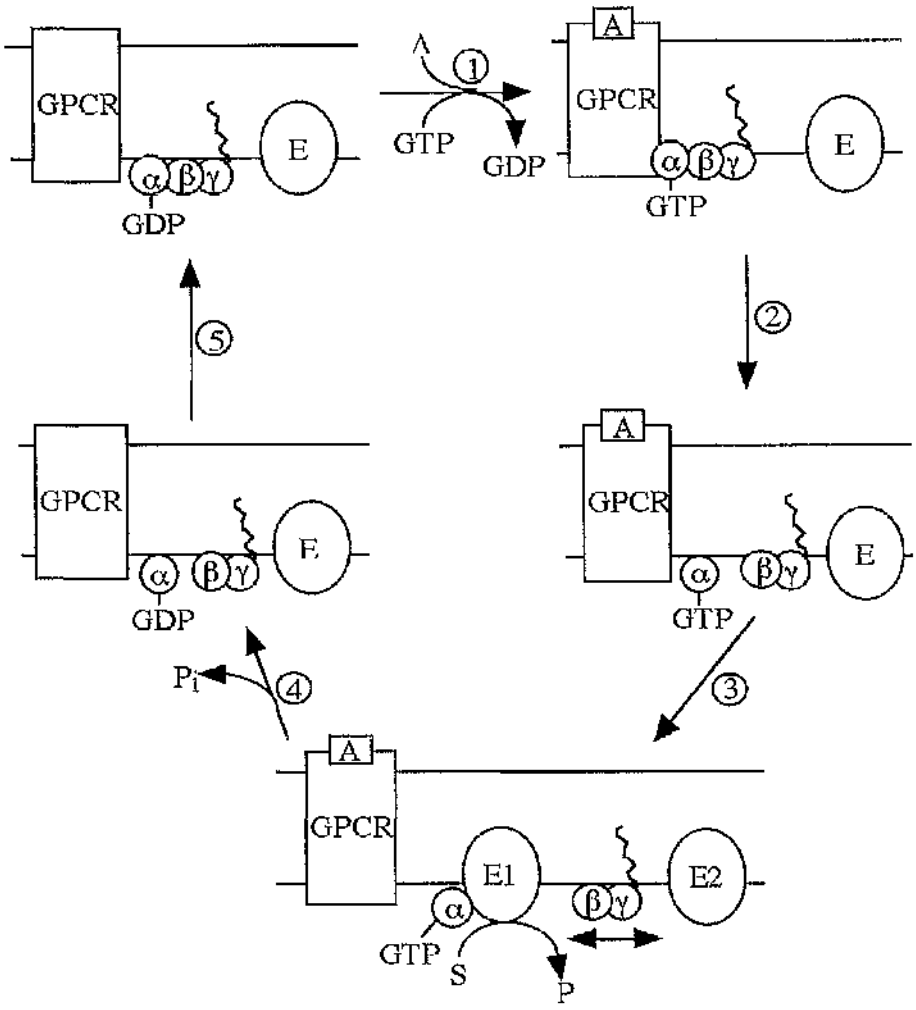

Figure 1.1 Transmembrane signalling by heterotrimeric G-proteins

Agonist (A)-mediated activation of the receptor stimulates a conformational change which favours the interaction of the receptor with the heterotrimeric G-protein (Step 1). This induces a conformational change in the α subunit which promotes dissociation of GDP from its binding site and permits GTP to bind (as it is present in significantly higher levels than GDP in normal cellular conditions). This induces the activated conformation of G_α which dissociates from the receptor as well as from $G_{\beta\gamma}$ (Step 2). This releases the receptor to interact with further G-proteins, and the α and βγ subunits to regulate effector proteins (Step 3). The active state persists until the intrinsic GTPase activity of G_α hydrolyses the bound GTP to GDP (Step 4) and so the duration of activity is determined by the rate of GTPase activity. The GDP-bound form of G_α favours reassociation with $G_{\beta\gamma}$ which switches off both subunits and primes the system to respond again (Step 5).

1.2.1 G_α-families and their function

The G-proteins were subclassified according to amino acid sequence relationships of the α subunits (see Table 1.1) although functional relationships follow this system closely as well. Much could be discussed as to the function of each of these subfamilies and their members, however, only a limited introduction to each of these will be given. The function and effect of the members of the G_{12} family is still poorly understood.

Table 1.1 Classes of mammalian G_α subunits

Class	Members	Toxin	Some Effector Functions
G_s	α_s, α_{olf}	Cholera	Stimulate adenylyl cyclase, regulate Ca^{2+} channels
G_i	α_{i1}, α_{i2}, α_{i3}, α_o, α_{t1}, α_{t2}, α_g, α_z	Pertussis (except α_z), Cholera (for α_t and α_g only)	Inhibit adenylyl cyclase, regulate Ca^{2+} and K^+ channels, activate phospholipase C
G_q	α_q, α_{11}, α_{14}, α_{15}, α_{16}	–	Activate phospholipase C
G_{12}	α_{12}, α_{13}	–	Regulate Na^+/K^+ exchange

1.2.1.1 G_s family

One of the earliest second messengers to be discovered was cAMP and its production is catalysed by a large family of proteins called the adenylyl cyclases (Sunahara *et al.*, 1996). Although these enzymes are regulated in diverse ways (De Vivo and Iyengar, 1994b), all of the mammalian adenylyl cyclases which have been identified thus far are stimulated by members of the G_s family. All members of the G_s family are sensitive to modification by the bacterial cholera toxin which catalyses the ADP-ribosylation of a specific Arg residue of the α subunit which is thought to play a key role in the GTP hydrolysis mechanism (Rens-Domiano and Hamm, 1995). This modification inhibits the GTPase activity thereby constitutively activating the protein.

1.2.1.2 G_i family

Pertussis toxin can catalyse the ADP-ribosylation of most members of the G_i family. This modifies a Cys residue four amino acids from the carboxy-terminus and thus inhibits receptor-G-protein coupling. Pertussis toxin sensitivity is often used to implicate G_i-proteins in signalling pathways. The G_i family couples receptors to various effector proteins. The most common and widely studied is the inhibition of adenylyl cyclase, but others include ion channels, phospholipases and the MAPK cascade (see later). The mechanism of inhibition of adenylyl cyclase by G_i-proteins depends, to a great deal, on the type of adenylyl cyclase which is present. This can occur by means of a direct inhibition of the enzyme by the $G_{i\alpha}$ subunit (especially on type V and VI isoenzymes) or by release of $\beta\gamma$ complex which can inhibit the activity of $G_{s\alpha}$ on type I cyclase (see below).

1.2.1.3 G_q family

Members of the G_q family, all of which are insensitive to both pertussis and cholera toxins, have been shown to be important in the regulation of members of the phosphoinositide-specific phospholipase C (PI-PLC) family (Exton, 1996). These enzymes catalyse the hydrolysis of phosphatidylinositol 4,5-bisphosphate to form two second messengers, inositol 1,4,5-trisphosphate (IP_3) and diacylglycerol (DAG). IP_3 regulates the release of intracellular Ca^{2+}, while DAG activates many isozymes of PKC. Specifically, it is members of the PLCβ sub-family (isozymes 1, 2, 3 and 4) which can be activated by G_q (Exton, 1996).

1.2.2 The role of $\beta\gamma$ complex

For a long time, the accepted viewpoint was that the $\beta\gamma$ complex was present only as a facilitator of the activity of the α subunits, stabilising the inactive form, localising it to membranes and presenting it to receptors. However, increasingly, the importance of the direct regulation of effector proteins by $\beta\gamma$ complexes has been realised (discussed in Sternweis, 1994; Clapham and Neer, 1995). Numerous effectors which are regulated by

$\beta\gamma$ subunits have now been found including K^+ and Ca^{2+} channels, adenylyl cyclase, PLCβ, GRKs and they are implicated in the regulation of the MAPK cascade (as will be discussed later). It is now clear that effectors can be regulated by G_α subunits alone, by $G_{\beta\gamma}$ alone, by both subunits acting independently of each other, or by both subunits acting synergistically or antagonistically. This presents a great potential for complexity in the regulation of effector molecules by GPCRs, especially when the ability of one receptor to interact with more than one type of G-protein (see next section) is also considered. Selectivity between the different possible effects probably relies heavily upon the cell-specific expression of different isoforms of the signalling components.

The different isoforms of adenylyl cyclase are regulated by some of these mechanisms involving $\beta\gamma$ and α subunits (Sternweis, 1994; Sunahara *et al.*, 1996). For example, type I adenylyl cyclase is susceptible to direct inhibition by $G_{\beta\gamma}$ and activation by $G_{s\alpha}$ whereas types II and IV are only modestly activated by $G_{s\alpha}$ but are synergistically activated further by $G_{\beta\gamma}$. In contrast type III is neither activated nor inhibited by $G_{\beta\gamma}$ but is still regulated by $G_{s\alpha}$.

PLCβ2 and 3 are stimulated by $\beta\gamma$ subunits as well as by $G_{q\alpha}$ (as mentioned above) although these effects are selective with regard to the preferred isoforms (Exton, 1996). The $\beta\gamma$ subunit acts independently of $G_{q\alpha}$ and activation is not conditional on priming by either subunit. This implies that these subunits act at distinct sites within the PLC molecule. The pertussis toxin-sensitive regulation of PLC activity by GPCRs is thought to occur by $\beta\gamma$-mediated activation of PLCβ .

In addition to enhancing receptor interaction with G_α, the $\beta\gamma$ complex has also been shown to regulate receptor desensitisation by localising GRKs (such as the β-adrenergic receptor kinase (βARK)) to the plasma membrane (Pitcher *et al.*, 1992) through a direct interaction mediated by the carboxy-terminal region of βARK (which includes a pleckstrin homology domain (see later)). Activation of the GRKs is achieved by a

synergy between the agonist-activated receptor and $G_{\beta\gamma}$ to stimulate phosphorylation and desensitisation of the agonist-bound receptor (Haga *et al.*, 1994). This mechanism may suggest a general model of membrane localisation and co-activation for the function of $G_{\beta\gamma}$ in regulating other effectors.

1.3 Multifunctional signalling by GPCRs

The mechanisms by which any one GPCR can regulate multiple effector pathways and how specificity in these pathways is achieved are of considerable interest (Milligan, 1993, Guderman *et al.*, 1996). There is a potential problem of proving experimentally that multiple effectors are regulated by a single receptor expressed in its physiological setting as there can be many genetic subtypes of one receptor which respond to the same ligand but activate distinct effector pathways. A frequent strategy to circumvent this problem involves heterologous expression of receptors in cells which do not usually contain them. If this technique is used, it must be taken into account that expressing the receptors in foreign genetic backgrounds to levels which are frequently considerably higher than in the cells which endogenously express the receptors may lead to non-physiological interactions of signalling components while the physiological situation may represent greater specificity of coupling (see Guderman *et al.*, 1996 for examples).

Nevertheless, heterologous expression has indeed demonstrated the coupling of a single receptor to multiple effector proteins and examples of such will be seen in this thesis. The mechanisms by which receptors produce these effects are currently under study but may involve the ability of one receptor to couple to distinct G-proteins which can then activate distinct signalling pathways, or both the α and $\beta\gamma$ subunits released from one G-protein regulating distinct effectors. Some of the mechanisms can be clearly seen in the regulation of the MAPK cascade by GPCRs.

1.4 THE MAPK CASCADE

MAPKs are important intermediates in signal transduction pathways that are initiated by many types of cell surface receptors. This family of MAPKs has been extensively studied over the past decade and is composed of three main groups: p42/p44^{MAPK} (ERKs), JNK/SAPK and p38/RK (Davis, 1994, Cano and Mahadevan, 1995). It is with the classical MAPKs or ERKs (extracellular regulated kinases) that this thesis will mainly deal, although the other subfamilies will be mentioned later in this Introduction. p42^{MAPK} and p44^{MAPK} are important enzymes involved in mitogenesis and differentiation and were initially described as regulated by growth hormones acting at tyrosine kinase-linked receptors. Subsequently it was realised that cytokines, antigens and GPCR agonists could also regulate their activity (for examples see Pelech and Sanghera, 1992; Pelech, 1993; Malarkey *et al.*, 1995). Numerous GPCR agonists have since been demonstrated to activate these enzymes via endogenously expressed receptors (including those for thrombin (van Corven *et al.*, 1993) and lysophosphatidic acid (LPA) (Hordijk *et al.*, 1994)) and via heterologously expressed receptors (including the muscarinic m2 acetylcholine receptor (Winitz *et al.*, 1993) and α_{2A}-adrenergic receptor (Alblas *et al.*, 1993)). Regulation of these MAPKs is achieved by means of intricate and complex cascades involving phosphorylation and protein-protein interactions which will be described in some detail (reviewed in Blenis, 1993; Crews and Erikson, 1993; Burgering and Bos, 1995; Malarkey *et al.*, 1995). Although the tyrosine kinase linked receptors and the GPCRs were originally thought to use largely distinct pathways in order to regulate these enzymes (Crews and Erikson, 1993), current research has increasingly suggested considerable similarity in the two cascades. It should be noted that there is great diversity in the pathways used by different receptors and cells and therefore some of the generalisations which will be mentioned will not be true in every system. A diagram illustrating the MAPK cascade as initiated by GPCRs is shown in Figure 1.2.

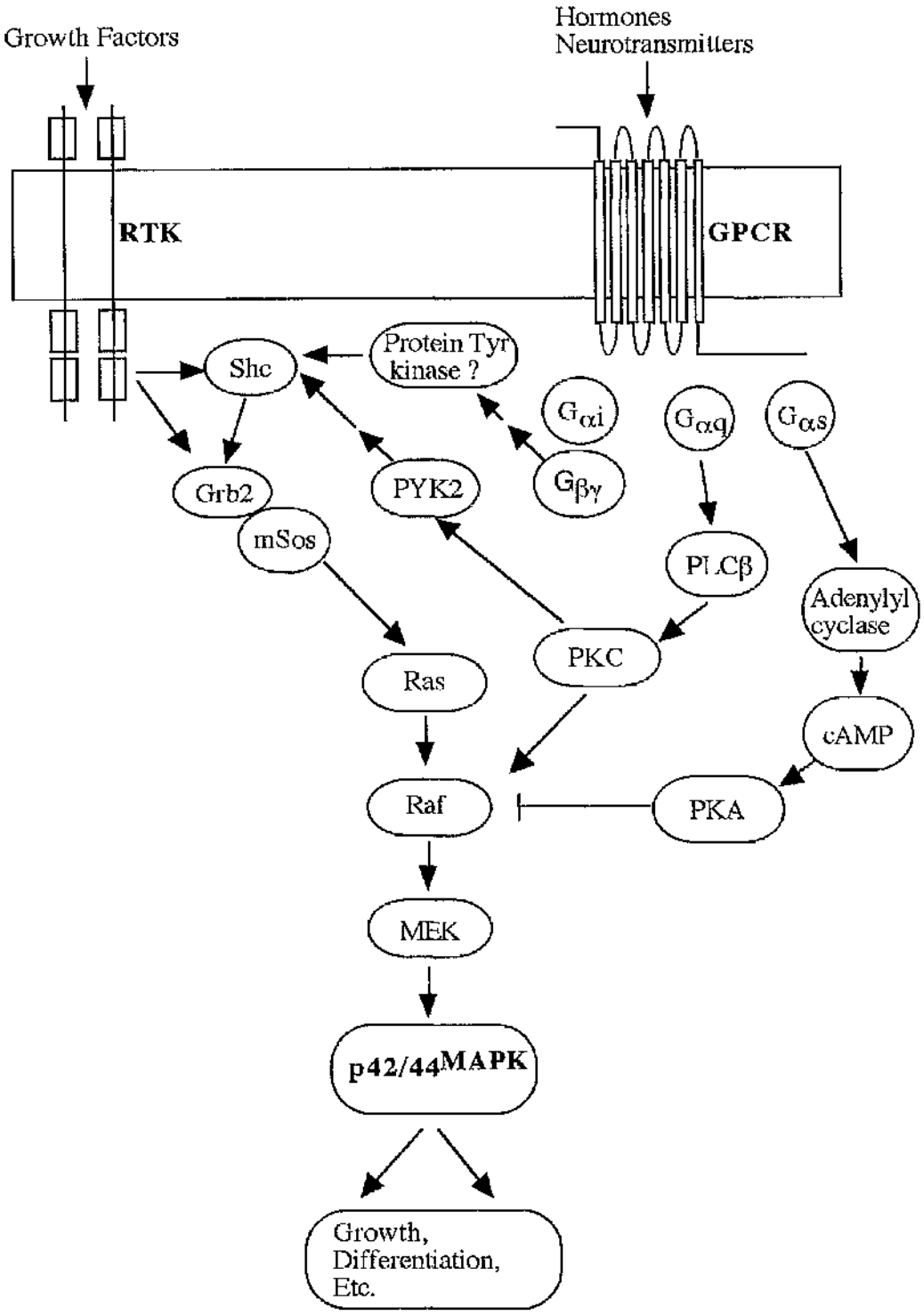

Figure 1.2 The G-protein coupled MAPK cascade

Schematic diagram of the regulation of $p42/44^{MAPK}$ by GPCRs via G_s, G_q and G_i-protein families and growth factor tyrosine kinase receptors (RTK). See main text for details and variations from this scheme.

1.4.1 $p42^{MAPK}$ and $p44^{MAPK}$

MAPK was first identified in adipocytes as an insulin-activated soluble serine/threonine kinase which catalysed the phosphorylation of microtubule-associated protein 2 (Ray and Sturgill, 1987). Two proteins of approximate molecular mass 42 kDa had previously been observed to be phosphorylated on tyrosine residues in response to growth factors and phorbol esters (Gilmore and Martin, 1983; Cooper *et al.*, 1984) and these proteins were found to mediate the activity observed by Ray and Sturgill (Rossomando *et al.*, 1989). Cloning and characterisation of these proteins (Boulton *et al.*, 1990 and 1991) demonstrated a family of kinases with two main isoforms, p42 and p44 (also called ERK 2 and 1 respectively but from now on these will be denoted as $p42^{MAPK}$ and $p44^{MAPK}$). These two forms of MAPK are coactivated by a variety of stimuli as will be seen later, however it should be noted that although selective activation of $p42^{MAPK}$ but not $p44^{MAPK}$ has been demonstrated in platelets (Papkoff *et al.*, 1994), this is thought to be unique to this system. Much of the work in this field was aided by the observed similarity in the MAPK cascade in signal transduction pathways in all eukaryotes. For example, genetic analysis of the pheromone-induced signalling pathways in yeast has been applied to the study of the MAPK pathway in mammalian systems (see Blumer, 1994; Nishida and Gotoh, 1993).

1.4.2 Regulated by phosphorylation

An early observation of the ability of phosphatase inhibitors to preserve the activity of MAPK suggested the importance of phosphorylation in the activation of MAPK (Ray and Sturgill, 1987). It is now known that the MAPK family is activated by dual phosphorylation on both threonine and tyrosine residues (Anderson *et al.*, 1990). This occurs in a TEY sequence for both $p42^{MAPK}$ and $p44^{MAPK}$ (Thr^{183} and Tyr^{185} in the mammalian $p42^{MAPK}$) (Nishida and Gotoh, 1993; Her *et al.*, 1993) and this defines these enzymes from the other members of the MAPK family (Cano and Mahadevan, 1995 and see later). Phosphorylation on both of these residues is essential for activity as shown by the loss of MAPK activity on mutation of either the phosphorylated threonine

or tyrosine residue (Alessandrini *et al.*, 1992). The phosphorylation of the TEY sequence is catalysed by a single dual specificity enzyme called MAPK kinase or MEK (**M**APK or **E**RK **K**inase) (Gomez and Cohen, 1991). Tyrosine and threonine residues can be phosphorylated by MEK independently of each other and in either order (Her *et al.*, 1993), and although autophosphorylation of the regulatory tyrosine residue can occur, MEK can catalyse the dual phosphorylation of a kinase-inactive MAPK (Nakielny *et al.*, 1992), demonstrating that this protein is indeed a dual specificity kinase. Control of the activity is also achieved by the action of phosphatases, both in the nucleus (CL100) and cytoplasm (Pyst1) and these will be discussed later.

The three-dimensional structure of $p42^{MAPK}$ was determined in its unphosphorylated low-activity conformation (Zhang *et al.*, 1994). This revealed that Thr^{183} is on the surface of the molecule while Tyr^{185} (the residue which is suggested to be phosphorylated first) is buried in a largely hydrophobic pocket and may interfere sterically with substrate binding. It is assumed that $p42^{MAPK}$ undergoes an initial conformational change on MEK binding in order to permit phosphorylation which occurs first on tyrosine and subsequently of threonine. Both global and local conformational changes are thought to be involved in the activation of $p42^{MAPK}$.

1.4.3 MAPK substrates

$p42/44^{MAPK}$ is a serine/threonine kinase with an optimal substrate consensus sequence of Pro-Xaa-Ser/Thr-Pro (hence the description of MAPK as a proline-directed kinase) (Davis, 1993). Following activation of MAPK, an important step is thought to be the translocation of a proportion of this enzyme to the nucleus (Chen *et al.*, 1992) and the activation of various transcription factors (Edwards, 1994; Cano and Mahadevan, 1995; Hill and Treisman, 1995). There are also important substrates of $p42/44^{MAPK}$ which are located in the cytoplasm such as cytosolic phospholipase A_2 which can be activated by GPCRs by a complex mechanism involving regulation by Ca^{2+}, PKC and MAPK (Lin *et al.*, 1993; Kramer *et al.*, 1993) and perhaps a further factor (Winitz *et al.*, 1994). Other

substrates of p42/44^{MAPK} include p90 ribosomal S6 kinase (p90^{rsk}) which can also activate transcription factors in the nucleus (Chen *et al.*, 1992; Blenis, 1993), MAPK activated protein (MAPKAP) kinase-2, as well as other kinases upstream of MAPK which perhaps function in a feedback pathway (reviewed in Davis, 1993).

1.4.4 MEK and its regulation

Two main mammalian isoforms of MEK have been identified and cloned, MEK1 and MEK2 (Seger *et al.*, 1992; Zheng and Guan, 1993a). These ubiquitous enzymes show remarkable selectivity for p42/44^{MAPK}; no other *in vitro* substrates for this enzyme have been discovered. The sufficiency of the MAPK cascade for cell growth was demonstrated by the ability of constitutively active MEK to transform mammalian cells (Mansour *et al.*, 1994, Cowley *et al.*, 1994). MEK was inactivated on treatment with phosphatases specific for phosphoserine/threonine, but not phosphotyrosine, demonstrating that these enzymes are regulated by serine/threonine phosphorylation (Crews and Erikson, 1992; Nakielny *et al.*, 1992). MEK and p42/44^{MAPK} were constitutively activated in NIH 3T3 cells expressing the oncogene v-*raf* (the transforming gene of the murine sarcoma virus), and recombinant v-Raf could also phosphorylate and activate MEK *in vitro* (Dent *et al.*, 1992). Activation and phosphorylation on Ser/Thr residues of MEK by the cellular counterpart of this oncogene, c-Raf, was subsequently demonstrated (Kyriakis *et al.*, 1992; Howe *et al.*, 1992) and phosphorylation at both Ser^{218} and Ser^{222} which is required for activation of human MEK1 can be catalysed by c-Raf (Zheng and Guan, 1994; Alessi *et al.*, 1994). In addition, MEK can also be phosphorylated by Mos and MEK kinase (Blumer and Johnson, 1994).

Raf-1 is a 72-76 kDa serine/threonine protein kinase which is activated by numerous growth factors. Its requirement in the activation of p42^{MAPK} and p44^{MAPK} (Schaap *et al.*, 1993) and cellular transformation (Troppmair *et al.*, 1994) induced by growth factors, serum and oncogenes has been demonstrated by the overexpression of dominant negative mutants of Raf-1 made from the N-terminal regulatory domain . The activation

of $p42^{MAPK}$ in response to LPA was also blocked by the expression of dominant negative mutants of Raf-1 and potentiated by overexpression of wild type Raf-1 in COS-1 cells (Howe and Marshall, 1993). The expression of a dominant negative mutant of Raf-1 also blocked the activation of $p44^{MAPK}$ by various GPCRs expressed in COS-7 cells (Hawes *et al.*, 1995) suggesting a general function for this enzyme. Three mammalian isoforms of Raf have been identified (c-Raf-1, A-raf and B-raf), of which c-Raf-1 is ubiquitous while they others display some tissue specificity (Daum *et al.*, 1994).

Raf may have other additional signal transduction roles involving the phosphorylation of substrates other than MEK. Recent work has implicated Raf-1 in a pathway leading to activation of $p70^{s6k}$ (see later) by a MAPK-independent mechanism (Lenormand *et al.*, 1996). At present these observations are poorly understood.

1.4.5 Ras

For many years, $p21^{ras}$ has been known to play a role in cell growth and transformation having been implicated in the formation of a considerable proportion of human tumours. This protein is the product of a proto-oncogene and one of a large number of small GTPase enzymes which are present in mammalian cells. Mammalian cells express four true Ras proteins and these proteins cycle between the active GTP-bound and the inactive GDP-bound forms and the ratio of Ras-GTP/Ras-GDP is thought to be the key determinant of downstream signalling from Ras proteins. This is regulated by guanine nucleotide exchange factors (GEFs) which stimulate the release of GDP and by stimulation of the low intrinsic GTPase activity by GTPase activating proteins (GAPs) (Boguski and McCormick, 1993).

Expression of oncogenic Ras was found to constitutively activate $p42^{MAPK}$ and $p44^{MAPK}$ (Leevers and Marshall, 1992; Cook *et al.*, 1993), although this appears to be cell-specific as this was not always observed in transfected Rat1 fibroblasts (Gupta *et al.*, 1992, Gardner *et al.*, 1993 contrasts with Hordijk *et al.*, 1994a). Ras has also been

implicated in the control of other transcriptional regulators (Deng and Karin, 1994). Overexpression of dominant negative mutants of $p21^{ras}$ (Asn^{17} to Ser, which might compete for a required GEF) in various cells blocked $p42^{MAPK}$ and $p44^{MAPK}$ activation by growth factors and GPCR agonists but not by phorbol esters (de Vries-Smits *et al.*, 1992; Cook *et al.*, 1993; Hawes *et al.*, 1995) which implicated a Ras-dependency of these pathways, although some GPCRs act by an apparently Ras-independent mechanism (Honda *et al.*, 1994; Hawes *et al.*, 1995). Experiments with the heterotrimeric G-protein activator AlF_4^- apparently also indicated that certain G-proteins may control this pathway in a Ras-independent manner (Robbins *et al.*, 1992).

1.4.6 Ras and Raf interaction

Experiments in which active Ras was shown to activate Raf-1 (Williams *et al.*, 1992), and dominant negative Raf prevented the effect of oncogenic Ras on the MAPK cascade (Schaap *et al.*, 1993; Troppmair *et al.*, 1994), positioned Ras upstream of Raf. These observations were taken further by the discovery of a direct interaction *in vitro* between the effector region of Ras and the amino-terminal regulatory domain of c-Raf, but only when Ras was present in its active GTP-bound state (Warne *et al.*, 1993). Specific interaction between Ras and Raf in intact mammalian cells in response to stimuli that cause Ras to be GTP-bound (phorbol esters and growth factors) was subsequently shown (Hallberg *et al.*, 1994). The native structure of Raf is a large multi-subunit complex made up of Raf and at least the chaperone proteins hsp90 and p50, and this complex was recruited to the membrane by Ras where Raf was found to be activated and interact with MEK (Wartmann and Davis, 1994). This led to the idea that the role of Ras was that of recruiting the inactive form of Raf to the membrane whereupon some other activation event occurs. The most convincing proof of this was presented by the loss of Ras-dependency when Raf was mutated to include the carboxy-terminal membrane localisation signal from K-ras (Stokoe *et al.*, 1994; Leevers *et al.*, 1994). This Raf-CAAX mutant was constitutively membrane localised and active, although growth factor treatment could further activate this protein. These activities were completely Ras-

independent, and so it is now thought that Ras acts as a regulated Raf membrane-recruiting agent, and then Raf is activated by some other means and anchored to the membrane (perhaps by cytoskeletal proteins) in a Ras-independent fashion.

The co-operation of Ras with other signals was indicated by experiments using an insect expression system which showed that $p21^{ras}$ and v-*src* could independently activate Raf-1 but only to a very limited extent. Maximal activation of Raf-1 required the coexpression of both genes (Williams *et al.*, 1992). Coexpression of Raf-1, $pp60^{src}$ and c-Ras was shown to be able to phosphorylate and activate recombinant MEK in a similar expression system (Dent *et al.*, 1994).

1.4.7 Phosphorylation of Raf

It would appear that phosphorylation of Raf is an important step in the activation of this kinase as physiological activation of Raf is paralleled by its hyperphosphorylation. Phosphorylation occurs on serine, threonine and tyrosine residues to various extents depending on the stimulus and the cell type involved (Daum *et al.*, 1994; Avruch *et al.*, 1994). Morrison and co-workers demonstrated that three serine residues (Ser^{43}, Ser^{259} and Ser^{621}) are the major *in vivo* phosphorylation sites of Raf-1 in mammalian cells and Sf9 insect cells expressing human Raf-1 (Morrison *et al.*, 1993). These sites varied in their basal level of phosphorylation, the level of phosphorylation in response to growth factors, and the functional consequences of their mutation to unphosphorylated residues.

1.4.7.1 PKC and Raf

PKCα has been a candidate Raf kinase due to the action of PKC-activating phorbol esters. Indeed, PKCα can activate Raf-1 by direct phosphorylation *in vitro* and *in vivo* (Kolch *et al.*, 1993) and the important sites in this regulation appear to be Ser^{499} (and Ser^{259}, although this is possibly an autophosphorylation site). However, although mutation of either of these residues impedes activation of Raf-1 by PKCα, this does not affect Ras/Src-mediated activation, implying that there is a complex activation of Raf-1.

Subsequent work also suggested that although the phosphorylation of Raf-1 by PKCα did stimulate the autokinase activity of Raf-1, it did not stimulate its ability to phosphorylate MEK (MacDonald *et al.*, 1993). Therefore PKCα-mediated phosphorylation of Raf-1 may activate this kinase for a specific, as yet unidentified, substrate.

1.4.7.2 Tyrosine phosphorylation of Raf

Although the phosphorylation on tyrosine residues of Raf is very limited in many cell systems, coexpression in the Sf9 insect expression system of activated tyrosine kinases (v-*src*) and Raf-1, produced phosphorylation on Tyr^{340} and Tyr^{341} of Raf-1 and activated its autokinase activity (Fabian *et al.*, 1993). This phosphorylation appears to have a functional role as a mutant Raf-1 in which these residues are altered to a negatively charged residue (presumably mimicking the effect of phosphorylation) has a higher basal activity and can transform mammalian cells and induce the meiotic transformation of Xenopus oocytes. Phosphorylation on tyrosine residues of Raf-1 has also been seen *in vivo*, in a T-cell line after treatment with interleukin 2 (Turner *et al.*, 1993). Treatment of immunoprecipitated Raf-1 from these cells with tyrosine-specific phosphatases, which selectively removed phosphate from the tyrosine residues, reduced the activity of Raf to near basal levels. Serine/threonine-specific phosphatases produced a much more modest reduction in Raf activity, and so this would suggest that phosphorylation of Raf-1 on tyrosine residues plays an important role in the interleukin 2-mediated activation of this kinase in these cells.

1.4.8 Other regulators of Raf

Other molecules which can phosphorylate Raf include MAPK (in a proposed feedback loop, but the physiological significance of this is unknown), and PKA (which will be discussed in detail below). Other proteins have been shown to bind to Raf proteins such as Rap1 which is a small Ras-related GTPase which may exert its inhibitory effect on

growth factor-mediated MAPK activation and stimulation of DNA synthesis by interrupting the interaction of Ras with Raf (Cook *et al.*, 1993).

Whether the phosphorylation of Raf is the initiating event in Raf activation is still a matter of some controversy. Therefore other candidates for the Raf-activator have been investigated. It has been suggested that some isoforms of the 14-3-3 family of proteins play a role in the regulation of Raf in mammalian systems, possibly through a stabilisation of the Raf kinase or through some interaction with PKC (Aitken, 1995).

1.4.9 Raf-independent MEK kinase activity

MEK can also be regulated by a MEK kinase (MEKK) activity which is independent of Raf. The similarity of signal transduction cascades in yeast and mammalian systems led to the discovery of a mouse MEKK (73 kDa) which was shown to be ubiquitously expressed and could phosphorylate and activate MEK independently of Raf-1 (Lange-Carter *et al.*, 1993). However, both MEKK and Raf appear to regulate MEK activity by phosphorylation on common residues (Gardner *et al.*, 1994). This MEKK was initially proposed to explain a number of observations in which G-protein-mediated activation of the MAPK cascade was not Ras/Raf dependent. For example, a Ras-independent activation of the MAPK cascade was stimulated by the G-protein activator AlF^-_4 (Robbins *et al.*, 1992), and thrombin activated MEK activity in fibroblasts without any detectable Raf activation (Gardner *et al.*, 1993). However, these are not general observations as, for example, Ras and Raf-dependent GPCR agonist-mediated $p42/44^{MAPK}$ regulation has subsequently been demonstrated for LPA in COS-1 cells (Howe and Marshall, 1993), and for the α_{2A} receptor expressed in COS-7 cells (Hawes *et al.*, 1995). Also, agonist-stimulation of the muscarinic m2 acetylcholine receptor activated Ras, Raf, MEK and MAPK in heterologously transfected Rat1 fibroblasts (Winitz *et al.*, 1993). Further variation was seen in the activation of $p42/44^{MAPK}$ by the α_{1B} adrenergic and the m2 muscarinic acetylcholine receptors expressed in COS-7 cells which was Raf-dependent, but Ras independent (Hawes *et al.*, 1995).

Raf-independent p42/44^{MAPK} activation has also been implied with other growth factors. Epidermal growth factor (EGF) and phorbol ester were shown to be able to utilise a Raf-independent pathway in order to activate p42/44^{MAPK} in murine fibroblasts (Chao *et al.*, 1994). In adipocytes, insulin-stimulated activation of Raf-1 which was Ras-dependent was not upstream of MAPK, but was required for insulin-mediated differentiation (Porras *et al.*, 1994). Insulin in these cells can activate (probably by serine/threonine phosphorylation) another member of the MEKK family distinct from c-Raf which can phosphorylate and activate MEK (Haystead *et al.*, 1994). Regulation of a MEKK by growth factors was also demonstrated in PC12 cells and this occurred in parallel with Raf activation, and both kinases were activated in a Ras-dependent fashion (Lange-Carter and Johnson, 1994). These results would indicate the presence of different parallel p42/44^{MAPK} pathways which may regulate diverse cellular functions. The role of MEKK in these cascades is not fully understood. In 293 cells, MEKK could indeed phosphorylate and activate MEK but this did not lead to a significant activation of p42^{MAPK} (Xu *et al.*, 1995) suggesting that additional, unidentified mechanisms were also involved in the activation of the p42/44^{MAPK}.

However, the physiological role of MEKK may be in another MAPK pathway - the JNK(c-Jun NH_2-terminal kinase)/SAPK(stress-activated protein kinase) cascade (see later). In NIH 3T3 cells, MEKK has been shown to be able to phosphorylate and activate the kinase and activator of SAPK (SEK1) but be unable to activate p42/44^{MAPK} (Yan *et al.*, 1994). Around the same time it was discovered that MEKK participated in the Ras-dependent activation of JNK by EGF and nerve growth factor (NGF), but only contributed to the activation of p42^{MAPK} when overexpressed. Raf-1 contributed to the Ras-dependent activation of p42^{MAPK} but not of JNK by these same growth factors (Minden *et al.*, 1994). Therefore this suggested that there are two distinct Ras-dependent pathways with one initiated by Raf-1 leading to p42/44^{MAPK} activation and the other involving JNK activation mediated by MEKK. Raf-independent MEK kinase activity

may also be achieved by c-Mos which can activate MEK and p42/44^{MAPK} in Xenopus oocytes (Blumer and Johnson, 1994; Nebreda and Hunt, 1993).

1.4.10 Effect of cAMP on the MAPK cascade

It has been known for some time that cAMP can affect the mitogenic response in numerous cells. Understanding the MAPK cascade has provided a molecular basis to the effects on growth of cAMP. Agents which elevated intracellular cAMP levels blocked the stimulation of DNA synthesis induced by growth factors in Rat1 fibroblasts (Cook and McCormick, 1993; Hordijk *et al.*, 1994a) and the activation of Raf-1, MEK and p42/44^{MAPK} by growth factors acting on tyrosine kinase receptors, GPCR agonists and phorbol esters in Rat1 and NIH 3T3 fibroblasts (Wu *et al.*, 1993; Cook and McCormick, 1993; Burgering *et al.*, 1993). cAMP, however, did not affect the stimulation of GTP loading of p21^{ras} or any of the other upstream proteins (Cook and McCormick, 1993; Burgering *et al.*, 1993). This indicated that the site of action was downstream of Ras but upstream of Raf, a conclusion which was strengthened by the ability of elevated concentrations of cAMP in *ras* transformed Rat1 and NIH 3T3 cells to deactivate constitutively active p42/44^{MAPK} and reverse the transformed phenotype, without altering the p21^{ras}GTP level (Hordijk *et al.*, 1994a; Chen and Iyengar, 1994). A model of competition for binding to Raf between a cAMP regulated protein and Ras was suggested by work which demonstrated that the block in the MAPK cascade could be overcome by increasing the total number of p21^{ras}GTP molecules by overexpression (Burgering *et al.*, 1993).

The involvement of PKA in the effect of cAMP in these cells was demonstrated by the loss of this effect in cells expressing a dominant negative form of PKA (Chen and Iyengar, 1994). Elevated cAMP levels in Rat1 fibroblasts were found to stimulate the phosphorylation of Raf-1 on Ser^{43}, which is the main site of PKA-directed phosphorylation of Raf-1 *in vitro* and *in vivo*. This residue is present in the regulatory amino-terminal domain of Raf-1 which binds to Ras and this phosphorylation

significantly reduced the affinity of binding of GTP-bound Ras for Raf-1 (Wu *et al.*, 1993). Therefore the PKA-directed phosphorylation of Raf-1 may contribute to the cAMP-mediated blockade of the MAPK cascade. Other mechanisms of cAMP-mediated inhibition of the MAPK cascade have been suggested including a role for members of the $p21^{rap}$ family.

In other cell lines, elevated cAMP levels have distinctly different effects on growth factor-induced MAPK activation. In PC12 cells (a neuroendocrine cell line) cAMP elevating agents stimulated the activity of $p42^{MAPK}$ and $p44^{MAPK}$ and MEK, and potentiated neurite formation induced by NGF (Frödin *et al.*, 1994). However, another study in PC12 cells described cAMP as having no effect on MEK and $p42^{MAPK}$ activation in the absence of growth factors but potentiating the effect of growth factor-mediated activation of MEK and $p42^{MAPK}$ (Vaillancourt *et al.*, 1994). Surprisingly, an inhibitory effect of cAMP on growth factor-activated Raf-1 and B-Raf was demonstrated in this same study. Similarly, in COS-7 (Faure *et al.*, 1994) and Swiss-3T3 cells (Faure and Bourne, 1995), elevated cAMP levels stimulated $p42/44^{MAPK}$ activity and did not inhibit LPA or EGF-mediated activation of $p42^{MAPK}$ or MEK. However, elevated cAMP levels did prevent mitogen-mediated Raf-1 activity, as was seen with Rat1 cells (Faure and Bourne, 1995). These studies would suggest that in these cells, growth factors can trigger a MAPK pathway which is both Raf-1-independent and cAMP-insensitive in addition to the Raf-regulated cascade. MEKK is not thought to be involved in this cAMP-insensitive pathway as its activation is blocked by cAMP as well (Lange-Carter and Johnson, 1994).

1.4.11 MAPK phosphatases

In contrast to the mechanisms of activation of $p42/44^{MAPK}$, and the pathway which controls this, the inactivation of these enzymes is poorly understood. The phosphorylation and activation of $p42/44^{MAPK}$ in most instances is a transient response and so there seems to be a requirement for a switch off mechanism, which could most

obviously be met by specific phosphatases. Indeed a family of apparently selective MAPK phosphatases has been discovered (Nebreda, 1994). *3CH134* was discovered as an immediate early gene which was rapidly and transiently expressed in mouse embryo fibroblasts during the G0/G1 transition and induced by various mitogens (Lau and Nathans, 1985). The product of this gene was a short-lived protein which displayed no similarity to any protein except a vaccinia virus tyrosine/serine phosphatase (Charles *et al.*, 1992). This led to the discovery that this protein displayed intrinsic protein tyrosine phosphatase activity with selectivity for $p42^{MAPK}$ *in vitro* (Charles *et al.*, 1993) and subsequently to the identification of this protein as MKP-1 (MAPK phosphatase-1), a dual-specificity phosphatase *in vitro* and *in vivo* with remarkable specificity for $p42^{MAPK}$ and $p44^{MAPK}$ (Sun *et al.*, 1993). Other members of this family were discovered including the human homologue of 3CH134 called CL100 or HVH1 (Keyse and Emslie, 1992; Zheng and Guan, 1993b). CL100 is highly inducible by oxidative stress and heat shock in skin cells (Keyse and Emslie, 1992) and is a highly MAPK-specific tyrosine/threonine phosphatase (Alessi *et al.*, 1993). Another similar MAPK phosphatase is PAC-1 which like 3CH134/CL100 is localised to the nucleus and induced by mitogens, but displays a distinctly different and limited tissue distribution (Rohan *et al.*, 1993). These enzymes can also be induced by agonists of GPCRs as demonstrated by the ability of angiotensin II (and thrombin) to induce expression of 3CH134 in vascular smooth muscle cells in a PKC and Ca^{2+}-dependent manner (Duff *et al.*, 1993).

The physiological relevance of this family of phosphatases have been demonstrated. The kinetics of MAPK deactivation coincided with the appearance of 3CH134 and treatment with cycloheximide (a protein synthesis inhibitor) led to a persistent activation of $p42^{MAPK}$ (Sun *et al.*, 1993), and constitutive expression of 3CH134, CL100 or PAC-1 blocked mitogen or oncogenic Ras and Raf-mediated activation of $p42/44^{MAPK}$ and MAPK-regulated reporter gene expression (Sun *et al.*, 1993; Alessi *et al.*, 1993; Ward *et al.*, 1994).

These enzymes were discovered to be localised to the nucleus and to have some, but lower, activity towards other members of the MAPK cascade (see later). However, recently discovered novel members of this family (called Pyst1 and Pyst2) are constitutively expressed in the cytoplasm of human skin fibroblasts and are much more selective for the $p42/44^{MAPK}$ members of the MAPK family (Groom *et al.*, 1996). Therefore the MAPK may be regulated by different MAPK phosphatases depending on their subcellular location.

Phosphatases would also be expected to act at other levels of the MAPK cascade. For example, protein phosphatase 2A (PP2A - a serine/threonine selective phosphatase) was implicated in the dephosphorylation and inactivation of MEK by the ability of SV40 small tumour antigen to activate MEK and $p44^{MAPK}$ through an interaction with PP2A (Sontag *et al.*, 1993). These examples underline the importance of controlling phosphorylation-signalled pathways by phosphatases as well as kinases (see Feng and Pawson, 1994; Sun and Tonks, 1994).

1.4.12 Growth factor receptors

The cascades initiated by growth factors and GPCR agonists were thought to converge at the level of the activation of Ras. However, there is striking similarity in some of the pathways which are used to couple the primary receptor events and the activation of the MAPK cascade indicating that convergence occurs at an earlier step. The early steps in the growth factor-mediated cascade will be explained briefly and then compared and contrasted with the pathways for various GPCR agonists (Schlessinger and Bar-Sagi, 1994; Malarkey *et al.*, 1995).

Growth factor receptors are characterised by an extracellular binding domain, a single transmembrane spanning region and a large intracellular catalytic domain. It is the autophosphorylation of these receptors on specific tyrosine residues and their associated dimerisation which are the essential events following growth factor binding. For the

EGF receptor (EGFR), the main sites of phosphorylation are in the carboxy-terminal tail, however, other receptors (e.g. the platelet derived growth factor (PDGF) receptor) contain kinase insert domains which are also phosphorylated. These receptors are called tyrosine kinase receptors because of their catalytic activity.

Phosphorylation of the receptor on tyrosine promotes the interaction of numerous proteins and enzymes including PLCγ, phosphatidylinositol 3-kinase (PI3-kinase), GAP, the growth-factor-receptor binding protein (Grb2), and members of the non-receptor Src family of tyrosine kinases. This interaction is mediated by Src homology-2 (SH2) domains (Feller *et al.*, 1994; Pawson, 1995) which are defined by approximately 100 amino acids which show considerable homology to the non-catalytic region of the Src family. The specificity of these various domains determine the specificity of the binding of these proteins with selective tyrosine residues of the receptors (Songyang and Cantley, 1995). It is the association of the adaptor protein Grb2 to the phosphorylated receptor which is the initial step in the $p21^{ras}$-MAPK cascade initiated by growth factor receptors (Gale *et al.*, 1993; McCormick, 1993). Some of the other proteins have been implicated in this cascade and will be dealt with later.

1.4.12.1 Grb2 and mSos

In addition to an SH2 domain, Grb2 contains two Src homology-3 (SH3) domains which are composed of approximately 60 amino acid residues and mediate binding to proline rich sequences (Feller *et al.*, 1994; Pawson, 1995). The SH3 domains of Grb2 mediate its binding to a proline rich sequence of the carboxy-terminal domain of mSos (the mammalian homologue of Drosophila Son of sevenless) (Li *et al.*, 1993; Egan *et al.*, 1993). mSos is a RasGEF, which activates Ras by stimulating guanine nucleotide exchange (Egan *et al.*, 1993; Boguski and McCormick, 1993). EGF-stimulated guanine nucleotide exchange of Ras was potentiated by Grb2 overexpression (Gale *et al.*, 1993) and the constitutive Grb2.mSos complex was associated with the EGFR to form a multi-protein complex, after EGF-mediated autophosphorylation (Li *et al.*, 1993). The

functional importance of mSos was demonstrated by the transforming ability of expression of this protein in Rat1 fibroblasts (Egan *et al.*, 1993). These, and many other studies (McCormick, 1993), indicate that tyrosine kinase linked receptors stimulate Ras.GTP loading by receptor autophosphorylation which recruits (via SH2 domains) the cytoplasmic Grb2.mSos complex which activates Ras by stimulation of guanine nucleotide exchange.

The way in which mSos is activated is not fully understood, however the primary mechanism is thought to simply involve its localisation to the plasma membrane at the vicinity of its substrate. This idea was strengthened by work performed with modified mSos proteins which were constitutively located at the plasma membrane by the introduction of sites of lipid modification. These mSos proteins activated the Ras.MAPK cascade and led to oncogenic transformation without external stimuli (Aronheim *et al.*, 1994). A carboxy-terminal truncated form of the plasma membrane-localised mSos displayed even greater activity, raising the possibility of a secondary mechanism of mSos activation through the relief of an inhibitory effect exerted by the carboxy-terminal region. Phosphorylation of mSos has been demonstrated but this is thought to be explained by MAPK-mediated feedback rather than by a primary activating stimulus (Burgering *et al.*, 1993).

1.4.12.2 GAP activation of Ras

Activation of Ras could also conceivably occur through inactivation of a basal GAP activity. Although such a decrease in GAP activity has been shown not to be the main mechanism of activation in a number of cell lines (e.g. Gale *et al.*, 1993), inactivation of GAPs has been demonstrated to be important in the activation of $p21^{ras}$ (in a PKC-dependent manner) on stimulation of the antigen receptor of T lymphocytes (Downward *et al.*, 1990). However the physiological role of GAPs may be more to do with restricting the length of any Ras activity stimulated by other means.

1.4.12.3 Src homology/collagen (Shc)

Alternative links between the tyrosine kinase linked receptors and downstream effectors can be mediated by other SH2 containing, adaptor proteins. One such protein is the insulin receptor substrate-1 (IRS-1) which is a major target for the insulin and insulin-like growth factor-1 (IGF-1) receptor tyrosine kinases and is implicated in the actions of PI3-kinase and Grb2 (Skolnik *et al.*, 1993). Another important adaptor protein is Src homology/collagen (Shc), which is a family of widely expressed proteins of size 46, 52 and 66 kDa (Pelicci *et al.*, 1992). These proteins contain an SH2 domain, a glycine/proline rich domain and a phosphotyrosine binding domain distinct from any SH2 domain, but they do not contain any detectable catalytic domain. These proteins were found to be complexed with, and tyrosine phosphorylated by, the activated epidermal growth factor receptor and the physiological involvement of these proteins in mammalian cell proliferation was demonstrated by the transforming and tumour creating ability of overexpressed Shc in NIH 3T3 cells and nude mice (Pelicci *et al.*, 1992). Shc's role in Ras signalling was demonstrated in PC12 cells by the ability of dominant negative Ras to block the neurite outgrowth induced by Shc overexpression (Rozakis-Adcock *et al.*, 1992). This was explained by the demonstration of Grb2 association (via its SH2 domain) with tyrosine phosphorylated Shc (Rozakis-Adcock *et al.*, 1992), and the association between Shc and mSos (Egan *et al.*, 1993), in *src* transformed Rat2 cells. Shc.Grb2 complexes were also found to be formed by, and associated with, ligand-activated EGF and NGF receptors (Rozakis-Adcock *et al.*, 1992) and insulin can also stimulate the formation of Shc.Grb2 complexes (Skolnik *et al.*, 1993).

The role of Shc in the mitogenic response to EGF and insulin in Rat1 cells overexpressing insulin receptors was demonstrated by the inhibitory effect of microinjection of anti-Shc antibodies on DNA synthesis (Sasaoka *et al.*, 1994b). However the anti-Shc antibodies did not inhibit the mitogenic effect of oncogenic *ras*. Immunoprecipitates of Shc from lysates of growth factor-stimulated cells removed a large proportion of the RasGEF activity (Sasaoka *et al.*, 1994a and b). These results would

therefore show that Shc was an important component in the mitogenic signal transduction cascade of insulin and EGF and appears to function upstream of Ras.

As the last piece of data suggests, the coupling of the activated EGFR to Shc is preferred over direct coupling to the Grb2.mSos complex. This was demonstrated by Sasaoka and co-workers who also demonstrated the presence of Shc.Grb2.mSos complexes which were formed on EGF stimulation but not associated with the activated EGFR (Sasaoka *et al.*, 1994a). The model of activation of Ras which is thought to predominate is that on EGF treatment, Shc associates with, and is tyrosine-phosphorylated by, the EGFR which leads to the formation of the EGFR.Shc.Grb2.mSos complex. Free Shc.Grb2.mSos complexes also exist which arise from the dissociation from the receptor or phosphorylation of Shc by other tyrosine kinases. In this way mSos is activated and the Ras.MAPK cascade is stimulated. It should be noted, however, that Shc has also been implicated in the control of other pathways in addition to the Ras.MAPK cascade (Bonfini *et al.*, 1996).

1.4.12.4 The non-receptor Src family of tyrosine kinases

As noted above, c-Src binds to activated tyrosine kinase linked receptors and this binding leads to the activation of these Src kinases. The mechanism of activation is quite complex and is not fully understood but is thought to involve the displacement of an internal phosphotyrosine residue from Src's SH2 domain, possibly by competition from the receptor phosphotyrosine, subsequent dephosphorylation of the inhibitory tyrosine residue and the autophosphorylation of another tyrosine on Src (Cooper and Howell, 1993). These steps are thought to be under the control of (one or many) phosphatases and kinases.

Members of the Src family have been proposed to be involved in signal transduction pathways that control growth and cellular architecture. The physiological role of Src has been suggested by the ability to activate or co-operate in the activation of the MAPK

cascade (see above; VanRenterghem *et al.*, 1993). Src is thought to play an important role for growth factor receptors (Erpel and Courtneidge, 1995), especially for those which do not contain intrinsic tyrosine kinase activity (especially important in haematopoietic cells). The activation of tyrosine kinase signalling pathways by these receptors is thought to be mediated by members of the Src protein tyrosine kinase family. However, Src has been demonstrated to be essential for PDGF receptor-induced mitogenic signalling even although these receptors contain intrinsic tyrosine kinase activity (Twamley-Stein *et al.*, 1993). Src family kinases are also essential for the mitogenic response of NIH 3T3 and Swiss 3T3 cells to PDGF, colony stimulating factor and EGF (Roche *et al.*, 1995). The implication of c-Src in the cascades initiated by GPCRs will be discussed below.

1.4.13 Regulation of the MAPK cascade by G-protein coupled receptors

There are now many agonists which act at GPCRs which have been demonstrated to stimulate growth and cell proliferation in numerous cells. This effect has been demonstrated for receptors coupling to G-proteins of the G_q, G_i, G_s and $G_{12/13}$ families (for reviews see Post and Brown, 1996; Malarkey *et al.*, 1995). These receptors have been shown to activate the p42/44^{MAPK} cascade, and although activation of this cascade is not always sufficient and may not be required for all GPCR-mediated growth responses it undoubtedly plays a central role in the mediation of many growth signals from GPCR to the nucleus. Other kinases may also be involved in these actions for example the JNK cascade (see later). The activation of the p42/44^{MAPK} cascade by receptors coupling to G_s, G_q and G_i are discussed below.

1.4.13.1 G_s-coupled receptors and MAPK

G_s-coupled receptors have very different effects on p42/44^{MAPK} activity and mitogenesis in various cell lines. Agonist-stimulation of G_s-coupled receptors stimulates p44^{MAPK} activity in COS-7 cells (Faure *et al.*, 1994; Crespo *et al.*, 1995), but reduces EGF-mediated p44^{MAPK} activity in Rat1 fibroblasts (Hordijk *et al.*, 1994a). Expression of a

constitutively active mutant of $G_{s\alpha}$ stimulates $p44^{MAPK}$ in COS-7 cells in some (Faure *et al.*, 1994) but not all studies (Crespo *et al.*, 1995), but blocks the Ras-induced stimulation of $p44^{MAPK}$ activity and DNA synthesis in NIH 3T3 cells (Chen and Iyengar, 1994). Stimulation of $G_{s\alpha}$ with cholera toxin also displayed a cell-specific effect on $p44^{MAPK}$ activity and DNA synthesis (Frondin *et al.*, 1994; Cook and McCormick, 1993). Most of these effects can also be reproduced using other cAMP elevating agents and can be correlated with the diverse effects of elevated cAMP levels on $p42/44^{MAPK}$ activity in these cells (as seen above).

1.4.13.2 G_q-coupled receptor activation of MAPK

There are many hormones which activate G_q-coupled receptors which can activate the Ras.MAPK cascade although the signalling pathways are less well defined than for G_i-coupled receptors. As seen before, the ability of G_q-coupled receptors to activate these pathways appears to depend not only on the specific receptor under investigation but also the cellular environment in which it is expressed. For example, endothelin-1 (ET-1) stimulated the phosphorylation and activation of $p42/44^{MAPK}$ in mouse astrocytes (Cazaubon *et al.*, 1993) and rat myocytes (Bogoyevitch *et al.*, 1994) but not in rat astrocytoma cell lines (Cazaubon *et al.*, 1993). In Rat1 fibroblasts, treatment with ET-1 has been reported to activate the Ras.MAPK cascade by Daub *et al.* (1996) but not by other groups (van Corven *et al.*, 1993; Alblas *et al.*, 1993; Hordijk *et al.*, 1994b).

There have been conflicting reports as to the involvement of Ras in the G_q-mediated activation of $p42/44^{MAPK}$ which may be a reflection of receptor and cell diversity. Agonist stimulation of the G_q-coupled prostaglandin $F_{2\alpha}$ (in NIH 3T3 cells) and α_1-adrenergic receptors (in COS-7 cells) activated Ras.GTP loading (Watanabe *et al.*, 1995; Koch *et al.*, 1994), and m1 muscarinic acetylcholine receptor-mediated MAPK activation (in COS-7 cells) was apparently blocked by expression of a dominant negative mutant Ras (Crespo *et al.*, 1994). However, it has been reported that the $p42/44^{MAPK}$ phosphorylation induced by the m1 muscarinic acetylcholine receptor in HEK 293 cells

(Ito *et al.*, 1995) and the α_1-adrenergic receptor expressed in CHO cells (van Biesen *et al.*, 1996) or by either receptor expressed in COS-7 cells (Hawes *et al.*, 1995) was unaffected by expression of the dominant negative Ras, thereby demonstrating Ras-independence.

1.4.13.2.1 Mediated by the α-subunit of G_q

The effect of G_q-coupled receptors is thought to be mediated by the $G_{q\alpha}$ subunit rather than the βγ complex, as shown by the lack of any effect of overexpression of $G_{t\alpha}$ or the C-terminus of the β-adrenergic receptor kinase (βARKct) on the agonist-mediated activation of the Ras.MAPK cascade by the bombesin, α1-adrenergic, or m1 muscarinic acetylcholine receptors expressed in COS-7 and CHO cells (Faure *et al.*, 1994; Koch *et al.*, 1994; Luttrell *et al.*, 1995a; Hawes *et al.*, 1995; van Biesen *et al.*, 1996). The ability of a constitutively active mutant of $G_{q\alpha}$ to activate the Ras.MAPK cascade and DNA synthesis in NIH 3T3 cells (Watanabe *et al.*, 1995) and $p44^{MAPK}$ activity in COS-7 cells (Faure *et al.*, 1994) seemingly confirms this view.

However, opposing findings have been reported. De Vivo and coworker failed to detect any stimulation of $p44^{MAPK}$ activity or DNA synthesis on expression of a constitutively active mutant of $G_{q\alpha}$ in NIH 3T3 cells, although they did show that expression potentiated the response to PDGF treatment (De Vivo and Iyengar, 1994a). Constitutively active mutants of $G_{q\alpha}$ and $G_{11\alpha}$ were unable to activate the Ras.MAPK cascade in COS-7 and HEK 293 cells (Crespo *et al.*, 1994; Ito *et al.*, 1995) and overexpressing $G_{t\alpha}$ inhibited m1 muscarinic receptor-mediated activation of $p42^{MAPK}$ in COS-7 cells (Crespo *et al.*, 1994). This may again indicate cell/receptor specificity in the mechanism of activation.

1.4.13.2.2 Involvement of PKC

The strong $p42/44^{MAPK}$ stimulation by phorbol esters and phosphorylation of Raf-1 by PKC-α (see above) has implicated PKC in the control of $p42/44^{MAPK}$. The activation of

PKC isoforms by diacylglycerol produced by PLC has been suggested as the mechanism for the activation of the MAPK cascade by G_q-coupled receptors (Faure *et al.*, 1994), and this is supported by the observations that PKC-downregulation by phorbol esters does attenuate the MAPK phosphorylation induced by some G_q-coupled receptors (Ito *et al.*, 1995; Hawes *et al.*, 1995; van Biesen *et al.*, 1996). However this does not explain all the available data. Although phorbol ester could stimulate p42/44^{MAPK} activity in vascular smooth muscle cells, it was not as potent as vasopressin which acts on a pertussis toxin-insensitive GPCR (Granot *et al.*, 1993). This suggested the presence of both PKC-dependent and independent pathways leading to p42/44^{MAPK} activation. Consistent with this idea is the partial block of ET-mediated activation of p42/44^{MAPK} by downregulation of (at least some isoforms of) PKC by prolonged treatment with phorbol esters (Cazaubon *et al.*, 1993; Bogoyevitch *et al.*, 1994). This was also demonstrated for the activation of p42^{MAPK} by carbachol acting on muscarinic m1 receptors in COS-7 cells (Crespo *et al.*, 1994). However, prostaglandin $F_{2\alpha}$-activated p42^{MAPK} by a mechanism which was sensitive to the protein kinase inhibitors staurosporine and H-7, was unaffected by prolonged phorbol ester treatment and so appears to utilise protein kinases independently of classical PKCs (Watanabe *et al.*, 1995). Some of these effects could possibly be explained by the involvement of phorbol ester-insensitive PKC isoforms.

1.4.13.2.3 Calcium and PYK2

A potential mechanism has been suggested for the coupling of the activation of PKC and an increase in cytoplasmic calcium to the Ras.MAPK cascade (Lev *et al.*, 1995). This involves a newly discovered protein tyrosine kinase, PYK2, which could be activated by phosphorylation on tyrosine residues stimulated by an influx of Ca^{2+}, and by bradykinin (an agonist for a G_q-protein coupled receptor) in a PKC-dependent and independent manner. Activated PYK2 stimulated p42^{MAPK} apparently by phosphorylating Shc thereby recruiting the Grb2.mSos complex which is quite similar to the mechanism utilised by receptor tyrosine kinases (also see later). PYK2 has since been shown to play

an important role in mediating the activation of $p42/44^{MAPK}$ in PC12 cells on stimulation with bradykinin and with LPA in a mechanism which involves an interaction with Src upstream of Grb2 and mSos (Dikic *et al.*, 1996). A role for increased cytoplasmic calcium in G_q-protein-mediated MAPK activation was suggested by a number of studies, for example the partial attenuation of the response to prostaglandin $F_{2\alpha}$ by a calcium chelator (Watanabe *et al.*, 1995).

1.4.13.3 G_i-protein coupled receptor activation of the MAPK cascade

Many agonists of GPCRs have demonstrated a pertussis-toxin sensitive activation of $p42/44^{MAPK}$ indicating that these effects are mediated by members of the G_i-protein family. The signalling pathway to $p42/44^{MAPK}$ activation has been shown to involve MEK, $p21^{ras}$ and Raf-1 (van Corven *et al.*, 1993; Howe and Marshall, 1993; Winitz *et al.*, 1993; Alblas *et al*, 1993; Crespo *et al.*, 1994; Luttrell *et al.*, 1995b; Ito *et al.*, 1995; Hawes *et al.*, 1995; and earlier discussions) but on the whole appears to be PKC-independent (van Corven *et al.*, 1993; Hordijk *et al.*, 1994; Crespo *et al.*, 1994; Luttrell *et al.*, 1995b; Hawes *et al.*, 1995; van Biesen *et al.*, 1996). LPA and thrombin acting on endogenous receptors in fibroblasts have the ability to signal via members of both the G_q and the G_i-protein family. Coupling to DNA synthesis and the Ras.MAPK cascade, however, has been shown by pertussis toxin sensitivity to be solely mediated by G_i-proteins (Gupta *et al.*, 1992; Gardner *et al.*, 1993; van Corven *et al.*, 1993; Howe and Marshall, 1993) and is independent of PLC pathways (van Corven *et al.*, 1993; Hordijk *et al.*, 1994b). LPA, in common with other G_q-coupled receptor agonists, stimulates the phosphorylation of many other substrates, such as $p125^{FAK}$, paxillin and p130, and this has been shown to involve PLC activation mediated by pertussis toxin-insensitive G-proteins (G_q) (Hordijk *et al.*, 1994b; Seufferlein and Rozengurt, 1994, Moolenaar, 1995).

1.4.13.3.1 Mediated by the βγ subunits

It has been suggested that the α subunit of G_{i2} is responsible for the activation of the $p42/44^{MAPK}$ cascade because expression of a GTPase deficient form of this protein (*gip2*) in Rat1 fibroblasts transforms these cells (Pace *et al.*, 1991) and constitutively activates $p42^{MAPK}$ (Gupta *et al.*, 1992) and MEK-1 (Gardner *et al.*, 1993). However the effects of this oncogene were highly cell specific as *gip2* failed to transform NIH 3T3 cells (Pace *et al.*, 1991) or to constitutively activate $p42^{MAPK}$ or MEK-1 in these cells (Gallego *et al.*, 1992; Gardner *et al.*, 1993), COS-7 cells (Faure *et al.*, 1994; Crespo *et al.*, 1994) or HEK 293 cells (Ito *et al.*, 1995). This may reflect a cell specific effect of this oncogene and may also demonstrate the problems in relating the results from oncogene studies to the signalling of GPCRs in untransformed cells which stimulate $p42/44^{MAPK}$ in all of the above cell lines.

The βγ complex derived from G_i-proteins is now thought to be the initiator of the Ras.MAPK cascade. The initial experiments which led to this conclusion involved the overexpression of β and γ subunits together (specifically β1γ2) which stimulated $p42/44^{MAPK}$ in a Ras-dependent and PKC-independent manner in COS-7 cells (Faure *et al.*, 1994; Crespo *et al.*, 1994; Hawes *et al.*, 1995) and stimulated $p42^{MAPK}$, Raf and Ras in HEK 293 cells (Ito *et al.*, 1995). These effects were dependent on membrane localisation of the βγ complex as shown by the failure of response with isoprenylation-deficient γ mutants.

The role of the βγ complex was further demonstrated by the expression of peptides which function as βγ-antagonists by competing with effector molecules for the binding of βγ subunits. Thus overexpression of $G_{t\alpha}$ inhibited the $p42/44^{MAPK}$ activation induced by the overexpression of βγ subunits as well as that induced by agonist-activated G_i-coupled receptors (Faure *et al.*, 1994; Crespo *et al.*, 1994). Expression of βARKct containing its βγ-binding domain which can specifically antagonise $G_{\beta\gamma}$ (and not G_α) mediated effects inhibited the activation of Ras and $p42^{MAPK}$ by LPA in Rat1 cells and

by agonists acting on heterologously expressed α_2-adrenergic and m2 muscarinic receptors expressed in COS-7 cells (Koch *et al.*, 1995; Hawes *et al.*, 1995). EGF-mediated responses and pertussis toxin-insensitive G-protein-mediated effects were unaffected in both cell lines. βARKct contains a pleckstrin homology (PH) domain and expression of the PH domains of several other proteins (including PLCγ, RasGAP, RasGRF) inhibited the stimulation of the Ras.MAPK cascade mediated by α_2-adrenergic receptors and βγ overexpression in COS-7 cells (Luttrell *et al.*, 1995a). PH domains of proteins are thought to be involved as βγ-subunit binding domains and so this data would seem to confirm the importance of the βγ-subunit in the Ras.MAPK cascade. The presence of PH domains in many proteins involved in signal transduction and growth control suggests that these domains may play a major role in the assembly of membrane-associated protein complexes involved in signal transduction cascades (see Inglese *et al.*, 1995).

A variation to this mechanism of pertussis toxin sensitive G-protein-mediated MAPK activation was seen with m2 muscarinic acetylcholine and platelet activating factor (PAF) receptors (van Biesen *et al.*, 1996). The m2 muscarinic receptor signals via G_q-proteins in order to stimulate $p44^{MAPK}$ activity when expressed in COS-7 cells in a pertussis toxin and βARKct-insensitive manner, (PAF does not stimulate $p44^{MAPK}$ in these cells). However, when expressed in CHO cells, these receptors stimulate $p44^{MAPK}$ in a G_o-coupled pathway which is sensitive to pertussis toxin inhibition and PKC-dependent. Signalling in these cells is still insensitive to βγ-antagonists and so represents a novel mechanism for the activation of the MAPK cascade mediated by the α subunit of G_o. PAF-induced $p42/44^{MAPK}$ activation has been reported to occur in the absence of any detectable Ras activation in these cells (Honda *et al.*, 1994) . This again reinforces the idea of the cellular specificity of pathways used to transduce mitogenic stimuli by GPCRs.

Another novel finding was that stimulation of $p44^{MAPK}$ induced by the IGF-1 receptor in Rat1 fibroblasts was pertussis toxin sensitive and was inhibited by the expression of βARKct (Luttrell *et al.*, 1995b). This stimulation was also similar to that induced by LPA in that it was PKC-independent, Ras-dependent and was inhibited by protein tyrosine kinase inhibitors (see later). This suggests that some tyrosine kinase-linked, growth factor receptors employ similar mechanisms for mitogenic signalling as GPCRs involving $G_{\beta\gamma}$ subunits derived from pertussis toxin-sensitive G-proteins.

1.4.13.3.2 βγ stimulation of Ras.MAPK cascade is mediated by Shc

Once the role of βγ in the stimulation of the Ras.MAPK cascade had been shown, the question of how this was achieved remained. The effect of βγ was not thought to be directly at the level of Ras because of the requirement for tyrosine kinase activity (see later) and is now thought to be mediated by the Shc adaptor protein. Shc was phosphorylated on tyrosine residues after agonist stimulation of G_i-protein coupled receptors in cardiac fibroblasts and COS-7 cells or by overexpressing $G_{\beta\gamma}$ in COS-7 cells (Schorb *et al.*, 1994; Touhara *et al.*, 1995; van Biesen *et al.*, 1995). The phosphorylation of Shc was followed by an increase in the functional association between Shc and the Grb2.mSos complex and the disruption of this interaction between Shc and Grb2 blocked βγ-mediated activation of $p42/44^{MAPK}$ (van Biesen *et al.*, 1995). These effects (but not those stimulated by EGF) were βγ-dependent as shown by the inhibitory effects of βARKct, but were not dependent on Ras or PKC activation. Tyrosine phosphorylation of Shc therefore appears to be an early step in the βγ-mediated activation of the Ras.MAPK cascade, and the subsequent signalling pathway appears to be common to both growth factor, tyrosine kinase linked receptors and GPCRs.

A similar pathway may also be induced by G_q-protein coupled receptors as demonstrated by the tyrosine phosphorylation of Shc and subsequent complex formation with Grb2.mSos stimulated by gastrin, thrombin (in this case by a pertussis toxin-insensitive manner) and muscarinic m1 receptors (Seva *et al.*, 1996; Chen *et al.*, 1996). This

pathway was shown to be PKC-independent (Chen *et al.*, 1996) and so may not be the mechanism used by all G_q-protein coupled receptors (see earlier).

Another possible role for the $G_{\beta\gamma}$ subunits in the MAPK cascade was suggested by the work of Pumiglia and co-workers which demonstrated a direct interaction between the βγ subunits and Raf-1 (Pumiglia *et al.*, 1995). This occurred *in vitro* and *in vivo* with similar affinity to that of the interaction of βARK and βγ. This raises the question as to the role of this interaction in signal transduction pathways. Suggestions include cross-talk mechanisms between growth factor receptor and GPCR-mediated pathways or the regulation of the MAPK cascade by GPCRs.

1.4.13.3.3 Tyrosine kinase activity required

The requirement for the tyrosine phosphorylation of Shc necessitates the activation of a tyrosine kinase as an early step in the GPCR-mediated activation of the Ras.MAPK cascade. In other systems, IRS-1 is apparently phosphorylated on tyrosine residues in cells stimulated by angiotensin II, suggesting its role as a different substrate for a GPCR-induced tyrosine kinase activity (Saad *et al.*, 1995). This conclusion is consistent with a number of observations of the inhibitory effects of genistein which is a tyrosine kinase-specific inhibitor (Akiyama *et al.*, 1987). Genistein inhibited LPA and thrombin-mediated Ras and $p42^{MAPK}$ activation in Rat1 fibroblasts at a lower concentration than that required for inhibition of EGF-mediated stimulation (van Corven *et al.*, 1993; Luttrell *et al.*, 1995b). Phorbol ester-activated $p42^{MAPK}$ was unaffected by genistein. Also, genistein prevented $p44^{MAPK}$ activation by overexpression of βγ or agonist activation of G_i but not G_q-coupled receptors expressed in COS-7 cells (Hawes *et al.*, 1995).

The genistein-sensitive protein tyrosine kinase has been located upstream of Shc in the Ras.MAPK cascade, and possibly may be responsible for the phosphorylation of Shc. Genistein had no effect on oncogenic Ras-mediated $p42/44^{MAPK}$ activation in both Rat1

and CHO cells (Luttrell *et al.*, 1995b; van Biesen *et al.*, 1995), but could inhibit the phosphorylation of p52 Shc by βγ overexpression and agonist stimulation of the α_{2A}-adrenoceptor in COS-7 cells (Touhara *et al.*, 1995) and could prevent the synergistic effect on $p44^{MAPK}$ activation of $G_{\beta\gamma}$ and mSos expression in CHO cells (van Biesen *et al.*, 1995). As usual there is some receptor specificity in this effect as the effect mediated by the muscarinic m2 receptor in Rat1 fibroblasts was not susceptible to inhibition by this agent (Winitz *et al.*, 1993). Other inhibitors of tyrosine kinases (but with less selectivity) e.g. staurosporine, have also been shown to have an inhibitory effect on this cascade (Hordijk *et al.*, 1994; Luttrell *et al.*, 1995b).

1.4.13.4 Receptor tyrosine kinases and GPCR-mediated $p42/44^{MAPK}$ activation

It has been proposed that receptor tyrosine kinases may play a role as downstream mediators in GPCR signalling to the Ras.MAPK cascade. In Rat1 fibroblasts, various GPCR agonists stimulated the phosphorylation of the EGFR and subsequent association of this receptor with the Shc adaptor proteins (which was tyrosine phosphorylated) and Grb2 (Daub *et al.*, 1996). Inhibition of EGFR function by either tyrphostin AG1478 (a selective EGFR kinase inhibitor (Levitzki and Gazit, 1995)) or a dominant negative mutant EGFR, suppressed these interactions as well as the stimulation of $p42/44^{MAPK}$ activity and DNA synthesis mediated by the GPCRs. EGF-mediated $p42/44^{MAPK}$ activity was less sensitive to inhibition by tyrphostin AG1478 and the actions of the dominant negative EGFR on EGF-mediated signalling could be overcome by a higher EGF concentration (PDGF-mediated responses were reported as insensitive to either inhibition). Therefore, this work suggests that the EGFR tyrosine kinase can act as a downstream mediator in the GPCR-mediated activation of the Ras.MAPK cascade. How this kinase activity would itself be activated independently of ligand-binding by the release of βγ subunits (at least in the case of LPA and thrombin) is not known. This work suggests that the point of convergence between the pathways by which GPCRs and

growth factor receptors activate p42/44^{MAPK} is at a much earlier step than previously proposed.

Similarly, the PDGF receptor has been implicated in the signalling pathway stimulated by angiotensin II in smooth muscle cells (Linseman *et al.*, 1995). Angiotensin II treatment of these cells phosphorylated the PDGF receptor on tyrosine residues and stimulated the association of this receptor with tyrosine phosphorylated Shc.Grb2 complex and also Src kinases. Therefore this GPCR may stimulate a pathway involving both a receptor (PDGF receptor) and the non-receptor (Src) tyrosine kinases.

1.4.13.5 Src and GPCR-mediated p42/44^{MAPK} activation

The Src family of tyrosine kinases was also implicated by the inhibitory effect of herbimycin A (an inhibitor of Src-family kinase (Levitzki and Gazit, 1995)) on GPCR and βγ-mediated activation of p44^{MAPK} and tyrosine phosphorylation of Shc (Hawes *et al.*, 1995; Touhara *et al.*, 1995). The role of Src in the stimulation of Shc.Grb2.mSos complexes was discussed earlier and this would seem to present a possible route to activation of the Ras.MAPK cascade. Activation of Src has been demonstrated by α_2-adrenergic, muscarinic m1 and thrombin receptors expressed in CCL39 cells acting through pertussis toxin sensitive, insensitive and partially sensitive pathways respectively (Chen *et al.*, 1994). Data has been reported which supports a role for Src in the GPCR-mediated activation of p42/44^{MAPK}. For example, angiotensin II acting at AT_1 receptors in smooth muscle cells has been shown to stimulate Ras.GTP loading and Ras.Raf-1 complex formation in a pathway which is dependent on selective members of the Src kinase family (Schieffer *et al.*, 1996). In PC12 cells, Src has been shown to act with PYK2 to link G_i- and G_q-coupled receptors (for LPA and bradykinin) to the cascade at a point upstream of Grb2 and Sos in order to activate p42/44^{MAPK} (Dikic *et al.*, 1996).

Again there appears to be a measure of diversity depending on the cell type studied because although the Src kinases were activated by LPA and bombesin treatment in

Swiss 3T3 cells, they were shown not to be involved in the mitogenic responses to LPA and bombesin (Roche *et al.*, 1995). It has been suggested that Src may play a role in the cytoskeletal rearrangements which accompany stimulation by LPA and thrombin in this case (Erpel and Courtneidge, 1995). Further studies are required to determine if the Src kinases are widely used as a mechanism of GPCR-mediated stimulation of the Ras.MAPK cascade.

1.4.13.6 Other tyrosine kinases and GPCR-mediated p42/44^{MAPK} activation

Other tyrosine kinases have also been shown to be required for the GPCR-mediated activation of the Ras.MAPK cascade. Avian B cells were shown to require the Src-related tyrosine kinase Lyn to permit the activation of p44^{MAPK} and MEK by a transiently transfected G_q-coupled m1 muscarinic acetylcholine receptor (Wan *et al.*, 1996). This kinase was not required for the G_i-coupled m2 muscarinic receptor to activate this cascade. However, another tyrosine kinase called Syk was essential for the activation by both types of receptors. This again illustrates that the pathway for GPCR-mediated Ras.MAPK activation depends upon both the receptors involved and their cellular environment.

1.4.14 PI3-kinase

PI3-kinase catalyses the formation of phosphatidylinositol 3,4,5-trisphosphate ($PI(3,4,5)P_3$) by direct phosphorylation of phosphatidylinositol 4,5-bisphosphate, and the first identified form of this enzyme was a heterodimer composed of an 85 kDa regulatory subunit and a 110 kDa catalytic subunit. This enzyme has been implicated in a number of intracellular signalling pathways, for example the activation of p70 ribosomal S6 kinase (p70^{s6k}) which is thought to play an important role in cellular regulation (Proud, 1996). However, the targets for the product of the enzyme ($PI(3,4,5)P_3$) are still being sought, although the serine/threonine kinase, Akt/PKB, has been suggested (Bos, 1995). The study of this enzyme has been greatly aided by the use of wortmannin

(and other similar inhibitors such as LY294002) which is a selective inhibitor of PI3-kinase (Ui *et al.*, 1995), although other effects have been reported (see Cross *et al.*, 1995). PI3-kinase can be activated by numerous receptors of both the tyrosine kinase family and the GPCR family (Ui *et al.*, 1995) and this enzyme is of particular interest to this discussion because of the recent implication of the role of PI3-kinase in the p42/44^{MAPK} pathway induced by GPCRs.

1.4.14.1 PI3-kinase and the p42/44^{MAPK} cascade

The involvement of PI3-kinase in the activation of the Ras.MAPK cascade was suggested by the ability of wortmannin to inhibit insulin and serum-mediated activation of p42/44^{MAPK} and p90^{rsk} in CHO cells overexpressing the insulin receptor (Welsh *et al.*, 1994). Wortmannin was thought to act at an early step in the pathway as Raf-1, MEK and p42^{MAPK} activation by IGF was blocked by this compound, although it did not appear to inhibit Ras-GTP loading (Cross *et al.*, 1994). In both these studies, rapamycin, (an inhibitor of the p70^{s6k} pathway (MacKintosh and MacKintosh, 1994)) had no effect on the MAPK pathway.

The use of wortmannin has also implicated PI3-kinase in the GPCR-mediated activation of p42/44^{MAPK}. PAF activates p42/44^{MAPK} through two distinct pathways in neutrophils, both of which are required for full activation. One is a Ca^{2+}-dependent pathway (inhibited by an intracellular Ca^{2+} chelator) and the other is a Ca^{2+}-independent but wortmannin-sensitive pathway (Ferby *et al.*, 1994). However this PAF-activated, wortmannin-sensitive MAPK pathway in a macrophage cell line appeared not to involve the p85/p110-type PI3-kinase (Ferby *et al.*, 1996), indicating that a different PI3-kinase isoform or a different wortmannin-sensitive protein was involved in this pathway. In COS-7 cells, the tyrosine phosphorylation of Shc stimulated by $\beta\gamma$ overexpression (but not by EGF) was inhibited by wortmannin (Touhara *et al.*, 1995) which would implicate the wortmannin-sensitive step early in the GPCR-mediated MAPK cascade. Agonist activation of α_1 adrenoceptors in vascular smooth muscle cells stimulated p42/44^{MAPK},

DNA synthesis and p85/p110 PI3-kinase activity in a wortmannin-sensitive but PKC- and Ca^{2+}-independent manner (Hu *et al.*, 1996). Stimulation was blocked by pertussis toxin pretreatment, implying that the receptors in this instance are coupled to proteins of the G_i family. Also reported was that the α_1 adrenoceptor-activated PI3-kinase was associated with an increase in the GTP loading of Ras and activation of some protein tyrosine kinase activity.

The activation of Ras and $p42/44^{MAPK}$ stimulated by LPA, agonist stimulated α_2 adrenoceptors and $\beta\gamma$ overexpression in COS-7 and CHO cells (but not by phorbol ester or EGF) was also inhibited by wortmannin, LY294002 and a dominant negative p85 subunit of PI3-kinase (Hawes *et al.*, 1996). PI3-kinase inhibitors did not affect $p42/44^{MAPK}$ activation by overexpression of mSos, constitutively active Ras or MEK. All of these results would indicate that PI3-kinase activity is required in the $G_{\beta\gamma}$-mediated MAPK signalling pathway at a point upstream of Shc, Sos and Ras activation.

There remains the question of how PI3-kinase is activated by GPCRs. A novel 110 kDa PI3-kinase subunit ($p110\gamma$) which is stimulated by thrombin via $G_{\beta\gamma}$ but does not bind to the p85 subunit has been cloned and expressed. In human platelets, this isoform of PI3-kinase was detected and was shown to be regulated by thrombin in a $G_{\beta\gamma}$-dependent manner (Zhang *et al.*, 1995). However, in addition, these cells also stimulated p85/p110 PI3-kinase activity and this was independent of $G_{\beta\gamma}$ subunits, but was apparently regulated by Rho. ADP-ribosylation of $p21^{Rho}$ by the Clostridium botulinum C3 exoenzyme has been shown to inhibit LPA-mediated PI3-kinase activation in Swiss 3T3 cells, although this did not totally block $p42^{MAPK}$ activation (Kumagai *et al.*, 1993). The Rho proteins form a subgroup of the Ras family of low-molecular weight G-proteins. These proteins were initially implicated in the reorganisation of the cytoskeleton stimulated by growth factors and GPCR agonists (Takai *et al.*, 1995). However, more recently these proteins have been shown to be involved in various multiple pathways including those transducing growth regulatory signals using MAPK-

like cascades (Symons, 1996). It has been suggested that the effect of the dominant negative p85 PI3-kinase subunit on $G\beta\gamma$-mediated $p42/44^{MAPK}$ activation which would apparently point to the involvement of p85/p110 PI3-kinase in this pathway, may not rule out the involvement of the p110γ subunit but rather be the result of the binding of a substrate common to both isoforms (Hawes *et al.*, 1996). Therefore the regulation of PI3-kinase activity may involve multiple kinase isoforms activated by distinctly different mechanisms. Src has also been suggested to play a role in coupling GPCR to PI3-kinase activity.

1.4.15 Functional outcome of MAPK activation

The importance of the $p42/44^{MAPK}$ cascade in the regulation of mitogenesis has been illustrated throughout this chapter in numerous ways, such as the ability of agents which activate $p42/44^{MAPK}$ to also stimulate DNA synthesis (for example van Corven *et al.*, 1989; Seuwen *et al.*, 1990; Gupta *et al.*, 1992; van Corven *et al.*, 1993; Hu *et al.*, 1996), by the correlation between the inhibition of the $p42/44^{MAPK}$ cascade and the inhibition of DNA synthesis by cAMP (Cook and McCormick, 1993; Hordijk *et al.*, 1994a; Frondin *et al.*, 1994), wortmannin (Hu *et al.*, 1996) and tyrphostin AG1478 (Daub *et al.*, 1996). This has also been demonstrated by the ability of constitutively active members of the cascade to transform mammalian cells (Dent *et al.*, 1992; Pelicci *et al.*, 1992; Mansour *et al.*, 1994; Aronheim *et al.*, 1994, Cowley *et al.*, 1994).

The role of $p42/44^{MAPK}$ in the mitogenic response has been more clearly demonstrated by the expression of kinase deficient mutants of $p42^{MAPK}$ and $p44^{MAPK}$. Using this method, the requirement for functional $p42/44^{MAPK}$ was demonstrated in the growth of quiescent cells infected with the SV40 small tumour antigen (Sontag *et al.*, 1993), the transformation of NIH 3T3 cells by v-*raf* (Troppmair *et al.*, 1994), the stimulation of gene transcription and cell proliferation by thrombin, fibroblast growth factor (FGF) or serum in lung fibroblasts (Pagès *et al.*, 1993), and in the induction of AP-1 activity by Ha-Ras, phorbol ester, and serum in rat embryo fibroblasts (Frost *et al.*, 1994). The last

two conclusions were also reached by use of RNA antisense expression and microinjection of specific substrate peptide inhibitors. Similar conclusions were achieved by the expression of dominantly interfering mutants of MEK1 (whose only known substrate is that of p42/44^{MAPK}) which reverted v-*src*- and *ras*-transformed NIH 3T3 cells (Cowley *et al.*, 1994). Therefore the growth factor-mediated activation of p42/44^{MAPK} is an absolute requirement for the triggering of proliferative responses in many cells.

In other cells, the functional response to the activation of p42/44^{MAPK} is not that of DNA synthesis and cellular proliferation, but sometimes that of differentiation or protein synthesis and hypertrophy. A constitutively active mutant of MEK1 stimulated the differentiation of PC12 cells, and a dominantly interfering mutant of the same enzyme inhibited growth factor-mediated differentiation of these cells (Cowley *et al.*, 1994). Agonist activation of the thromboxane A_2 GPCR in rat aortic smooth muscle cells stimulated p42^{MAPK} activation by a pathway involving Shc and Grb2, but this did not result in the stimulation of DNA synthesis. However, protein synthesis was stimulated as measured by an increase in the incorporation of [^{14}C]leucine (Jones *et al.*, 1995). The absolute requirement for the p42/44^{MAPK} cascade in the stimulation of protein synthesis by tyrosine kinase growth factors (insulin and FGF) and GPCR agonists (angiotensin II and thrombin) in smooth muscle cells was demonstrated by the inhibition by a MEK inhibitor (PD 98059) of protein synthesis and p42/44^{MAPK} activation (Servant *et al.*, 1996). However, the p42/44^{MAPK} cascade is not sufficient for protein synthesis activation as demonstrated by the inhibition by rapamycin (a p70^{s6k} cascade-selective inhibitor) and the additive effects of rapamycin and PD 98059. It appears that both of these distinct pathways operate to increase protein synthesis.

It should be noted that the activation of the MAPK cascade and protein synthesis by the one agonist does not necessarily indicate a functional connection between these two effects. This was seen in the activation of p42/44^{MAPK} by various GPCR agonists in

neonatal ventricular myocytes (Post *et al.*, 1996). In these cells, GPCR agonists which could stimulate hypertrophy stimulated p42/44^{MAPK} with similar kinetics to agonists which were not hypertrophic. Also expression of dominantly-interfering mutants of p42^{MAPK} and p44^{MAPK} and treatment with PD 98059 failed to block the atrial natriuretic factor (ANF) expression of the hypertrophic GPCR agonists, but did inhibit Ras-induced gene expression and p42/44^{MAPK} activation. Therefore p42/44^{MAPK} activation is apparently not sufficient for GPCR-mediated induction of cardiac cell growth and gene expression (G_q-coupled PLC activation correlates better with hypertrophy) and is not required for transcriptional activity of the ANF gene. This would again illustrate the cell and stimulus-specificity which can occur in these pathways especially at this level of functional output.

1.4.15.1 Duration of activation and response

The picture of the functional outcome of activation of the MAPK cascade is more complex as it depends not only upon the extent of stimulation of p42/44^{MAPK}, but also on the duration of the activation of these enzymes (Schlessinger and Bar-Sagi, 1994; Marshall, 1995). It is thought that a more sustained activation permits time for nuclear translocation and transcriptional activation of genes which are not regulated by a more transient activation (Edwards, 1994; Hill and Treisman, 1995). NGF promoted the differentiation of PC12 cells whereas EGF treatment led to a proliferative signal, even although both growth factors activated p42/44^{MAPK} (Marshall, 1995). However, in these cells, NGF stimulated a prolonged activation of p42/44^{MAPK} and MEK for several hours and a significant translocation of p42/44^{MAPK} to the nucleus, while EGF-mediated activation was significantly more transient and translocation was not detected (Traverse *et al.*, 1992). The sustained activation of p42/44^{MAPK} permitted nuclear translocation and supposedly phosphorylation of transcription factors which produced the differentiation. This idea was strengthened by the observation of a differentiative response on EGF treatment of PC12 cells which overexpressed the EGFR. In this case, EGF stimulated the activation of p42/44^{MAPK} with a significantly more prolonged time course and its

translocation to the nucleus was clearly seen (Traverse *et al.*, 1994). The opposite effect was seen by reducing the level of expression of NGF receptors in these cells thereby converting a differentiation response to one of proliferation by a more transient p42/44^{MAPK} activation (Marshall, 1995). Therefore the quantitative difference in activation of p42/44^{MAPK} was translated into a qualitative difference in transcription factor activation and cellular response.

A similar model can be used to explain observations in other cells with GPCR agonists where the sustained activation of p42/44^{MAPK} is apparently important in producing a proliferative response. In CCL39 (hamster lung fibroblasts), thrombin was strongly mitogenic and stimulated cell proliferation presumably through its ability to stimulate p70^{s6k} and p44^{MAPK} with a biphasic time course of an initial transient peak of activity followed by a delayed, sustained peak over many hours (Kahan *et al.*, 1992; Meloche *et al.*, 1992). Treatment with pertussis toxin or a thrombin inhibitor nearly totally prevented the mitogenic activity and the sustained activation of p44^{MAPK} by thrombin, but only partially inhibited the initial transient phase (Meloche *et al.*, 1992). Activation of a serotonin receptor or a transfected m1 muscarinic receptor was not sufficient to induce full mitogenesis and could only stimulate the initial transient peak of activity. Therefore, there appears to be a correlation between the ability of a growth factor to stimulate a sustained phase of p44^{MAPK} activity and its mitogenic potential.

The duration of MAPK activation can also determine between a hyperplastic (cell proliferation) and hypertrophic (cell growth) response. In rat mesengial cells, PDGF stimulated a prolonged activation of p42/44^{MAPK}, MEK and Raf and stimulated DNA synthesis ([^{3}H]thymidine incorporation) and protein synthesis ([^{3}H]leucine incorporation). In contrast, angiotensin II stimulated a significantly less potent and more transient activation of the MAPK cascade coupled with an inability to stimulate DNA synthesis, although protein synthesis was still stimulated (Huwiler *et al.*, 1995).

Therefore the critical determinant between a hyperplastic and a purely hypertrophic response appears to be the magnitude and duration of the stimulation of p42/44^{MAPK}.

1.4.16 Other MAPK cascades

As stated earlier there are three distinct groups of mammalian MAPKs (see Davis, 1994; Cano and Mahadevan, 1995). The JNK/SAPK family has limited homology to p42/44^{MAPK} and its members are activated by UV irradiation, protein synthesis inhibitors, heat shock and cellular stress. The defining property of these kinases is that they contain the TPY sequence which must be phosphorylated on threonine and tyrosine in order to be activated (this is TEY in p42/44^{MAPK}). This can be achieved by a dual specificity kinase called SEK which is thought to be regulated by MEKK in a Ras-dependent manner (see earlier; Yan *et al.*, 1994; Minden *et al.*, 1994), although at present the pathway of regulation is not as well defined as that for p42/44^{MAPK}. The JNK/SAPK cascade can also be activated by mitogens and recent evidence has demonstrated their activation by G_q and G_i-coupled receptors in Rat1a cells (Mitchell *et al.*, 1995) and NIH 3T3 cells (Coso *et al.*, 1995). Like the p42/44^{MAPK} cascade, the JNK/SAPK cascade is thought to play an important role in the induction of the transcription factors c-fos and c-jun (Cano and Mahadevan, 1995).

The third member of the MAPK family is p38 which was discovered as a kinase which was tyrosine phosphorylated in mammalian cells in response to lipopolysaccharide and changes in osmolarity (Han *et al.*, 1994). This kinase also contains a dual phosphorylation motif, in this case in a TGY sequence (Cano and Mahadevan, 1995). There is much still to be explained in connection with this, and the other MAPKs, especially in the area of how specificity in the parallel cascades is achieved allowing the activation of specific pathways in cells (especially if Ras is involved in them all) and also the question of substrate selectivity of these kinases.

GPCRs have also been implicated in the activation of the JAK/STAT pathway (Marrero *et al.*, 1995) which is a recently identified tyrosine kinase signalling cascade involved in the control of transcription (Edwards, 1995; Malarkey *et al.*, 1995; Hill and Treisman, 1995).

1.4.17 Why use a cascade?

One question which arises from the identification and study of this cascade is the reason for (or more properly the benefit from) its presence and complexity. A much simpler mechanism for the activation of MAPK could be envisioned, however one probable benefit from this complexity is the increase in the number of targets for positive and negative crossregulation by other signalling pathways (for example the stimulation by PKC and the various effects of cAMP) as well as for positive and negative feedback loops within the cascade. This permits this cascade to respond to numerous signals in a cell-specific manner (for example with elevated cAMP levels) and so synchronise the response to mitogenic signals with other environmental factors. Also, such a cascade allows an increased number of steps at which diversification or branching in the mitogenic signal can occur (such as seen with the various Ras effectors), which when coupled to the need of many downstream targets for more than one input for functional regulation, introduces cross-checks which could ensure that conditions are ideal before a commitment to a functional response such as mitogenesis is made.

1.5 Research aims

Although there has been an extensive amount of work detailing the cascade from GPCRs to $p42/44^{MAPK}$, as detailed above, there is currently little information on the quantitative aspects of this regulation such as the level of GPCR expression or degree of G-protein stimulation which is required in order to permit this activation, and how this compares with the other effectors of these receptors. Chapter 3 will address these questions with the α_{2A} adrenoceptor expressed in Rat1 fibroblasts to different densities as well as with a mutant form of this receptor which displays a reduced coupling efficiency. Chapter 4

will determine the ability of the δ opioid receptor to activate p42/44^{MAPK} when expressed at a low and high density and will contrast the quantitative relationship between G-protein and p42/44^{MAPK} activation in this system to other receptor/effectors systems. This work will be continued in Chapter 5 by use of opioid agonists with a range of intrinsic activities. In addition, the involvement or influence of various kinases and other effector pathways in the regulation of the MAPK cascade by GPCRs will be investigated in Chapters 3 and 5.

Chapter 2: Materials and Methods

Chapter 2: Materials and Methods

2.1 Materials

Materials were obtained from the following suppliers:

2.1.1 General Reagents

Aldrich Chemical Company, Gillingham, Dorset, U.K.

2,2,4-trimethylpentane.

Amersham International plc., Little Chalfont, Bucks., U.K.

ECL reagents, Biotrak p42/44 MAP kinase enzyme assay system.

Appligene, Chester-le-Street, Co. Durham, U.K.

Water saturated phenol.

Boehringer Mannheim U.K. Ltd., Lewes, East Sussex, U.K.

App(NH)p, creatine phosphokinase, dibutyryl cAMP, hygromycin B, GDP, GTPγS, DNAase free RNAase.

Calbiochem-Novabiochem (U.K.) Ltd., Beeston, Nottingham, U.K.

Pansorbin cells, tyrphostin AG1478.

Costar Scientific Corporation U.K., Gordon Road, Bucks., U.K.

Nitrocellulose.

Fisons Scientific Equipment, Loughborough, U.K.

Ammonium formate, $CaCl_2.6H_2O$, DMSO, EDTA, EGTA, ethylacetate, ethylene glycol, formic acid, glucose, glycine, HEPES, H_2O_2, hydrochloric acid, KCl, KH_2PO_4, K_2HPO_4, $MgCl_2.6H_2O$, NaCl, Na_2CO_3, $NaHCO_3$, NaH_2PO_4.

Gibco BRL Life Technologies Inc, Paisley, U.K.

Agarose, lipofectin, tris, urea, 1 kb DNA ladder.

Koch-Light Lab. Ltd., Colinbrook, Bucks., U.K.

NaK tartrate, $MgSO_4.7H_2O$.

Lipid Products, South Nutfield, Surrey, U.K.

Phosphatidylbutanol.

May & Baker Ltd., Dagenham, U.K.

$CuSO_4$, sodium tetraborate.

Merck Ltd., Poole, Dorset, U.K.

Acrylamide, ammonium persulphate, bacto-agar, bacto-tryptone, bacto-yeast extract, butan-1-ol, chloroform, DTT, ethanol, Folin and Coicalteu's phenol reagent, glacial acetic acid, glycerol, imidazole, isoamyl alcohol, isopropanol, methanol, N,N'-methylene-bisacrylamide, NaOH, $NaHPO_4$, orthophosphoric acid, SDS, sucrose, trichloroacetic acid.

Packard Instrument Company, Meriden, CT, U.S.A.

Ultima-Flo AF scintillant.

Pfizer Central research, U.K.

UK14304.

Promega Ltd., Southampton, U.K.

Restriction enzymes.

Research Biochemicals Inc., Semat Technical (U.K.) Ltd., St. Albans, Herts., U.K.
Buprenorphine, diprenorphine, ICI174864, levorphanol tartrate, morphine, TIPPΨ.

Sigma Chemical Company, Poole, Dorset, U.K.
Alumina, ampicillin, aprotonin, L-arginine HCl, ascorbic acid, ATP, bromophenol blue, BSA, cAMP, charcoal (activated), chelerythrine chloride, cholera toxin, Coomasie blue, DADLE, o-dianisidine, Dowex 1, Dowex 50W, EGF, endothelin-1, ethidium bromide, forskolin, gelatin, genistein, GTP, idazoxan, LiCl, LPA, MBP, MOPS, $MnCl_2$, NaF, naloxone, p-nitrophenol phosphate, NP40, ouabain, PEG8000, pepstatin A, phenylmethylsulphonyl fluoride, phosphocreatine, ponceau S, potassium acetate, prestained molecular weight standards, $RbCl_2$, sodium azide, sodium deoxycholate, sodium orthovanadate, TEMED, thimerasol, N-tris(hydroxymethyl)methylglycine-NaOH, Triton-x100, trypsin, Tween 20, wortmannin.

Speywood Ltd., Berkshire, U.K.
Pertussis toxin.

Upstate Biotechnology Inc., Lake Placid, New York, U.S.A.
EGF (human, recombinant).

2.1.2 Radiochemicals

Amersham International plc., Little Chalfont, Bucks., U.K.
[γ-^{32}P]ATP (s.a. 3000 Ci/mmol), [α-^{32}P]ATP (s.a. 400 Ci/mmol), [8-^{3}H]cAMP (s.a. 24 Ci/mmol), [15,16(n)-^{3}H]diprenorphine (s.a. 39 Ci/mmol), [ethyl-^{3}H]RS-79948-197 (s.a. 90 Ci/mmol), [γ-^{32}P]GTP (s.a. > 10 Ci/mmol), myo-[2-^{3}H]inositol (s.a. 16.5 Ci/mmol), [9,10(n)-^{3}H]palmitic acid (s.a. 51 Ci/mmol).

Du Pont NEN (U.K.) Ltd., Stevenage, Herts., U.K.

[adenylate-^{32}P]NAD (s.a. 800 Ci/mmol), [methyl-^{3}H]yohimbine (s.a. 81 Ci/mmol), [^{35}S]GTPγS (s.a. 1175 Ci/mmol).

2.1.3 Tissue culture plasticware

Costar Scientific Corporation U.K., Gordon Road, Bucks., U.K.

25 cm^2 and 75 cm^2 flasks, 10 cm dishes, 6 and 24 well plates.

Bibby Sterilin Ltd., Stone, Staffs., U.K.

Sterile disposable plastic pipettes.

Nunc, Nalge Nunc Inc., Denmark.

Cryovials.

2.1.4 Cell culture Media

Gibco BRL Life Technologies Inc, Paisley, U.K.

10x DMEM, 200 mM glutamine , inositol free DMEM, 7.5% (w/v) $NaHCO_3$, newborn calf serum, 10000 units/ml penicillin / 10 mg/ml streptomycin.

2.1.5 Standard Buffers:

Phosphate Buffered Saline (PBS)

2.7 mM	KCl
1.5 mM	KH_2PO_4
140 mM	NaCl
8 mM	Na_2HPO_4
pH	7.4

This was made as a 10x solution and stored until required. When required, a 1x solution was prepared by dilution giving the above composition and pH was set to 7.4 with concentrated HCl.

Hanks Modified Medium

1.3 mM	$CaCl_2.6H_20$
5.4 mM	KCl
490 μM	$MgCl_2.6H_20$
410 μM	$MgSO_4.7H_20$
137 mM	NaCl
4.2 mM	$NaHCO_3$
270 μM	NaH_2PO_4
pH	7.2-7.4 at 4°C

This was made as a 2x stock and stored at 4°C until required.

Laemmli Buffer

5 M	urea
0.4 M	DTT
0.17 M	SDS
50 mM	Tris/HCl (pH 8)
0.01% (w/v)	bromophenol blue

Stored aliquoted at -20°C until required.

2.1.6 Antisera

Anti-$p44^{MAPK}$ used for immunoblotting was a gift from Dr. Neil Anderson, Dept. of Surgery and School of Biological Sciences, University of Manchester, Manchester, U.K.

Anti-$p42^{MAPK}$ was a gift from Dr. Ailsa Campbell, Division of Biochemistry and Molecular Biology, Institute of Biomedical and Life Sciences, University of Glasgow, Glasgow, U.K.

Anti-$p44^{MAPK}$ used for IP kinase assay was from Dr. Simon Cook, Onyx Pharmaceuticals, Richmond, California, U.S.A.

HRP-linked donkey anti-rabbit IgG and HRP-linked sheep anti-mouse IgG were obtained from the Scottish Antibody Production Unit, Carluke, Lanarkshire, U.K.

Anti phosphotyrosine antiserum was obtained from Upstate Biotechnology Inc., Lake Placid, New York, USA.

2.1.7 cDNAs

pCMV4 expressing haemmaglutinnin tagged wild type and Asn^{79} porcine α_{2A} adrenoceptor was a gift from Dr. Lee Limbird, Dept. of Pharmacology, Vanderbilt University Medical Centre, Nashville, Tennessee, U.S.A.

pCMV-ms12 expressing the mouse δ opioid receptor was a kind gift from Dr. Graeme Bell, Howard Hughes Medical Institute, University of Chicago, Chicago, Illinois, U.S.A.

2.2 Methods

2.2.1 Cell culture

2.2.1.1 Cell growth

Growth Medium for Rat1 fibroblasts: 5% DMEM

10% (v/v)	Dulbecco's Modified Eagle's Medium
0.375% (w/v)	sodium bicarbonate
2 mM	glutamine
100 units/ml	Penicillin
100 μg/ml	Streptomycin
5% (v/v)	newborn donor calf serum

Medium for serum starvation was as above without, or with a lower concentration (0.05% (v/v)) of, newborn calf serum.

Rat1 fibroblasts were grown to confluency in 5% DMEM in 75 cm^2 tissue culture flasks at 37°C and in a humidified atmosphere of 95% air / 5% CO_2. At confluency, the medium was removed and replaced with 2 ml of a sterile solution of PBS containing 0.1% (w/v) trypsin, 0.025% (w/v) EDTA and 10 mM glucose. This was incubated at 37°C until the cells were removed from the surface of the flask. 4.5 vols of 5% DMEM were added in order to stop the action of the trypsin and the cell suspension was

transferred to a 50 ml tube and centrifuged at 800 x g in a MSE centaur centrifuge for 5 min. The cell pellet was resuspended and transferred to other tissue culture flasks or plates as required.

2.2.1.2 Cell line maintenance

After trypsinisation and centrifugation, as above, the cell pellet was resuspended in newborn calf serum containing 10% (v/v) DMSO and transferred to cryovials. These were placed at -80°C for 24 hours and stored in liquid nitrogen.

2.2.1.3 Harvesting cells

Just prior to confluency, cells were scraped off the surface of the flasks into the growth medium using a disposable cell scraper (Costar). The suspension was pipetted into 50 ml tubes and centrifuged in a Beckman TJ-6 Benchtop centrifuge at 800 x g and 4°C for 5 min. The cell pellet was washed twice in ice-cold PBS and stored at -80°C.

2.2.1.4 Crude membrane preparation

Membranes were prepared from the frozen cell pellet prepared as above. The cells were resuspended in 3 ml of ice-cold TE buffer (10 mM Tris-HCl (pH 7.5), and 0.1 mM EDTA) and homogenised with at least 30 strokes of a teflon on glass homogeniser. The suspension was then centrifuged at 500 x g in a Ti50 rotor in a Beckman L5-50B ultracentrifuge for 10 min. The pellet contained unbroken cells and the nuclear fraction, and the supernatant was centrifuged again at 48,000 x g for 10 min. This pellet was washed in 5 ml of ice-cold TE buffer and then centrifuged again at 48,000 x g for 10 min. The pellet containing the crude membrane fraction was resuspended in TE buffer, passed through a fine gauge needle 10 times, then aliquoted and stored at -80°C.

2.2.2 Protein determination

Protein determination was performed using the method of Lowry *et al.* (1951). Reagent solutions were prepared as follows:

1% (w/v) $CuSO_4$

2% (w/v) NaK tartrate

2% (w/v) Na_2CO_3 in 0.1 mM NaOH

These were mixed in the ratio of 1 : 1 : 100 respectively, 20 min prior to assaying. 1 ml of the above reagent mix, and then 10 min later 100 μl of 50% (v/v) Folin and Ciocalteu's phenol reagent, were added to the protein sample (made up to a constant volume with TE buffer). After mixing and incubating at room temperature for at least 20 min, absorbance at a wavelength of 750 nm was determined with a spectrophotometer (Shimadzu). By comparison to a standard curve prepared with various volumes of a standard concentration of BSA in TE buffer, the concentration of protein in each sample was determined.

2.2.3 Radioligand binding assay

Levels of expression of receptors were determined using radioligand binding assays. Borosilicate glass tubes were set up on ice containing:

50 μl of membrane suspension diluted from a frozen aliquot (prepared as in 2.2.1.4) with ice-cold TE buffer to give appropriate protein concentration,

25 μl of appropriate concentration of tritiated ligand,

175 μl of TSM buffer (10 mM Tris/HCl (pH 7.4), 50 mM sucrose and 20 mM $MgCl_2$).

Some tubes also contained 25 μl of competing non-radioactive ligand (compensated by a reduction in volume of TSM buffer added) to define non-specific binding. The reaction was incubated at 30°C for 45 min and terminated by filtration through Whatman GF/C filters using a Brandel cell harvester. After three (approximately 5 ml) washes with ice-cold TSM buffer, the filters were soaked overnight in 5 ml Ultima-Flo AF scintillant prior to liquid scintillation counting.

2.2.4 High affinity GTPase assay

These assays were performed essentially as described in Koski and Klee (1981). Each incubation contained the following:

20 μl of membrane suspension prepared as in 2.2.1.4 and diluted to the required concentration with TE buffer,

50 μl of [^{32}P]GTP mix which contained: 20 mM phosphocreatine, 100 units/ml creatine phosphokinase, 2 mM ATP (pH 7.5), 200 μM App(NH)p, 2 mM Ouabain, 200 mM NaCl, 10 mM $MgCl_2$, 4 mM DTT, 80 mM Tris/HCl (pH 7.5), 200 μM EDTA (pH 7.5), 1 μM non-radioactive GTP (pH 7.5), and approximately 50,000 cpm of [γ-^{32}P]GTP (specific activity 30 Ci/mmol),

10 μl of various ligands,

H_20 to make volume up to 100 μl.

Membranes, water and ligands were mixed on ice and the assay was started by the addition of the [^{32}P]GTP mix and transfer to a 30°C water bath. Incubation was allowed for 30 min, after which the reaction was terminated by the transfer to an ice slurry and addition of 900 μl of ice-cold 5% (w/v) activated charcoal in 10 mM H_3PO_4. The charcoal was pelleted by centrifugation at 12,000 x g for 20 min in a benchtop microfuge. 500 μl of the supernatant was transferred to insert scintillation vials and counted by Cherenkov counting. 50 μl aliquots of the [^{32}P]GTP mix were also counted directly and this allowed calculation of data as pmol of GTP hydrolysed per min per mg of membrane protein.

2.2.5 GTPγS binding assay

These assays were performed as in Wieland and Jakobs (1994). Borosilicate glass tubes were set up on ice containing the following:

25 μl of membranes (diluted from a stock with ice-cold TE to give the required concentration),

50 μl of [^{35}S]GTPγS reaction mix which contained: 40 mM HEPES (pH 7.4), 6 mM $MgCl_2$, 200 mM NaCl, 20 μM GDP, 0.2 mM ascorbic acid (all of these can be

prepared as a 10 x stock and aliquotted and frozen at -20°C), 50 nCi [^{35}S]GTPγS (stored at -80°C diluted in 10 mM N-tris(hydroxymethyl)methylglycine-NaOH (pH 7.6), 10 mM DTT),

25 μl remaining was made up with water, agonists and/or 10 μl of 100 μM GTPγS (to determine non-specific binding).

The membranes were always added last and then the contents of the tubes were mixed well. Incubations were performed at 4°C for 60 min and were terminated by the addition of 3 ml of ice-cold filter wash (20 mM HEPES (pH 7.4) and 3 mM $MgCl_2$) to each tube and immediate filtration through a Whatman GF/C filter using a Brandel cell harvester. Each filter was then washed with a further 2 x 5 ml of the filter wash buffer and then soaked in 10 ml Ultima-Flo AF scintillant overnight before liquid scintillation counting.

2.2.6 Adenylyl cyclase assay

These were performed as in Johnson and Salomon (1991).

This assay measured the production of [^{32}P]cAMP from [^{32}P]ATP. Separation of [^{32}P]cAMP from the [^{32}P]ATP was achieved using the method of Salomon *et al.* (1974) which made use of Dowex and Alumina columns.

2.2.6.1 Sample preparation

Each incubation tube was prepared on ice to contain the following:

20 μl of membrane suspension (diluted from a frozen stock aliquot with TE buffer to give appropriate concentration),

50 μl of [^{32}P]ATP reaction mix containing: 2 μM GTP (pH 7.5), 2 mM cAMP, 400 μM ATP (pH 7.5), 200 mM Tris/HCl (pH 7.5), 100 mM NaCl, 10 mM $MgCl_2$, 40 mM phosphocreatine, 100 units/ml creatine phosphokinase and 10^6 cpm [α-^{32}P]ATP,

30 μl remaining was made up with water and 10 μl additions of ligands as required.

The reaction was initiated by transfer of the tubes to a 30°C water bath, and incubation was allowed for 15 min. The reaction was terminated by removal of tubes to an ice

slurry and the addition of 100 μl of 2% (w/v) SDS, 45 mM ATP, 1.3 mM cAMP (stopper solution). 50 μl (10,000 cpm) of a solution of [^{3}H]cAMP was added and the samples were boiled for 10 min. 750 μl of H_2O was added and the [^{32}P]cAMP content in the sample was determined using the chromatography columns prepared as below.

2.2.6.2 Preparation of the columns

Dowex 50W (50x4-400) (1 g per column) was washed twice with twice its volume of water to remove fines. It was then washed with twice its volume of 1 M NaOH and then 1 M HCl. After further washes with water, a 1 : 1 slurry with water was produced and 2 ml was added to each glass wool stoppered column. A cold reaction mix (50 μl of reaction mix without the [^{32}P]ATP, 100 μl of stopper solution and made up to 1 ml with water) was added to each column and allowed to drip to waste. These columns were then stored until required at room temperature. On day of use, the columns were washed with 2 x 2 ml of 1 M NaOH, followed by 2 x 2 ml of 1 M HCl and 6 x 2 ml of H_2O.

The alumina columns were prepared by adding a 50% (w/v) alumina solution in 0.1 M imadazole (pH 7.3) to glass wool stoppered columns (2 ml per column). As with the Dowex columns, a cold reaction mix was dripped through each column prior to storage at room temperature. On the day of use, the columns were washed with 4 x 2 ml of 0.1 M imadazole (pH 7.3).

2.2.6.3 Nucleotide elution profile of columns

This was performed to determine the elution volume of the nucleotides for both the Dowex and alumina columns.

A solution containing 50 μl of [^{32}P]ATP reaction mix as used in assay with 50 μl (10,000 cpm) of [^{3}H]cAMP, 100 μl of stopper solution and the volume made up to 1 ml with water was applied to a Dowex column. The eluted solution was collected in vials containing 10 ml of Ultima-Flo AF scintillant. Successive washes of the column with 0.5 ml of water were collected in further vials containing scintillant and counted by liquid

scintillation on a dual label programme. The elution profiles of both nucleotides were then produced and the efficiency of recovery was determined by reference to a direct count of the radioactive mixture. An elution profile of the alumina columns could be produced in a similar fashion, using a reaction mix containing only the [^{3}H]cAMP and 0.1 M imidazole (pH 7.3) instead of water as the elution buffer.

2.2.6.4 Determining cAMP production

Once the volume of the samples had been made up to 1 ml by the addition of H_2O, as described above, the samples were loaded onto prepared Dowex columns and the ATP was eluted with 0.5 ml H_2O. 4 x 2 ml washes of H_2O were then applied and the eluate was allowed to drip onto the prepared alumina columns. The cAMP fraction was then eluted from the alumina columns with 4 x 1.5 ml of 0.1 M imidazole (pH 7.3) into 12 ml of Ultima-Flo AF scintillant. The samples were counted on a dual label liquid scintillation counting programme and so the amount of cAMP produced was calculated taking into account the efficiency of recovery from each column determined from the recovery of the internal [^{3}H]cAMP standard. Results were thus calculated in pmol of cAMP produced per min per mg of membrane protein.

2.2.7 SDS-polyacrylamide gel electrophoresis (SDS-PAGE)

2.2.7.1 10% Acrylamide resolving gels

10% (w/v) acrylamide/0.25% (w/v) N,N'-methylene-bisacrylamide resolving gels were prepared as follows:

8.2 ml	H_2O
1.6 ml	50% (v/v) glycerol
8 ml	30% (w/v) acrylamide, 0.8% (w/v) N,N'-methylene-bisacrylamide
6 ml	5 M Tris/HCl (pH 8.8), 0.4 % (w/v) SDS
90 μl	10% (w/v) ammonium persulphate
8 μl	TEMED

This was mixed and immediately poured into a Hoefer Gel Caster with two 180 x 160 mm glass plates and 1.5 mm spacers. The gel was layered with 0.1 % (w/v) SDS and allowed to set at room temperature for 90 min.

14% acrylamide resolving gels were prepared as above with the following alterations: 5 ml of H_20 and 11.2 ml of 30% (w/v) acrylamide, 0.8% (w/v) N,N'-methylene-bisacrylamide.

2.2.7.2 Stacking gels

After the resolving gel had set, the SDS was washed off and the stacking gel was prepared:

9.75 ml	H_20
1.5 ml	30% (w/v) acrylamide, 0.8% (w/v) N,N'-methylene-bisacrylamide
3.75 ml	0.5 M Tris/HCl (pH 6.8), 0.4 % (w/v) SDS
150 μl	10% (w/v) ammonium persulphate
8 μl	TEMED

This was mixed and layered on top of the resolving gel around a 15 well Teflon comb and left to set for another 90 min.

The buffer used in the upper and lower reservoir of the gel electrophoresis tank was 25 mM Tris base, 0.192 M glycine and 0.1% (w/v) SDS. Once set, the gels were assembled into a Hoefer vertical gel electrophoresis kit, loaded using a Hamilton syringe and electrophoresis was performed at 60 V overnight.

2.2.7.3 Sample preparation

Samples were sometimes prepared for gel electrophoresis by sodium deoxycholate/trichloroacetic acid precipitation:

To the desired amount of protein, the following was added in the correct order:

750 μl	H_2O
10 μl	2% (w/v) sodium deoxycholate
250 μl	24% (w/v) trichloroacetic acid

This was centrifuged in a microfuge for 20 min at 12,000 x g. The supernatant was removed and the pellet dissolved in 15 μl of 2 M Tris base. 15 μl of Laemmli buffer was then added and the sample loaded onto the gel.

2.2.7.4 6M Urea containing polyacrylamide gels

In order to provide adequate separation of proteins as part of the MAPK electrophoretic mobility shift assay (see 2.2.9.1), an SDS-PAGE system which contained 6 M urea and had a low level of N,N'-methylene-bisacrylamide was used (Kim and Milligan, 1994). This was made by preparing three individual solutions on the day of use:

Solution 1:	6 M	urea
Solution 2:	6 M	urea
	1.5 M	Tris/HCl (pH 8.8)
	0.4% (w/v)	SDS
Solution 3:	6 M	urea
	30% (w/v)	acrylamide
	0.15% (w/v)	N,N'-methylene-bisacrylamide

The resolving gel was then prepared from these solutions as follows:

12.2 ml	solution 1
9.6 ml	solution 2
16.2 ml	solution 3
30 μl	10% (w/v) ammonium persulphate
6 μl	TEMED

This was mixed and immediately poured into a 20 cm Bio-Rad Protean II gel casting apparatus with 1.5 mm spacers. The gel was layered with butan-1-ol and allowed to set for 2 hours at room temperature.

The butanol was then thoroughly washed off and stacking gel was prepared as before. Electrophoresis was performed at 120 V for 18-20 hours.

2.2.8 Western blotting

Subsequent to electrophoresis overnight with any of the above gel types, proteins were transferred to a nitrocellulose sheet in an LKM Transphor apparatus filled with 25 mM Tris base, 0.192 M glycine and 20% (v/v) methanol at 1.5 mA for 2 hours. The sheet was then temporarily stained with 0.1% (w/v) ponceau S, 3% (w/v) trichloroacetic acid in order to check transfer efficiency and protein loadings. After washing in transfer buffer and distilled water in order to remove the stain, the nitrocellulose sheet was treated in different ways depending on the antibody used.

Immunoblotting against $p44^{MAPK}$ was with a polyclonal antiserum and the nitrocellulose sheet was blocked with 5% (w/v) gelatin in PBS for 2 hours at 37°C. The gelatin was washed off with distilled water and the sheet incubated in a 1 : 500 dilution of anti-$p44^{MAPK}$ antiserum in 1% (w/v) gelatin, 0.2% (v/v) NP40 in PBS overnight at 37°C. The next day, the primary antiserum was washed off with three changes of distilled water and at least five changes of 0.2% (v/v) NP-40 in PBS (over a time period of 30 min). The secondary antibody (horse-radish peroxidase conjugated goat anti-rabbit IgG) was then added (in 1% (w/v) gelatin, 0.2% (v/v) NP40 in PBS) and incubation at 37°C was allowed for at least 2 hours. The secondary antibody was then removed and the same washes were performed as before, with the addition of two washes of PBS at the end. The blot was then developed in 50 ml of 0.02% (w/v) o-dianisidine in PBS after the addition of 5 μl of H_2O_2. Development was terminated by immersion in 1% (w/v) sodium azide.

When the monoclonal anti-$p42^{MAPK}$ or anti-phosphotyrosine antisera were used, the nitrocellulose sheet was blocked in 10% (w/v) milk protein, 0.1% (v/v) Tween 20 in PBS at 25°C while shaking. The primary and secondary antisera were prepared in 0.5%

(w/v) milk protein, 0.1% (v/v) Tween 20 in PBS. Horse-radish peroxidase conjugated anti-mouse IgG was used as the secondary antiserum. Washes were as above but with 0.1% (v/v) Tween 20 in PBS and blots were developed using Amersham's ECL kit according to the manufacturer's procedure.

Anti-$p44^{MAPK}$ primary antibodies could be used up to fifteen times, other primary and the secondary antibodies were routinely used up to three times. All antibodies were stored at 4°C using thimerasol as an anti-bacterial agent.

2.2.8.1 Quantitation of immunoblots

Immunoblots were quantified by densitometric scanning using a Bio-Rad imaging densitometer.

2.2.9 MAPK assays

The activation of the $p42/p44^{MAPK}$ pathway was determined by three different methods. The electrophoretic mobility shift assay was used to demonstrate the phosphorylation of $p42^{MAPK}$ or $p44^{MAPK}$ as determined by a retardation in mobility in SDS-PAGE. The activity of $p42/44^{MAPK}$ was determined by the immunoprecipitation (IP) kinase assay or by the Biotrak p42/44 MAP kinase enzyme assay system (Amersham International). The first assay measures the ability of immunoprecipitated $p44^{MAPK}$ to catalyse the phosphorylation of an exogenously added substrate myelin basic protein (MBP), and the kit from Amersham uses a peptide which is highly selective for $p42/44^{MAPK}$ as an exogenous substrate in a kinase reaction.

2.2.9.1 Electrophoretic mobility shift assay

This assay was performed as in Leevers and Marshall (1992). Cells were grown in 5% DMEM to confluency in 10 cm tissue culture dishes at 37°C and 5% CO_2 after which they were serum starved in low or zero serum DMEM for 24 to 48 hours. The cells were then incubated with the appropriate ligands in serum free DMEM for various lengths of

time at 37°C and 5% CO_2. The incubation was terminated when the cells were transferred to 4°C, the medium was removed and the cells washed in ice-cold PBS. 450 μl of ice-cold lysis buffer was then added to each dish. This lysis buffer contained 25 mM Tris/HCl (pH 7.5), 25 mM NaCl, 10% (v/v) ethylene glycol, (stored as a stock solution at -20°C) and added immediately prior to use 40 mM p-nitrophenol phosphate, 10 μM DTT, 0.2% (v/v) NP40, 1 μg/ml aprotonin, 1 mM sodium orthovanadate, 3.5 μg/ml pepstatin A, and 200 μM phenylmethylsulphonyl fluoride. Cells were scraped into tubes and passed through a fine gauge needle approximately ten times in order to complete cell lysis. The cell suspension was then centrifuged at 4°C in a microfuge at 12,000 x g for 5 min. 450 μl of the supernatant was then transferred to 115 μl Laemmli buffer in fresh tubes and boiled at 100°C for 5 min. These samples were then analysed directly by SDS-PAGE using 6 M urea containing polyacrylamide gels (as described in 2.2.7.4). Western blotting of these gels and immunoblotting with anti-$p42^{MAPK}$ or anti-$p44^{MAPK}$ antisera permitted the gel shift, and therefore the phosphorylation, of these MAPKs to be determined. Densitometric scanning allowed quantitation of these blots and calculation of the results as the percentage of the total detectable $p42^{MAPK}$ or $p44^{MAPK}$ which was present in the lower mobility form.

2.2.9.2 IP kinase assay

Cells were grown to confluence in 5% DMEM in 6 well plates and serum starved for 24 to 48 hours. The cells were treated with the appropriate ligands in serum free DMEM for various times. The incubation was terminated as the medium was removed and the cells washed in ice-cold PBS. 400 μl of lysis buffer was then added. This lysis buffer contained: 20 mM Tris/HCl (pH 8), 137 mM NaCl, 1 mM EGTA, 1% (v/v) Triton x-100, 10% (v/v) glycerol, 1.5 mM $MgCl_2$, stored at 4°C as a 2x stock solution, and added just prior to use 0.1 mM sodium orthovanadate, 10 μg/ml aprotonin, 25 mM NaF and 0.2 mM phenylmethylsulphonyl fluoride. Cells were scraped off the plate and transferred to microfuge tubes. These were mixed for 20 min at 4°C and centrifuged at

4°C in a microfuge at 12,000 x g for 5 min. The cell lysate was then assayed for protein concentration.

The volume of cell lysate which contained 300 μg of protein was mixed with 4 μl of anti-$p44^{MAPK}$ antiserum for 2 hours at 4°C. 50 μl of pansorbin cells (washed and resuspended in lysis buffer) were added for the last 30 min. After this time, the pansorbin cells were pelleted by a pulse centrifugation and the supernatant removed by aspiration. The pellet was washed in 3 x 0.5 ml of lysis buffer and once with 0.5 ml of kinase buffer (30 mM Tris/HCl (pH 8), 1 mM $MnCl_2$, 10 mM $MgCl_2$). The kinase reaction was initiated by resuspending the washed pansorbin pellet in 30 μl of kinase buffer containing 1 μM ATP (pH 8), 0.23 mg/ml MBP and 2 μCi of [γ-^{32}P]ATP. This reaction was incubated at 30°C for 30 min and terminated when 7.5 μl Laemmli buffer was added. These samples were boiled for 5 min at 100°C and centrifuged at 12,000 x g for 2 min. The supernatant was then analysed by SDS-PAGE using a 14% acrylamide gel in a Bio-Rad Mini-Protean II electrophoresis system run at 200 V until the dye front was 1 cm from the end of the gel. The stacker and bottom part of the gel (containing the dye front and ATP) were discarded, and the gel was stained in 0.1% (w/v) Coomasie blue in 40% (v/v) methanol, 10% (v/v) glacial acetic acid for 30 min and destained for a further 30 min in 40% (v/v) methanol, 10% (v/v) glacial acetic acid. The gel was washed in water and then dried under vacuum in a Bio-Rad gel dryer. These were exposed to a phosphor storage plate for about 30 min and analysed using a FUJIX BAS1000 image analyser and the radioactivity associated with the MBP band was quantified.

2.2.9.3 Biotrak p42/44 MAP kinase activity assay

Cells were grown to confluence in 5% DMEM in 60 mm plates and serum starved for 24 to 48 hours. The cells were treated with appropriate ligands in serum free DMEM for various times and the incubation was terminated and cell lysates were prepared as for the IP kinase assay, using 150 μl per plate of the same lysis buffer. After protein determination, the cell lysates were assayed using the Biotrak p42/44 MAP kinase

enzyme assay system (Amersham International) according to the manufacturers instructions in the presence of 0.2 μCi/μl [γ-^{32}P]ATP. Samples were counted by liquid scintillation and results presented as pmol phosphate transferred per min per mg protein.

2.2.10 Transphosphatidylation assay

This was performed as in Cook and Wakelam (1991). This assay was used to monitor the activity of PLD by measuring the transphosphatidylation activity of [^{3}H]palmitate-labelled cells in the presence of butan-1-ol. This produced [^{3}H]phosphatidylbutanol which was not metabolised further and could be isolated by phase separation and thin layer chromatography. Cells were grown to 70% confluency in 5% DMEM at 37°C and 5% CO_2 in 24 well plates. The medium was replaced with fresh 5% DMEM containing 4 μCi/ml [^{3}H]palmitate and cells were incubated for another 24 hours. The cells were then incubated at 37°C for 20 min in 0.5 ml per well of HBG (Hanks modified medium containing 2% (w/v) BSA and 10 mM glucose). This was removed and replaced by 0.5 ml HBG containing 0.3% (v/v) butan-1-ol (HBGbutanol) for a further 5 min incubation. This was removed and the reaction was initiated by adding 0.2 ml HBGbutanol with or without the required ligands. After the required incubation time, the medium was removed and replaced by ice-cold methanol (0.5 ml per well) to terminate the reaction. The cell debris was scraped into glass vials and each well was washed with a further 0.2 ml methanol. 0.7 ml chloroform was added and the vials were vortexed and allowed to stand at room temperature for 15 min. 585 μl of H_2O was added and the solutions were again mixed. These vials were then stored overnight at -20°C.

Centrifugation at 1,500 x g for 5 min was performed, and 450 μl of the lower phase (which contained the phospholipids) was transferred to fresh vials and dried down under vacuum in a Jouan centrifugal evaporator for 60 min. This was resuspended in 2 x 25 μl chloroform : methanol mix (19 : 1, v/v) and loaded onto Whatman silica gel thin layer chromatography plates which had been pre-run and activated at 120°C. In addition, 7.5 μl of phosphatidylbutanol (Lipid Products) was loaded on top of each sample. Plates

were developed in the organic phase of a 5 : 11 : 2 : 10 mix of 2,2,4 trimethylpentane, ethylacetate, acetic acid and water under non-equilibrated conditions.
Phosphatidylbutanol displayed an Rf value of approximately 0.4, and was detected by visualising the exogenously added phosphatidylbutanol by staining with iodine vapour. The strip of silica containing this band was then scraped off the plate and subjected to liquid scintillation counting. Thus the radioactivity associated with this band, and hence the production of [^{3}H]-labelled phosphatidylbutanol, was determined.

2.2.11 Total inositol phosphate assay

This was performed as described in MacNulty *et al.* (1992).

2.2.11.1 Inositol free medium

A stock of inositol free medium was prepared, filter sterilised and stored at 4°C:

6.685 g inositol free DMEM

1.85 g sodium bicarbonate

Made up to 500 ml with H_2O.

When ready to label, the cells were incubated in this inositol free medium containing 2 mM glutamine, 2% (v/v) dialysed newborn calf serum, and 1 μCi/ml [^{3}H]inositol.

Newborn calf serum was dialysed prior to use in order to remove endogenous inositol and so improve [^{3}H]inositol labelling of the cells:
Dialysis tubing was boiled twice in fresh 10 mM EDTA for 10 min and was then stored until required in 20% (v/v) ethanol at 4°C.
50 ml newborn calf serum was put into dialysis tubing and the ends were sealed. This was placed into 2 l of Earles Salts (120 mM NaCl, 1.3 mM KCl, 810 μM $MgSO_4.7H_2O$, 900 μM NaH_2PO_4, and 5.6 mM Glucose) and left to stir gently at 4°C. The dialysis solution was changed every 12 hours for 2 days and then the serum was aliquoted and stored at -20°C.

2.2.11.2 Preparation of Dowex formate

Dowex chloride (Dowex 1x8-200) was converted to Dowex formate prior to use in this assay. This was carried out in stages due to the strength of the electrostatic interaction between the Dowex and chloride ions. 100 g Dowex 1 was washed 3 x 1 l of water in order to remove fines. This was then transferred to a scintered funnel and washed with 2 l of 2 M NaOH and then with 6 l of H_2O (to remove NaCl and excess NaOH). The Dowex was then washed with 500 ml of 1 M formic acid, followed by approximately 20 l of H_2O until the pH was constant at 5 to 5.5. This was then stored at room temperature until required in an approximate 1 : 1 ratio with H_2O.

2.2.11.3 Phospholipase C assay

70% confluent cells in 24 well plates were labelled with [^{3}H]inositol by a 24 hour incubation at 37°C and 5% CO_2 in inositol free medium containing [^{3}H]inositol as detailed above. The cells were then washed with 0.5 ml per well of HBG, and incubated at 37°C for 15 min in HBG containing 10 mM LiCl. Treatment with various ligands was then performed in 150 μl of HBG containing LiCl for 10 min and terminated with the addition of 0.5 ml of ice-cold methanol. The cells were then scraped into insert vials (Sterlin) and each well was washed with a further 200 μl of ice-cold methanol. 310 μl of chloroform was added to each vial to allow extraction of the lipids for 30 min at room temperature. (Sometimes the samples were stored at 4°C overnight at this stage). 500 μl of H_2O and a further 310 μl of chloroform was then added. The vials were then spun at 1,500 x g for 5 min to split the phases.

200 μl of the lower phase was removed to a fresh vial and dried down under vacuum in a centrifugal evaporator. 4 ml of Ultima-Flo AF scintillant was added and the vials were analysed by liquid scintillation counting. 750 μl of the upper phase was removed to fresh vials and analysed by batch chromatography: 500 μl of the Dowex formate prepared as above was added to each vial. This was allowed to settle and the supernatant was removed by aspiration. The Dowex was then washed with 2 x 3 ml of H_2O, followed by

a 3 ml wash with 5 mM sodium tetraborate, 60 mM ammonium formate. After another 3 ml wash with H_20, 1 ml of 1 M ammonium formate, 0.1 M formic acid was added, the Dowex was again allowed to settle and 750 μl of the supernatant was removed and subjected to liquid scintillation counting. Knowledge of the radioactivity associated with the lower phase permitted correction (for differences in the number and labelling of cells) of the values obtained by batch chromatography for the total inositol phosphates released from the cells.

2.2.12 Agonist-driven cholera toxin-catalysed [^{32}P]ADP ribosylation

This assay was performed as in Milligan *et al.* (1991).

Each incubation was prepared on ice to contain the following:

20 μl of membrane suspension (diluted with TE buffer from a frozen stock aliquot to give appropriate concentration),

5 μl of cholera toxin (activated as a 1 mg/ml solution with equal volume of 100 mM DTT for at least 60 min at room temperature) or 50 mM DTT as negative control,

5 μl of ligand, or water as control,

20 μl of [^{32}P]NAD reaction mix containing: 50 mM thymidine, 625 mM NaH_2PO_4 (pH 7.0), 625 mM Na_2HPO_4 (pH 7.0), 1.3 mM ATP (pH 7.5), 50 mM arginine HCl, and 0.1 μCi/μl of [^{32}P]NAD.

The reaction was incubated at 37°C for 2 hours and terminated by cooling on ice. After sodium deoxycholate/trichloroacetic acid precipitation (Section 2.2.7.3), the samples were analysed by SDS-PAGE with 10% (w/v) acrylamide / 0.25% (w/v) N,N'-methylene-bisacrylamide resolving gels (Section 2.2.7.1). The gels were dried down under vacuum, exposed to a phosphor storage plate and analysed using a FUJIX BAS1000 image analyser.

2.2.13 Data Analysis

Analysis of data curves was performed using the Kaleidagraph curve fitting package driven by an Apple Macintosh computer. Statistical significance of data was measured by Student *t*-tests.

2.2.14 Molecular Biology

The methods below were derived from Sambrook *et al.* (1989).

2.2.14.1 Solutions for molecular biology

LB medium

To make 1 l

10 g	bacto-tryptone
5 g	bacto-yeast extract
10 g	NaCl

These were dissolved in 950 ml of H_2O, set to pH 7.0 with 5 M NaOH, made up to 1 l and sterilised by autoclaving at 126°C for 11 min.

Terrific Broth

To make 1 l

12 g	bacto-tryptone
24 g	bacto-yeast extract
4 ml	glycerol

These were dissolved in 900 ml of H_2O and sterilised at 126°C for 11 min. This was allowed to cool to at least 60°C and 100 ml of 170 mM KH_2PO_4 and 720 mM K_2HPO_4 (previously sterilised) was then added.

SOC medium

To make 1 l

20 g	bacto-tryptone
5 g	bacto-yeast extract
0.5 g	NaCl
10 ml	250 mM KCl

These were dissolved in 950 ml of H_2O, the pH was set to 7.0 with 5 M NaOH, the volume was made up to 1 l, and the solution was autoclaved. Just prior to use, 5 ml of a sterile solution of 2 M NaCl and 20 ml of 1 M glucose (filter sterilised) was added.

Agar plates

1.5% (w/v) bacto-agar in LB medium was autoclaved and poured into 10 cm petri dishes while still warm. Ampicillin was added to some plates prior to pouring to give final concentration of 60 μg/ml.

TAE buffer

40 mM	Tris-acetate
1 mM	EDTA

This was prepared as a 50x stock solution by adding 242 g of Tris base, 57.1 ml of glacial acetic acid, and 100 ml of EDTA (pH 8) to H_20 to give a final volume of 1 l. On day of use, this was diluted with H_20 to give 1x stock.

2.2.14.2 Alkaline lysis and purification of plasmid DNA from transformed *E. coli*

2.2.14.2.1 Harvesting and lysis of bacteria

Minipreparations of plasmid DNA were obtained by the alkaline lysis method.

Solution I:	50 mM	glucose
	25 mM	tris/HCl (pH 8)
	10 mM	EDTA (pH 8)

This was autoclaved at 126°C for 11 min and stored at 4°C.

Solution II:	0.2 M	NaOH
	1% (w/v)	SDS

This was made fresh on the day of use.

Solution III:	3 M	potassium acetate
	5 M	acetic acid

This was autoclaved at 126°C for 11 min and stored at room temperature.

Bacterial cultures of transformed *E. coli* were grown overnight at 37°C with vigorous shaking in LB medium or terrific broth. Various volumes (3 to 6 ml) of these cultures were centrifuged in a microfuge at 12,000 x g for 30 seconds at 4°C. The supernatant was removed by aspiration and the pellet was resuspended in 200 μl of ice-cold solution I by vigorous vortexing. 400 μl of freshly prepared solution II was added and the tubes were mixed by inversion. After a 5 min incubation on ice, 300 μl of ice-cold solution III was added. After a gentle vortex and incubation on ice for another 5 min, the tubes were centrifuged at 12,000 x g for 10 min and the supernatant was transferred to a fresh tube.

2.2.14.2.2 RNAase treatment

The supernatant was then incubated with 0.5 mg/ml (DNAase-free) RNAase at 37°C for 20 min. (DNAase-free) RNAase was prepared as a 10 mg/ml stock in 10 mM Tris/HCl (pH 7.5) and 15 mM NaCl, it was heated to 100°C for 15 min, cooled to room temperature slowly, and stored aliquoted at -20°C.

2.2.14.2.3 Phenol : chloroform extractions

After RNAase treatment, the DNA solution was phenol : chloroform extracted in order to remove protein. 0.5 vols. each of choloroform (96% (v/v) chloroform, 4% (v/v) isoamyl alcohol) and water saturated phenol (pH 8) were added to the RNAase-treated supernatant

and the tube was mixed by vortexing. The phases were separated by cetrifugation at 12,000 x g in a microfuge for 2 min and the upper, aqueous phase was removed to a fresh tube. This phenol : chloroform extraction was repeated, and then it was finally repeated with an equal volume of chloroform.

2.2.14.2.4 DNA precipitation

An equal volume of isopropanol was added to the purified DNA solution and this was incubated on ice for 15 min. After a 5 min centrifugation at 12,000 x g in a microfuge, the DNA pellet was allowed to dry. The pellet was then rinsed with 0.5 ml of 70% (v/v) ethanol at 4°C and dried in air for 10 min. The DNA was dissolved in sterile H_2O and stored at -20°C until required.

2.2.14.2.5 PEG purification

DNA which was required for transfection was further purified by this procedure which was performed by preparing a mix composed of DNA solution : 4 M NaCl : autoclaved 13% (w/v) PEG8000 in a ratio of 4 : 1 : 5. This was thoroughly mixed and incubated on ice for 20 min. The DNA was then pelleted by centrifugation at 12,000 x g at 4°C for 15 min. The supernatant was removed, the pellet was rinsed with 70% (v/v) ethanol, and dried as before. It was then redissolved in sterile H_2O and stored at -20°C.

2.2.14.2.6 Quantitation of DNA

Spectrophotometric determination of the amount of DNA was performed by measuring the absorbance of 5 μl of the stock DNA solution (made up to 1 ml with H_2O) at wavelengths 260nm and 280nm with a Shimadzu spectrophotometer and quartz cuvettes. The absorbance at 260 nm allows the concentration of DNA to be calculated using the assumption that a 50 μg/ml solution of double-stranded DNA gives an absorbance of 1. The ratio between the absorbances at 260 and 280 nm provides an estimate of the purity of the sample. Pure solutions of DNA are expected to give an Abs_{260}/Abs_{280} ratio of approximately 1.8.

2.2.14.3 Restriction enzyme digests

These were performed for a minimum of 1 hour at 37°C in the following solution:

5 μl	DNA (1-10 μg)
2 μl	buffer (10x stock, appropriate for enzyme used)
0.5 μl	restriction enzyme
12.5 μl	H_2O (sterile)

2.2.14.4 Agarose gel electrophoresis

Electrophoresis through agarose gels was used to separate and identify DNA fragments. Agarose was melted in a microwave oven in TAE buffer to give a concentration of 1% (w/v) (or any other required concentration). This was allowed to cool to approximately 60°C and ethidium bromide was added to a concentration of 0.5 μg/ml (from a stock concentration of 10 mg/ml). This was then poured into a Horizon electrophoresis kit (Gibco-BRL) and allowed to set around a 8 well comb. The comb and kit ends were removed and enough TAE buffer was poured into the tank to cover the gel to a depth of about 1 mm. The DNA solutions were mixed with 6x gel loading buffer (0.25% (w/v) bromophenol blue, 30% (v/v) glycerol) and loaded into the wells of the gel. Electrophoresis was performed at 75 V for about 1-2 hours, or until separation of the DNA fragments was achieved. Visualisation of the ethidium bromide-stained DNA was performed using a UVP ultraviolet transilluminator.

2.2.14.5 Preparation of competent *E. coli*

Buffer 1:	3 ml	1 M potassium acetate
	10 ml	1 M $RbCl_2$
	1 ml	1 M $CaCl_2$
	5 ml	1 M $MnCl_2$
	18.75 ml	80% (v/v) glycerol

pH was set to 5.8 with 100 mM acetic acid, the volume was made up to 100 ml and the solution was filter sterilised and stored at 4°C.

Buffer 2:	4 ml	100 mM MOPS (pH 6.5)
	3 ml	1 M $CaCl_2$
	0.4 ml	1 M $RbCl_2$
	7.5 ml	80% (v/v) glycerol

pH was set to 6.5 with HCl, the volume was made up to 40 ml and the solution was filter sterilised and stored at 4°C.

100 ml of LB medium was inoculated with 5 ml of an overnight culture of *E. coli* (DH5α). This was incubated at 37°C with shaking until the optical density at 550 nm was 0.48. The culture was chilled on ice for 5 min, then centrifuged at 3000 rpm in a TJ6 Beckman centrifuge for 10 min at 4°C. The medium was poured off and the pellet was resuspended in 40 ml of buffer 1. After 5 min on ice, the cells were pelleted as before and resuspended in 2 ml of buffer 2. After a 15 min incubation on ice, the competent cells were aliquoted and stored at -80°C.

2.2.14.6 Transformation of competent *E. coli*

1-10 ng (in 1-5 μl) of DNA was added to 50 μl of competent cell suspension and this was incubated on ice for 15 min. The mix was then heat shocked at 42°C for 90 seconds and returned to ice for 2 min. 450 μl of SOC medium was added and the cell suspension was shaken at 37°C for 45 min. 200 μl of this mix was then plated out on an agar plate (containing the appropriate antibiotic) and left to grow at 37°C overnight. Colonies were then picked from the plate and grown in LB medium overnight. From these cultures, plasmid DNA could be prepared as above.

2.2.14.7 Stable Transfections

Rat1 fibroblasts were grown on 10 cm dishes until approximately 40-50% confluency and then washed twice in serum free DMEM. 5 μg of plasmid DNA (and 0.5 μg of additional plasmid DNA used for selection - pBABE hygro) were mixed with sterile Hank's modified medium to a final volume of 100 μl. Lipofectin (100 μl) mixed with 200 μl of sterile Hank's modified medium was then added to the DNA mix. This was

mixed gently and incubated at room temperature for 15 min. The DNA/lipofectin mixture was mixed with 9.6 ml of serum free DMEM and added carefully to the plate of cells. After a 16 hour incubation, this medium was removed and the cells were washed twice in 5% DMEM and incubated for a further 48 hours in fresh 5% DMEM. The medium was then replaced by 5% DMEM containing 50 μg/ml hygromycin B in order to select for those cells expressing the antibiotic resistance gene. After approximately 12 days, discrete colonies became visible on the plate, and they were picked (by scraping with sterile pipette tip) and transferred to 24 well plates. Clones were expanded and stored in liquid nitrogen as they were produced. Clones were harvested and analysed for expression of the desired protein.

Chapter 3

The regulation of $p44^{MAPK}$ by the α_{2A} adrenergic receptor when expressed in Rat1 fibroblasts: effect of expression levels and the Asn^{79} mutation.

Chapter 3: The regulation of p44^{MAPK} by the α_{2A} adrenergic receptor when expressed in Rat1 fibroblasts: effect of expression levels and the Asn^{79} mutation.

3.1 Introduction

The α_{2A} adrenoceptor has been extensively studied at the biochemical and pharmacological level. This provided a good model receptor to study the regulation of p44^{MAPK} by GPCRs because a range of pharmacological tools were available, the receptor had been cloned and a considerable amount was already known about its signalling. The study of endogenously expressed receptors can be difficult because the population of the receptors could be mixed with other subtypes and sometimes the physiological host cells are more difficult to manage in the laboratory. Much of the work described in this introduction, as well as the results which will be presented in this thesis, were obtained from heterologously transfected cells which transiently or stably expressed the α_{2A} adrenoceptor.

An α_2 adrenoceptor (called α_2-C10) was cloned from a human genomic DNA library with oligonucleotide probes corresponding to sequences from purified human platelet α_2 adrenoceptors (Kobilka *et al.*, 1987) and this was found to correspond to the α_{2A} adrenoceptor subtype by pharmacological analysis. There are possibly four subtypes of α_2 adrenoceptors which have been cloned and classified by pharmacological analysis (MacKinnon *et al.*, 1994) and the α_{2A} adrenoceptor is found in many tissues such as the brain, kidney and adipose tissue. Stimulation of the receptor in these tissues resulted in the inhibition of adenylyl cyclase and this was also found following heterologous expression in Chinese hamster lung fibroblasts and COS-7 cells (Cotecchia *et al.*, 1990) and in Rat1 fibroblasts (MacNulty *et al.*, 1992). However in these cells, the α_2-C10 adrenoceptor also displayed an ability to couple to multiple signal transduction pathways inducing stimulation of phosphoinositide hydrolysis in Chinese hamster lung

fibroblasts and COS-7 cells and stimulation of PLD-mediated hydrolysis of phosphatidylcholine in Rat1 fibroblasts. In cells of neuronal origin this receptor coupled to the inhibition of adenylyl cyclase and L-type Ca^{2+} channels and the activation of K^+ channels (Surprenant *et al.*, 1992). These effects of the α_{2A} adrenoceptor were all mediated by members of the G_i-protein family as judged by the attenuation of the responses with pertussis toxin pretreatment.

Further study of the G-protein coupling of the α_2-C10 adrenoceptor expressed in Rat1 fibroblasts (in a cell line called 1C which expressed the receptor to a high level) demonstrated that this receptor had the ability to functionally couple to both G_{i2} and G_{i3} (Milligan *et al.*, 1991). This was shown by the ability of a selective α_2 adrenergic receptor agonist (UK14304) to stimulate cholera toxin-catalysed ADP-ribosylation of these proteins in the absence of guanine nucleotides, an assay which defines the interaction of these G-proteins with the receptor. This effect was blocked by yohimbine, a selective α_2 adrenergic antagonist. Although coupling to these two G-proteins, G_{i2} but not G_{i3} contributed to the inhibition of adenylyl cyclase in these cells (McClue *et al.*, 1992) which is in line with the widely held view of the cellular role of G_{i2}. However, regulation of other signalling pathways was possible as illustrated by Raymond and co-workers who demonstrated that the human α_{2A} adrenoceptor could couple to the inhibition of cAMP accumulation in murine embryonic stem cells which lack $G_{i2\alpha}$ (Raymond *et al.*, 1994). Heterologous expression of this receptor in some cell systems also permitted coupling to G_s leading to the stimulation of adenylyl cyclase at high agonist concentrations. This produced biphasic concentration-response curves (Eason *et al.*, 1992). The coupling to G_s can be more clearly seen after pertussis toxin pretreatment which attenuates the coupling to the G_i-proteins (Cotecchia *et al.*, 1990; Eason *et al.*, 1992). Overexpression of $G_{q\alpha}$ and $G_{s\alpha}$ also forced the interaction of the α_{2A} adrenoceptor with these G-proteins in HEK 293 cells leading to agonist-mediated stimulation of phospholipase C and adenylyl cyclase respectively (Chabre *et al.*, 1994).

However, this required a 1000-fold greater concentration of agonist than the physiological coupling to G_i which led to the inhibition of adenylyl cyclase.

The α_{2A} adrenoceptor can also couple to the $p42/44^{MAPK}$ cascade, an ability common to many G_i-coupled receptors (see Section 1.4.13.3). Many of the original studies on G_i-mediated $p42/44^{MAPK}$ regulation were performed using the activity of LPA, acting on a putative GPCR which can couple to members of both G_i and G_q protein families (although only G_i-proteins mediated Ras.MAPK activation (see Moolenaar, 1995)). However, this receptor has not been identified at the molecular level and there is a very limited pharmacology at this site, therefore many groups have chosen to study the signalling of GPCRs heterologously expressed in fibroblast cell lines. A proliferative response to agonist stimulation of the α_2 adrenoceptor had been demonstrated previously in intestinal crypt cells (Tutton and Barkla, 1987), expression of the α_2-C10 adrenoceptor in Chinese hamster lung fibroblasts permitted α_2 agonists to act as co-mitogens (Seuwen *et al.*, 1990) and there was extensive pharmacology and signal transduction information available and so this receptor appeared to be potentially useful to continue these studies. Agonist stimulation of the α_{2A} adrenoceptor in the 1C cell line (derived from Rat1 fibroblasts) was shown to stimulate the GTP loading of $p21^{ras}$ and the phosphorylation of $p44^{MAPK}$ (Alblas *et al.*, 1993). It was concluded that this was not the result of the stimulation of the other known effectors of the α_{2A} adrenoceptor but occurred independently of both adenylyl cyclase and phospholipase C activity. The work in this chapter continues this research and makes use of the endogenous receptors for LPA and EGF as controls for G_i-coupled and tyrosine-kinase linked receptor-mediated stimulation of $p42/44^{MAPK}$.

Site-directed mutagenesis has permitted the characterisation of some of the specific amino acid residues important in various facets of the receptor's function (Wang *et al.*, 1991). One residue was found to play an important role in receptor-G-protein coupling and allosteric regulation by monovalent cations. This work was originally performed

on the porcine species-variant of the α_{2A} adrenoceptor (Guyer *et al.*, 1990). This study demonstrated a phenomenon which had been seen before, that of allosteric modulation by monovalent cations which manifested itself in the accelerated dissociation of an antagonist when expressed in COS-M6 cells. This allosteric modulation was dependent on the presence of an aspartate residue at position 79 (Asp^{79}) shown by the loss of this effect, but not the selectivity of adrenergic binding, when this residue lost its side chain negative charge through a mutation to an asparagine (Horstman *et al.*, 1990). Similar results had been recorded with an aspartate at an analogous position in other GPCRs and so possibly this is a general function of this residue in these receptors (see Ceresa and Limbird, 1994).

Expression of the Asn^{79} mutant of the human α_{2A} adrenergic receptor in CHO cells took this research further as it demonstrated this mutation altered receptor-G-protein coupling as shown by both the insensitivity of agonist binding to guanine nucleotides and the loss of agonist-mediated inhibition of cAMP accumulation (Wang *et al.*, 1991). The suggestion was made that the Asp^{79} residue was critical for the agonist-induced conformational change that catalyses G-protein activation and possibly involves cation transfer. However, a significantly different scenario was seen with this mutant receptor expressed in mouse pituitary cells (Surprenant *et al.*, 1992). In this system, a selective loss of effector output was shown in that agonist-induced inhibition of adenylyl cyclase and voltage dependent Ca^{2+} currents were preserved but the activation of inwardly rectifying K^+ currents was lost. Two theories were suggested to explain this: either the coupling to the Ca^{2+} channel and adenylyl cyclase-associated G-proteins, but not the K^+ channel-associated G-protein(s), was preferentially retained by the Asn^{79} mutant or that the reduced receptor-G-protein coupling of Asn^{79} is still sufficient to couple to the Ca^{2+} channels and adenylyl cyclase but not to the activation of K^+ currents. The latter explanation now appears to be more likely due to the work of Chabre and co-workers. They demonstrated that although the α_{2A} adrenoceptor preferentially couples to G_i, it could be 'forced' to couple G_s and G_q by overexpression in HEK 293 cells. However,

the Asn^{79} mutant was only able to couple to G_i and inhibition of adenylyl cyclase, and this was with lower potency (Chabre *et al.*, 1994). Therefore the mutation apparently reduced the efficiency of coupling of this receptor to all G-proteins thus eliminating the signal transduction pathways which were coupled less efficiently to the α_{2A} adrenoceptor. This explanation is, however, too simple to account for the nonreciprocal disruption of receptor-G-protein coupling which was detected in mouse pituitary cells by Ceresa and Limbird (1994). They demonstrated that loss of the negative charge at position 79 (glutamate could substitute for aspartate with limited differences) produced loss of allosteric regulation by Na^+, as seen before. This was paralleled by an attenuation, but not elimination, of anterograde information transfer (receptor to G-protein) as seen by a reduction in GTPase stimulation by agonist at the Asn^{79} mutant. However, retrograde information transfer (G-protein to receptor) was completely lost as demonstrated by the lack of sensitivity of agonist binding to guanine nucleotides.

The experiments using this mutant receptor described in this chapter attempted to determine if this selective, or general loss of G-protein coupling, leads to the loss of coupling to the Ras.MAPK cascade. In addition these experiments may also give an indication as to the coupling efficiency of the receptor to this pathway in comparison to the coupling to the other signalling effectors/G-proteins.

3.2 Results and Discussion

The level of α_{2A} adrenoceptor expression in the 1C cell line was regularly monitored as expression was not as stable or as great as previously reported (Milligan *et al.*, 1991). The mean level of expression was found to be 850 ± 140 fmol/mg membrane protein (mean ± SEM, n = 9) as determined by the specific binding of [^{3}H]yohimbine at saturating concentrations (10^{-8} M). This level of expression was still sufficient to substantially stimulate high affinity GTPase activity on agonist treatment. Maximally effective concentrations (10^{-5} M) of UK14304 increased the high affinity GTPase activity by 70 ± 5 pmol/min/mg membrane protein (mean ± SEM of triplicate assays) as compared with the level in the absence of this ligand.

As mentioned previously, agonist stimulation of these cells had been reported to increase the GTP loading of $p21^{ras}$ and the level of phosphorylation of $p42^{MAPK}$, as determined by a mobility shift after SDS-PAGE (Alblas *et al.*, 1993). This effect was seen to be maximal after 5 min of treatment with 5 x 10^{-7} M UK14304. It was therefore decided to determine if the coupling to the $p21^{ras}$.MAPK cascade could also be detected by an increase in the activity of the $p44^{MAPK}$. This was performed by measuring the ability of immunoprecipitated $p44^{MAPK}$ to phosphorylate myelin basic protein as an exogenously added substrate. The phosphorylation can be measured by a phosphorimager because a trace amount of [γ-^{32}P]ATP was added to the reaction mixture. Figure 3.1 shows that the stimulation of cells of clone 1C with either 10^{-6} M UK14304 or 10^{-8} M EGF (a maximally effective dose) for 5 min significantly activated $p44^{MAPK}$. The percentage increase over the basal activity of $p44^{MAPK}$ on stimulation with UK14304 from a number of experiments was calculated to be 160 ± 25% and for EGF was 240 ± 35% (mean ± SEM, n = 12 in each case).

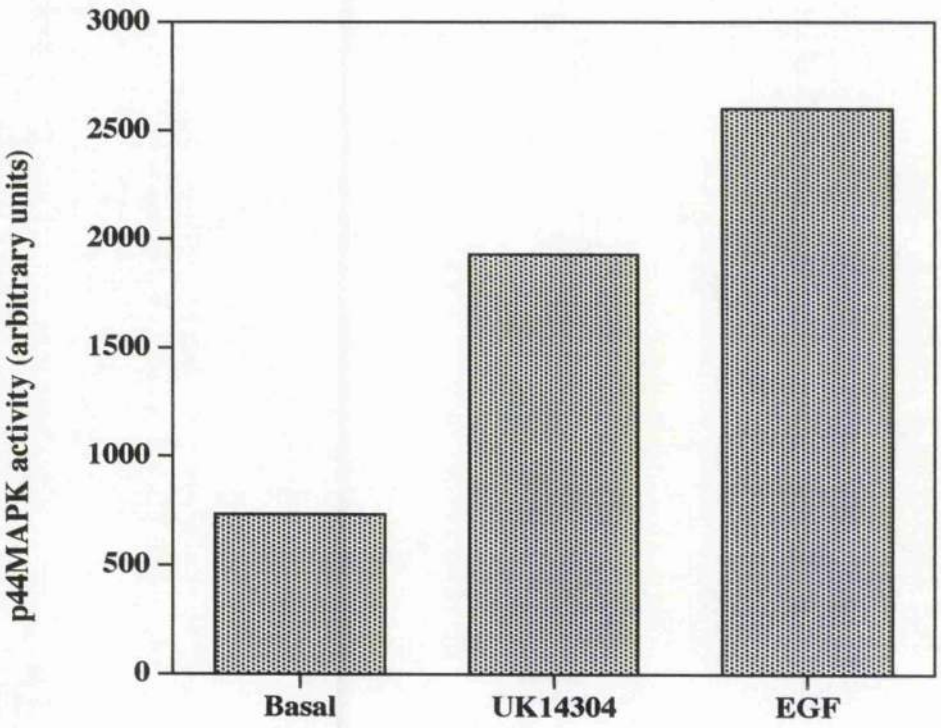

Figure 3.1 Stimulation of the activity of $p44^{MAPK}$ in cells of clone 1C by EGF and UK14304.

Serum starved 1C cells were treated with serum free DMEM containing either no agonist (basal), 10^{-6} M UK14304 or 10^{-8} M EGF for 5 min and $p44^{MAPK}$ activity was determined by the IP kinase method as described in Section 2.2.9.2. Representative results of one of at least 12 observations are displayed.

Pretreatment of the cells with 10^{-3} M dibutyryl cAMP (a cAMP analogue) for 20 min significantly attenuated the activation of $p44^{MAPK}$ in response to maximally effective concentrations of UK14304 and EGF (Figure 3.2A and Table 3.1). This result is consistent with the reported effects of elevated cAMP levels on growth factor and GPCR-mediated activation of the Ras.MAPK cascade in Rat1 fibroblasts (Cook and McCormick, 1993; Wu *et al.*, 1993; Hordijk *et al.*, 1994). It has been suggested that cAMP acts via PKA-mediated phosphorylation of Raf or MEKK (see Section 1.4.10) and this would be consistent with the reported lack of effect of elevated cAMP levels on the GTP loading of $p21^{ras}$ by the α_{2A} adrenoceptor as well as the results here. Therefore, although the conclusion made by Alblas and co-workers that the activation of the $p42/44^{MAPK}$ cascade was not secondary to the inhibition of adenylyl cyclase (Alblas *et al.*, 1993) is correct, these two signal transduction pathways do not exist independently of each other.

Pretreatment with 10^{-5} M forskolin for 15 min produced a similar attenuation of EGF-mediated $p44^{MAPK}$ activation as would be expected because of the ability of forskolin to directly stimulate adenylyl cyclase activity in these cells. Forskolin pretreatment also consistently reduced the activity of $p44^{MAPK}$ on UK14304 treatment but the attenuation was not as complete or as significant as with EGF (Figure 3.2B and Table 3.1). The reason for this is not certain, however UK14304-mediated stimulation of the α_{2A} adrenoceptor can reduce forskolin amplified adenylyl cyclase activity in crude membrane preparations (see Figure 3.8) and so the inhibitory effects of the forskolin-mediated increase in cAMP may be antagonised by the α_{2A} adrenoceptor. This may illustrate the point made earlier as to the fact that the Ras.MAPK cascade initiated by the α_{2A} adrenoceptor could be influenced by the other effector pathways of the receptor.

Table 3.1 The effect of various pretreatments on UK14304 and EGF-mediated p44^{MAPK} activation in 1C cells.

		% increase in p44^{MAPK} activity over basal		
Pretreatment	Agonist	Control	Pretreated	Significance
Dibutyryl cAMP	UK14304	170 ± 30	11 ± 5	0.010
	EGF	310 ± 60	40 ± 25	0.007
Forskolin	UK14304	170 ± 40	110 ± 20	0.130
	EGF	240 ± 30	30 ± 6	0.030
Genistein	UK14304	190 ± 70	340 ± 50	0.024
	EGF	235 ± 80	340 ± 90	0.270

The stimulation of p44^{MAPK} activity by 5 min treatment with 10^{-6} M UK14304 or 10^{-8} M EGF was determined by the IP kinase assay as described in Section 2.2.9.2 and in the legends to Figure 3.2 and 3.3 after pretreatment with 10^{-3} M dibutyryl cAMP, 10^{-5} M forskolin or 5×10^{-5} M genistein. Data is displayed as mean ± SEM (n = 4 for dibutyryl cAMP and n = 3 for forskolin and genistein) and the significance of the effect of each of the treatments was calculated using the paired students t-test.

Figure 3.2 The effect of elevated cAMP levels on $p44^{MAPK}$ activation in cells of clone 1C.

A Serum starved 1C cells in 6 well plates were pretreated for 20 min with serum free DMEM with (shaded bars) and without (hatched bars) 10^{-3} M dibutyryl cAMP and were then left untreated or treated with 10^{-6} M UK14304 or 10^{-8} M EGF for a further 5 min. The activity of $p44^{MAPK}$ was then determined by the IP kinase assay as described in Section 2.2.9.2. The data displayed is from one of four similar observations.

B 1C cells were treated as in Figure 3.2A but pretreatment for 15 min was with (shaded bars) or without (hatched bars) 10^{-5} M forskolin prior to treatment with agonists and $p44^{MAPK}$ activity determination. Data is from one of three similar observations.

Figure 3.2

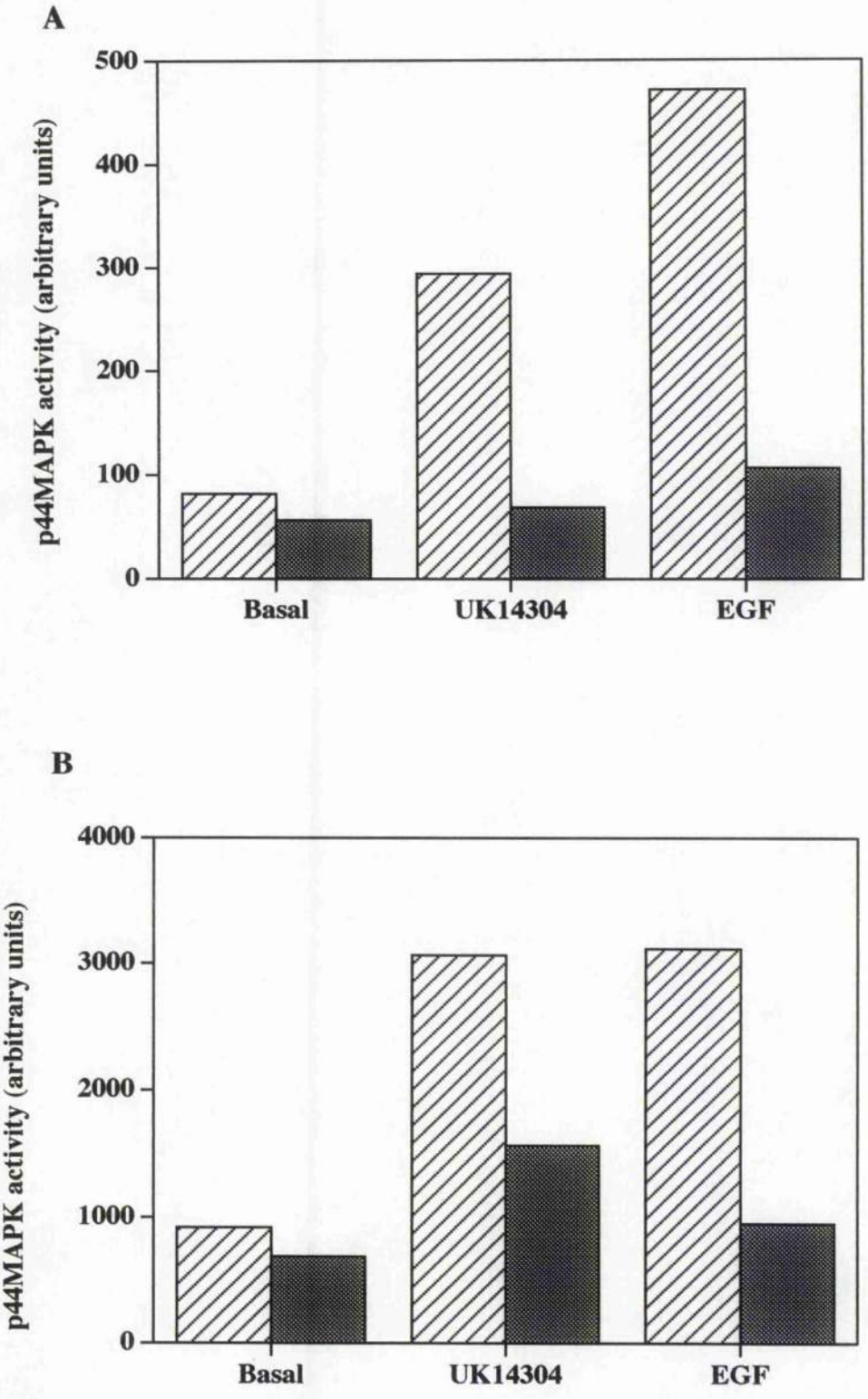
A
500
400
300
200
100
0
p44MAPK activity (arbitrary units)
Basal
UK14304
EGF
B
4000
3000
2000
1000
0
p44MAPK activity (arbitrary units)
Basal
UK14304
EGF

Genistein is a selective tyrosine kinase inhibitor that can inhibit the activation of $p42/44^{MAPK}$ by many but not all of the G_i coupled receptors that have been studied (see Section 1.4.13.3.3). In cells of clone 1C, however, very different effects were observed. A concentration of genistein (5×10^{-5} M) was used which was found to inhibit LPA and thrombin receptor peptide-mediated $p21^{ras}$ GTP loading but not that stimulated by EGF in Rat1 fibroblasts (van Corven *et al.*, 1993). Often a reduction in the basal activity after pretreatment with 5×10^{-5} M genistein for 10 min was observed, but this was coupled with a consistent enhancement of the UK14304 and EGF-mediated stimulation of $p44^{MAPK}$ activity (Figure 3.3). As can be seen in Table 3.1 which was calculated from three separate experiments, the increase in activity after genistein pretreatment was not found to be significant for the EGF response, but a probability of 0.024 was calculated for the increased response to UK14304.

Although this would seem to contradict most of the literature as to the effect of this agent on G_i-coupled receptor-mediated stimulation of the $p42/44^{MAPK}$ cascade, there is some similarity to the effect on the activation by muscarinic m2 receptor expressed in Rat1 fibroblasts (Winitz *et al.*, 1993). In this case, genistein (at a concentration of 3×10^{-4} M) did not display any inhibitory effect on the agonist-mediated stimulation of the activity of $p42/44^{MAPK}$ or MEK, or on the GTP loading of Ras. However, genistein did slightly enhance the agonist-mediated stimulation of Raf. The lack of an inhibitory effect of genistein in these experiments could possibly be explained by the presence of a genistein-insensitive tyrosine kinase involved in the $p42/44^{MAPK}$ pathway but the reason for the enhancement of stimulation is puzzling.

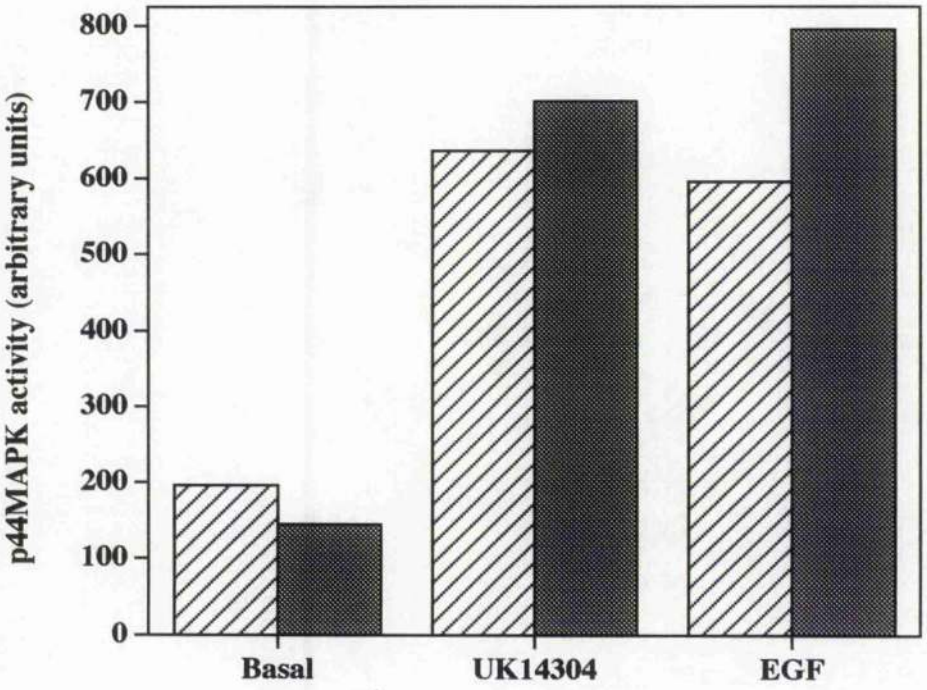

Figure 3.3 The effect on agonist-stimulated p44^{MAPK} activity after pretreatment with genistein of cells of clone 1C.

Serum starved 1C cells in 6 well plates were pretreated for 30 min with serum free DMEM with (shaded bars) and without (hatched bars) 10^{-5} M genistein and then left untreated (basal) or treated with 10^{-6} M UK14304 or 10^{-8} M EGF for a further 5 min. The activity of p44^{MAPK} was then determined by the IP kinase assay as described in Section 2.2.9.2. The data displayed is from one of three observations. (Table 3.1 contains means of the data from all experiments).

The next section of work attempted to determine whether the mutation of Asp^{79} to Asn would prevent the coupling of the α_{2A} adrenoceptor to the $p42/44^{MAPK}$ cascade. Rat1 fibroblasts were stably co-transfected with either the wild type or Asn^{79} mutant of the haemaglutinnin-tagged porcine α_{2A} adrenoceptor expressed in pcmv4 with the hygromycin resistance expression vector pBABE hygro in a 10 : 1 ratio. Clones were selected on the basis of resistance to 50 μg/ml hygromycin B and subsequently analysed by the radioligand binding assay (with 10^{-8} M [^{3}H]yohimbine) in order to identify and quantify the expression of the α_{2A} adrenoceptor. Clones expressing the wild type and Asn^{79} mutant receptor were selected for further analysis (called clones TAGWT and ASN79 respectively). There was some degree of variation in the level of expression throughout different passages, however, the receptor level was monitored frequently and the mean expression level for each clone is shown in Table 3.2. From this Table it can be clearly seen that three of the clones (TAGWT 17, ASN79 4 and 9) expressed reasonably similar levels of receptor (3 - 5.6 pmol/mg protein) and that clone TAGWT 3 expressed the receptor at considerably lower levels (0.5 pmol/mg protein).

Table 3.2 Receptor expression levels of TAGWT and ASN79 clones.

	Specific Binding
Clone	(fmol/mg membrane protein)
TAGWT 3	460 ± 70
TAGWT 17	5600 ± 550
ASN79 4	3000 ± 430
ASN79 9	4300 ± 580

Specific binding of 10^{-8} M [^{3}H]yohimbine to membranes prepared from cells of the above clones as determined by the radioligand binding assay described in Section 2.2.3. Non-specific binding was determined in the presence of 10^{-4} M idazoxan. Data is presented as mean ± SEM, from at least 8 observations.

Scatchard analyses of the two higher expressing clones were performed using [ethyl-^{3}H]RS-79948-197 (a high affinity ligand for the α_{2A} adrenoceptor) (see Figure 3.4). Calculated values of B_{max} for TAGWT 17 and ASN79 9 were 7900 and 6900 fmol/mg membrane protein and of K_d were 0.38 and 0.31 nM respectively. The similarity in the dissociation constants for the two clones would suggest that the Asn^{79} mutation does not significantly affect the binding affinity of antagonists to the receptor as described previously (Wang *et al.*, 1991). This would justify the use of the radioligand binding results to compare the receptor expression levels in each of the clones. Any difference between the radioligand binding in TAGWT and ASN79 clones was therefore not due to a difference in the affinity for the ligand but in the number of binding sites available.

High affinity GTPase assays were performed to demonstrate and measure the coupling of these transfected receptors to their G-proteins (Figure 3.5). As would be expected the maximum UK14304-mediated stimulation of GTPase activity over basal in membranes prepared from cells of clone TAGWT 17 was much greater ($p = 0.001$) than in the lower expressing clone TAGWT 3 (42 ± 4 and 14 ± 2.5 pmol/min/mg membrane protein respectively; mean ± SEM, from at least three independent experiments). The maximum possible stimulation by UK14304 of GTPase activity in membranes prepared from cells of both of the ASN79 clones was also significantly ($p < 0.0015$) lower than that seen with TAGWT 17 (6.9 ± 1.3 and 8.5 ± 1.5 pmol/min/mg membrane protein for clones ASN79 4 and ASN79 9 respectively; mean ± SEM, from at least three independent experiments). In addition, the wild type receptor expressed in drastically lower levels in TAGWT 3 stimulated a significantly greater level of GTPase activity than the much higher level of expression of the mutant receptor in ASN79 4 ($p = 0.027$). Therefore the Asn^{79} receptor expressed in Rat1 fibroblasts displayed a much reduced, but still measurable ability to couple to the G-protein machinery compared to the wild type receptor. A similar situation occurred when these receptors were expressed in mouse anterior pituitary cells (Ceresa and Limbird, 1994), when the Asn^{79} mutation attenuated but did not eliminate the G-protein coupling.

Figure 3.4 Scatchard analysis of clones TAGWT 17 and ASN79 9.

A Saturation specific binding curves of [ethyl-^{3}H]RS-79948-197 to membranes prepared from cells of clones TAGWT 17 and ASN79 9 were produced using the radioligand binding assay as described in Section 2.2.3. Results are presented as concentration of [^{3}H]RS-79948-197 added (as determined by measuring the radioactivity of samples of each dilution added to each tube) against specific binding to the membranes. Specific binding was determined as the difference between the total binding and the binding in the presence of 10^{-4} M idazoxan. This data was then subjected to Scatchard analysis (Scatchard, 1949) and displayed in panel **B**.
For both graphs, the open circles and broken line represent clone TAGWT 17, and the filled squares and full line represent clone ASN79 9.

Figure 3.4

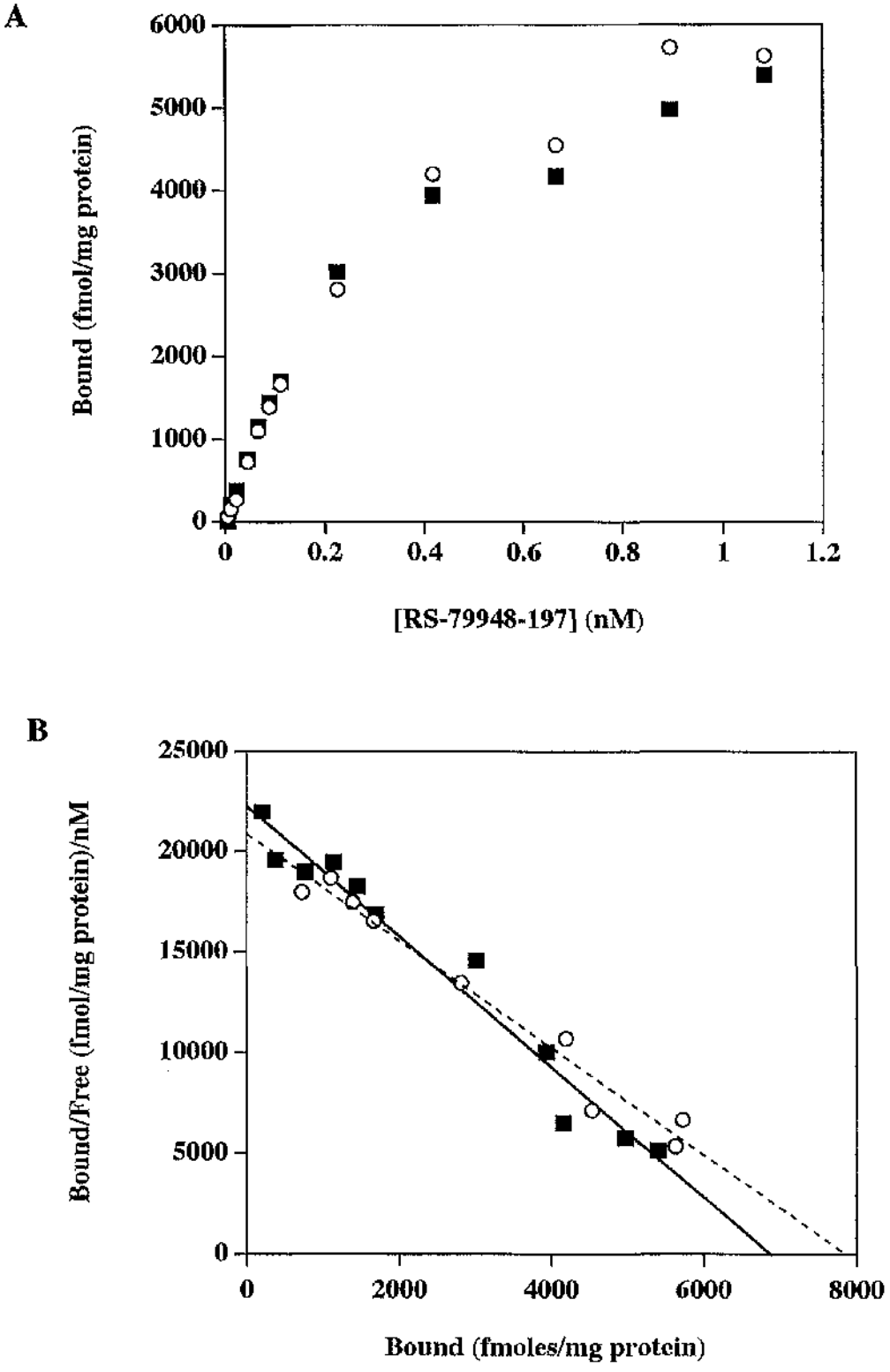
A
Bound (fmol/mg protein)
6000
5000
4000
3000
2000
1000
0
0
0.2
0.4
0.6
0.8
1
1.2
[RS-79948-197] (nM)
B
Bound/Free (fmol/mg protein)/nM
25000
20000
15000
10000
5000
0
0
2000
4000
6000
8000
Bound (fmoles/mg protein)

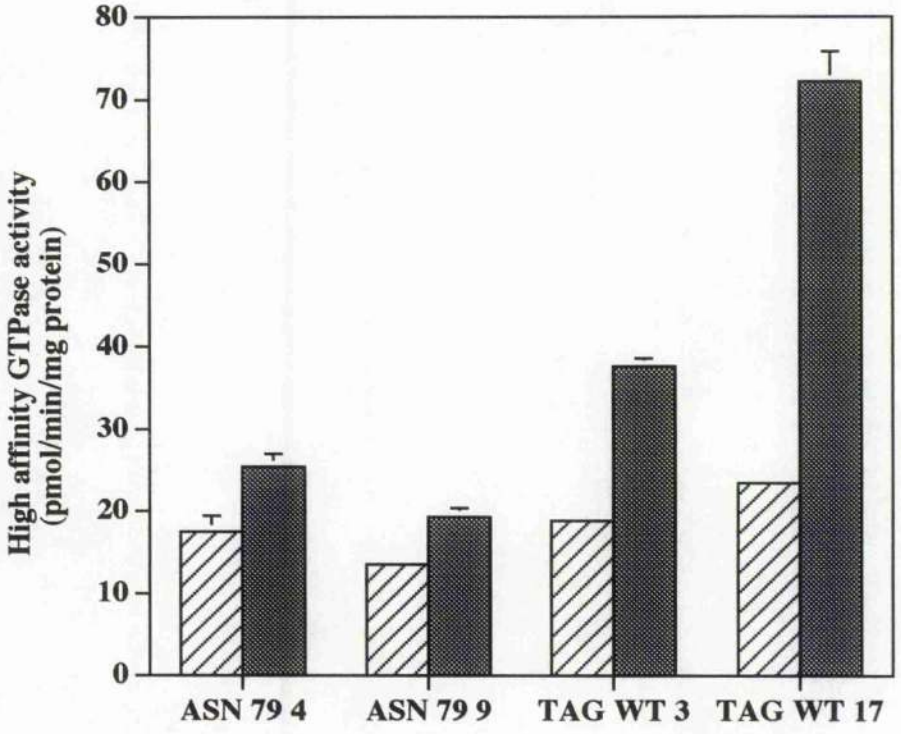

Figure 3.5 Stimulation of high affinity GTPase activity in membranes of clones TAGWT and ASN79 by UK14304.

High affinity GTPase activity was determined in membranes of cells of clones TAGWT 3 and 17 and of clones ASN79 4 and 9 according to Section 2.2.4. Hatched bars represent basal activity and the shaded bars represent GTPase activity on treatment with 10^{-5} M UK14304. Activity is presented as mean ± SEM of triplicate assays from a representative experiment of at least three independent experiments.

Concentration-response curves to UK14304 for high affinity GTPase activity in each of the four clones are shown in Figure 3.6. As would be expected, the EC_{50} value was 10 fold lower for the clone expressing the wild type receptor at the higher level (EC_{50} value for TAGWT 17 was 3.7×10^{-9} M and for TAGWT 3 was 3.0×10^{-8} M). This was also reflected in the EC_{50} values for the mutant receptors (EC_{50} for ASN79 9 was 5.8×10^{-9} M and for ASN79 4 was 5.0×10^{-8} M). Hill slopes of the concentration-response curves ranged from 0.6 to 0.9. It was noticeable that the differences in the EC_{50} values were less pronounced compared to the differences seen in the maximum stimulation of GTPase and that there was no significant difference in the concentration of UK14304 required to produce half-maximal stimulation of GTPase activity between the two higher receptor level expressing clones (TAGWT 17 and ASN79 9).

Under normal circumstances, cholera toxin catalyses the ADP-ribosylation of G proteins belonging to the G_s family. However, in the absence of guanine nucleotides, cholera toxin can catalyse the ADP-ribosylation of G_i-like proteins if they are coupled to an agonist-activated receptor. A similar experimental approach has been used previously to establish the coupling of the α_2-C10 adrenoceptor expressed in Rat1 fibroblasts to two G_i-proteins (Milligan *et al.*, 1991). Maximally effective concentrations of UK14304 stimulated a large increase in the level of [^{32}P]ADP-ribosylation of G_i-like proteins by cholera toxin in membranes of clone TAGWT 17 (Figure 3.7). Results are displayed as the relative stimulation over the level of G_s labelling which was unaffected by the presence of UK14304. Very little increase in labelling of G_i-like proteins occurred on treatment of membranes of clone TAGWT 3 with UK14304 and there was little or no detectable increase in the cholera toxin-catalysed [^{32}P]ADP-ribosylation of G_i-like proteins in the ASN79 mutant cell lines. This is consistent with the lower level of expression of the wild type α_{2A} adrenoceptor in TAGWT 3 permitting coupling to fewer G_i-proteins and the lower ability of the Asn^{79} mutant to couple to the G-protein machinery. These results therefore concur with those conclusions which were based on the high affinity GTPase assays.

Figure 3.6 Concentration-response curves for UK14304 stimulated high affinity GTPase activity in TAGWT and ASN79 clones.

A High affinity GTPase activity was measured (as in Section 2.2.4) in response to various concentrations of UK14304 in membranes from cells of clones TAGWT 3 (filled circles, full line), TAGWT 17 (open circles, broken line).

B High affinity GTPase activity was measured in response to various concentrations of UK14304 in membranes from cells of clones ASN79 4 (open squares, broken line) and ASN79 9 (filled squares, full line).

As the amount of stimulation of GTPase activity was different for each clone (see Figure 3.5), data is presented as % of the maximum level achieved by the agonist in each of the clones, mean ± SEM of triplicate assays.

Figure 3.6

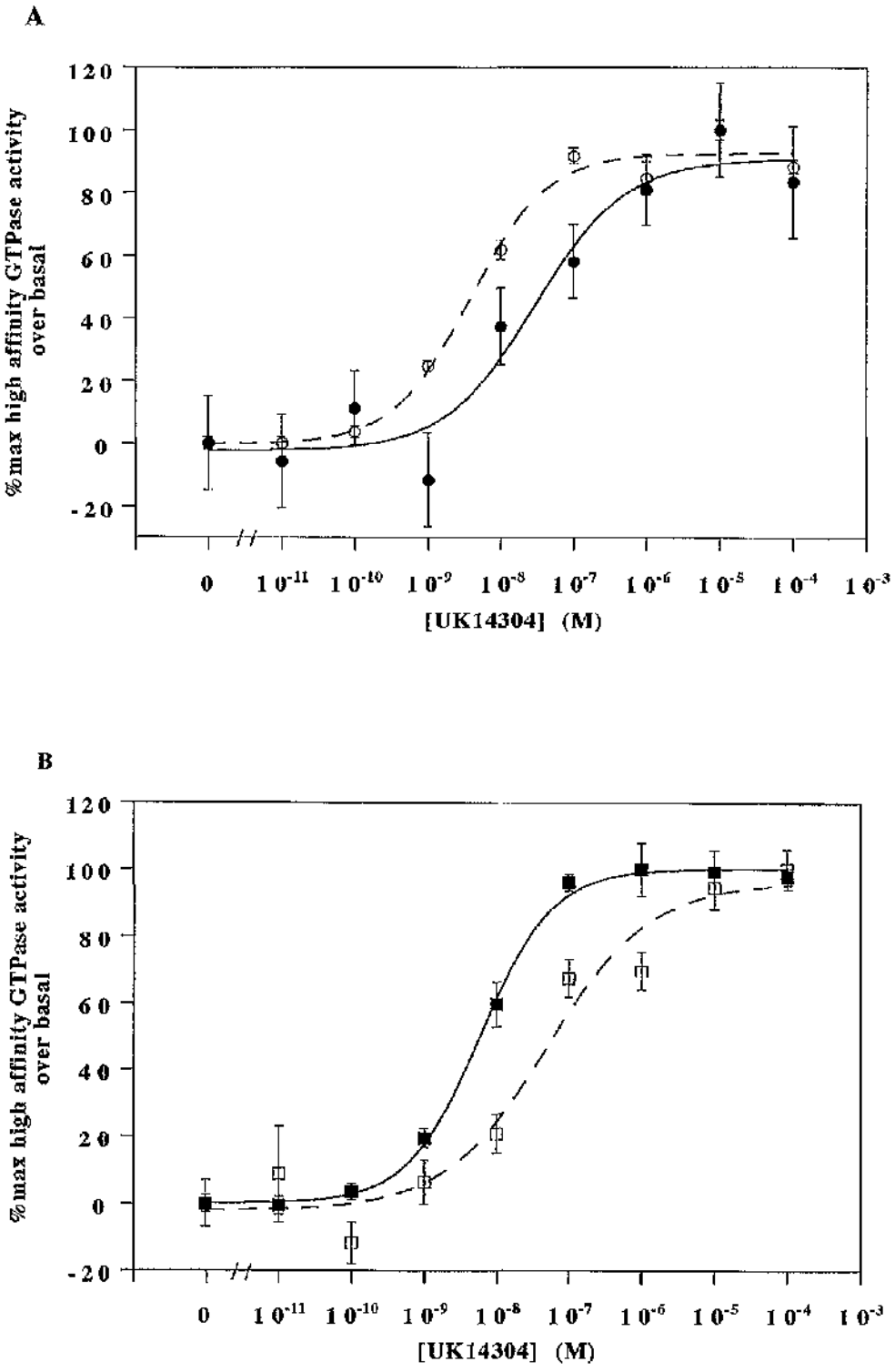
A
120
100
80
60
40
20
0
-20
% max high affinity GTPase activity over basal
0
10-11
10-10
10-9
10-8
10-7
10-6
10-5
10-4
10-3
[UK14304] (M)
B
120
100
80
60
40
20
0
-20
% max high affinity GTPase activity over basal
0
10-11
10-10
10-9
10-8
10-7
10-6
10-5
10-4
10-3
[UK14304] (M)

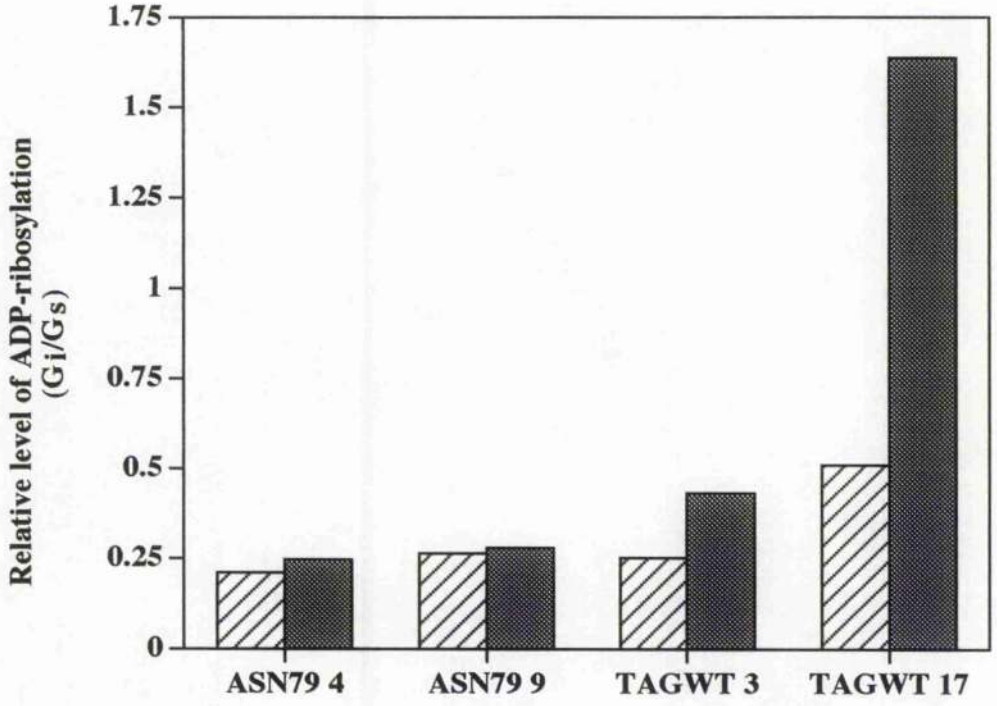

Figure 3.7 UK14304 -driven cholera toxin-catalysed [^{32}P]ADP-ribosylation of the α subunit of G_i-like proteins in TAGWT and ASN79 clones.

Membranes of cells of the clones noted were subjected to cholera toxin-catalysed [^{32}P]ADP-ribosylation performed in the absence (hatched bars) or presence of 10^{-5} M UK14304 (shaded bars). Quantitation of the phosphorimage is shown in the graph and the data has been displayed as the relative labelling of G_i-like proteins as compared with that of G_s-like proteins (whose labelling does not significantly alter on agonist treatment) for each of the samples analysed.

The inhibition of forskolin-amplified adenylyl cyclase activity by UK14304 was determined in order to demonstrate the functional output of the receptors beyond the level of the G-protein. Figure 3.8 demonstrates that the largest level of inhibition by UK14304 was achieved in clone TAGWT 17. The % inhibition of forskolin-amplified adenylyl cyclase activity by UK14304 was calculated to be 54 ± 9% (mean ± SEM, n = 3). The level of agonist-mediated inhibition possible in clone TAGWT 3 was smaller than this (38 ± 2%, mean ± SEM, n = 3). It is of interest to note however that the difference in the maximal inhibition of adenylyl cyclase between these two clones was not as pronounced as the difference at the GTPase level (Figure 3.5). This lesser response at the level of adenylyl cyclase to higher receptor expression has been reported previously (Ashkenazi *et al.*, 1987) and tends to implicate the adenylyl cyclase catalytic element, rather than the receptor, as the limiting component in this pathway in these cells.

The two mutant clonal cell lines also displayed a significant degree of agonist-mediated inhibition of forskolin-amplified adenylyl cyclase activity (Figure 3.8; mean ± range of two individual experiments for ASN79 4 was 24 ± 11% and for ASN79 9 was 25 ± 7%). Therefore the mutant receptor has a reduced ability to produce a functional output, however this is not as pronounced as at the GTPase level. It was reported that the Asn^{79} mutant receptor was able to couple to the inhibition of adenylyl cyclase and Ca^{2+} currents in mouse anterior pituitary cells, although the activation of K^+ currents was lost (Surprenant *et al.*, 1992) and when expressed in HEK 293 cells, the mutant receptor could also still couple to the inhibition of adenylyl cyclase but with reduced potency (Chabre *et al.*, 1994). In contrast, agonist stimulation of this mutant receptor failed to produce any effect on cAMP production in CHO cells (Wang *et al.*, 1991). Therefore the Asn^{79} receptor in Rat1 fibroblasts displayed a similar coupling ability to when it was expressed in pituitary and HEK 293 cells in that coupling to at least one of its effectors was still detectable.

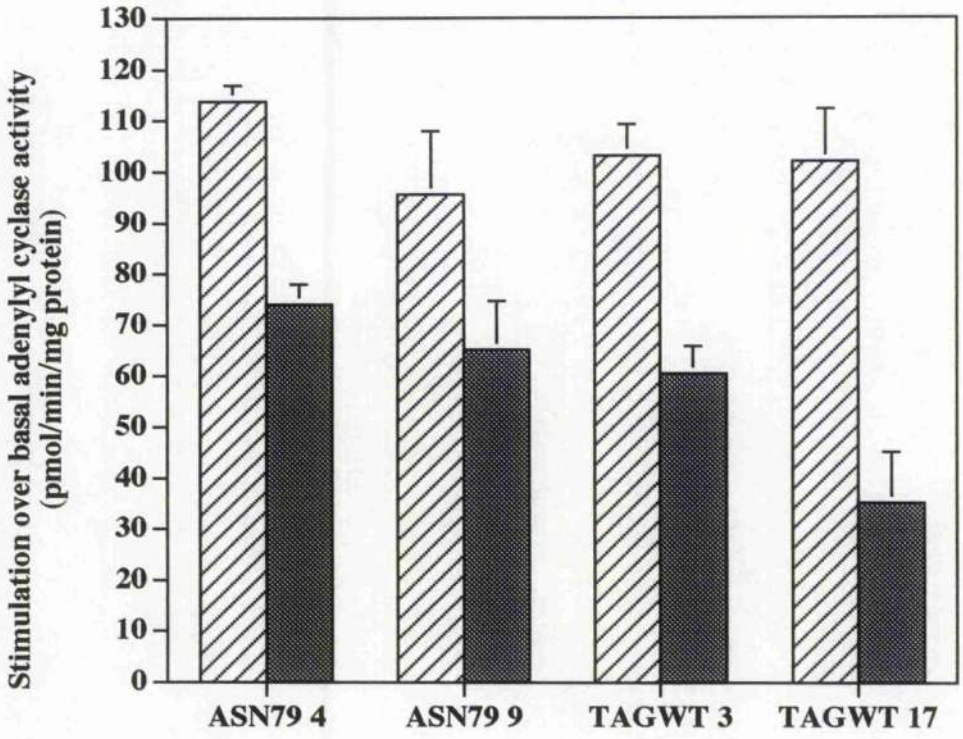

Figure 3.8 Inhibition of forskolin-amplified adenylyl cyclase activity by UK14304 in membranes of clones TAGWT and ASN79.

Adenylyl cyclase activity was determined as in Materials and Methods in membranes prepared from cells of the clones TAGWT and ASN79 as indicated. The basal activity was determined in the absence of any agonist and the stimulation over this activity on treatment with 10^{-5} M forskolin is represented by the hatched bars. The shaded bars represent the activity on treatment with both forskolin and 10^{-5} M UK14304 and thus the difference between these two values represent the inhibition of forskolin-amplified adenylyl cyclase activity by the agonist-stimulated α_{2A} adrenoceptor. Results shown are presented as mean ± SEM of triplicate assays from one of two or three independent experiments performed.

The extent of the similarity of signalling between the receptor expressed in Rat1 fibroblasts and pituitary cellular systems was then tested by attempting to determine whether the Asn^{79} receptor could still couple to the Ras.MAPK cascade. From the literature, coupling to the Ras.MAPK cascade can be mediated by the βγ complex (see Section 1.4.14.3.1) and the K^+ channel in pituitary cells may be regulated by G_i-protein coupled receptors via $G_{\beta\gamma}$ as well. It was of interest to determine if there was any selective loss of signalling pathways regulated by this mutant receptor in Rat1 fibroblasts and also to determine whether the efficiency of coupling of the receptor to the Ras.MAPK cascade was significantly less than to other effectors.

Figure 3.9 shows that treatment of serum starved cells of TAGWT and ASN79 clones with 10^{-6} M UK14304 for 5 min phosphorylated a significant proportion of the $p44^{MAPK}$ in the cells. The basal levels of phosphorylation in the absence of any ligand were somewhat variable ranging from 0% for TAGWT 3 to 40% for ASN79 9. The actual level of basal phosphorylation was not consistent over a number of passages but the significance of this observation is not clear. There was only a limited pattern to this level of 'basal' phosphorylation in that the cells expressing higher receptor levels invariably produced a larger basal level of phosphorylation (seen especially with TAGWT clones). Therefore some level of empty-receptor activation of the $p44^{MAPK}$ cascade might possibly have been observed (see chapter 4 for more on this).

It is obvious, however, that both of the TAGWT clones produced a strong phosphorylation of $p44^{MAPK}$ after treatment with UK14304. This would suggest that, in a similar fashion to what was observed at the level of adenylyl cyclase, there is no requirement to produce the maximum level of G-protein activation possible in these cells in order to produce a strong signal at the level of $p44^{MAPK}$. For many years it was suggested that the heterologously expressed G_i-coupled receptors could couple to the Ras.MAPK pathway because of the overexpression of such receptors in the experiments performed (see Malarkey *et al.*, 1995). However, this data would suggest that this is

not necessarily the case as the much lower expression level in TAGWT 3 was able to produce a substantial phosphorylation of $p44^{MAPK}$.

The UK14304-mediated phosphorylations of $p44^{MAPK}$ observed with both of the ASN79 clones (stronger in ASN79 9) are also in agreement with such a conclusion. These results also demonstrated that the Asn^{79} mutation did not produce a selective loss of coupling to the Ras.MAPK cascade but a reduction in coupling efficiency. Therefore the coupling efficiency to the Ras.MAPK pathway appears not to be substantially lower than that to adenylyl cyclase as both effects are reduced, but not eliminated by this mutation. When this mutant receptor was expressed in HEK 293 cells, the coupling to G_q and G_s-coupled effectors was selectively lost while the signalling through G_i-proteins was reduced (Chabre *et al.*, 1994). This was interpreted as a reduction in general G-protein coupling efficiency due to the mutation of the receptor with the selective elimination of those G-protein systems less efficiently coupled. Ceresa and co-workers suggested that the apparently selective effects of the mutation (such as in Surprenant *et al.*, 1992) may be explained by the difference in the stoichiometry of receptor-G-protein coupling required for each effect. They suggested that perhaps the activation of the K^+ channel was mediated by $\beta\gamma$ subunits and that this would explain the requirement for the greater stoichiometry. However, the results presented here would not really support this view because the coupling to the Ras.MAPK cascade (also mediated by $G_{\beta\gamma}$) was apparently not affected to a significantly greater extent than the inhibition of adenylyl cyclase (mediated selectively by $G_{i2\alpha}$, McClue *et al.*, 1992).

As would be expected with cells from the same parental Rat1 fibroblasts, EGF and LPA stimulated very similar levels of $p44^{MAPK}$ phosphorylation in all of the clones (Figure 3.9), demonstrating that the differences in the response to UK14304 was due to the expressed α_{2A} adrenoceptors.

Figure 3.9 Effect of UK14304, EGF and LPA on p44^{MAPK} phosphorylation in cells of clones TAGWT and ASN79.

A Serum starved cells of clones TAGWT 3 and 17 and ASN79 4 and 9 were treated for 5 min with serum free DMEM containing no agonist, 10^{-6} M UK14304, 10^{-8} M EGF or 10^{-5} M LPA. The cells were lysed according to the electrophoretic mobility shift assay (see 2.2.9.1) and fractions were resolved by SDS-PAGE in 6 M urea-containing polyacrylamide gels and immunoblotted for p44^{MAPK}. The shift from the higher mobility to the lower mobility form is representative of the phosphorylation of p44^{MAPK}.

B The percentage of the total detectable p44^{MAPK} which was present in the lower mobility form was then be calculated by densitometric scanning and this represented the percentage phosphorylation of p44^{MAPK} in these cells. The quantitation of the above immunoblot is shown where hatched bars represent no agonist, darkly shaded bars 10^{-6} M UK14304, striped bars with 10^{-8} M EGF and lightly shaded bars 10^{-5} M LPA.

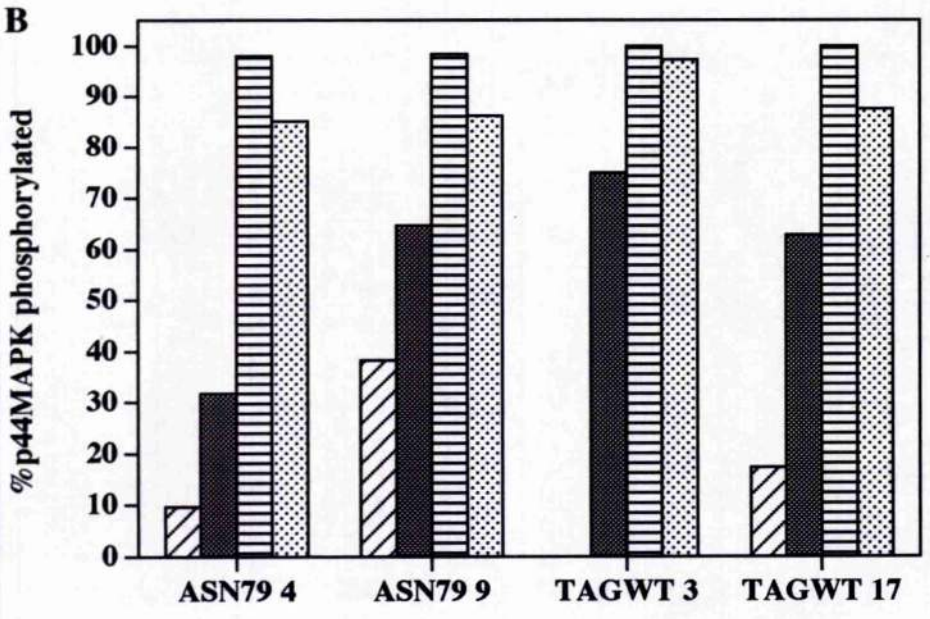

Figure 3.9A

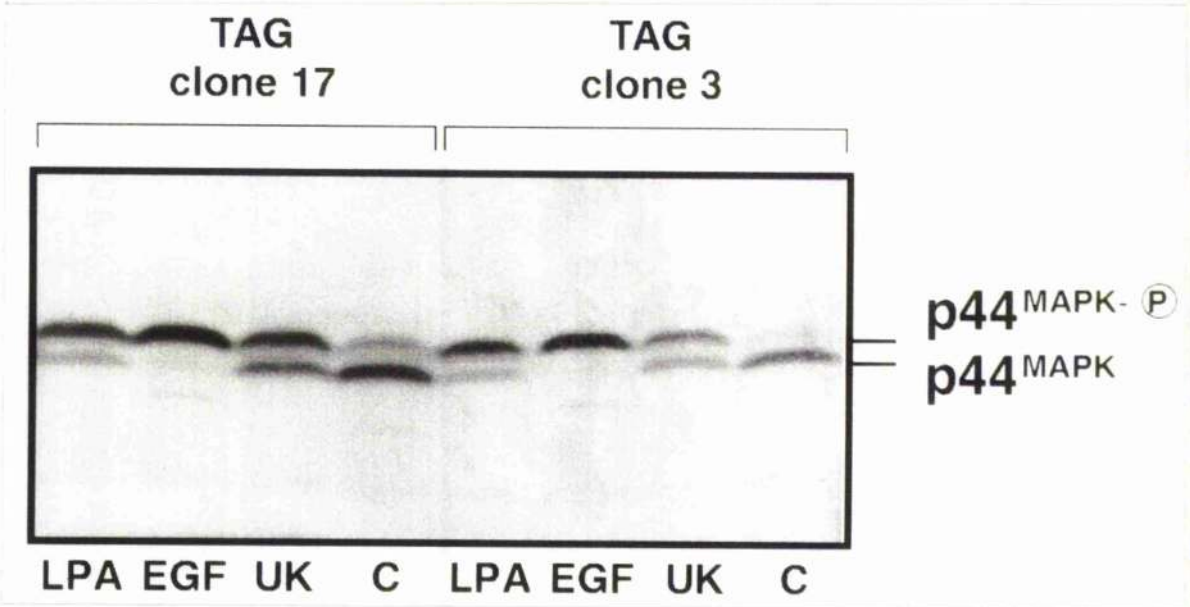
TAG
clone 17
TAG
clone 3
p44 MAPK- P
p44 MAPK
LPA EGF UK C LPA EGF UK C

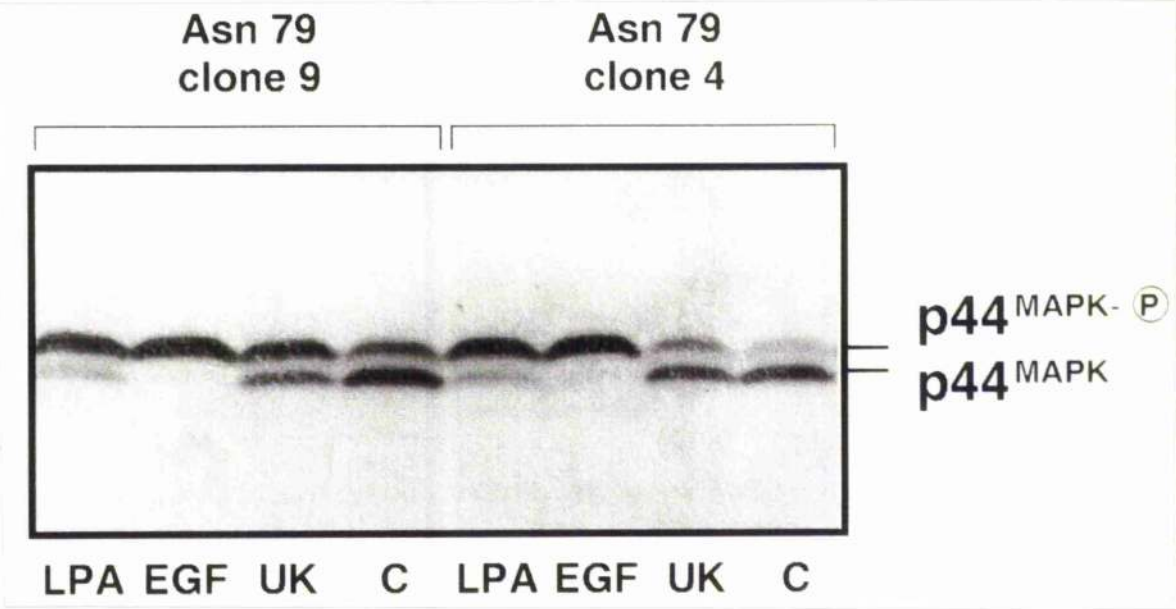
Asn 79
clone 9
Asn 79
clone 4
p44 MAPK- P
p44 MAPK
LPA EGF UK C LPA EGF UK C

The time courses of phosphorylation of $p44^{MAPK}$ by UK14304 were very similar in both the wild type and mutant α_{2A} adrenoceptor clones, as shown in Figure 3.10. It is obvious from Figure 3.10A that in both TAGWT clones, nearly all of the detectable $p44^{MAPK}$ was phosphorylated after 5 min of UK14304 treatment and this was sustained for at least 5 min. Thereafter the phosphorylation decreased, so that by 20 min, approximately 40% remained phosphorylated in clone TAGWT 17 and 20% in clone TAGWT 3. Therefore the only slight difference in the time courses between these two clones appears to be that the phosphorylation of $p44^{MAPK}$ was slightly more sustained in the higher receptor expressing clone. This would be consistent with the reported effects on the time course of $p42/44^{MAPK}$ activation by insulin or EGF in PC12 cells which overexpress either receptor and could be important for the determination of the functional response to the activation of the Ras.MAPK cascade by the α_{2A} adrenoceptor (see Section 1.4.15.1 and Chapter 4 discussion).

In the ASN79 clones, the highest detected level of phosphorylation was on average approximately 50% (Figure 3.10B). These clones followed a similar time course to the wild type clones, although some differences were detected. The maximum level of phosphorylation was achieved by 10 min, while typically only 50-70% of this maximum was seen after 5 min (the point at which the maximal level was achieved in the TAGWT clones). Only very limited detectable phosphorylation of $p44^{MAPK}$ persisted beyond 20 min. These differences between the time courses can perhaps be more clearly seen when the data is presented as a percentage of the maximum level of phosphorylation over the basal level achieved in each experiment for each clone (displayed in Figure 3.10C). Therefore the maximum effect and time course of phosphorylation of $p44^{MAPK}$ can be correlated to some extent to the level of G-protein coupling (as measured by the GTPase assay) in each of the clones. This will be discussed further in Chapters 4 and 5.

Figure 3.10 Time courses of the phosphorylation of $p44^{MAPK}$ by 10^{-5} M UK14304 in cells of clones TAGWT and ASN79.

Cells of TAGWT and ASN79 clones were treated with 10^{-5} M UK14304 for various times and the levels of phosphorylation of $p44^{MAPK}$ in these samples were determined as in Section 2.2.9.1.

A Percentage of the total detectable $p44^{MAPK}$ which was present after various times of treatment with 10^{-5} M UK14304 for clones TAGWT 3 (filled circles, full line) and for TAGWT 17 (open circles and broken line). Data is presented as mean ± SEM (n = 3).

B Percentage of the total detectable $p44^{MAPK}$ which was present after various times of treatment with 10^{-5} M UK14304 for clones ASN79 4 (open squares, broken line) and for ASN79 9 (filled squares and full line). Data is presented as mean ± SEM (n = 3).

C Results used to produce Figures 3.10A and B were converted to the percentage of the maximal phosphorylation of $p44^{MAPK}$ achieved over the basal level in each of the clones for each experiment, and the data was averaged. The clones are represented by the same symbols but SEM are not displayed in this graph for clarity of presentation.

Figure 3.10

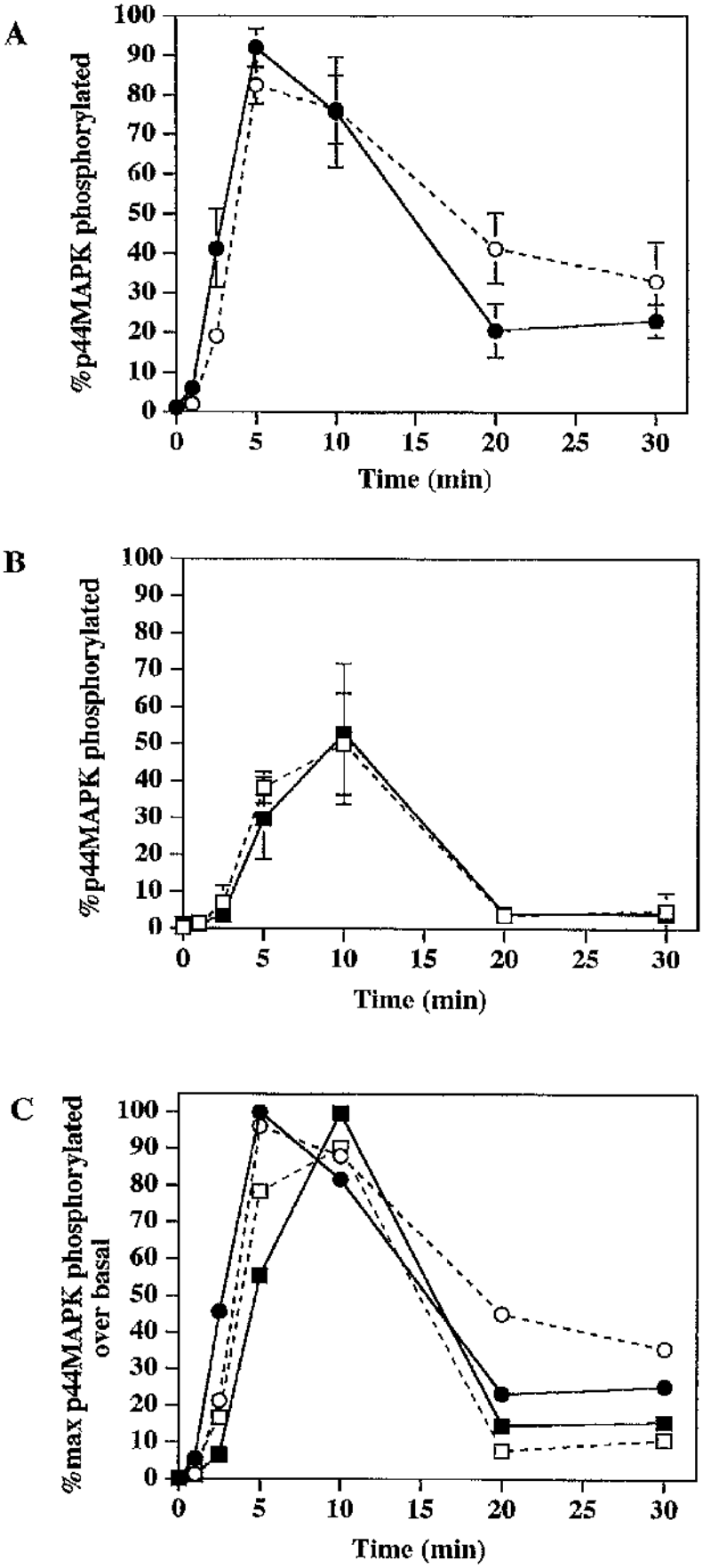
A
%p44MAPK phosphorylated
Time (min)
B
%p44MAPK phosphorylated
Time (min)
C
%max p44MAPK phosphorylated over basal
Time (min)

The assumption made above was that the observed differences between the time courses of the clones was solely due to the transfected adrenoceptors and their level of expression. This would seem reasonable because they were produced from the same parental cell line. The similarity in the time course of LPA-mediated $p44^{MAPK}$ phosphorylation (acting on endogenous receptors) in TAGWT 17 and ASN79 9 (Figure 3.11) clearly demonstrated that indeed there were no intrinsic differences in the time courses of phosphorylation of $p44^{MAPK}$ in these two clones.

Concentration-response curves to UK14304 in clones TAGWT 3 and 17 (Figure 3.12) clearly demonstrated that significantly ($p = 0.008$) higher concentrations of UK14304 were required to give half maximal agonist-mediated phosphorylation of $p44^{MAPK}$ in the lower expressing cell line (EC_{50} for TAGWT 17 = $1.3 \pm 0.6 \times 10^{-9}$ M (mean ± SEM, n = 4) and for TAGWT 3 = $1.7 \pm 0.5 \times 10^{-8}$ M (mean ± range, n = 2)). These values are similar to the EC_{50} values determined for the stimulation of high affinity GTPase activity in the same clones (3.7×10^{-9} M for TAGWT 17 and 3.0×10^{-8} M for TAGWT 3) and so can be explained in the context of a higher concentration of agonist being required in the lower expressing cells to provide the required level of G-protein stimulation to achieve stimulation of the MAPK cascade.

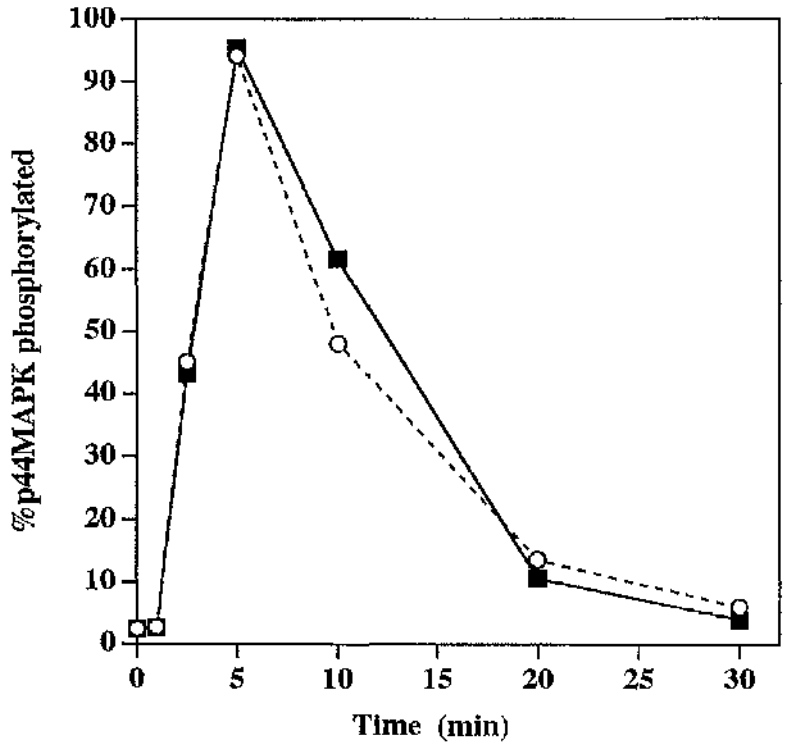

Figure 3.11 Time courses of the phosphorylation of $p44^{MAPK}$ by 10^{-5} M LPA in cells of clones TAGWT 17 and ASN79 9.

Cells of clones TAGWT 17 (open circles, broken line) and ASN79 9 (filled squares, full line) which had been serum starved for 24 hours were treated with 10^{-5} M LPA for various times and the levels of phosphorylation of $p44^{MAPK}$ in these samples were determined as in Section 2.2.9.1.

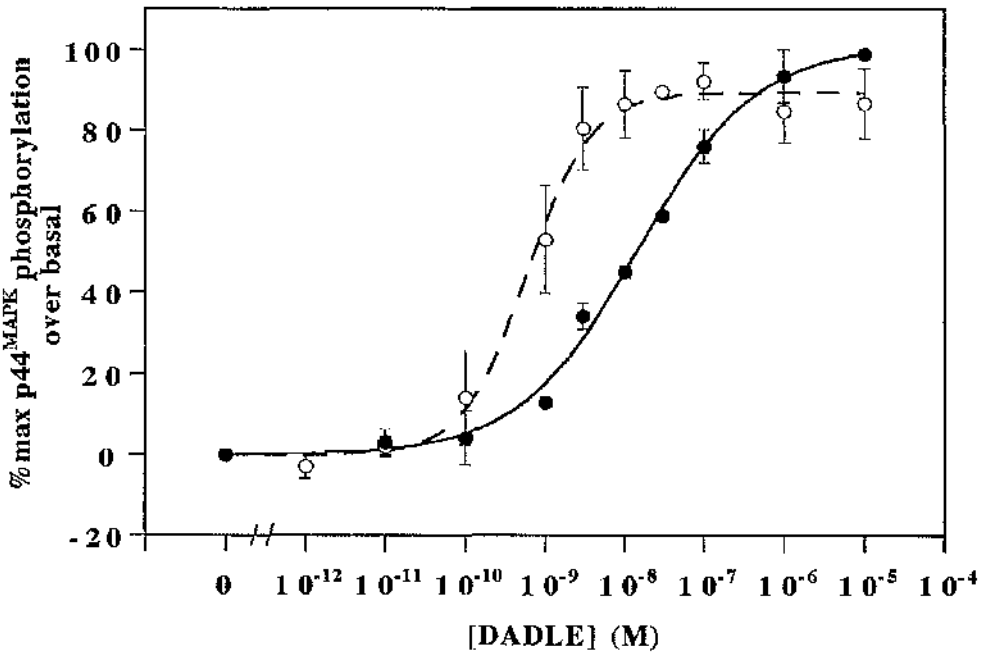

Figure 3.12 Concentration-response curves to UK14304 for p44^{MAPK} phosphorylation in cells of clone TAGWT 3 and TAGWT 17.

Serum starved cells of clones TAGWT 3 and TAGWT 17 were treated with various concentrations of UK14304 for 5 min and samples were analysed by SDS-PAGE and immunoblotted to determine the percentage of the total detectable p44^{MAPK} which was in its phosphorylated state as described in Section 2.2.9.1. Results were converted into percentages of the maximal level of phosphorylation achieved over the basal level in each experiment and are presented as the mean ± SEM (n = 4) for TAGWT 17 (open circles, broken line) and mean ± range (n = 2) for TAGWT 3 (filled circles, full line).

However there is some inconsistency with this data. Maximal phosphorylation of $p44^{MAPK}$ after 5 min UK14304 treatment was achieved in both TAGWT 3 and 17 clones. However, the level of G-protein activation which produced this maximal phosphorylation of $p44^{MAPK}$ in TAGWT 3 cells occurred in TAGWT 17 cells at a concentration of agonist which stimulated less than 50% of total $p44^{MAPK}$ phosphorylation. In other words, maximum phosphorylation of $p44^{MAPK}$ required nearly maximum G-protein activation in both clones. However, this maximum level of G-protein activation was very different in each of the clones and so different levels of G-protein activation in each clone were required to stimulate the activation $p44^{MAPK}$. A possible contribution to this inconsistency may be a variation of the receptor expression levels between the various passages. In addition the averaging of data from a number of experiments could magnify this inconsistency. A comparison between assays using membrane preparations and those in whole cells may be expected to produce inconsistencies like this, however no such problems were seen in similar experiments presented in Chapter 4.

It is of interest to note that the Hill coefficient for $p44^{MAPK}$ phosphorylation for clone TAGWT 17 was on average 1.2 ± 0.3 ($n = 4$), and for TAGWT 3 was 0.6 ± 0.06 ($n = 2$). These values are also similar to those achieved for GTPase activity (0.8 and 0.7 respectively). Therefore no co-operative nature was seen in the concentration-response curves for these receptors. The significance of these observations will be discussed in more detail in Chapter 4.

3.3 Conclusions

The work presented in this chapter attempted to further the knowledge of the control of the p42/44^{MAPK} cascade by the α_{2A} adrenoceptor when expressed in Rat1 fibroblasts. The first part of this chapter measured the activation of p44^{MAPK} by the agonist-stimulated human α_2-C10 adrenoceptor expressed in the 1C cell line and studied the effects of cAMP-elevating agents and a tyrosine kinase inhibitor in these cells. Although it is clear that the α_{2A} adrenoceptor's activation of the Ras.MAPK cascade is not mediated by an inhibition of adenylyl cyclase, the attenuation of UK14304 -mediated activation of p44^{MAPK} by dibutyryl cAMP or forskolin pretreatment demonstrated that these pathways do not act independently of each other. The data may also suggest that the inhibitory effect of the α_{2A} adrenoceptor on adenylyl cyclase could enhance the effect of the coupling to the p42/44^{MAPK} cascade. The enhanced effect of UK14304 and EGF on p44^{MAPK} activation after genistein pretreatment is in contrast with most of the reported effects of this agent and would appear to be unexplainable at this stage.

The second part of the chapter was concerned with determining the relative efficiency of the coupling of the adrenoceptor to the Ras.MAPK cascade and the effect of site directed mutagenesis of this receptor at residue Asp^{79}. Clones of Rat1 fibroblasts transfected with the wild type α_{2A} adrenoceptor displayed greater ability to couple to the G-protein machinery than clones expressing the Asn^{79} mutant receptor as measured by the agonist-mediated stimulation of GTPase activity and cholera toxin-catalysed ADP-ribosylation of G_i-like proteins. A similar effect was seen at the level of adenylyl cyclase, but the magnitude of the differences were less, possibly because the limiting factor in this system is the catalytic element of adenylyl cyclase. The effects seen in the two wild type clones could also be correlated to their relative receptor expression levels.

Both the wild type and Asn^{79} mutant receptors coupled to the phosphorylation of $p44^{MAPK}$ in all four clones studied. The time course of activation was studied for all clones as was the concentration-response relationships for both wild type clones. From the data produced it was concluded that significant phosphorylation of $p44^{MAPK}$ occurred with much less than full G-protein stimulation, indicating that the coupling efficiency of the receptor to the Ras.MAPK cascade is not exceptionally less than to adenylyl cyclase. Thus a large overexpression is not required in order for significant stimulation of the cascade to occur, although increased expression led to a more sustained time course and so perhaps a greater functional response. These results would indicate that the rate of phosphorylation and dephosphorylation is related to the level of G-protein activation achieved on agonist stimulation.

No selective loss of signalling ability to the Ras.MAPK cascade was determined for the Asn^{79} mutation but rather it appeared that a general reduction in coupling efficiency could explain the results presented. This manifested itself as a reduction in the maximum level of stimulation of $p44^{MAPK}$ phosphorylation achieved, coupled with a time course which displayed a delay in reaching the maximum level and a reduction in the length of time this level was sustained.

The concentration-response curves were difficult to interpret as they appeared not to be consistent with previous results. However, they did appear to correlate the level of G-protein stimulation with the level of phosphorylation of $p44^{MAPK}$ and showed that there was no co-operativity in this response The relation of G-protein activation to $p44^{MAPK}$ phosphorylation will be discussed further in the next chapter.

Chapter 4

Agonist-mediated regulation of $p42^{MAPK}$ and $p44^{MAPK}$ following expression of the mouse δ opioid receptor in Rat1 fibroblasts: effects of receptor expression levels and comparison with G-protein activation and coupling to other effectors.

Chapter 4: Agonist-mediated regulation of p42^{MAPK} and p44^{MAPK} following expression of the mouse δ opioid receptor in Rat1 fibroblasts: effects of receptor expression levels and comparison with G-protein activation and coupling to other effectors.

4.1 Introduction

The results presented in Chapter 3 provided information concerning the quantitative aspects of GPCR-regulation of the p42/44^{MAPK} cascade. However, there were some inconsistencies within this data which were difficult to reconcile. Another system was therefore chosen to attempt to reconcile some of these inconsistencies and to determine how general these observations were for G_i-coupled receptors expressed in fibroblasts. Previous work in the laboratory provided clones which expressed the mouse δ opioid receptor in Rat1 fibroblasts at two markedly different levels, and there is considerable pharmacology and signalling information available for this receptor. Therefore this seemed to be a potentially useful system.

The opioid receptors have been extensively studied because opioid drugs are the principal agents used for treating chronic severe pain. There are numerous ligands for these receptors (see Knapp *et al.*, 1995) displaying a range of effects and specificities and some of these will be used in Chapter 5. Pharmacological studies suggested the presence of three opioid receptor types (δ, μ and κ) and these have now been cloned and sequenced and shown to belong to the seven transmembrane-spanning GPCR family (Knapp *et al.*, 1995; Zaki *et al.*, 1996). These three types are very similar and display an overall homology of approximately 70%. Recent reports have suggested the presence of additional subtypes (Zaki *et al.*, 1996). Primary cellular responses of opioid receptors culminate in the inhibition of neuronal activity via inhibition of

adenylyl cyclase, increase in K^+ current, or inhibition of Ca^{2+} channel activity which are all mediated by pertussis toxin-sensitive G-proteins.

In a similar observation to that for the α_{2A} adrenoceptor, the δ opioid receptor which is expressed endogenously in mouse neuroblastoma x rat glioma hybrid (NG108-15) cells was shown to specifically couple to G_{i2} to inhibit adenylyl cyclase activity (McKenzie and Milligan, 1990). However, also in common with the α_{2A} adrenoceptor, functional coupling to multiple G_α subunits and other effectors has been demonstrated. Coupling of the δ opioid receptor to multiple members of the G_i-protein family was demonstrated in stably transfected CHO cells, and there was no requirement for overexpression of the receptor to force these interactions (Prather *et al.*, 1994). Coexpression studies in HEK 293 cells demonstrated the ability of the δ opioid receptor to couple to G_z (a member of the G_i-protein family which lacks the required Cys residue for pertussis toxin modification) and this coupling permitted opioid agonist-mediated inhibition of cAMP accumulation in a pertussis toxin-insensitive manner (Tsu *et al.*, 1995). Coupling of opioid receptors (μ and/or δ) to the stimulation of basal adenylyl cyclase activity, mediated apparently by G_s, has also been demonstrated (Cruciani *et al.*, 1993).

Other effectors of the δ opioid receptor have been described. These include a stimulatory effect on intracellular Ca^{2+} in differentiated NG108-15 cells which was observed at a lower agonist concentration than that required for the inhibitory effect (Jin *et al.*, 1992). A δ opioid receptor-mediated stimulation of type I phosphodiesterase activity in a pertussis toxin-insensitive manner was demonstrated in NG108-15 cells (Law and Loh, 1993). This was shown not to be due to an increase in intracellular Ca^{2+} levels. In addition, stimulation of PI-PLC activity has been observed as a consequence of agonist stimulation of the δ opioid receptor (Tsu *et al.*, 1995). In this case, the stimulation was sensitive to inhibition by pertussis toxin.

Previous studies on the δ opioid receptor in our laboratory have included an investigation of the spontaneous activity of the receptor to couple to G_i-like proteins in the absence of agonist treatment when expressed in Rat1 fibroblasts (Mullaney *et al.*, 1996). Agonist treatment ([D-Ala^2, D-Leu^5] enkephalin or DADLE) enhanced this activity and ICI 174864 acting as an inverse agonist attenuated this activity. These studies used a clonal cell line named clone D2 which expressed a considerable level (some 6 pmol/mg membrane protein) of the mouse δ opioid receptor cloned from a mouse brain cDNA library (Yasuda *et al.*, 1993) and measured the functional output at the level of the G-protein.

The δ opioid receptor displays many signalling properties similar (but not identical) to those described for the α_{2A} adrenoceptor (see Chapter 3) and so it was expected that this receptor would also display an ability to couple to the p42/44^{MAPK} cascade. This was indeed shown, and the availability of another clone which expressed the receptor in considerably lower levels (170 fmol/mg membrane protein, called clone DOE) provided data to support some of the conclusions made in chapter 3 such as the relation of expression levels to the time course of activation of p42/44^{MAPK}. Further study of this signalling ability uncovered some surprising conclusions in regard to the receptor and activated G-protein reserve and to the co-operativity which was present in these clones for the activation of p42/44^{MAPK}.

4.2 Results and Discussion

Rat1 fibroblasts (which do not endogenously express an opioid receptor) were cotransfected in a 10 : 1 ratio with pCMV-ms12 encoding the mouse δ opioid receptor (Yasuda *et al.*, 1993) and pBABE hygro, which permits the expression of resistance to hygromycin B. Clones which demonstrated resistance to 200 μg/ml hygromycin B were selected and expanded and the expression of the heterogenous receptor was determined by reverse transcriptase-polymerase chain reaction (RT-PCR) (results not shown but see Mullaney *et al.*, 1996) and expression of high-affinity binding sites for the opioid ligand [^{3}H]diprenorphine. Two clones of interest were chosen because of their considerably different levels of receptor expression. Clone D2 was found to express 6400 ± 100 fmol/mg membrane protein of the δ opioid receptor while clone DOE expressed considerably lower levels of 170 ± 30 fmol/mg membrane protein (mean ± SEM, n = 3 in each case).

The δ opioid receptor expressed in these clonal cell lines was effectively coupled to the cellular G-protein signal transduction machinery as evidenced by the ability of the δ opioid agonist DADLE to stimulate high affinity GTPase activity in both these clones (Figure 4.1). The stimulation of activity by a maximally effective concentration of DADLE (10^{-5} M) was found to be significantly ($p = 0.0001$) greater in membranes of clone D2 (20.9 ± 1.0 pmol/min/mg protein, mean ± SEM, n = 4) compared to clone DOE (6.9 ± 1.2 pmol/min/mg protein, mean ± SEM, n = 4). This is consistent with the higher receptor expression level in D2 cells which would be anticipated to permit greater coupling to the G-protein machinery. This coupling was predominantly, if not exclusively, to G-proteins which are members of the G_i-subfamily as pretreatment of these cells with pertussis toxin drastically attenuated the DADLE-mediated stimulation of GTPase activity.

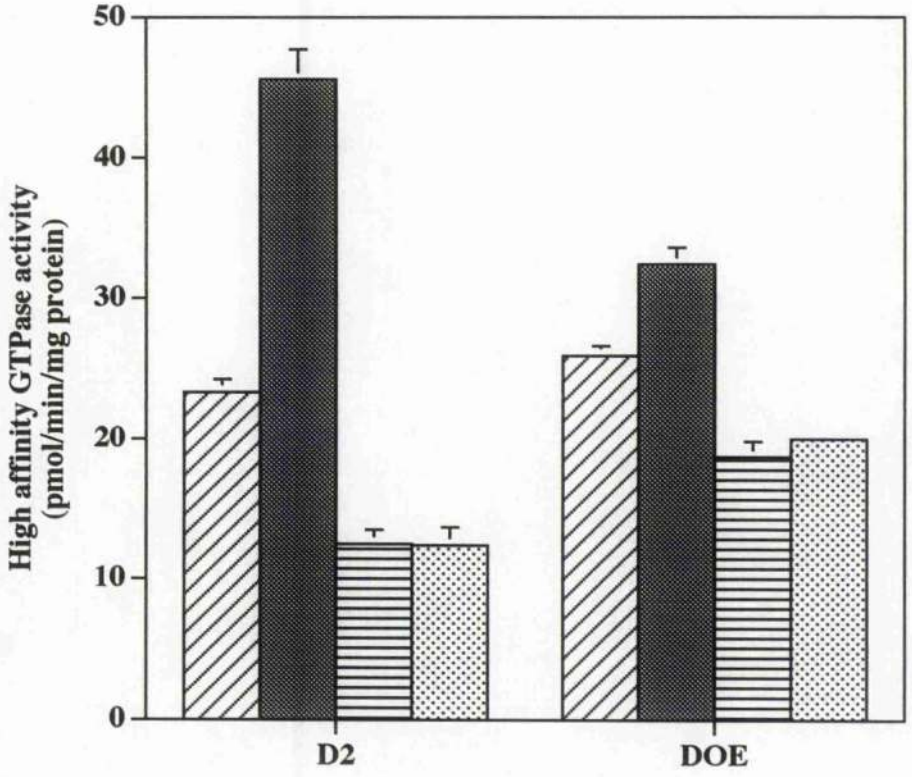

Figure 4.1 The effect of pertussis toxin on DADLE-mediated stimulation of high affinity GTPase activity in membranes of clones D2 and DOE.

Membrane preparations from cells of clone D2 and clone DOE which were either untreated or treated with 25 ng/ml pertussis toxin for 16 hours prior to harvesting, were assayed for basal and 10^{-5} M DADLE-stimulated high affinity GTPase activity as described in Section 2.2.4. Basal activity is represented by the hatched bars, DADLE-stimulated activity by the shaded bars, both in membranes from untreated cells. GTPase activities of membranes from pertussis toxin treated cells are represented by striped bars (basal) and speckled bars (10^{-5} M DADLE stimulated). Results represent mean ± SEM, of triplicate assays.

The coupling of the δ opioid receptor to the G-protein population in both clones was further demonstrated by the stimulation by DADLE of [^{35}S]GTPγS binding to membranes from these cells (Figure 4.2). It was obvious again that the stimulation of [^{35}S]GTPγS binding after DADLE treatment was greater in membranes of the higher expressing clone D2 compared to DOE (200 ± 8 compared to 17 ± 2 fmol/mg protein). In contrast, the stimulation of [^{35}S]GTPγS binding by 10^{-5} M LPA, acting at endogenous GPCRs (Figure 4.2), was very similar in both of the clones (32 ± 2 and 27 ± 2 fmol/mg protein for clone D2 and clone DOE respectively). This would indicate that the observed differences on stimulation with DADLE was indeed due to the level of expression of the δ opioid receptor and not some intrinsic property of the clonal cell line such as variation in G-protein level.

The functional interaction of these heterogenously expressed receptors and the G_i-like population of the cellular G-proteins was further shown by the ability of DADLE to stimulate cholera toxin-catalysed [^{32}P]ADP-ribosylation of G_i-like proteins in membranes from both clone D2 and DOE (Figure 4.3). The greater coupling to the G-protein machinery in D2 cells was again obvious from the considerably greater stimulation of cholera toxin-catalysed [^{32}P]ADP-ribosylation by maximally effective concentrations of DADLE in membranes of clone D2 as compared with membranes from clone DOE. Therefore three separate strategies demonstrated the ability of the δ opioid receptor expressed in Rat1 fibroblasts to functionally couple to G_i-like G-proteins and the considerably greater possible activation of the cellular G_i-like population in the higher expressing clone D2.

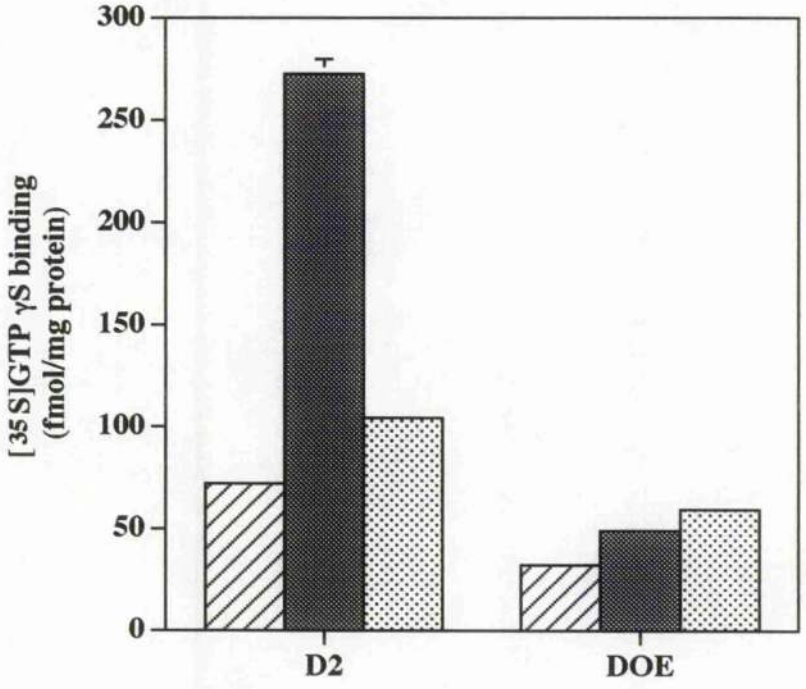

Figure 4.2 The effect of DADLE and LPA treatment on [^{35}S]GTPγS binding to membranes of clones D2 and DOE.

[^{35}S]GTPγS binding to membrane preparations of clones D2 and DOE was assessed with and without treatment with 10^{-5} M DADLE or 10^{-5} M LPA according to Section 2.2.5. Basal binding is represented by hatched bars, binding stimulated by 10^{-5} M DADLE is represented by the shaded bars and 10^{-5} M LPA by speckled bars. Results are presented as mean ± SEM, of triplicate assays.

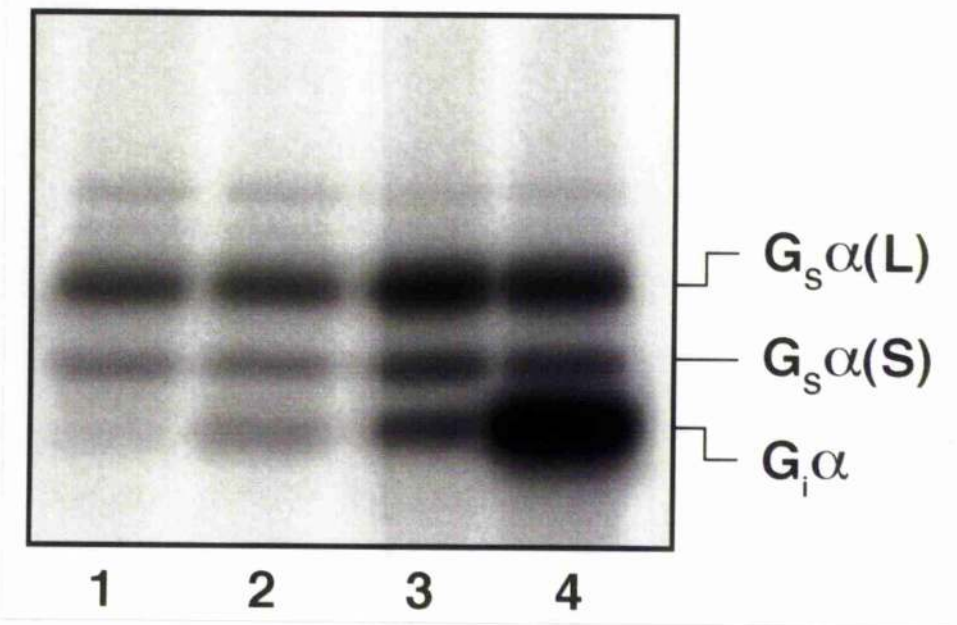

Figure 4.3 DADLE-mediated stimulation of cholera toxin-catalysed [^{32}P]ADP-ribosylation in membranes of clones D2 and DOE.

Cholera toxin-catalysed [^{32}P]ADP-ribosylation was performed as in Section 2.2.12 on membranes (20 μg) of either clone DOE (lanes 1-2) or clone D2 (lanes 3-4) in the absence (lanes 1 and 3) and presence (lanes 2 and 4) of 10^{-5} M DADLE. One representative autoradiograph is shown from four produced.

The greater level of expression of the receptor also altered the concentration of agonist which was required to produce stimulation of G-protein activation. This was illustrated by the concentration-response curves for DADLE-mediated stimulation of high affinity GTPase activity as shown in Figure 4.4. As the maximum output in the two clones was markedly different (see Figure 4.1), the results are presented as a percentage of the maximum achievable stimulation over the basal level in each of the clones. A significantly ($p = 0.03$) higher concentration of DADLE was required to produce half-maximal GTPase activity in cells of clone DOE ($EC_{50} = 4.2 \pm 0.6 \times 10^{-8}$ M, mean ± range, $n = 2$) compared to the higher expressing D2 cells ($EC_{50} = 5.7 \pm 2.2 \times 10^{-9}$ M, mean ± range, $n = 2$). The Hill coefficients for both clones ranged from 1.2 to 0.7 for the experiments performed. The significance of this observation will become clearer later.

These previous two conclusions that a greater activation of the G_i-like proteins was possible in the higher expressing clone D2 and that the concentrations of agonist required to produce a half-maximal response was less in the higher expressing clone were similar to those made for the α_{2A} adrenoceptor (Chapter 3). However, these results are distinctly different from observations made with the δ opioid receptor expressed in CHO cells where although the maximal G-protein response was greater with higher expression levels, the EC_{50} values did not show any change (Prather *et al.*, 1994).

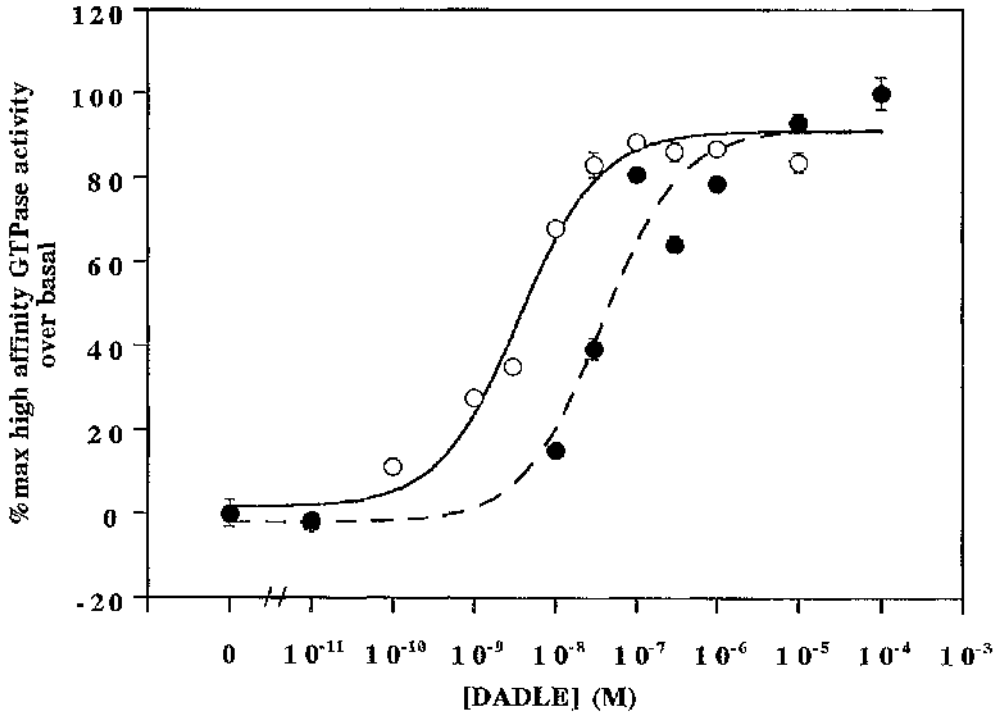

Figure 4.4 Concentration-response curves for DADLE-mediated stimulation of high affinity GTPase activity in membranes of clones D2 and DOE.

High affinity GTPase activity in response to various concentrations of DADLE was determined in membranes from cells of clone D2 (open circles and full line) and DOE (filled circles and broken line) as described in Section 2.2.4. The maximum DADLE-mediated stimulation of GTPase activity in the two clones were markedly different (between 27.1 and 29.1 pmol/min/mg protein for clone D2, and between 6.9 and 7.3 pmol/min/mg protein for clone DOE) and so the results are presented as a percentage of the maximum achievable stimulation over the basal level in each of the clones. Results are presented as mean ± SEM of triplicate assays, from one of two experiments performed.

As previously illustrated for both endogenously and heterologously expressed δ opioid receptors (e.g Knapp *et al.*, 1995; McKenzie and Milligan, 1990), agonist stimulation of the δ opioid receptor expressed in Rat1 fibroblasts inhibited forskolin-amplified adenylyl cyclase activity (Figure 4.5). This was mediated by G_i-like proteins as shown by the attenuation of this response after pretreatment of the cells with pertussis toxin. The percentage inhibition of forskolin-amplified adenylyl cyclase activity on treatment with a maximally effective concentration of DADLE was higher in clone D2 (37.7 ± 7.5%, mean ± SEM, n = 4) than in clone DOE (24.6 ± 5.2%, mean ± SEM, n = 5). This was as expected because of their respective receptor expression levels and a similar observation has been made before for this receptor (Tsu *et al.*, 1995). However, the difference in maximum output due to the receptor level was not as pronounced as that demonstrated at the level of G-protein activation (Figures 4.1 to 4.3). This supports the similar observation with the α_{2A} adrenoceptor expressed in these fibroblasts (Figure 3.8) which was interpreted to indicate that the catalytic element of adenylyl cyclase was the limiting factor in this system.

It is of interest to note that the basal level of adenylyl cyclase activity was consistently higher in membranes from cells of clone DOE in comparison with cells of clone D2 (Figure 4.5). This is consistent with the suggestion that a higher level of spontaneous activity would be produced when the receptor was expressed to higher levels (Mullaney *et al.*, 1996). This conclusion was also supported by the [^{35}S]GTPγS binding and agonist driven, cholera toxin-catalysed [^{32}P]ADP-ribosylation experiments. However, for some unknown reason, such an increased basal G-protein activation was not detected with the high affinity GTPase assays.

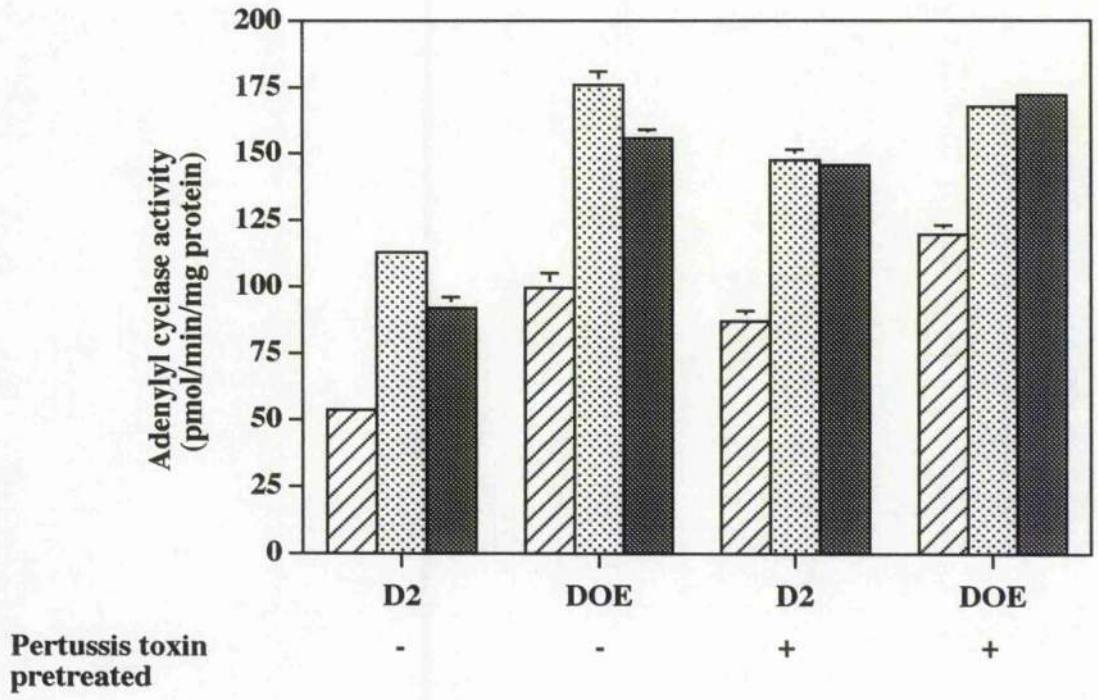

Figure 4.5 Inhibition of forskolin-amplified adenylyl cyclase activity by DADLE in membranes of clones D2 and DOE.

Adenylyl cyclase activity was assayed in membranes from cells of clone D2 and clone DOE, with and without pertussis toxin pretreatment (25 ng/ml for 16 hours) as described in Section 2.2.6. Basal activity is represented by the hatched bars, the activity on treatment with 10^{-5} M forskolin is represented by the speckled bars and the activity after treatment with both 10^{-5} M forskolin and 10^{-5} M DADLE is represented by the shaded bars. Results are presented as mean ± SEM of triplicate assays.

When the α_{2A} adrenoceptor was expressed in Rat1 fibroblasts, agonist treatment stimulated PLD-mediated hydrolysis of phosphatidylcholine in addition to adenylyl cyclase inhibition and both effects were mediated by G_i-like proteins (MacNulty *et al.*, 1992). In addition, opioid peptide mediated-stimulation of PLD activity has been reported (Mangoura and Dawson, 1993). It was subsequently discovered that the δ opioid receptor displayed a similar signalling ability when expressed in Rat1 fibroblasts as evidenced by the stimulation of transphosphatidylation in [^{3}H]palmitate labelled cells. Figure 4.6 shows that in cells of both clones D2 and DOE, 10^{-5} M DADLE stimulated the transphosphatidylation activity as determined by the radioactivity present in the phosphatidylbutanol-containing band after thin layer chromatography. As was expected, maximally effective concentrations of ET-1 (acting on endogenously expressed $G_{q/11}$-coupled receptors) and LPA also stimulated PLD activity. ET-1 consistently demonstrated the strongest stimulation of PLD activity in both clones which was also expected due to its known signalling properties. However it is obvious that the tyrosine kinase linked receptor agonist, EGF, did not significantly stimulate this activity.

Direct comparison of the absolute levels of transphosphatidylation activity between the clones was not possible as correction for variation in the numbers of cells assayed or the labelling efficiency in each clone was not performed. Each experiment therefore depended on plating down similar numbers of cells in each well when the plates were seeded. However, DADLE-mediated transphosphatidylation activity was consistently stronger in cells of D2 as compared with DOE. This can be clearly demonstrated if the DADLE-mediated stimulation is calculated as a percentage of the stimulation obtained with ET-1 (34 ± 1.5% of the ET-1 response in D2 cells, and 16 ± 1.6% in DOE cells, mean ± SEM, n = 3). Therefore, once again the greater expression of the δ opioid receptor in clone D2 permitted coupling of the receptor to the effector (in this case PLD) to a greater extent than in clone DOE.

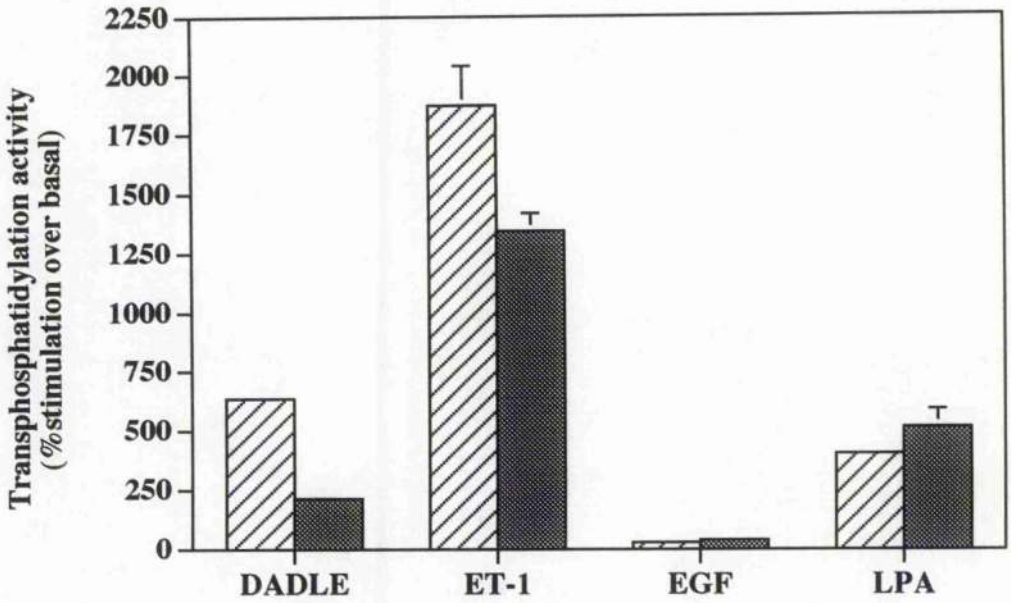

Figure 4.6 Transphosphatidylation activity in response to various ligands in [^{3}H]palmitate-labelled cells of clones D2 and DOE.

The transphosphatidylation activity was determined in cells of clone D2 (hatched bars) and clone DOE (shaded bars) which had been labelled with 4 μCi/ml [^{3}H]palmitate for 24 hours. Stimulation by 10^{-5} M DADLE, 10^{-7} M ET-1, 10^{-8} M EGF and 10^{-5} M LPA was performed in HBGbutanol as described in Section 2.2.10 for 15 min prior to stopping the reaction with ice-cold methanol. Phase separation was performed and the aqueous layers were subjected to thin layer chromatography and bands containing phosphatidylbutanol (as detected by an internal standard after iodine staining) were counted by liquid scintillation. Results (mean ± SEM, of triplicate assays) are presented as the percentage activation achieved by each of the agonists over the basal activity in each of the clones.

The coupling of the δ opioid receptor to PLD was indeed mediated by G_i-like proteins as shown by the complete attenuation of this response after pertussis toxin pretreatment (Figure 4.7). As stated before, ET-1 acts on $G_{q/11}$-coupled receptors and so its response was, not surprisingly, unaffected by pertussis toxin.

The time course of DADLE-mediated activation of PLD was quite distinct from that induced by ET-1 (Figure 4.8). Production of phosphatidylbutanol was complete within 2 min of stimulation with 10^{-5} M DADLE, and levels were maintained thereafter. In contrast, the rate of production of phosphatidylbutanol was greater with ET-1 and continued beyond 2 min although the rate of production began to decrease after 5 min. These differences may be produced because the δ opioid receptor activated PLD through G_i-proteins but the endothelin receptor used $G_{q/11}$-proteins. However, the stimulation of PLD activity was apparently rapidly desensitised for both receptors and so the difference in time courses may reflect variation in rates of receptor desensitisation. This result is similar to the observed time course of activation of PLD by agonist-stimulated thrombin and m1 muscarinic receptors in hamster lung fibroblast-derived cell lines (McKenzie *et al.*, 1992).

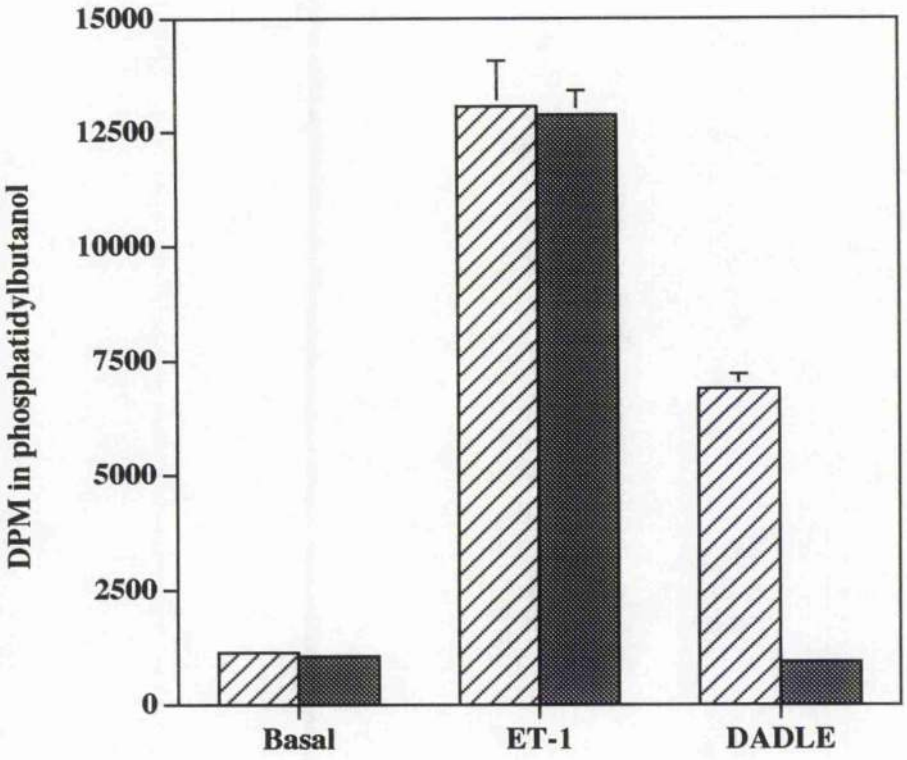

Figure 4.7 The effect of pertussis toxin pretreatment on ET-1 and DADLE-mediated stimulation of transphosphatidylation activity in cells of clone D2.

The transphosphatidylation activity in [^{3}H]palmitate (4 μCi/ml) labelled D2 cells was determined as in Section 2.2.10 with (shaded bars) and without (hatched bars) pertussis toxin pretreatment (25 ng/ml for 16 hours). Stimulation by no agonist (basal), 10^{-7} M ET-1 and 10^{-5} M DADLE was performed for 15 min. Results are presented as mean ± SEM, of triplicate assays from one experiment of two performed.

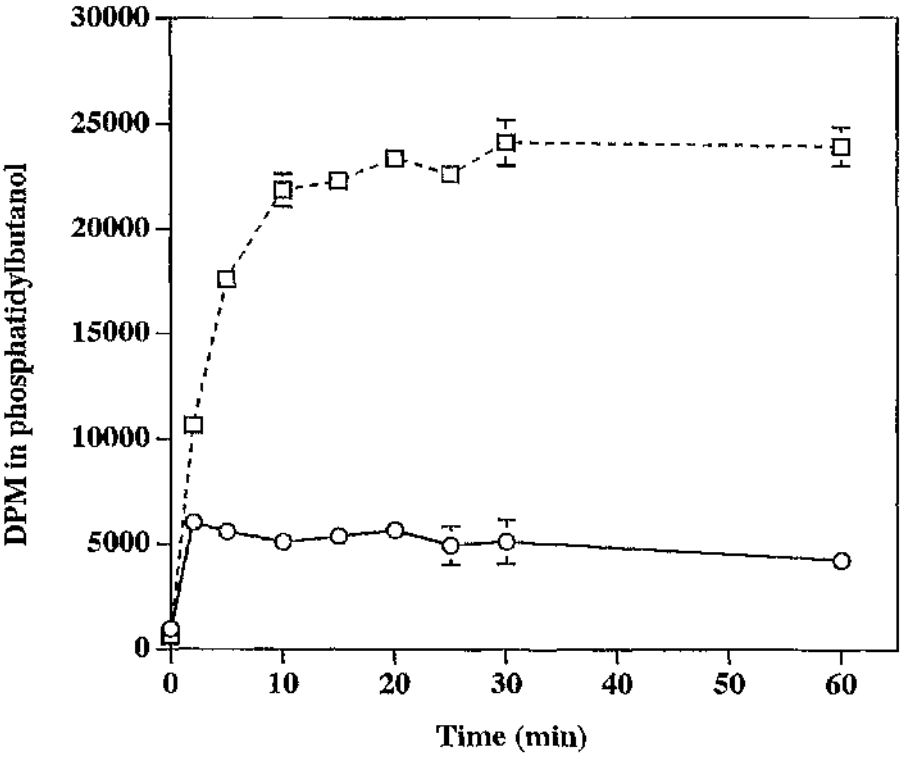

Figure 4.8 Time course of ET-1 and DADLE-mediated stimulation of transphosphatidylation activity in [^{3}H]palmitate labelled cells of clone D2. [^{3}H]palmitate labelled (4 μCi/ml) cells of clone D2 were treated with 10^{-5} M DADLE (open circles, full line) or 10^{-7} M ET-1 (open squares, broken line) in the presence of butan-1-ol for various times and transphosphatidylation activity was assayed as described in Section 2.2.10. Results are presented as mean ± SEM (of triplicate assays) for ET-1, and mean ± SEM (of three independent experiments) for DADLE, of measured DPM in the phosphatidylbutanol-containing band of the thin layer chromatography plate.

It can be seen from Figure 4.8 that 15 min treatment of agonist produced a response that was maximal for both ET-1 and DADLE. This result therefore justifies the use of a 15 min time point for treatments in the experiments presented in Figures 4.6 and 4.7. In subsequent concentration-response curves, treatments with various concentrations of DADLE in cells of clone D2 and DOE were also performed for 15 min (Figure 4.9). There was only a very limited response to DADLE in cells of clone DOE and so the concentration-response curves were difficult to produce and the shape of the curve was quite different from clone D2. Therefore, although the calculated EC_{50} value (2.3×10^{-9} M) is apparently lower than that for D2 cells, it can be seen that this is not because the stimulation of PLD activity is detectable at a lower concentration of DADLE, but rather that the maximal stimulation is achieved very abruptly. The average EC_{50} value calculated from the concentration-response curves to DADLE in clone D2 was $2.5 \pm 0.6 \times 10^{-8}$ M (mean ± SEM of three independent experiments) and the Hill coefficient was 1.0 ± 0.3. These values were very similar to those for the GTPase activity and so would correlate the level of transphosphatidylation activity with the level of G-protein activation.

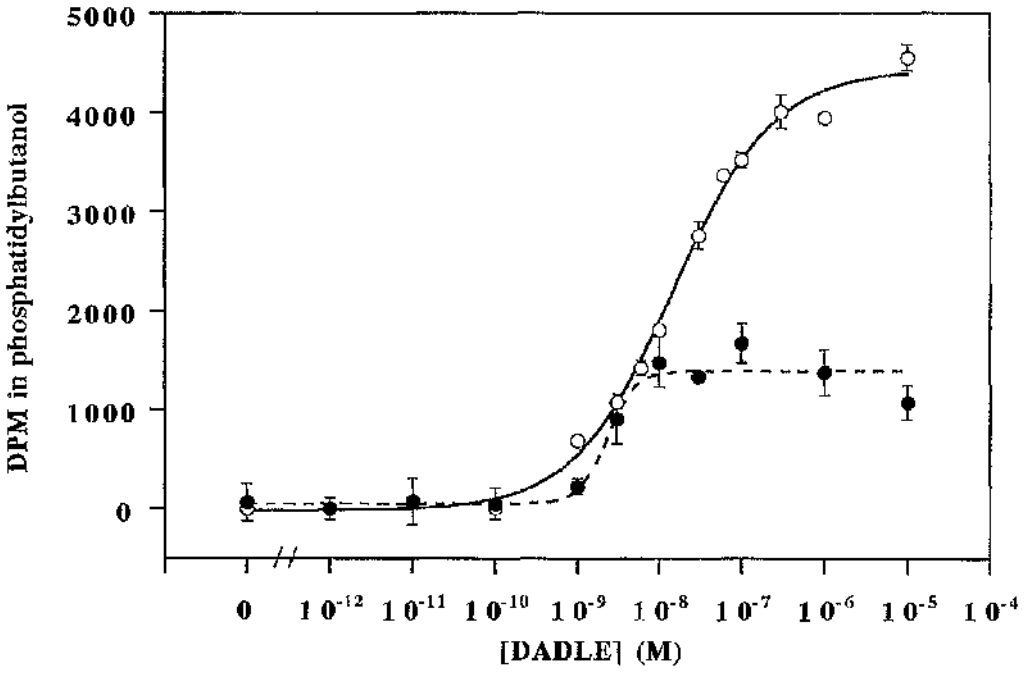

Figure 4.9 Concentration-response curves of DADLE-mediated stimulation of transphosphatidylation activity in cells of clones D2 and DOE.

[^{3}H]palmitate labelled (4 μCi/ml) cells of clone D2 (open circles, full line) and DOE (filled circles, broken line) were treated with various concentrations of DADLE for 15 min in the presence of butan-1-ol and the transphosphatidylation activity was assayed as described in Section 2.2.10. Results are presented as mean ± SEM of triplicate assays from one representative experiment of three performed.

The activation of PLC by the α_{2A} adrenoceptor in Rat1 fibroblasts was reported as negligible (MacNulty *et al.*, 1992), however an activation of PLC activity was reported for the δ opioid receptor expressed in Ltk$^-$ fibroblasts (Tsu *et al.*, 1995). This was also detected in cells of clone D2 on treatment with 10^{-5} M DADLE (Figure 4.10). The response was rather variable over the experiments which were performed with between 480% and 100% increase of activity over basal levels on treatment with DADLE. Pretreatment of the cells with pertussis toxin attenuated the response to DADLE, and so would indicate that this response was mediated by G_i-like proteins, however some DADLE-mediated activation was still detectable over the basal level (which also was often increased on pertussis toxin pretreatment). The response to ET-1 was of a similar magnitude, and as expected for a $G_{q/11}$-protein coupled agonist, was largely unaltered after pretreatment with pertussis toxin. However, some reduction in ET-1-mediated activation was sometimes seen after pertussis toxin treatment, but may be partly explained by the previously mentioned altered basal levels. The significance of the slightly unusual aspects of these results is not known.

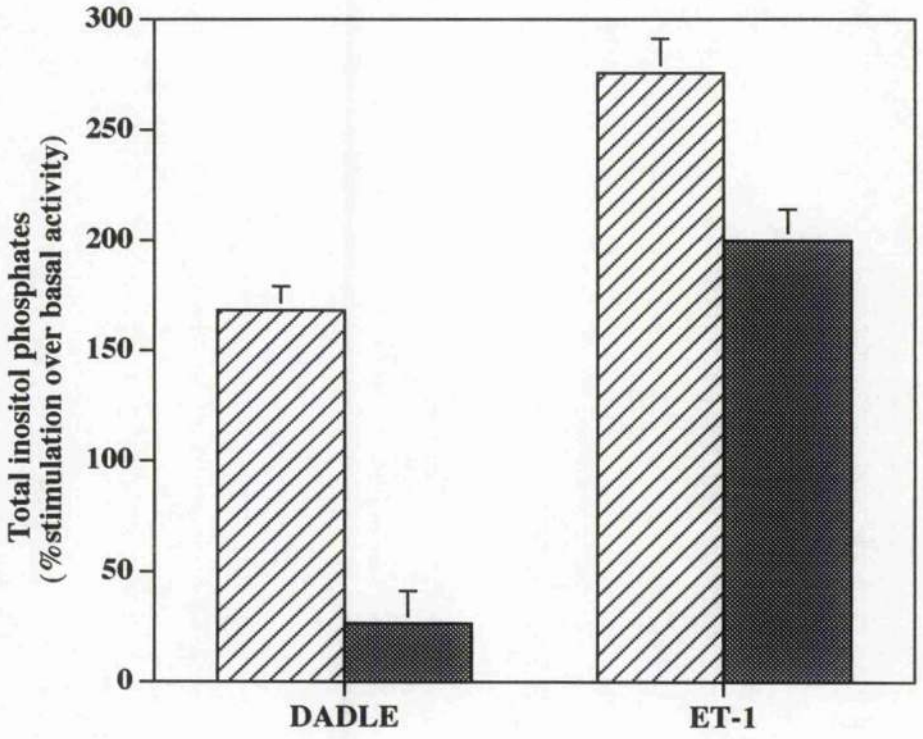

Figure 4.10 The effect of pertussis toxin pretreatment on the stimulation of production of total inositol phosphates by DADLE and ET-1 in cells of clone D2. Cells of clone D2 were labelled with [^{3}H]inositol (1.5 μCi/ml, 24 hours) in inositol free medium with (shaded bars) and without (hatched bars) pertussis toxin pretreatment (25 ng/ml for 24 hours) and stimulated with 10^{-5} M DADLE or 10^{-7} M ET-1 in the presence of Li^+ for 10 min as described in Section 2.2.11. The radioactivity associated with the total inositol phosphates was determined by batch elution from Dowex formate. Results are presented as percentage stimulation of activity over the basal level, mean ± SEM of triplicate assays, and is a representative experiment of three performed.

The above results demonstrated the coupling of the δ opioid receptor via G_i-like proteins to adenylyl cyclase, PLD and PLC. As mentioned previously, the signalling of this receptor in Rat1 fibroblasts was very similar to that described for the α_{2A} adrenoceptor (Chapter 3) and so it was no surprise that the agonist-stimulated δ opioid receptor was able to activate $p42/44^{MAPK}$. Treatment of serum starved cells of clone D2 and clone DOE with maximally effective concentrations of DADLE for 5 min stimulated the phosphorylation of virtually the entire population of $p44^{MAPK}$ as detected by immunoblotting with a specific anti-$p44^{MAPK}$ antibody (Figure 4.11). This phosphorylation was seen as a gel shift from the higher mobility unphosphorylated form to the lower mobility, phosphorylated form and the data is presented as the percentage of the total detected $p44^{MAPK}$ which was in the phosphorylated form. DADLE failed to have any effect on the phosphorylation of $p44^{MAPK}$ in serum starved parental Rat1 fibroblasts but in all three cell lines, 5 min treatment with maximally effective concentrations of EGF phosphorylated the entire population of $p44^{MAPK}$ (Figure 4.11). For cells of clone D2 the average percentage phosphorylations of $p44^{MAPK}$ were 22 ± 6% (basal), 92 ± 3% (10^{-5} M DADLE) and 99 ± 1% (10^{-8} M EGF) and for cells of clone DOE were 12 ± 5% (basal), 94 ± 2% (10^{-5} M DADLE) and 99 ± 1% (10^{-8} M EGF), mean ± SEM from at least 6 independent experiments. Stimulation of the phosphorylation on tyrosine residues of proteins apparently corresponding to $p42^{MAPK}$ and $p44^{MAPK}$ by DADLE and EGF in cells of clone D2 was also demonstrated by means of immunoblotting with a phosphotyrosine specific antiserum (data not shown).

Therefore in contrast to the other effects measured, apparently maximum output could be achieved in the lower receptor expressing clone DOE. In these clones (in a similar manner to what was seen with clone TAGWT 3 in Chapter 3), maximum G-protein activation was not required in order to stimulate maximal phosphorylation of $p44^{MAPK}$ as measured after 5 min agonist treatment.

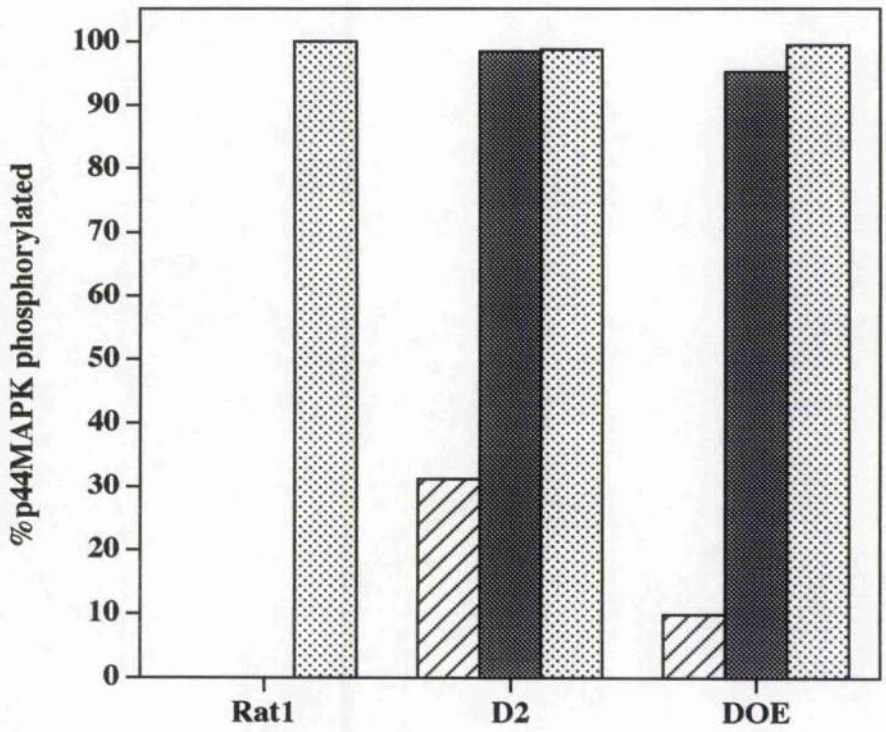

Figure 4.11 Effect of DADLE and EGF on the phosphorylation of $p44^{MAPK}$ in cells of clones D2 and DOE and in parental Rat1 fibroblasts.

Serum starved cells of clone D2, DOE or parental Rat1 fibroblasts were treated for 5 min with serum free DMEM containing no agonist (hatched bars), 10^{-5} M DADLE (shaded bars) or 10^{-8} M EGF (speckled bars). The phosphorylation of $p44^{MAPK}$ was then measured by the electrophoretic mobility shift assay as described in Section 2.2.9.1. This assay involved subjecting the cell lysates to SDS-PAGE (in the presence of 6 M urea) and immunoblotting with an antiserum specific for $p44^{MAPK}$. The proportion of the total detectable $p44^{MAPK}$ which was present in the lower mobility, phosphorylated form was then calculated by densitometric scanning. Results for clones D2 and DOE are representative of at least six experiments performed.

As expected, the phosphorylation of $p44^{MAPK}$ was associated with an increase in the activity of $p42/44^{MAPK}$ (Figure 4.12). These results were obtained with the Biotrak p42/44 MAP kinase activity assay (Amersham) which measured the labelling of a peptide specific for $p42^{MAPK}$ and $p44^{MAPK}$ with [^{32}P] which was determined by liquid scintillation counting (Section 2.2.9.3). With this assay, the measured activity stimulated by maximally effective concentrations of DADLE in cells of clone DOE was often lower than that seen in cells of clone D2. This was also commonly seen for treatment with EGF, but the maximum response of DADLE was of a similar magnitude to the maximum EGF response. This was interpreted to imply that a similar maximum level of activation was achieved in each clone on DADLE treatment and that the differences in actual levels of activity was somehow related to clonal differences. The actual measured activity did vary quite substantially between different experiments, however the same basic effects of the ligands were noted each time. DADLE and EGF-mediated stimulation of $p44^{MAPK}$ activity was also demonstrated using the IP kinase method (Section 2.2.9.2) where the activity of immunoprecipitated $p44^{MAPK}$ was determined by its ability to [^{32}P]-label exogenously added myelin basic protein (data not shown).

The phosphorylation of $p44^{MAPK}$ stimulated by DADLE in clones DOE and D2 was attenuated by pretreating the cells with pertussis toxin (Figure 4.13 and data not shown). Pertussis toxin displayed a similar effect on the LPA-mediated phosphorylation of $p44^{MAPK}$, but had no effect on the phosphorylation stimulated by EGF. This is consistent with both LPA and DADLE signalling via G_i-like proteins and EGF acting on a tyrosine kinase-linked receptor. Pertussis toxin pretreatment also sometimes reduced the basal level of phosphorylation of $p44^{MAPK}$, however, this was not always observed.

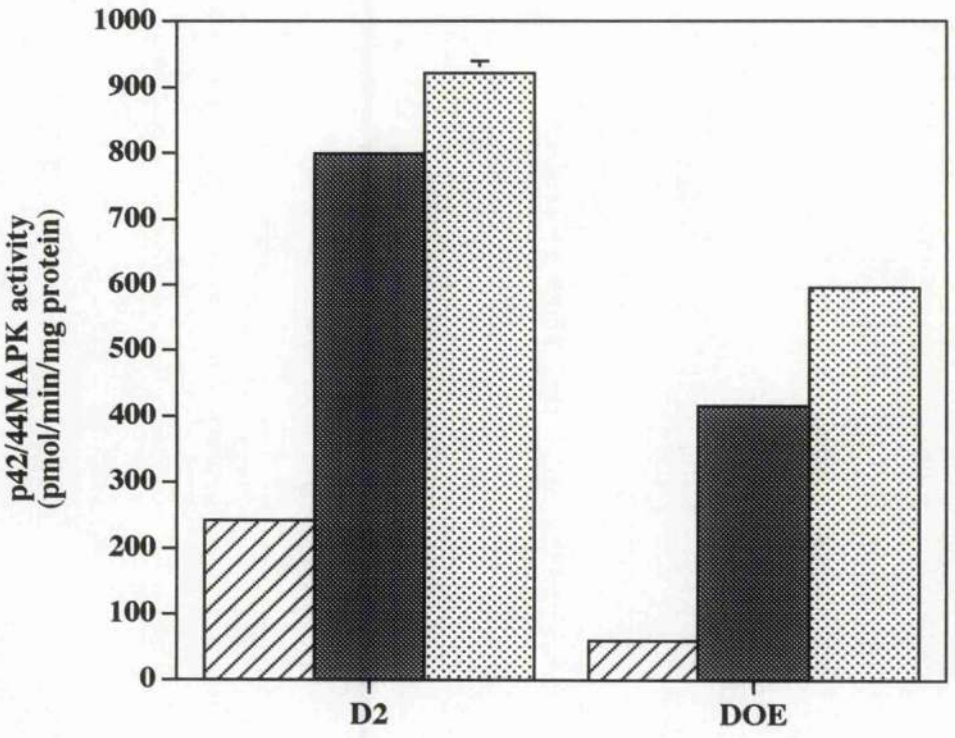

Figure 4.12 Stimulation of p42/44^{MAPK} activity in cells of clones D2 and DOE by EGF and DADLE.

Serum starved cells of clone D2 or clone DOE were treated for 7.5 min with serum free DMEM containing no agonist (hatched bars), 10^{-5} M DADLE (shaded bars) or 10^{-8} M EGF (speckled bars). The activity of p42/p44^{MAPK} in cellular lysates was then measured by the Biotrak p42/44 MAP kinase activity assay (Amersham) as described in Section 2.2.9.3. The activity of the p42/44^{MAPK} was calculated as pmol phosphate transferred/min/mg protein. Results are presented as mean ± range of duplicate assays from a representative experiment of two (D2) or three (DOE) performed.

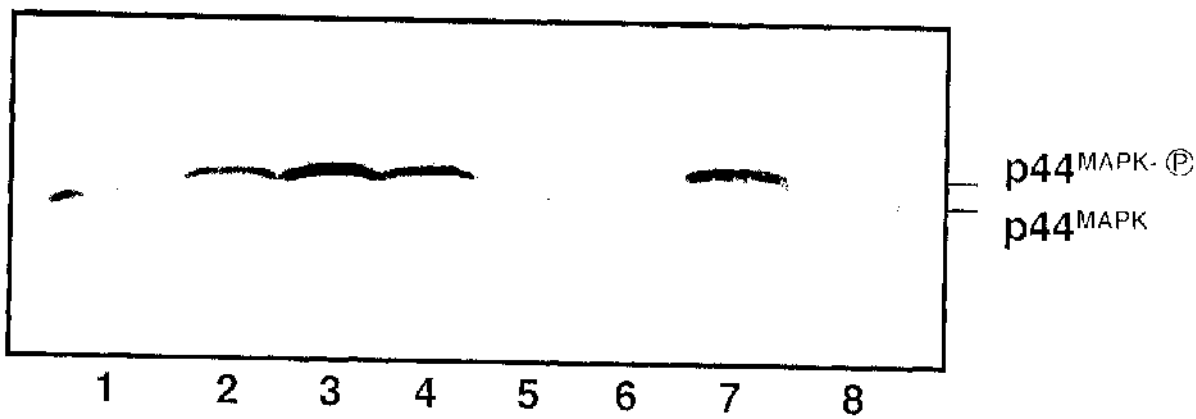

Figure 4.13 Effect of pertussis toxin on $p44^{MAPK}$ phosphorylation stimulated by DADLE, LPA and EGF in cells of clone DOE.

Serum starved cells of clone DOE, some of which had been pretreated for 16 hours with 25 ng/ml pertussis toxin, were stimulated for 5 min with serum free DMEM containing no agonist (lanes 1 and 5), 10^{-6} M DADLE (lanes 2 and 6), 10^{-8} M EGF (lanes 3 and 7) or 10^{-5} M LPA (lanes 4 and 8). The cells were lysed according to Section 2.2.9.1, fractions resolved by SDS-PAGE (in the presence of 6 M urea) and immunoblotted with a specific antiserum raised against $p44^{MAPK}$. A representative immunoblot is shown. Lanes 5-8 were pretreated with pertussis toxin, lanes 1-4 were not.

In order to prove that DADLE-mediated phosphorylation of $p44^{MAPK}$ was indeed mediated by the transfected δ opioid receptor, the ability of naloxone (a general opioid receptor antagonist (Knapp *et al.*, 1995)) to prevent the effect of DADLE was investigated in DOE and D2 cells (Figure 4.14 and data not shown). In cells of clone DOE, the presence of 10^{-5} M naloxone significantly reduced and totally prevented the phosphorylation of $p44^{MAPK}$ stimulated by 10^{-6} M and 10^{-8} M DADLE, respectively. In D2 cells, an inhibitory effect could only be seen on 10^{-8} M DADLE-mediated phosphorylation. Therefore, it would appear that higher concentrations of the agonist can compensate for the actions of the antagonist as anticipated for a competetive interaction. However, the ability of this antagonist to have any inhibitory effect would support the conclusion that the phosphorylation of $p44^{MAPK}$ by DADLE is indeed mediated by the opioid receptor. As expected naloxone had no effect on EGF-mediated phosphorylation of $p44^{MAPK}$ in either clone.

It was noted in several experiments that $p44^{MAPK}$ was not always totally unphosphorylated after 5 min of treatment with serum free DMEM without any agonist. There seemed to be some pattern to this in that the basal levels of phosphorylation in the DOE cells and in the parental Rat1 fibroblasts were commonly lower than that seen in cells of clone D2 (for an example see Figure 4.11). It was suggested that this could be a manifestation of spontaneous activity (mentioned above). In order to investigate this, the phosphorylation of $p44^{MAPK}$ in serum starved cells of clone D2, clone DOE and parental Rat1 fibroblasts was monitored after various times of incubation with serum free DMEM (Figure 4.15). In cells of clone D2, a peak of $p44^{MAPK}$ phosphorylation which was stimulated only by the change of medium was commonly seen, but the magnitude of this peak was highly variable and sometimes it was not detected at all. A much more limited agonist-independent phosphorylation was observed in cells of clone DOE, and no effect was seen in the parental Rat1 fibroblasts. $p42/44^{MAPK}$ activity in these 'basal' conditions as measured with the Biotrak activity assay, followed a similar pattern as the phosphorylation of $p44^{MAPK}$ (data not shown).

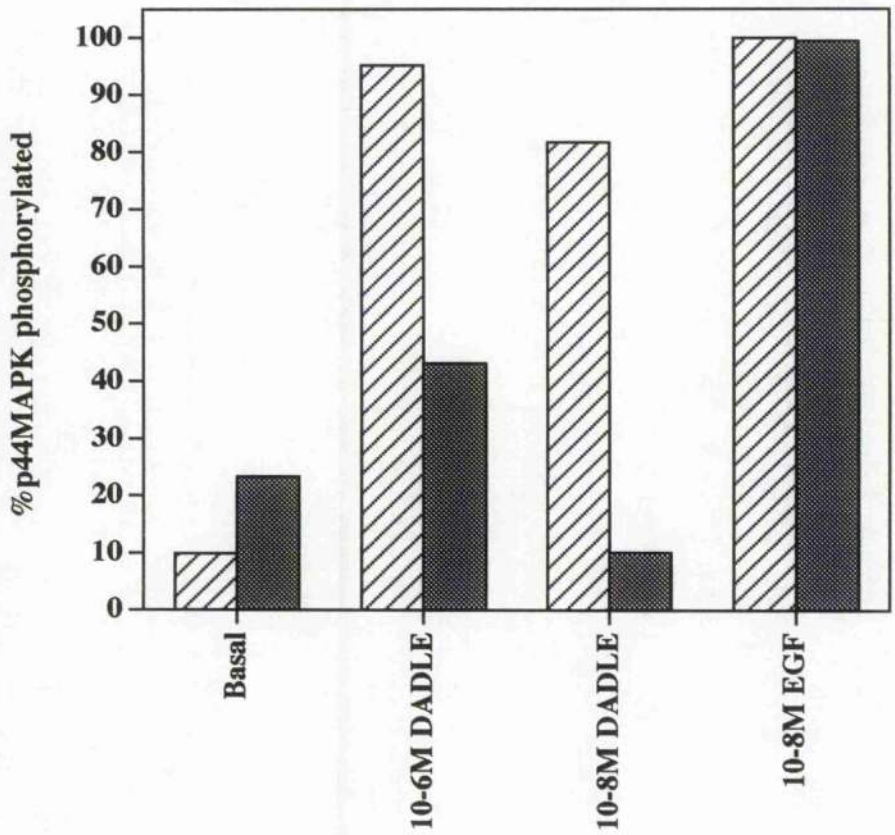

Figure 4.14 The antagonistic effects of naloxone on DADLE-mediated phosphorylation of p44^{MAPK} in cells of clone DOE.

Cells of clone DOE were serum starved for 24 hours and treated with no agonist, 10^{-6} or 10^{-8} M DADLE or 10^{-8} M EGF in the presence (shaded bars) or absence (hatched bars) of 10^{-5} M naloxone. The phosphorylation status of p44^{MAPK} was determined using the electrophoretic mobility shift assay as described in Section 2.2.9.1.

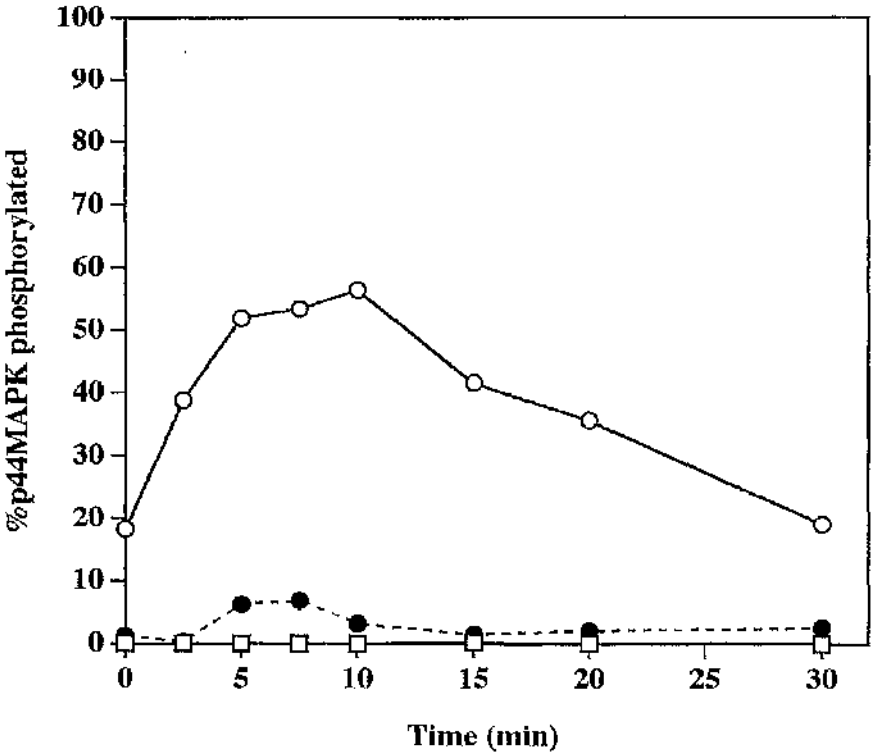

Figure 4.15 Time course of phosphorylation of $p44^{MAPK}$ on treatment with 'control' serum free DMEM in cells of clones D2 and DOE and parental Rat1 fibroblasts.

Cells of clone D2 (open circles, full line), clone DOE (filled circles, broken line) or parental Rat1 fibroblasts (open squares, full line) were serum starved for 24 hours and then treated with fresh serum free DMEM for various times as noted. The phosphorylation level of $p44^{MAPK}$ was determined by the electrophoretic mobility shift assay (as described in Section 2.2.9.1) and the percentage of the total detectable $p44^{MAPK}$ which was present in the lower mobility, phosphorylated form was calculated.

The variation according to the receptor level would suggest that this observation may indeed be due to an 'empty' receptor-activation of the G_i-mediated-p42/44^{MAPK} cascade. These results could also be consistent with the presence of low levels of an opioid agonist in DMEM (which could be studied further by determining the effect of naloxone on the 'basal' peak of activity). Some agonist-independent phosphorylation of p44^{MAPK} was still detected after pertussis toxin pretreatment in control time courses (data not shown) which would suggest a different, but at this stage unknown, mechanism. The significance which should be attached to these observations is not obvious and they might just be an artefact of the method used in these experiments, however, they do present the possibility that the δ opioid receptor has some sort of agonist-independent activity on this cascade which becomes observable when the receptors are expressed to a high level.

By pretreating the cells with serum free DMEM for 30 min after the serum starvation but prior to the agonist treatment, the 'control' peak had decayed to negligible levels and the stimulation induced solely by the added ligand could be observed. Time courses and concentration-response curves (see later) were not significantly altered depending on whether the cells were pretreated as above or whether the percentages of the maximum response achieved over the various basal levels were calculated. Therefore this slightly odd observation is not thought to have any bearing on the conclusions drawn from any of the experiments performed.

The time course of phosphorylation of $p44^{MAPK}$ stimulated by maximally effective concentrations of DADLE was more prolonged in cells of clone D2 as compared with clone DOE (Figure 4.16). In both clones the phosphorylation was rapid and was easily detected within 1 min, and maximal by 5 min of agonist treatment. This maximum level of phosphorylation of $p44^{MAPK}$ in cells of clone DOE was not maintained so that levels had returned close to basal by 15 min. In cells of clone D2, however, the elevated level of phosphorylation was still detectable at 30 min after the agonist had been added. The time course of phosphorylation of $p42^{MAPK}$ by 10^{-5} M DADLE was found to be very similar to that observed for $p44^{MAPK}$ (Figure 4.17). The same increased duration of the phosphorylation of $p42^{MAPK}$ was seen in clone D2 as compared to clone DOE.

Very similar time courses were displayed at the level of the activity of $p42/44^{MAPK}$ as measured by the Biotrak p42/44 MAP kinase activity assay (Figure 4.18). The slight delay on the activation of $p42/44^{MAPK}$ in cells of clone D2 was observed to be the only consequence of the 30 min pretreatment with serum free DMEM (after the 24 hour serum starvation) prior to treatment with 10^{-5} M DADLE. The reduced duration of the activation in these cells as compared with the phosphorylation data is not thought to be significant and can be explained in terms of variation over the different passages of cells involved.

Figure 4.16 Time course of DADLE-mediated phosphorylation of $p44^{MAPK}$ in cells of clones D2 and DOE.

A and **B** Serum starved cells of clone D2 (A) and clone DOE (B) were treated with 10^{-5} M DADLE for various times. The phosphorylation of $p44^{MAPK}$ was then assessed by the electrophoretic mobility shift assay as described in Section 2.2.9.1. Representative immunoblots from such experiments are shown in A (clone D2) and B (clone DOE). **C** Scanning by densitometry was used to quantify immunoblots such as in A and B from a number of experiments and the data was calculated as the percentage of the maximal level of phosphorylation achieved over the basal level. Results are represented by open circles and full line for D2 and filled circles and broken line for DOE. Data is presented as mean ± SEM, from three (clone DOE) and six (clone D2) independent observations.

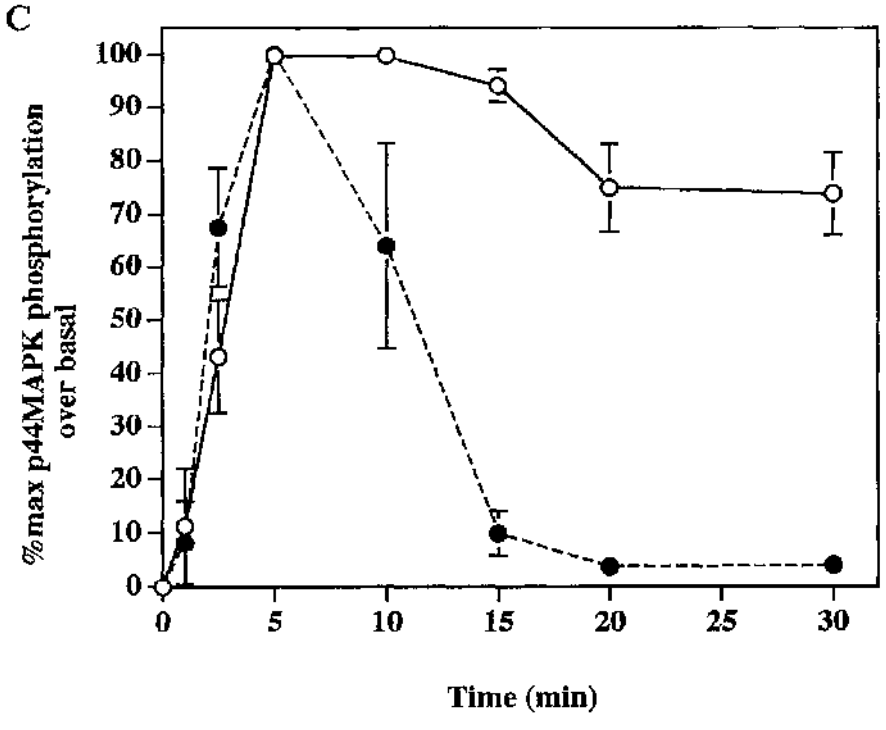

Figure 4.16

A

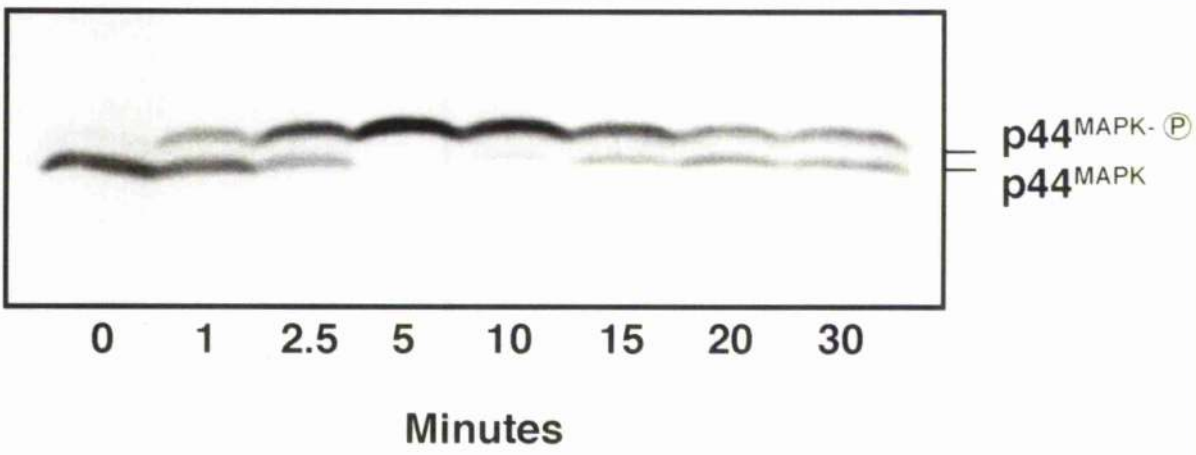

B

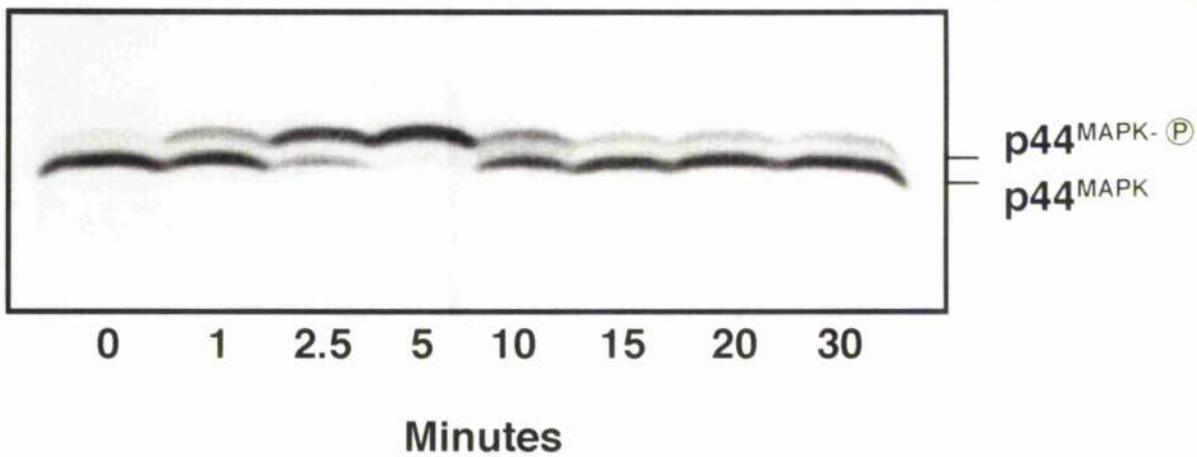

Figure 4.17 Time course of DADLE-mediated phosphorylation of $p42^{MAPK}$ in cells of clones D2 and DOE.

A and **B** In similar experiments to Figure 4.16, serum starved cells of clone D2 (A) and clone DOE (B) were treated with 10^{-5} M DADLE for various times. Samples were processed as described in Section 2.2.9.1 by the electrophoretic mobility shift assay and after SDS-PAGE, immunoblotting was performed with a specific anti-$p42^{MAPK}$ antiserum and the immunoblots are displayed.

C Scanning by densitometry was used to quantify the immunoblots in A and B and the data was calculated as the percentage of the maximal level of phosphorylation of $p42^{MAPK}$ achieved over the basal level. Results are represented by open circles and full line for D2 and filled circles and broken line for DOE.

Figure 4.17

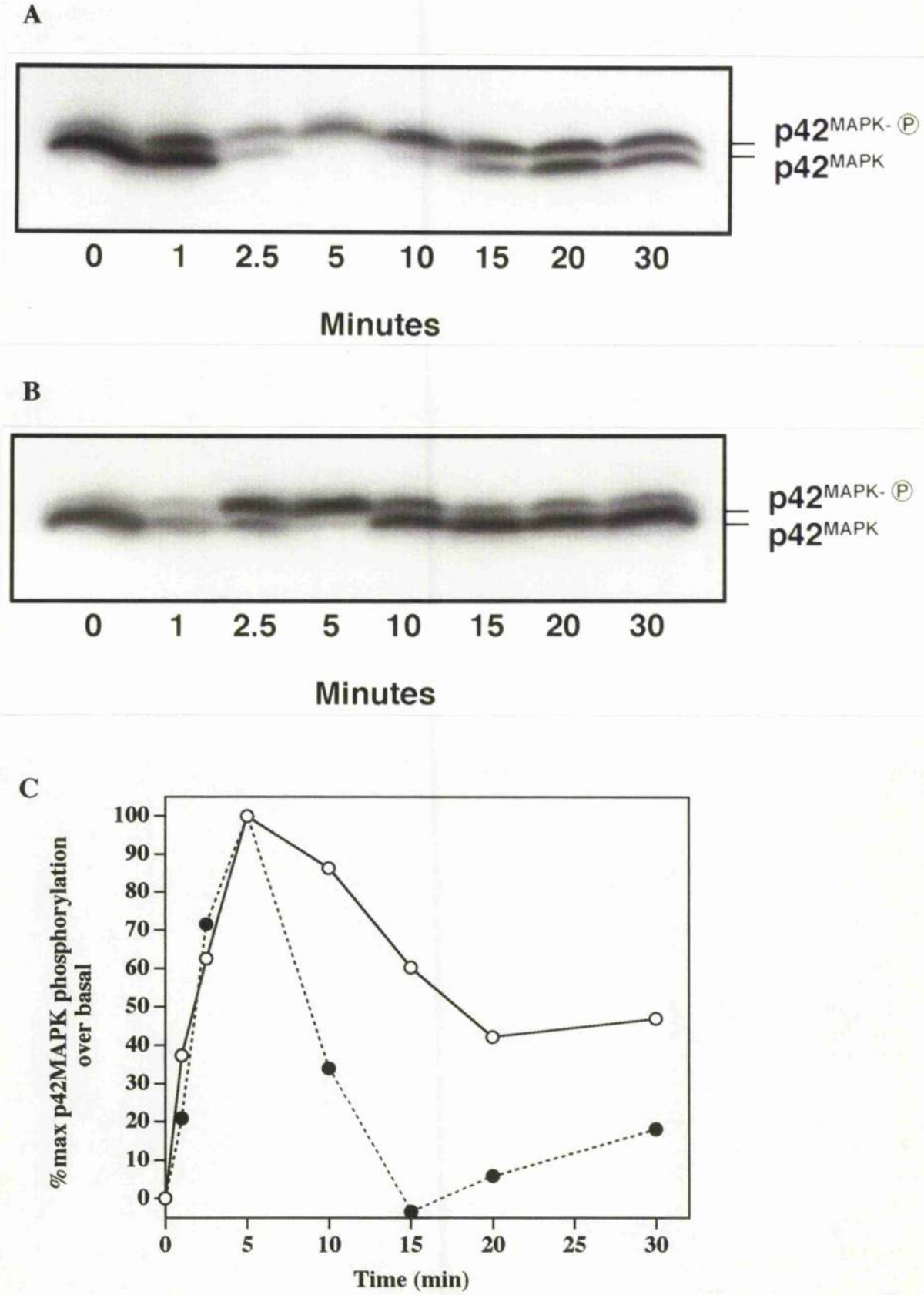
A
p42MAPK-Ⓟ
p42MAPK
0 1 2.5 5 10 15 20 30
Minutes
B
p42MAPK-Ⓟ
p42MAPK
0 1 2.5 5 10 15 20 30
Minutes
C
%max p42MAPK phosphorylation over basal
100
90
80
70
60
50
40
30
20
10
0
0 5 10 15 20 25 30
Time (min)

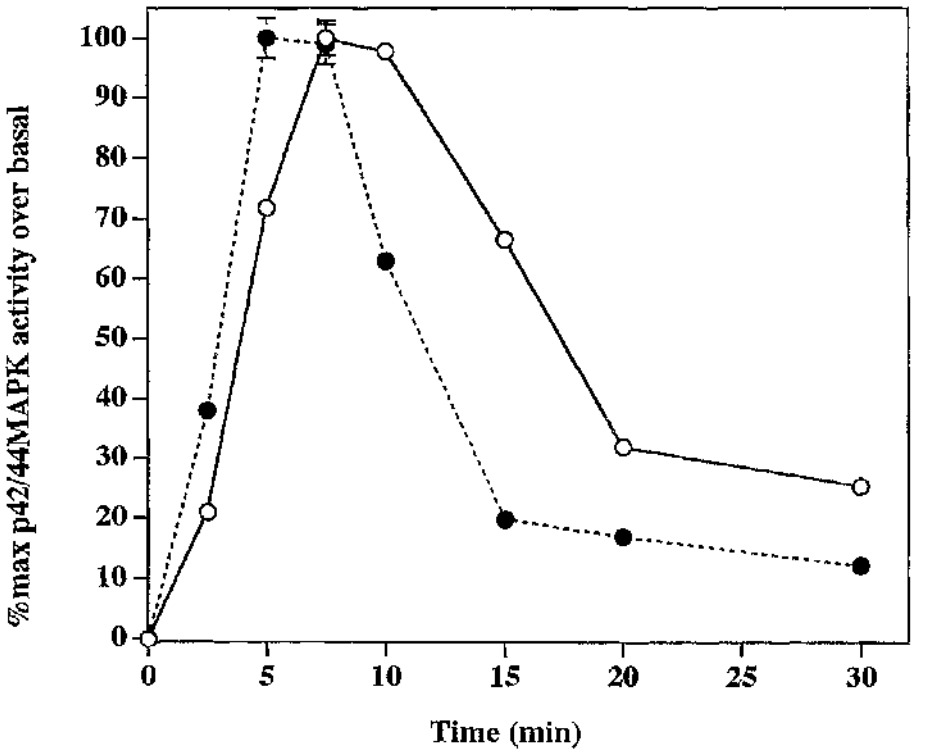

Figure 4.18 Time course of stimulation of p42/44^{MAPK} activity by DADLE in cells of clones D2 and DOE.

Serum starved cells of clone D2 and clone DOE were pretreated for 30 min in serum free DMEM and then treated with a final concentration of 10^{-5} M DADLE for various times. Cellular lysates were prepared as described in Section 2.2.9.3 and the activity of p42/44^{MAPK} in these samples was assessed by the Biotrak p42/44 MAP kinase activity assay from Amersham. Results are presented as % of maximum activity over basal, mean ± range of duplicate assays from one of two experiments performed. Data is represented by open circles and full line for clone D2 and filled circles and broken line for clone DOE.

These three separate pieces of evidence therefore support the idea suggested in Chapter 3 that a greater level of GPCR expression can produce a more sustained stimulation of $p42/44^{MAPK}$. The importance of this observation lies in the fact that the final effect on the cell of the stimulation of the Ras.MAPK cascade is believed to be dependent on the length of time the activation is sustained as this determines if significant nuclear translocation of activated $p42/44^{MAPK}$ can occur (see Section 1.4.15.1). Therefore, although the clone expressing lower levels of the receptor can stimulate the phosphorylation of essentially all the detectable $p42/44^{MAPK}$ in these cells, this activation is more transient and so the effect of DADLE on these cells may be very different from the effect on clone D2. Similar effects on the time course of activation of $p42/44^{MAPK}$ have been demonstrated for the overexpression of tyrosine kinase linked receptors, including receptors for EGF and insulin in PC12 cells (Marshall, 1995; Schlessinger and Bar-Sagi, 1994).

The time courses of phosphorylation of $p44^{MAPK}$ upon treatment with 10^{-5} M LPA were not noticeably different between clone D2 and clone DOE (Figure 4.19). Maximal phosphorylation was achieved 5 min after LPA treatment and this decayed to greatly reduced levels by 30-60 min. LPA acts on GPCRs which are endogenous to the parental Rat1 fibroblasts and so should be present in similar levels in each of the clones. The observed differences between the clonal cell lines for DADLE-mediated activation of $p42/44^{MAPK}$ are clearly due to the levels of expression of the δ opioid receptor and not because of some variation in the individual clonal cell lines.

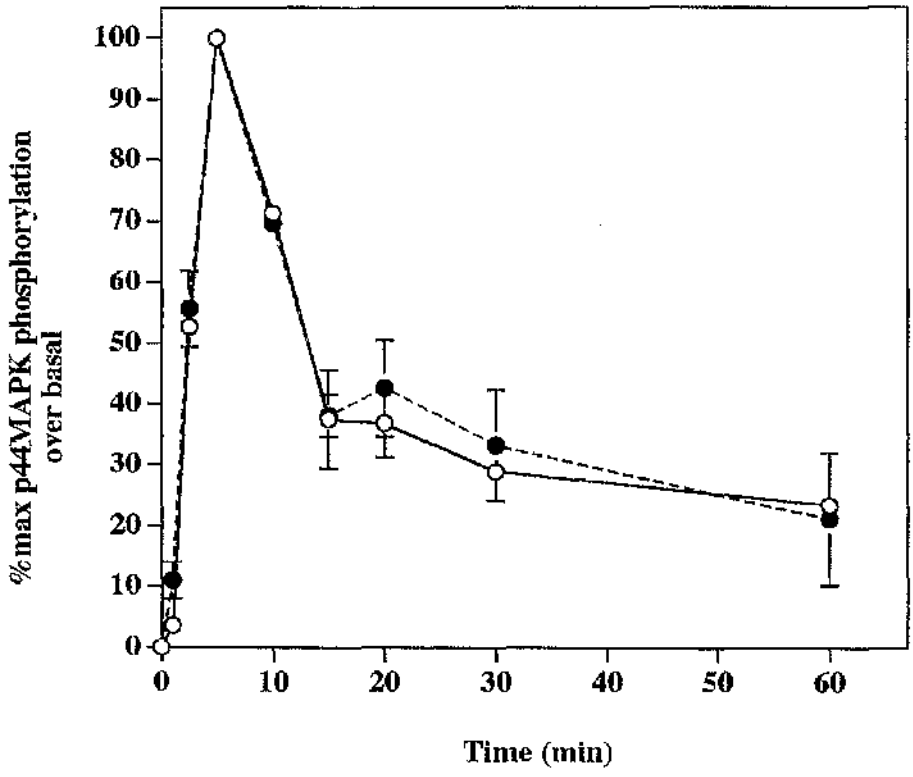

Figure 4.19 Time course of the phosphorylation of $p44^{MAPK}$ in cells of clones D2 and DOE on treatment with LPA.

Cells of clone D2 and clone DOE were serum starved for 24 hours and then subjected to 10^{-5} M LPA for various times. The phosphorylation level of $p44^{MAPK}$ was then assessed by the electrophoretic mobility shift assay (Section 2.2.9.1). $p44^{MAPK}$ immunoblots were scanned by densitometry and the data was calculated as the percentage of the maximal phosphorylation of $p44^{MAPK}$ over the basal which was present at each of the time points. Results are presented as mean ± range from two independent experiments. Data is represented by open circles and full line for clone D2 and filled circles and broken line for clone DOE.

Two proposals could possibly explain the sustained kinetics in clone D2: possibly the receptor level in clone D2 but not clone DOE was high enough such that full desensitisation could not occur therby the receptor could continue to stimulate the phosphorylation of $p42/44^{MAPK}$; or the higher receptor expression was able to stimulate a greater level of G-protein activation which stimulated the Ras.MAPK cascade to a greater extent which could not be overcome as rapidly by the cellular turn off mechanisms (presumably MAPK phosphatases). In order to test these ideas further the time courses of phosphorylation of $p44^{MAPK}$ mediated by different concentrations of DADLE were determined in cells of clone D2 (Figure 4.20). The time courses of 10^{-6} M and 10^{-8} M DADLE were very similar. Maximal phosphorylation was achieved after 5 min of agonist treatment and this was maintained for a further 10 min. However, the dephosphorylation was slightly more rapid in cells which had been treated with 10^{-8} M DADLE as near basal levels were seen after 20 min while 50% of $p44^{MAPK}$ was still phosphorylated at this time in 10^{-6} M DADLE-treated cells. 10^{-10} M DADLE stimulated nearly complete phosphorylation of the $p44^{MAPK}$ population but 10 min was required for this to be reached, and the dephosphorylation was more rapid.

These results can be very approximately correlated with the level of high affinity GTPase stimulation which can be achieved by each of these concentrations of ligand in clones D2 and DOE. 10^{-8} M DADLE (and 10^{-6} M DADLE) produced greater GTPase activity than could be achieved by maximally effective concentrations in clone DOE and so produced a more sustained time course of phosphorylation of $p44^{MAPK}$. 10^{-10} M DADLE produced a stimulation of GTPase activity which was less than the maximal level in clone DOE and so the time course of phosphorylation of $p44^{MAPK}$ for this concentration of DADLE was more delayed and possibly more transient than for clone DOE cells. These results therefore support the model in which the magnitude and duration of the phosphorylation of $p42/44^{MAPK}$ is dependent on the level of G-protein stimulation achieved and indicate that an inability to desensitise the receptors was not the reason for the more sustained kinetics in clone D2.

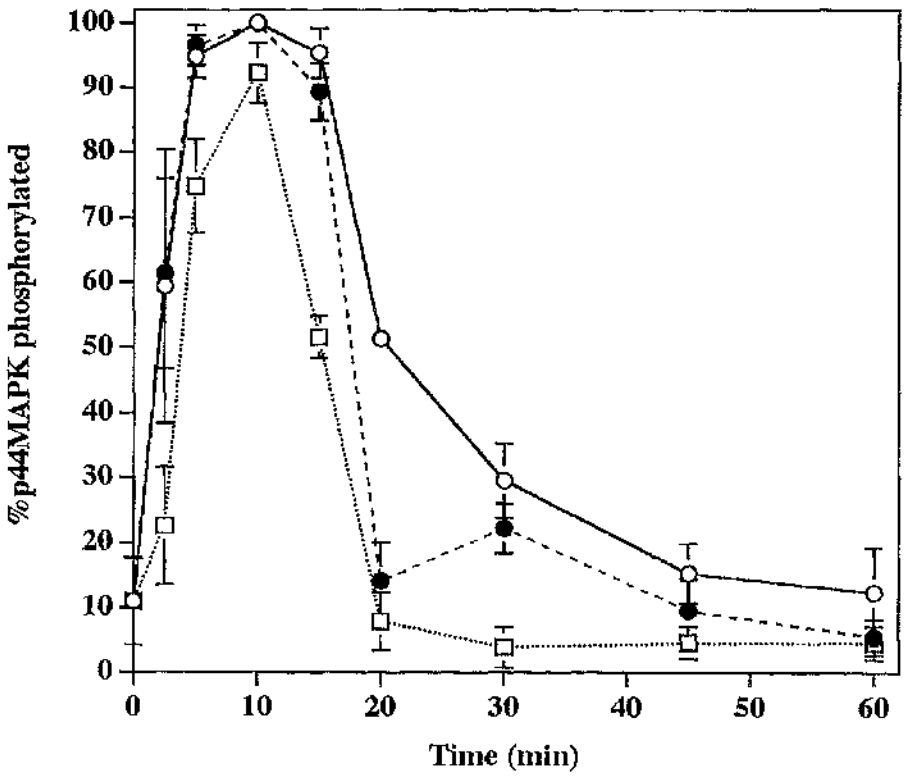

Figure 4.20 Time course of $p44^{MAPK}$ phosphorylation stimulated by treatment with various concentrations of DADLE in cells of clone D2.

Serum starved cells of clone D2 were treated with DADLE at 10^{-6} M (open circles, full line), 10^{-8} M (filled circles, broken line) and 10^{-10} M (open squares, dotted lines) for various times. The phosphorylation status of $p44^{MAPK}$ in each sample was assessed by the electrophoretic mobility shift assay as described in Section 2.2.9.1. Results are presented as mean ± SEM from three independent experiments.

Concentration-response curves of DADLE-mediated $p44^{MAPK}$ phosphorylation demonstrated that a significantly ($p = 0.04$) larger concentration of DADLE was required to produce half-maximal phosphorylation of $p44^{MAPK}$ in cells of clone DOE compared with clone D2 (Figure 4.21). This was similar to what was expected on the basis of the GTPase results in these cells and the $p44^{MAPK}$ phosphorylation results in Chapter 3. The average EC_{50} for phosphorylation of $p44^{MAPK}$ by 5 min treatment of DADLE in clone DOE was $3.1 \pm 0.9 \times 10^{-9}$ M which was some 40 fold higher than for clone D2 which displayed an EC_{50} value of $7.3 \pm 2.4 \times 10^{-11}$ M (mean ± SEM, $n = 3$ for clone D2, $n = 4$ for clone DOE). It is of note that these concentration-response curves were co-operative in nature as shown by the Hill coefficients of 2.3 ± 0.4 for clone D2 and 1.9 ± 0.2 for clone DOE.

The concentration-response curves of DADLE-mediated stimulation of $p42/44^{MAPK}$ activity in clones D2 and DOE were very similar to those for phosphorylation (Figure 4.22). The EC_{50} values displayed for each clone were similar to the phosphorylation data, with a significantly ($p = 0.005$) larger concentration required to produce a half-maximal effect in cells of clone DOE as compared to clone D2 (EC_{50} value for clone D2 was $1.4 \pm 0.3 \times 10^{-10}$ M and for DOE was $2.8 \pm 0.2 \times 10^{-9}$ M, mean ± range, $n = 2$ for each clone). Hill coefficients were typically calculated at approximately 2.5, showing co-operativity in these concentration-response curves.

Figure 4.21 Concentration-response curves of DADLE-mediated phosphorylation of $p44^{MAPK}$ in cells of clone D2 and clone DOE.

A and B Serum starved cells of clones D2 and DOE were treated with various concentrations of DADLE for 5 min. Samples were prepared as described in Section 2.2.9.1 for the electrophoretic mobility shift assay and resolved by SDS-PAGE and immunoblotted with an anti-$p44^{MAPK}$ antiserum. Representative immunoblots are shown for clone D2 (A) and DOE (B).

C Immunoblots such as in A and B were scanned by densitometry and the percentage of the maximal phosphorylation of $p44^{MAPK}$ which was produced with each concentration was calculated. Results are presented as mean ± SEM, n = 3 for clone D2 (open circles, full line) and n = 4 for clone DOE (filled circles, broken line).

Figure 4.21

A

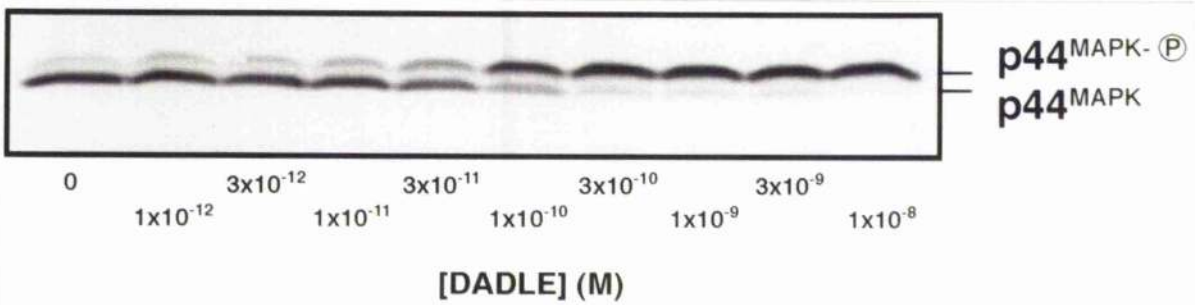

B

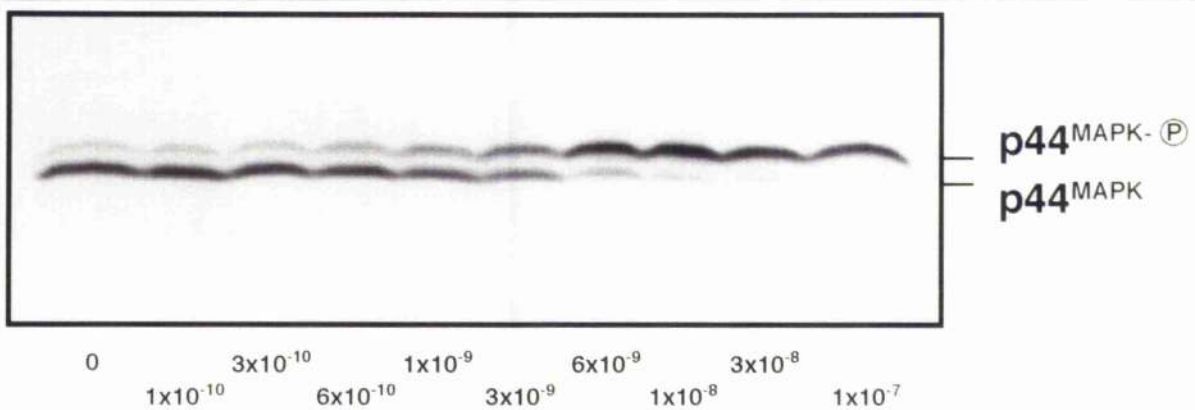

C

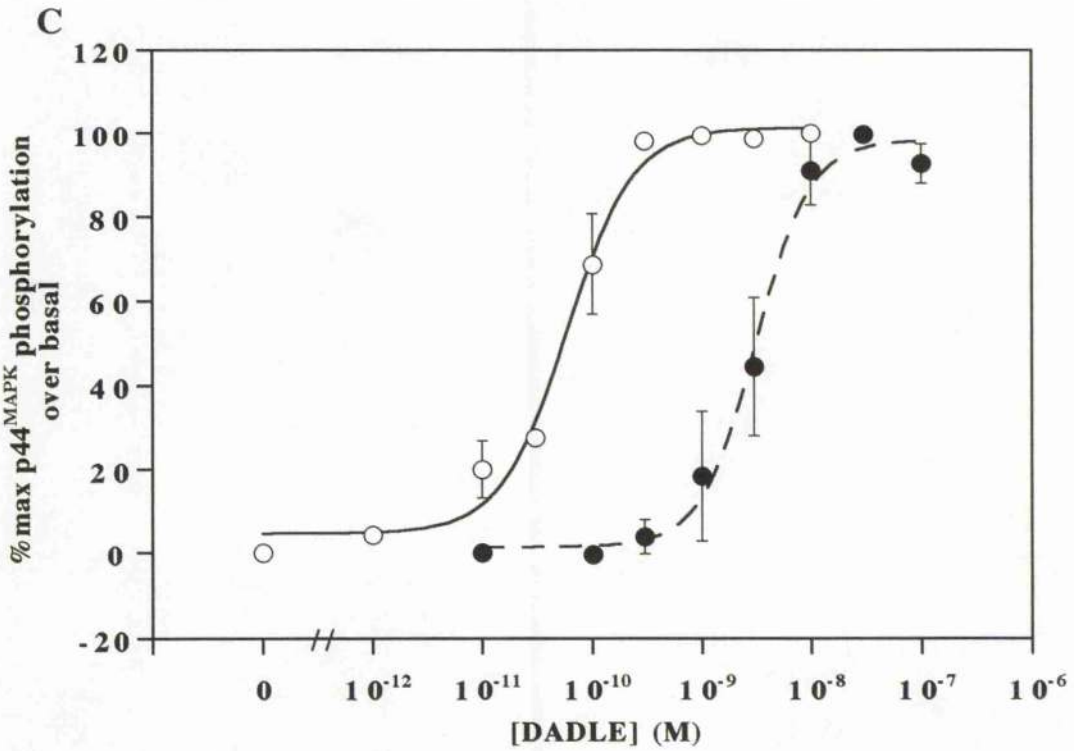

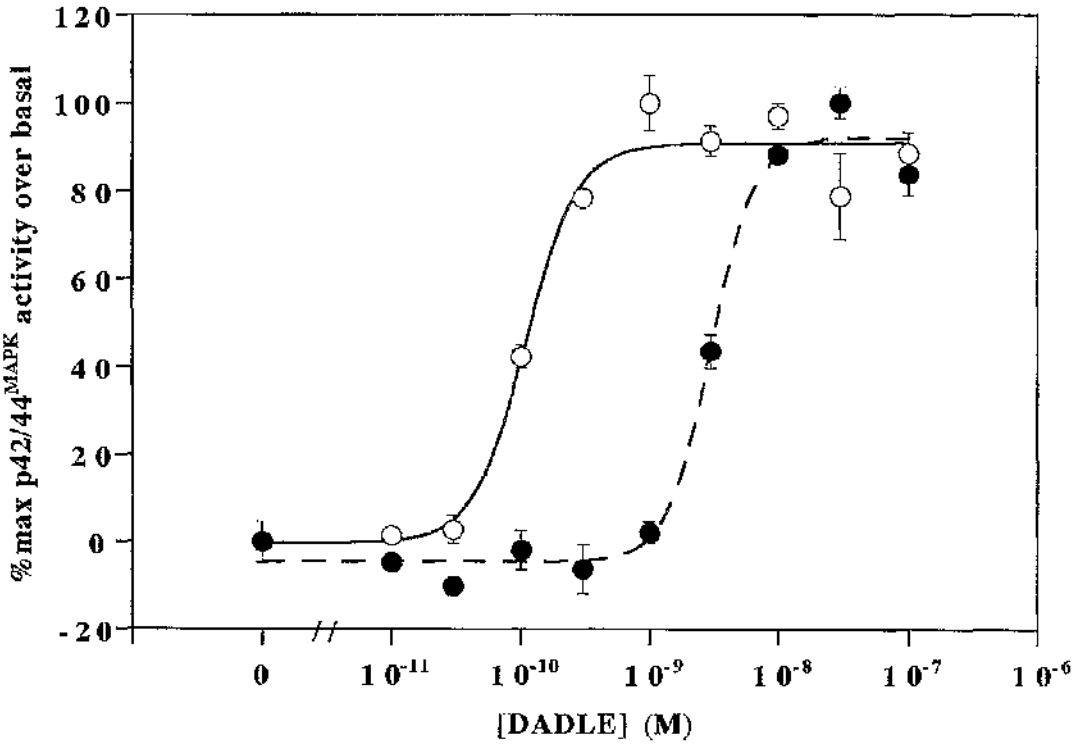

Figure 4.22 Concentration-response curves of DADLE-mediated stimulation of the activity of p42/44^{MAPK} in cells of clone D2 and clone DOE.

The activity of p42/44^{MAPK} in serum starved cells of clone D2 and DOE was determined by the Biotrak activity assay (as described in Section 2.2.9.3) in response to 7.5 min treatment of various concentrations of DADLE after a 30 min pretreatment with serum free DMEM. Results are presented as mean ± range of duplicate assays of the percentage of the maximal response achieved over the basal level in cells of clone D2 (open circles, full line) and clone DOE (filled circles, broken line). Data is shown from one of two experiments performed.

In contrast, the concentration-response curves to LPA-mediated phosphorylation of $p44^{MAPK}$ were not significantly ($p = 0.11$) different between the two clones (Figure 4.23). The EC_{50} for clone D2 was $1.2 \pm 0.3 \times 10^{-7}$ M and for clone DOE was $1.1 \pm 0.5 \times 10^{-6}$ M, mean ± SEM, $n = 3$ in each case. Therefore the above marked differences in the concentration-response curves for DADLE were clearly due to the difference in the expression levels of the δ opioid receptor in the clones. The LPA-mediated concentration-response curves surprisingly did not show any co-operativity. The values of the Hill coefficients were calculated as 1.1 ± 0.2 for clone D2 and 0.8 ± 0.2 for clone DOE and were significantly ($p = 0.04$ for clone D2 and $p = 0.007$ for clone DOE) different to that calculated for the DADLE-mediated $p44^{MAPK}$ phosphorylation.

As displayed in Figure 4.4 the concentration-response curves of DADLE-mediated high affinity GTPase activity also displayed a requirement for a higher concentration of DADLE to produce a half-maximal effect in clone DOE compared to clone D2. However, this was not as pronounced as for the $p44^{MAPK}$ phosphorylation. Direct comparison of the concentration-response curves to DADLE-mediated $p44^{MAPK}$ phosphorylation and high affinity GTPase activity demonstrated that in cells of clone D2, only a very small proportion of the cellular G_i-protein population was required to be activated to cause maximal phosphorylation of $p44^{MAPK}$ (Figure 4.24A). Therefore only a small fraction of the δ opioid receptor population was required to be occupied to produce this maximal effect and a large receptor and activated G_i-protein reserve exists in these cells. This is consistent with the maximum $p44^{MAPK}$ phosphorylation response to DADLE (5 min treatment) in clone DOE where the maximal agonist-stimulated GTPase response is much lower than in clone D2. However, the receptor and activated G-protein reserve was also obvious in cells of clone DOE (Figure 4.24B), although the magnitude of this was significantly ($p = 0.03$) smaller: a 94 ± 23 fold higher concentration of DADLE was required to produce the half-maximal GTPase activation compared with $p44^{MAPK}$ phosphorylation in clone D2, whereas this was only 27 ± 14 fold higher in clone DOE (mean ± SEM, $n = 3$ (D2) or 4 (DOE)).

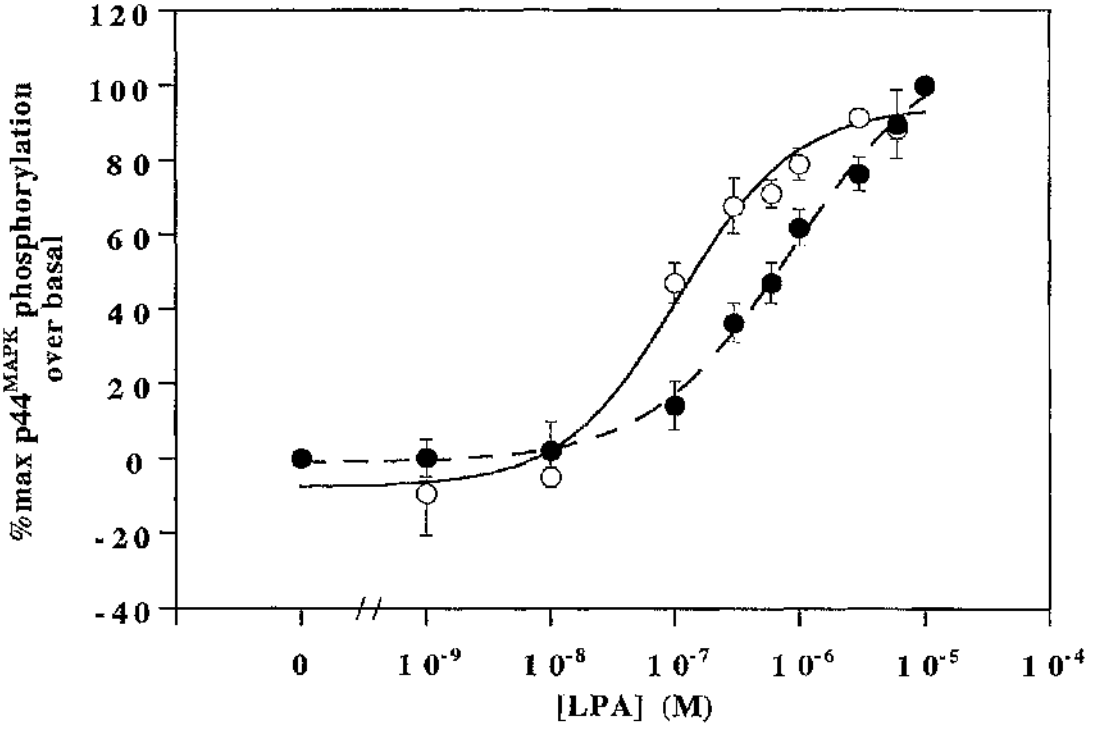

Figure 4.23 Concentration-response curves of LPA-mediated phosphorylation of $p44^{MAPK}$ in cells of clone D2 and clone DOE.

The level of phosphorylation of $p44^{MAPK}$ was determined by the electrophoretic mobility shift assay (Section 2.2.9.1) in serum starved cells of clones D2 and DOE in response to 5 min treatment of various concentrations of LPA. The results from densitometric scans of the immunoblots were calculated as the percentage of the maximal response achieved over the basal level for each of the clones and the data is presented as mean ± SEM from three independent experiments. The results for clone D2 are represented by open circles and full line and for clone DOE by filled circles and broken line.

Figure 4.24 Comparison of the concentration-response curves of the stimulation of high affinity GTPase activity and phosphorylation of $p44^{MAPK}$ by DADLE in cells of clone D2 and DOE.

Data from concentration-response curves to DADLE for high affinity GTPase (as in Figure 4.4) and for phosphorylation of $p44^{MAPK}$ (as in Figure 4.21) for cells of clone D2 (A) and clone DOE (B) are presented as the percentage of the maximal effect produced by DADLE. Experimental details are as in the legends to the figures mentioned.

A For cells of clone D2, the phosphorylation of $p44^{MAPK}$ is represented by open circles and full line, and high affinity GTPase activity by open squares and dotted line.

B For cells of clone DOE, the phosphorylation of $p44^{MAPK}$ is represented by filled circles and broken line, and high affinity GTPase activity by filled squares and dotted line.

Figure 4.24

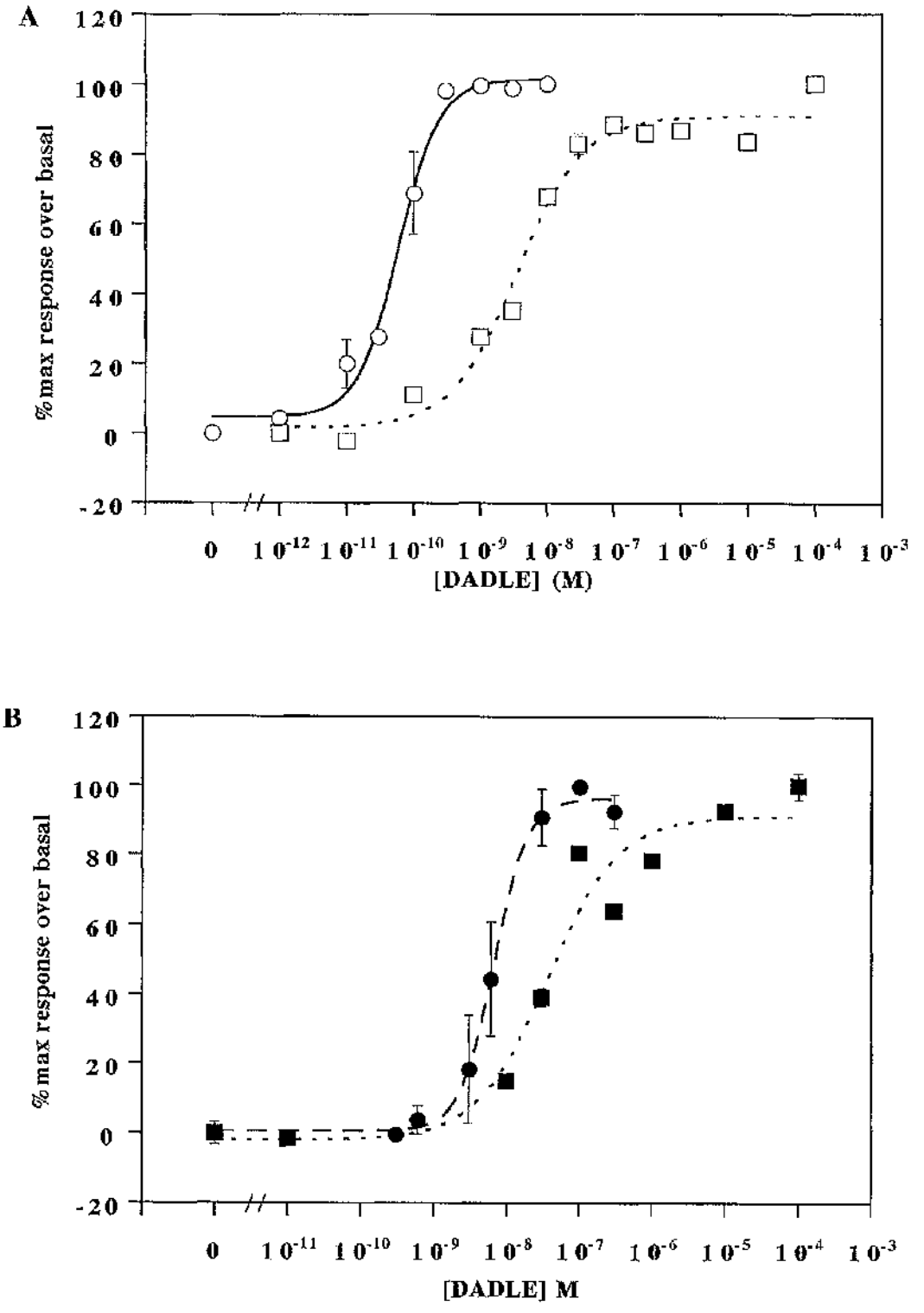
A
120
100
80
60
40
20
0
-20
% max response over basal
0
10-12
10-11
10-10
10-9
10-8
10-7
10-6
10-5
10-4
10-3
[DADLE] (M)
B
120
100
80
60
40
20
0
-20
% max response over basal
0
10-11
10-10
10-9
10-8
10-7
10-6
10-5
10-4
10-3
[DADLE] M

The suggestion was made that these differences in concentration-responses might occur because the comparison is between the response to a treatment with DADLE on whole cells ($p44^{MAPK}$ phosphorylation) and treatment on membrane preparations (GTPase activity). In order to exclude this explanation, the concentration-response curve for clone D2 of $p44^{MAPK}$ phosphorylation was compared with that for transphosphatidylation activity (from Figure 4.9) as both involve whole cell treatments. Again the curves displayed a similarly significant ($p = 0.02$) difference in the EC_{50} values (Figure 4.25) indicating that the large receptor and activated G_i-protein reserve in the response of δ opioid receptor-mediated activation of $p44^{MAPK}$ was not general for all effectors of this receptor and was not just a consequence of the experimental method.

As noted previously, the Hill coefficients for the concentration-response curves for DADLE-mediated phosphorylation of $p44^{MAPK}$ displayed marked co-operativity. In contrast the Hill coefficients for the transphosphatidylation assay in clone D2 and the GTPase assays in both clones were significantly ($p = 0.04$) smaller, with values less than or equal to 1. Thus there was no co-operativity at the level of the G-protein or PLD activation. This might suggest that the receptor feeds into the Ras.MAPK pathway at more than one distinct point which would create the co-operativity as well as the observed highly potent effect.

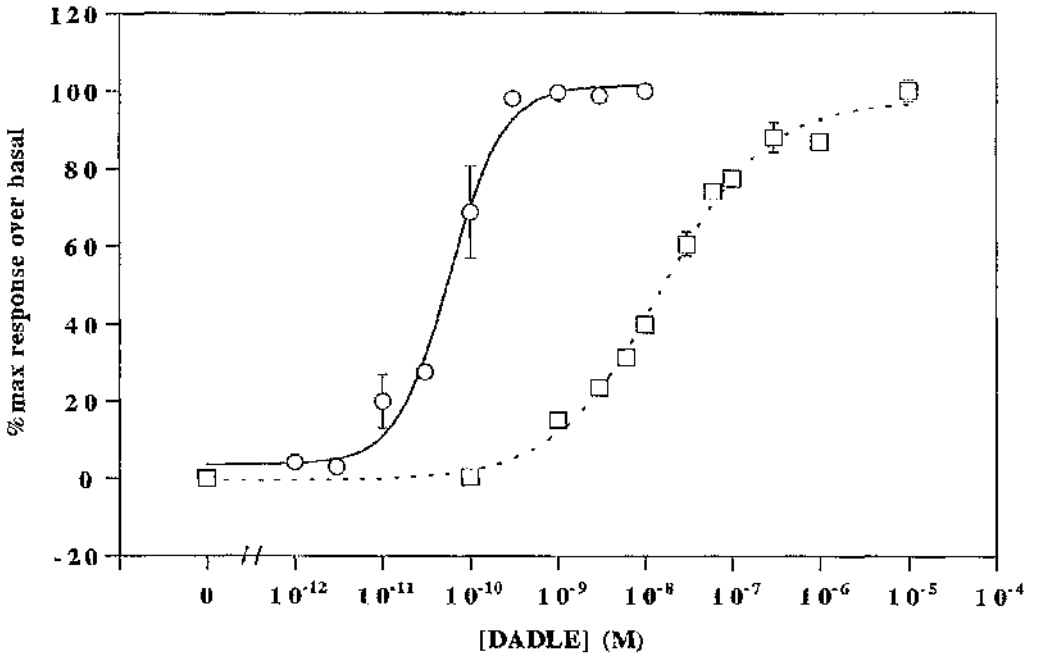

Figure 4.25 Comparison of the concentration-response curves for DADLE-mediated stimulation of transphosphatidylation activity and phosphorylation of p44^{MAPK} in cells of clone D2.

Data from concentration-response curves to DADLE for transphosphatidylation activity (as in Figure 4.9) and for phosphorylation of p44^{MAPK} (as in Figure 4.21) for cells of clone D2 are presented as the percentage of the maximal effect produced by DADLE. The phosphorylation of p44^{MAPK} is represented by open circles and a full line, and transphosphatidylation activity by open squares and a dotted line. The experimental details are as reported in the legends to the figures mentioned.

That these observations were not just artefacts of the experimental methods used was further demonstrated by the fact that they were not common to other G_i-protein coupled receptors expressed in these cells. The activation of endogenous receptors with LPA, led to the phosphorylation of $p44^{MAPK}$ in a manner which did not display any co-operativity but displayed a similar EC_{50} value to that calculated for GTPase activation in parental Rat1 fibroblasts (Carr *et al.*, 1994). In addition, the results presented in Chapter 3 with the α_{2A} adrenoceptor expressed in Rat1 fibroblasts did not show any co-operativity and were inconsistent as to the presence of a receptor or activated G-protein reserve. Therefore, although there were many similarities between the signalling of the α_{2A} adrenoceptor and the δ opioid receptor when expressed in these cells, they display quantitatively different features in their ability to couple to the $p42/44^{MAPK}$ cascade. Since the δ opioid receptor in these experiments demonstrated a peculiarly efficient coupling ability to the activation of $p42/44^{MAPK}$ it would be interesting to determine if there is any variation in the pathways used by these three GPCRs to activate the cascade which might explain these results.

The reason for this difference between the signalling of these receptors is puzzling and at this stage is a matter of pure speculation. The coupling to the Ras.MAPK cascade by G_i-protein coupled receptors has been suggested to be mediated by βγ subunits released from pertussis toxin sensitive G-proteins (see Section 1.4.13.3.1). These results may suggest that the δ opioid receptor may couple to the Ras.MAPK cascade not only by this pathway, in common with the other G_i-protein coupled receptors, but also through another as yet undefined point in the pathway which is exclusively available to the δ opioid receptor. Other speculations to explain this property may include an ability of the δ opioid receptor to selectively couple to G-proteins containing βγ subunits with greater (and selective) potency to couple to the Ras.MAPK cascade. It would be interesting to determine if these observations are specific for the δ opioid receptor or if other receptors could reproduce these results creating a subset of G_i-protein coupled receptors which would display these properties.

Previous studies which recorded the various concentration-response relationships for p42/44^{MAPK} and other effectors have failed to demonstrate any markedly greater efficiency of coupling to the MAPK cascade in contrast with other effectors. Such examples include the activation of p42/44^{MAPK} by agents which use pertussis toxin insensitive pathways such as prostaglandin $F_{2\alpha}$ (Watanabe *et al.*, 1995), pertussis toxin sensitive pathways such as thrombin (Chen *et al.*, 1994) and pathways which are partially sensitive to pertussis toxin such as platelet activating factor (Honda *et al.*, 1994). Therefore, although the stoichiometry of the GPCR-mediated activation of p42/44^{MAPK} had not previously been studied to any great extent, the available data does suggest that the observations described for the δ opioid receptor expressed in the Rat1 fibroblasts cannot be applied in general to all GPCRs.

4.3 Conclusions

For the first time, the activation of p42/44^{MAPK} by the δ opioid receptor has been described and so the range of GPCRs which can activate this cascade has been extended. However, this result is perhaps not surprising considering the opioid receptor's previously described ability to signal via the G-proteins of the G_i family and the knowledge of a mechanism of G_i-protein-mediated activation of the Ras.MAPK pathway by $G_{\beta\gamma}$. Much more surprising and novel conclusions, however, were made regarding the quantitation of this coupling and the relationship between the receptor expression level and the response to agonist stimulation.

The δ opioid receptor expressed in Rat1 fibroblasts at a high and low density could functionally couple to the G-protein machinery as shown with three different assays: agonist stimulation of high affinity GTPase activity, [^{35}S]GTPγS binding and cholera toxin catalysed [^{32}P]ADP ribosylation of G_i-like proteins. The maximal agonist-mediated stimulation was dependent on the receptor level in the two clones and the concentration of agonist which produced a half-maximal GTPase stimulation was lower in the higher receptor expressing clone. A greater inhibition of forskolin-stimulated adenylyl cyclase activity was also possible in the higher receptor expressing clone. In keeping with previously described multiple signalling ability, the receptor could also stimulate transphosphatidylation activity in a dose and receptor level-dependent manner. In addition, a somewhat variable δ opioid agonist-stimulated PI-C activity was demonstrated. All these responses were mediated by pertussis toxin-sensitive, G_i-like, G-proteins.

Maximally effective concentrations of DADLE stimulated the phosphorylation of all the detectable p42^{MAPK} and p44^{MAPK} in both of these clones at a 5 min time point. This was sensitive to inhibition by both naloxone and pertussis toxin and therefore indicated that it was indeed mediated by the δ opioid receptor signalling through G_i-like proteins. An increase in activity of p42/44^{MAPK} accompanied their

phosphorylation in both clones. The time courses of activation and phosphorylation demonstrated distinct differences between the two clones which supported the idea proposed in chapter 3 that a greater expression of the GPCR would produce a more sustained time course due to the activation of a greater proportion of the G-protein population. This was further supported by the time course of $p44^{MAPK}$ phosphorylation in response to different concentrations of DADLE which appeared to allow some correlation between the possible GTPase activation and the activation of $p42/44^{MAPK}$. The more sustained activation of $p42/44^{MAPK}$ in clone D2 may make a great difference to the functional outcome of DADLE-treatment in these cells. It has been shown that DADLE-treatment of D2 cells is mitogenic as determined by its ability to stimulate DNA synthesis (Wilson *et al.*, submitted), however, it remains to be seen if this occurs with DADLE-treatment of cells of clone DOE. It is unlikely that $p42/44^{MAPK}$ activation is sufficient for this effect as $p70^{s6k}$ activity appears to be required.

Perhaps the most novel and surprising conclusions arose from the concentration-response curves for DADLE-mediated phosphorylation and activation of $p42/44^{MAPK}$. These results displayed a very large receptor and activated G-protein reserve in both clones, although the magnitude was greater in the higher expressing clone D2. This would indicate that the coupling between the receptor and this cascade is highly efficient. The inconsistencies which could not be reconciled in Chapter 3 do not arise from the data presented in this chapter. Another interesting observation was that the concentration-response curves for DADLE-mediated phosphorylation of $p44^{MAPK}$ displayed marked co-operativity (Hill coefficients were approximately 2.5). This was not observed, however, for the DADLE-mediated stimulation of GTPase activity and PLD activity nor for the phosphorylation of $p44^{MAPK}$ by LPA nor by the α_{2A} adrenoceptor. Therefore this indicates that the δ opioid receptor, when expressed in the Rat1 fibroblasts, has some novel signalling ability with regards to the $p42/44^{MAPK}$ cascade which may involve an additional input site into this pathway.

Chapter 5

Further studies on the regulation of the phosphorylation of p42/44^{MAPK} by the δ opioid receptor: partial agonists, inhibitors and cross-talk.

Chapter 5: Further studies on the regulation of the phosphorylation of p42/44^{MAPK} by the δ opioid receptor: partial agonists, inhibitors and cross-talk.

5.1 Introduction

The previous chapter quantitatively described the regulation of p42/44^{MAPK} activity by the δ opioid receptor following expression in Rat1 fibroblasts. This chapter initially will continue this work and provide evidence in support of the conclusions of the coupling efficiency to this cascade by a study on the ability of opioid agonists with a range of intrinsic activities at this receptor to stimulate the phosphorylation of p42/44^{MAPK}. The influence that other signalling pathways have on the p42/44^{MAPK} activation by the δ opioid receptor will be examined by means of second messenger analogues and selective enzyme inhibitors in the second part of this chapter.

The different expression levels of the δ opioid receptor in clone D2 and clone DOE were used in Chapter 4 to study the relationship between the level of G_i-protein activation and stimulation of the p42/44^{MAPK} cascade. In this chapter, the regulation will be studied using ligands which have different levels of intrinsic activity and so would be expected to stimulate the G-protein machinery and the p42/44^{MAPK} cascade to different extents. These ligands have been described as full agonists, partial agonists (which display lower intrinsic activity as measured by their inability to produce a maximal response, even at maximal receptor occupancy), neutral antagonists (which have no intrinsic activity), and one ligand has been described as an inverse agonist because it reduced the spontaneous activity of the receptor (Mullaney *et al.*, 1996). The relative efficacy of the ligands used in these experiments was determined in NG108-15 cells (Klee *et al.*, 1984). A ligand can display a range of intrinsic activities and potencies at a given receptor depending on a combination of different factors including the receptor expression level, receptor reserve and the level at which the output is

measured (Hoyer and Boddeke, 1993) and, to some extent, these factors will be illustrated in this system.

The activation of p42/44^{MAPK} by GPCRs does not occur in isolation of the other signal transduction pathways in a cell but rather the cross-talk between pathways provides a further level of complexity and control. This could be of benefit to the cell because the functional output of the p42/44^{MAPK} cascade (for example mitogenesis or differentiation) is synchronised with various environmental and cellular conditions. An example of this is the inhibitory effect of elevated cAMP levels on the G-protein coupled receptor-mediated activation of p42/44^{MAPK} as described in Section 1.4.10 and illustrated for the α_{2A} adrenoceptor in Chapter 3. This chapter will extend this observation to include the δ opioid receptor and will further examine cAMP's inhibitory effect on the time course of activation.

Phospholipases have been implicated in the control of mitogenesis by a number of GPCRs. The activation of p42/44^{MAPK} by many but not all G_q-protein coupled receptors has been shown to be dependent on PKC activation following the activation of PLC (for examples see Section 1.4.13.2). The activation of p42/44^{MAPK} by many G_i-protein coupled receptors has been shown to be independent of PKC activity, however, it was thought that because the δ opioid receptor stimulated a measurable PLC activity, it would be worthwhile to determine whether a PKC-selective inhibitor (chelerythrine) affected the δ opioid-induced activation of p42/44^{MAPK}. A slightly less well defined relationship is the role of PLD activity in the mitogenic response to both tyrosine kinase and G-protein-linked receptors (discussed in Boarder, 1994). PLD-derived phosphatidic acid has been implicated in the mitogenic response to ET-1 and angiotensin II in vascular smooth muscle cells (Wilkes *et al.*, 1993; Wilkie *et al.*, 1996). This was demonstrated by the selective inhibition mediated by butan-1-ol which diverted the PLD-formed phosphatidic acid to phosphatidylbutanol. However, there is no evidence to link the activities of p42/44^{MAPK} and PLD and, for example, the

vasopressin-mediated activation of p42/44^{MAPK} and PLD in rat vascular smooth muscle cells were shown to be concurrent, but independent of each other (Jones *et al.*, 1994). The relationship between the stimulation of PLD and p42/44^{MAPK} activity was examined in these cells as agonist stimulation of the δ opioid receptor expressed in cells of clone D2 led to a strong stimulation of PLD activity (see Chapter 4).

As discussed in Chapter 1, the EGFR tyrosine kinase, PI3-kinase and a genistein-sensitive tyrosine kinase have been implicated in G_i-protein-mediated activation of p42/44^{MAPK}. The final part of this chapter will attempt to determine if these kinases are involved in the pathway initiated by the δ opioid receptor by use of tyrphostin AG1478, wortmannin and genistein. In addition, the effect of the level of receptor expression on the potency of the inhibitors will be examined.

5.2 Results and Discussion

Maximally effective concentrations of opioid ligands, which displayed a range of intrinsic activities at the level of adenylyl cyclase inhibition and GTPase activation in the NG108-15 cell line (Klee *et al.*, 1984), produced a range of stimulations of high affinity GTPase activity in membranes from cells of clone D2 and clone DOE (Figure 5.1). DADLE stimulated the greatest GTPase activity in both of the clones, although the maximal effect was larger in membranes of clone D2 compared with clone DOE as observed earlier (Figure 4.1). In membranes of clone D2, the other ligands, except TIPPΨ, produced a range of stimulations of GTPase activity which were greater than the stimulation with DADLE in clone DOE. However, these ligands struggled to produce a measurable stimulation of GTPase activity in membranes from clone DOE and DADLE and possibly levorphanol were the only ligands which produced a stimulation over the basal level. TIPPΨ was previously described as a neutral antagonist and no efficacy of this ligand was detected at this level in either clone. The relative order of intrinsic activity of the ligands for GTPase activity in clone D2 was similar to that previously observed (Klee *et al.*, 1984):

DADLE > Levorphanol > Diprenorphine > Morphine > Buprenorphine > TIPPΨ

This order of intrinsic activity in cells of clone D2 was also observed using other assays of G-protein coupling namely [^{35}S]GTPγS binding and cholera toxin-catalysed [^{32}P]ADP-ribosylation experiments (data not shown). Therefore DADLE could be described as a full agonist, TIPPΨ as a neutral antagonist and the other four ligands as partial agonists.

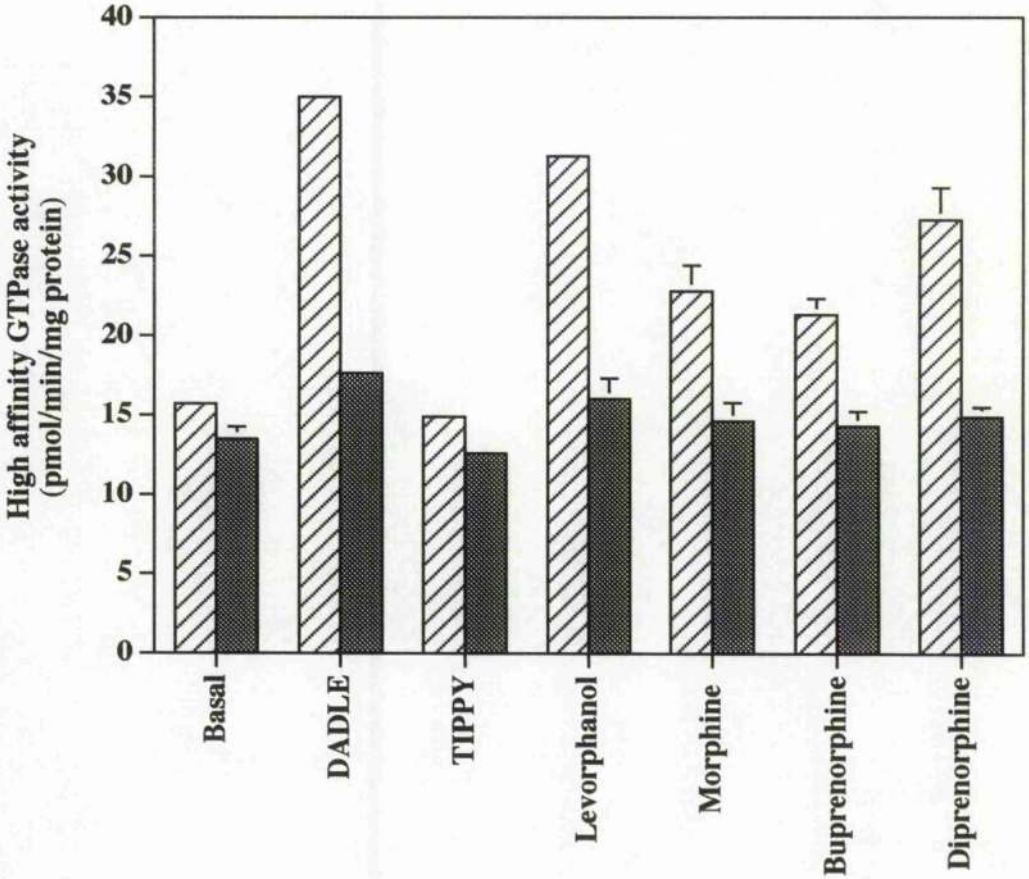

Figure 5.1 Effect of various opioid ligands on the high affinity GTPase activity in membranes from cells of clone D2 and clone DOE.

High affinity GTPase activity was measured as described in Section 2.2.4 on treatment of membranes derived from cells of clone D2 (hatched bars) and clone DOE (shaded bars) with various ligands (all at 10^{-6} M). Results are presented as mean ± SEM of triplicate assays of the activity in pmol/min/mg membrane protein and were calculated from one representative experiment from two (DOE) and three (D2) independent experiments performed.

Treatment of cells of clone D2 and DOE with maximally effective concentrations of these ligands for 5 min stimulated the phosphorylation of $p44^{MAPK}$ to an extent which was generally consistent with the observed stimulation of GTPase activity (Figure 5.2). As was expected from the previous chapter, DADLE stimulated the phosphorylation of the entire detectable population of $p44^{MAPK}$ in both clones. In cells of clone D2, every other opioid ligand produced a near maximal phosphorylation of $p44^{MAPK}$ while only levorphanol produced a measurable effect in cells of clone DOE. The effect of the partial agonists in clone D2 is not surprising as the level of stimulation of GTPase activity by these ligands in these cells was greater than that achieved by DADLE in clone DOE. TIPPΨ, however, was not expected to produce this maximal (or any) effect as it is classed as a neutral antagonist. This ligand may stimulate the G_i-protein machinery to a slight degree which cannot be measured at the level of GTPase activity (there is no data to support this), but which is sufficient to induce the phosphorylation of $p44^{MAPK}$. This explanation, however, is inadequate as the level of GTPase activation by TIPPΨ in clone D2 is lower than that produced by levorphanol in DOE cells, which can stimulate only a partial phosphorylation of $p44^{MAPK}$. The other unexpected result was that ICI174864 consistently stimulated the phosphorylation of $p44^{MAPK}$ over the basal levels in clone D2. This ligand has been reported to be an inverse agonist in these cells (Mullaney *et al.*, 1996) and so stimulation of phosphorylation of $p44^{MAPK}$ was totally unexpected. Although difficult to explain, the stimulation by TIPPΨ and ICI174864 does appear to have been mediated by the δ opioid receptor and not through some other effect on the cells as neither ligand displayed any detectable effect on the lower receptor expressing clone DOE. The lack of effect of the partial agonists in cells of clone DOE can perhaps be understood in terms of the low or undetectable level of G_i-protein stimulation as measured by the GTPase assay.

These results are similar in some ways to the effect of ligands with a range of intrinsic activities on the β_2-adrenoceptor-mediated activation of adenylyl cyclase in two clones with differing levels of receptor expression (MacEwan *et al.*, 1995). These ligands displayed higher intrinsic activities in the higher receptor expressing clone and the ligands with a relatively lower intrinsic activity were more sensitive to a reduction in receptor expression level. Therefore, the elimination of a greater fraction of the receptor population was required to reduce the effect of a full agonist compared to that of a partial agonist. As presented in Figure 5.2, DADLE produced essentially maximal phosphorylation of $p44^{MAPK}$ (at this time point) in both clone D2 and in clone DOE, whereas the agonists with lower intrinsic activity could produce a maximal response only in the clone expressing the higher level of receptors, and struggled to produce any effect in the lower expressing cell line. Therefore a similar differential sensitivity to the level of receptor expression was seen with partial agonists in this system.

EGF stimulated maximal phosphorylation of $p44^{MAPK}$ in both cell lines, again indicating that both clones were sensitive in this assay. Treatment with ET-1 was included in this experiment because there were conflicting reports of the effect of this agonist in Rat1 fibroblasts (discussed in Section 1.4.13.2). In cells of clone D2 and DOE, the effect of 5 min treatment with ET-1 was somewhat inconsistent, however, usually a strong (but not maximal) stimulation of $p44^{MAPK}$ phosphorylation was detected. ET-1 stimulated PLD and PLC activity more strongly than DADLE in clone D2 (see Figure 4.6 and 4.10) and the DADLE-mediated stimulation of PLD activity in clone DOE was very limited. This data indicates that it is highly unlikely that DADLE-mediated activation of PLD or PLC was responsible for the activation of $p42/44^{MAPK}$, but would not rule out the involvement of PLD or PLC activity in this pathway (see below).

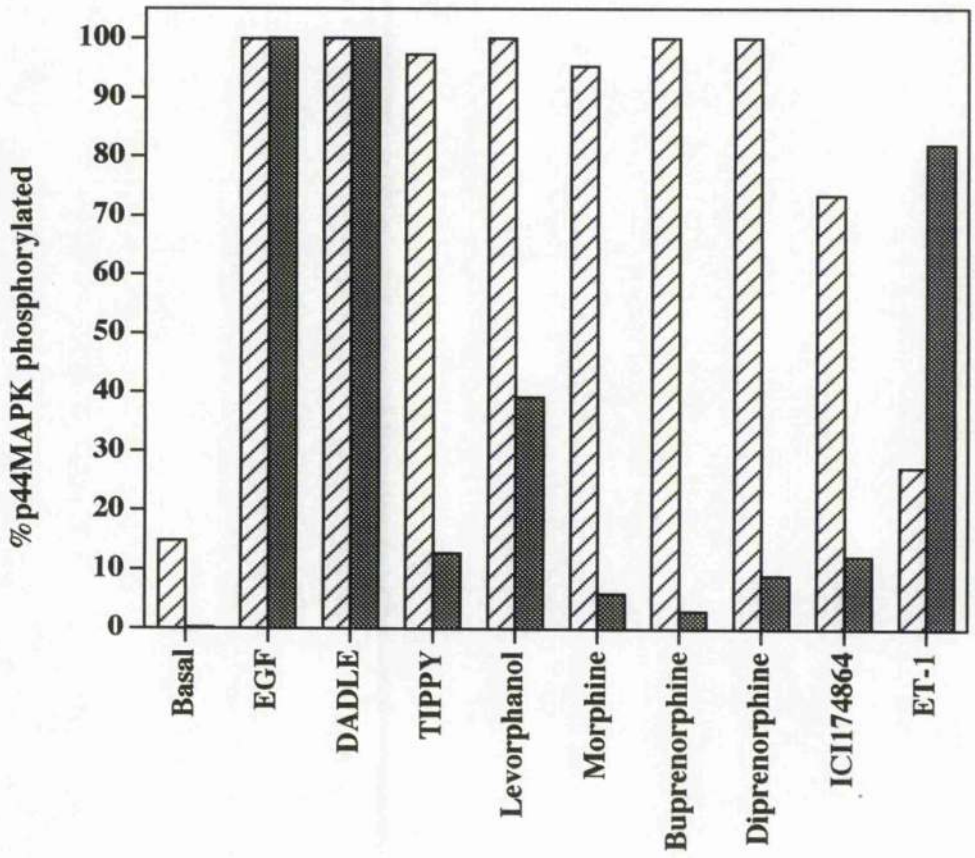

Figure 5.2 Phosphorylation of $p44^{MAPK}$ after 5 min treatment with maximally effective concentrations of various agonists in cells of clones D2 and DOE.

Serum starved cells of clone D2 (hatched bars) and clone DOE (shaded bars) were treated with various agonists for 5 min at a concentration of 10^{-6} M apart from EGF (10^{-8} M) and ET-1 (10^{-7} M). The percentage of $p44^{MAPK}$ which was present in its phosphorylated form in each sample was measured by the electrophoretic mobility shift assay as described in Section 2.2.9.1. The result is representative of two (DOE) or three (D2) experiments performed.

Although the opioid partial agonists could maximally phosphorylate $p44^{MAPK}$ in clone D2, differences were seen in the duration of this response (Figure 5.3A). Buprenorphine and morphine were chosen to be compared with DADLE as they were two of the less efficacious partial agonists and so it was assumed that any differences would be greater and more easily observed for these ligands. Although the average maximum phosphorylation reached was perhaps slightly less than 100%, essentially the only difference between the time courses was that the duration of phosphorylation was consistently less for buprenorphine and morphine compared to that for DADLE (Figure 5.3A). By 15 min of buprenorphine or morphine treatment, phosphorylation levels of $p44^{MAPK}$ had fallen to approximately 45%, whereas on average 90% was still phosphorylated after treatment with DADLE. This is consistent with the differences in the DADLE-mediated time courses between clones D2 and DOE (see Figure 4.16) and time courses produced by different concentrations of DADLE in clone D2 (Figure 4.20) and supports the conclusion that a greater level of G-protein stimulation induces a more sustained activation of $p42/44^{MAPK}$. The phosphorylation of $p44^{MAPK}$ on treating clone D2 with TIPPΨ or ICI174864 was rather inconsistent and 100% phosphorylation was not usually detected. However, the time course of phosphorylation stimulated by these ligands, as shown in Figure 5.3B, followed similar patterns to that seen for the other partial agonists with perhaps a more transient peak of activity which would be consistent with a lesser degree of G-protein stimulation.

The time courses of two of the more efficacious opioid partial agonists in cells of clone DOE are displayed in Figure 5.4. The phosphorylation by diprenorphine and levorphanol was also rather variable from experiment to experiment (perhaps because they are more sensitive to variations in receptor expression levels over different passages) but it was noted that the phosphorylation was more delayed than that observed with DADLE in these cells (seen in Figure 4.16). These results are consistent with a lower level of G-protein stimulation (detected by the GTPase assay) producing a delayed, weaker and more transient stimulation of the phosphorylation of $p44^{MAPK}$.

Figure 5.3 Time course of phosphorylation of $p44^{MAPK}$ by various opioid ligands in cells of clone D2.

Serum starved cells of clone D2 were treated for various times with different opioid ligands (all at 10^{-5} M) and the phosphorylation status of $p44^{MAPK}$ in each of the samples was measured by the electrophoretic mobility shift assay (according to Section 2.2.9.1). Results are presented as the percentage of the total detectable $p44^{MAPK}$ which was present in its phosphorylated form.

A Time courses for DADLE (open circles, full line), buprenorphine (closed circles, broken line) and morphine (open squares, dotted line). Results presented are mean ± SEM from at least three independent experiments.

B Time courses for TIPPΨ (open triangles, broken line) and ICI174864 (closed triangles, dotted line). Results presented are from one of two experiments performed.

Figure 5.3

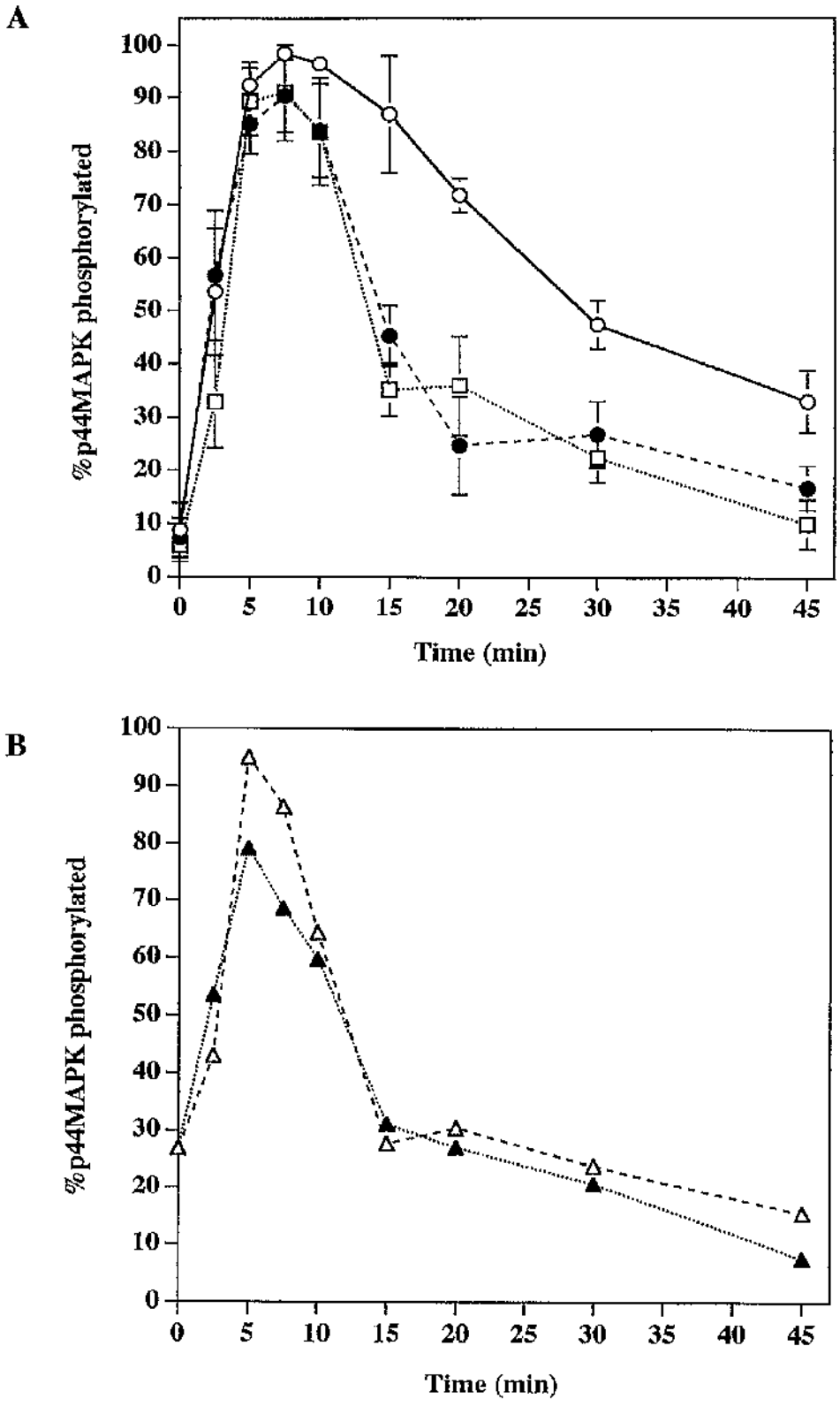
A
%p44MAPK phosphorylated
Time (min)
B
%p44MAPK phosphorylated
Time (min)

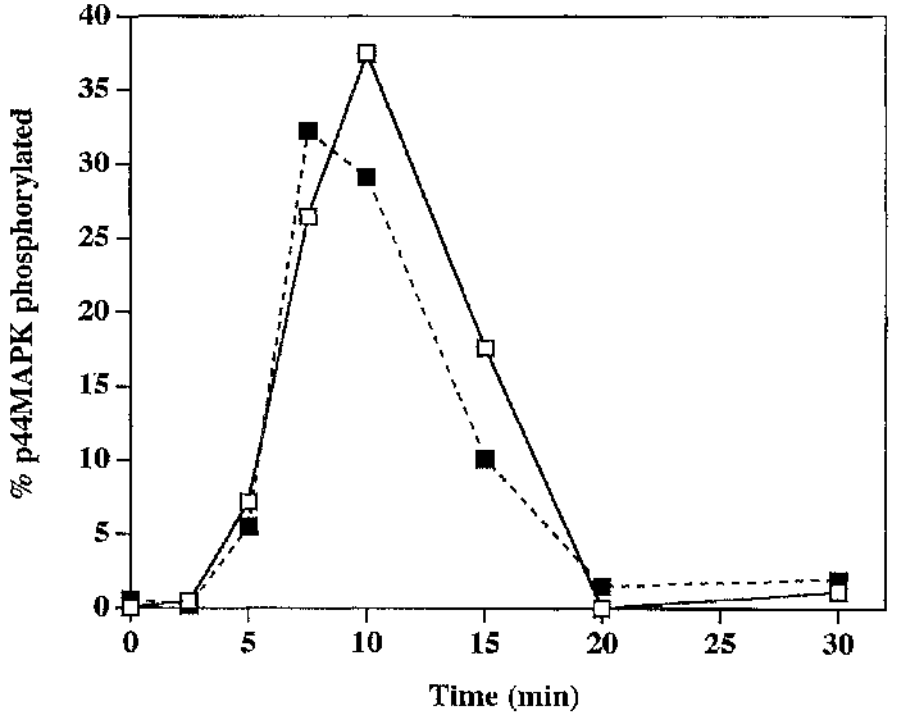

Figure 5.4 Time course of phosphorylation of $p44^{MAPK}$ by diprenorphine and levorphanol in cells of clone DOE.

Serum starved cells of clone DOE were treated with 10^{-5} M diprenorphine (open squares, full line) or 10^{-5} M levorphanol (closed squares, broken line) for various times. The percentage of phosphorylation of $p44^{MAPK}$ present in each of the samples was measured by the electrophoretic mobility shift assay as described in Section 2.2.9.1 and results presented are from one of two experiments performed.

Therefore the results produced with these opioid ligands confirm the conclusions presented in Chapter 4 concerning the relationship of the extent of G-protein stimulation by the receptor and the magnitude and time course of activation of $p42/44^{MAPK}$.

It has already been stated that the ET-1-mediated phosphorylation of $p44^{MAPK}$ in cells of clone DOE and D2 indicated that PLD activity was not responsible for the DADLE-mediated phosphorylation of $p42/44^{MAPK}$. The involvement of PLD activity in the regulation of $p44^{MAPK}$ was investigated further by pretreating the cells with 0.3% (v/v) butan-1-ol which trapped the PLD-derived phosphatidic acid as phosphatidylbutanol and prevented its action (Wilkes *et al.*, 1993). This treatment produced no effect on the stimulation of $p44^{MAPK}$ phosphorylation in clone D2 by maximally effective concentrations of DADLE or EGF, however, there was some inhibition of the ET-1 response (Figure 5.5A), (a reduction in basal phosphorylation of $p44^{MAPK}$ was also sometimes detected). The results were insufficient to conclusively prove that butanol had a significant effect on ET-1, and although work described later in this chapter would suggest that inhibitor studies using only cells which express high levels of receptor should be interpreted with caution, the data presented here would support the conclusion that PLD activity is not involved in the δ opioid receptor-mediated activation of $p44^{MAPK}$. The stimulation of PLD activity may still play a role in the mitogenic response to agonist-activation of the δ opioid receptor as demonstrated for angiotensin II-mediated mitogenesis in vascular smooth muscle cells (Wilkie *et al.*, 1996). Activation of $p42/44^{MAPK}$ was necessary, but not sufficient, for the mitogenic response to angiotensin II, and the inhibitory effect of butan-1-ol on this response suggested that PLD activity was one of the other required signalling components.

Chelerythrine similarly displayed no consistent, inhibitory, effect on DADLE-mediated phosphorylation of $p44^{MAPK}$ in clone D2 (Figure 5.5B). This compound is a protein kinase inhibitor which displays selectivity for PKC (Herbert *et al.*, 1990) and so this data would tend to rule out an involvement of PKC in the δ opioid receptor-mediated activation of $p44^{MAPK}$ (consistent with previous results for G_i-coupled receptors as discussed in Section 1.4.13.3). However, these results should be treated with caution as although chelerythrine did inhibit the phosphorylation induced by ET-1, this was not a complete effect and so the lack of effect on the response to DADLE could conceivably be due to the strong stimulation of the MAPK cascade being able to overcome a weak inhibition (see later for a similar observation with tyrphostin AG1478). Therefore, although not proved conclusively, the data would tend to exclude the involvement of PLD or PKC activity in the δ opioid mediated phosphorylation of $p44^{MAPK}$ but would indicate that these activities contribute to the ET-1-induced phosphorylation of $p44^{MAPK}$ as was observed in vascular smooth muscle cells (Wilkes *et al.*, 1993).

The involvement of the adenylyl cyclase pathway in the MAPK cascade was investigated by elevating cAMP levels with either dibutyryl cAMP or forskolin. Pretreatment of cells of clone D2 and DOE with 10^{-3} M dibutyryl cAMP significantly ($p < 0.05$) attenuated the phosphorylation of $p44^{MAPK}$ stimulated by 5 min treatment with maximally effective concentrations of DADLE and EGF (Figure 5.6 and data not shown). 10^{-5} M forskolin pretreatment of cells of clone D2, however, only attenuated the phosphorylation in response to EGF and not to DADLE. A similar observation was made with the α_{2A} adrenoceptor (see Table 3.1) and is possibly because of δ opioid receptor-mediated inhibition of forskolin-amplified adenylyl cyclase activity (see Figure 4.5). Therefore, the δ opioid receptor-mediated phosphorylation of $p44^{MAPK}$ in Rat1 fibroblasts was also attenuated by elevated cAMP levels as observed for numerous other GPCRs (see Section 1.4.10).

Figure 5.5 The effect of pretreatment of butanol and chelerythrine on the phosphorylation of $p44^{MAPK}$ by DADLE, EGF and ET-1 in cells of clone D2.

A Serum starved cells of clone D2 were pretreated for 10 min with serum free DMEM containing 0.3% (v/v) butan-1-ol (shaded bars) or with no additions (control - hatched bars). The cells were then treated for a further 5 min by the addition to final concentrations of 10^{-8} M EGF, 10^{-5} M DADLE, 10^{-7} M ET-1 or no addition (basal). The percentage phosphorylation of $p44^{MAPK}$ was then assessed by the electrophoretic mobility shift assay as described in Section 2.2.9.1.

B Serum starved cells of clone D2 were pretreated for 30 min with serum free DMEM containing 10^{-5} M chelerythrine (shaded bars) or with 0.1% (v/v) DMSO (control - hatched bars). The cells were then treated and $p44^{MAPK}$ phosphorylation was assessed as in part A.

Results for both parts are from one of two experiments performed.

Figure 5.5

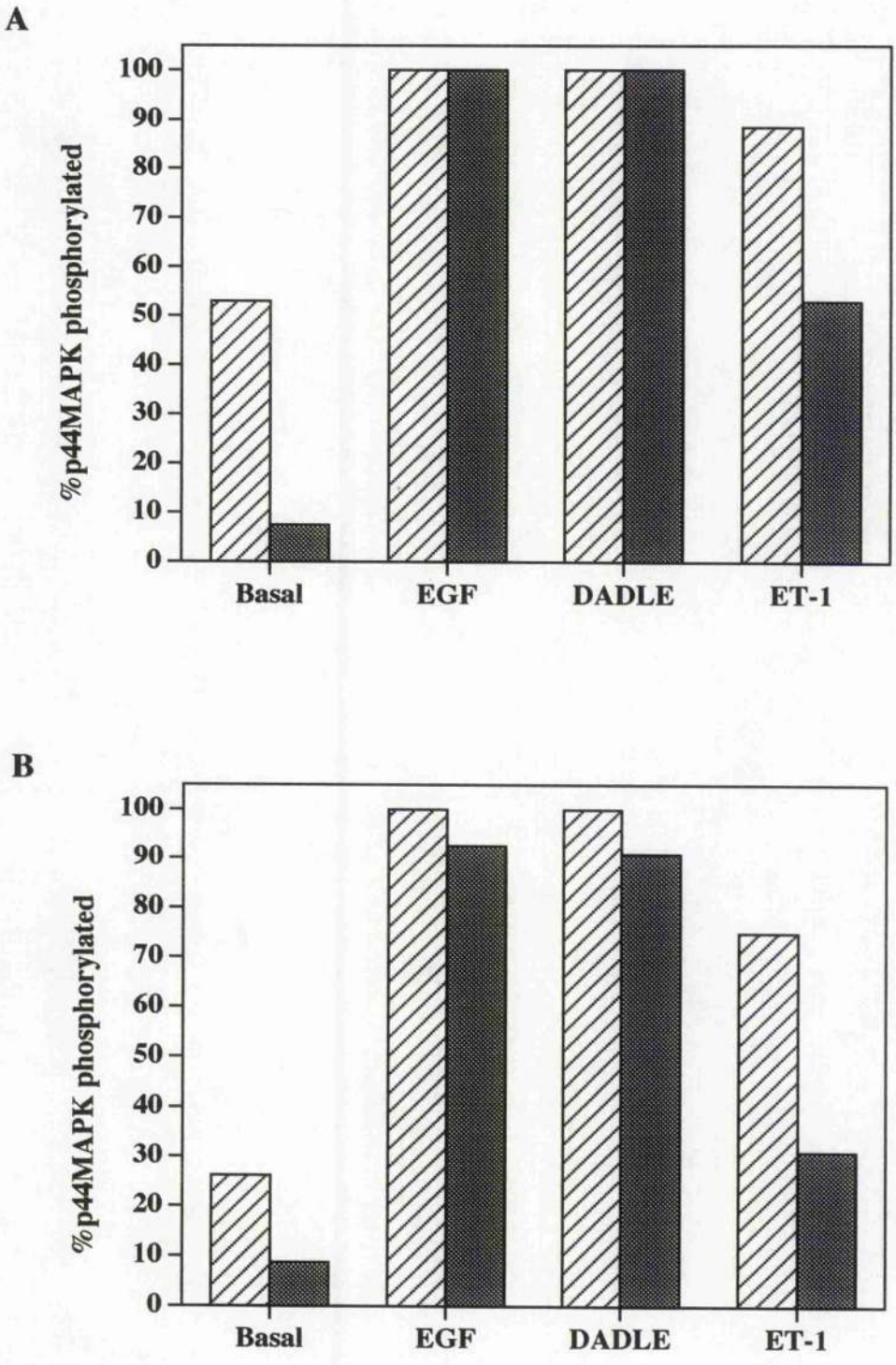
A
%p44MAPK phosphorylated
100
90
80
70
60
50
40
30
20
10
0
Basal
EGF
DADLE
ET-1
B
%p44MAPK phosphorylated
100
90
80
70
60
50
40
30
20
10
0
Basal
EGF
DADLE
ET-1

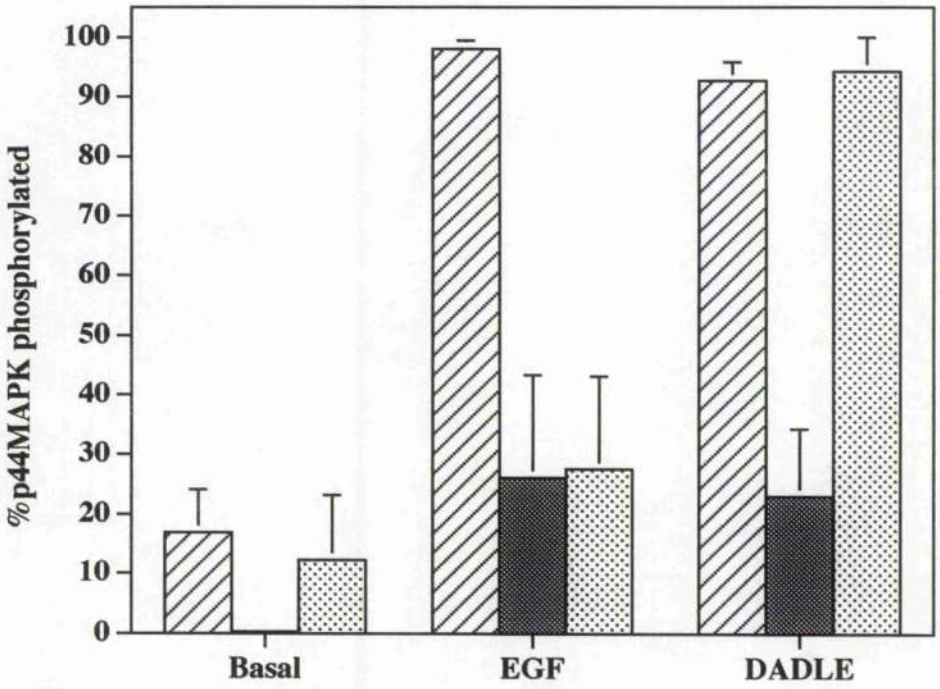

Figure 5.6 The effect of pretreatment of cells of clone D2 with dibutyryl cAMP or forskolin on DADLE and EGF-mediated phosphorylation of $p44^{MAPK}$.

Serum starved cells of clone D2 were pretreated with serum free DMEM containing no addition (hatched bars), 10^{-3} M dibutyryl cAMP (shaded bars), or 10^{-5} M forskolin (speckled bars) for 20 min prior to 5 min treatment with 10^{-5} M DADLE, 10^{-8} M EGF or no ligand (basal). The percentage phosphorylation of $p44^{MAPK}$ was assessed in each of the samples by the electrophoretic mobility shift assay (Section 2.2.9.1) and the data is presented as mean ± SEM, from three independent experiments.

The attenuation by dibutyryl cAMP of the phosphorylation of $p44^{MAPK}$ in response to 5 min treatment with DADLE in clone D2 was not usually complete (on average 20% phosphorylation remained). It was subsequently discovered that pretreatment of these cells with 10^{-3} M dibutyryl cAMP did not eliminate the DADLE-mediated phosphorylation of $p44^{MAPK}$ but rather produced a time course which was delayed, more transient and had a reduced maximum (Figure 5.7A). It typically took a further 5 min after the maximum was achieved in the control cells for the maximal phosphorylation to be reached in the dibutyryl cAMP-treated cells and this maximum was only 70% phosphorylation. This level was not sustained, in contrast with the elevated phosphorylation in the control cells which was still detected after 30 min. A similar but greater effect was observed in cells of clone DOE (Figure 5.7B). The delay of phosphorylation was perhaps even more obvious and the greater magnitude of inhibition of phosphorylation was sometimes such that a complete elimination of DADLE-mediated phosphorylation was observed. This perhaps was because the stimulation of this cascade by the lower expression level of δ opioid receptors in clone DOE was sometimes unable to overcome the inhibitory effect of the dibutyryl cAMP. Alterations in the time course of activation can have profound effects on the functional outcome of the stimulation of the MAPK cascade (as discussed in Section 1.4.15.1) and so these results illustrate how the functional effect on a cell of the stimulation of the MAPK cascade could be modified by other signal transduction pathways.

Figure 5.7 Effect of dibutyryl cAMP pretreatment on the time course of DADLE-mediated phosphorylation of $p44^{MAPK}$ in cells of clone D2 and DOE.

Serum starved cells of clone D2 (**A**) or clone DOE (**B**) were pretreated for 20 min with serum free DMEM containing 10^{-3} M dibutyryl cAMP (closed circles, broken lines) or left untreated (open circles, full lines). The cells were then treated with the addition of DADLE to a final concentration of 10^{-5} M and incubated for various times. The phosphorylation of $p44^{MAPK}$ was assessed in each of the samples by the electrophoretic mobility shift assay (Section 2.2.9.1) and the results are presented as percentage of the total detectable $p44^{MAPK}$ which was phosphorylated. Data in part A represents mean ± SEM from three independent experiments, data in part B is from one of two experiments performed.

Figure 5.7

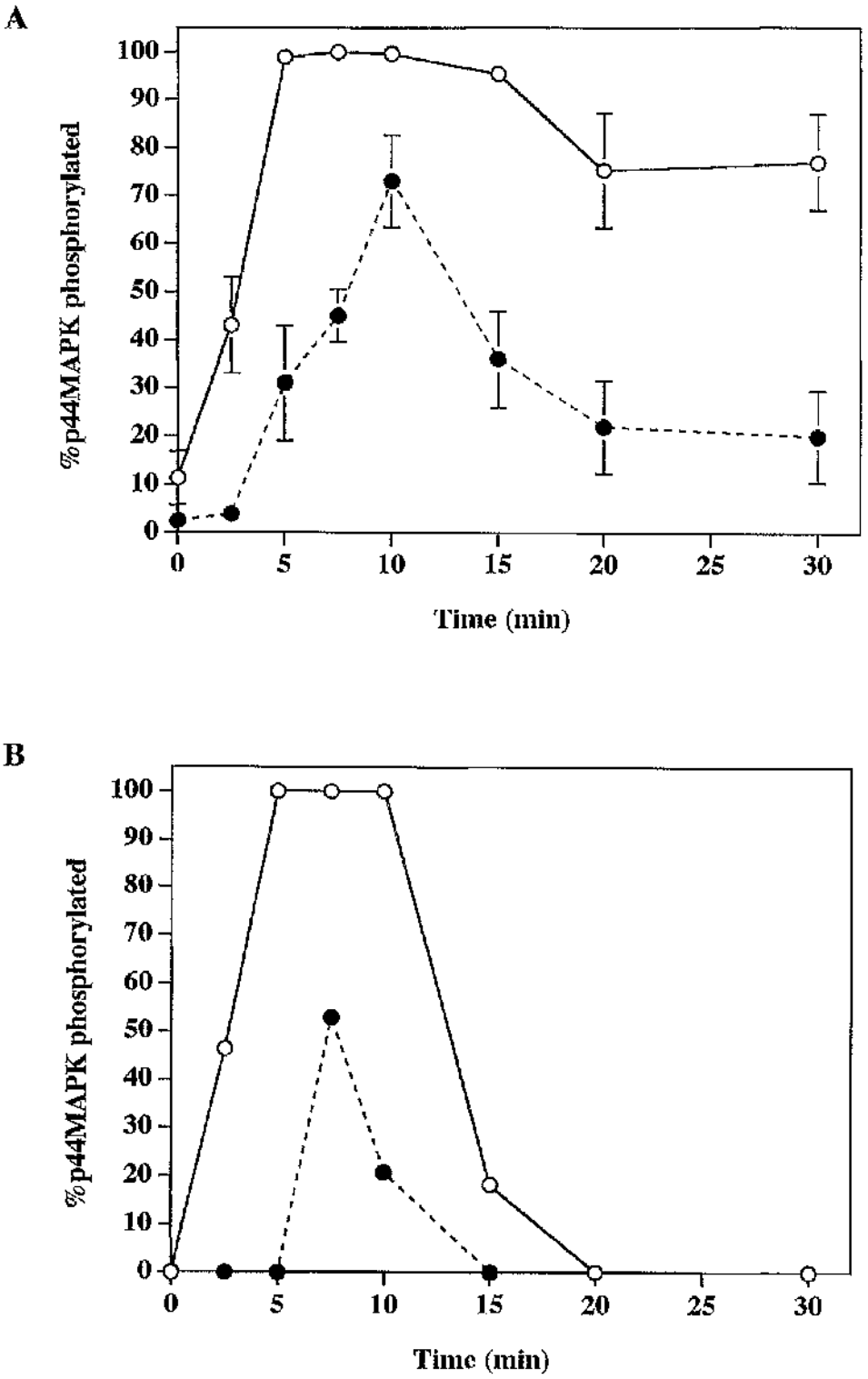
A
%p44MAPK phosphorylated
100
90
80
70
60
50
40
30
20
10
0
0
5
10
15
20
25
30
Time (min)
B
%p44MAPK phosphorylated
100
90
80
70
60
50
40
30
20
10
0
0
5
10
15
20
25
30
Time (min)

The effect of elevated levels of cAMP is thought to be mediated by a PKA-directed phosphorylation of Raf or other MEKK (see Section 1.4.10). These results would therefore suggest that this inhibition can be overcome by a greater stimulatory signal on these MEKKs or that the greater expression of the δ opioid receptor in clone D2 permits the activation of a cascade which does not involve a PKA-sensitive component. They might also suggest that the second input into the MAPK cascade suggested from the co-operativity observed in the concentration-response curves of DADLE-mediated activation of $p42/44^{MAPK}$ (see Figure 4.21-4.23) could possibly be provided by a reduction in cAMP (by an inhibition of adenylyl cyclase or stimulation of a phosphodiesterase). Although this idea is currently purely speculative a similar dual input to the $p42/44^{MAPK}$ cascade has been proposed for the β-adrenoceptor in COS-7 cells (Crespo *et al.*, 1995). In this case the simultaneous signals are opposing with the balance between the stimulatory signal (mediated by $G_{s\beta\gamma}$) and the inhibitory signal (by $G_{s\alpha}$-mediated elevation of cAMP and PKA activation) determining the outcome. However, in the case of the δ opioid receptor, the two signals appear to be stimulatory which could possibly produce the observed co-operativity.

Pretreatment with 10^{-3} M dibutyryl cAMP also reduced the transphosphatidylation activity in response to DADLE in cells of clone D2 (Figure 5.8A). However the results are not conclusive because the basal activity was reduced by the pretreatment so that although the actual activity in the presence of DADLE was reduced, there was still a substantial stimulation over basal in the presence of dibutyryl cAMP. The pretreatment had no consistent effect on the response to ET-1. There was no obvious change in the time course of DADLE-mediated activation of PLD other than a slight decrease in the maximal activation (Figure 5.8B). Elevated cAMP levels in these cells, therefore, did not have the same effect on the PLD activity as it does on the MAPK cascade which would indicate that the inhibitory effect of this compound did not occur at the level of the receptor.

Figure 5.8 The effect of pretreatment with 10^{-3} M dibutyryl cAMP on the ET-1 and DADLE-mediated activation of transphosphatidylation activity in cells of clone D2.

A Cells of clone D2 were labelled with [^{3}H]palmitate (4 μCi/ml) for 24 hours and then pretreated with HBGbutanol for 20 min with (shaded bars) or without (hatched bars) 10^{-3} M dibutyryl cAMP (after the usual washes of HBG and HBGbutanol). The cells were treated for 15 min by the addition of agonists to final concentrations of 10^{-5} M DADLE or 10^{-7} M ET-1 or there was no addition (basal activity). The transphosphatidylation activity was then measured as described in Section 2.2.10 and the activity in each sample is presented as the radioactivity measured in phosphatidylbutanol in DPM. Results displayed are mean ± SEM of triplicate assays from one of three experiments performed.

B Cells were treated, in an identical fashion to part A, with a final concentration of 10^{-5} M DADLE for various periods of time. Transphosphatidylation activity was then assayed as before. Results are mean ± SEM of triplicate assays from one of two experiments performed. Control cells are represented by the open circles and full line, cells which were pretreated with 10^{-3} M dibutyryl cAMP are represented by filled squares and broken line.

Figure 5.8

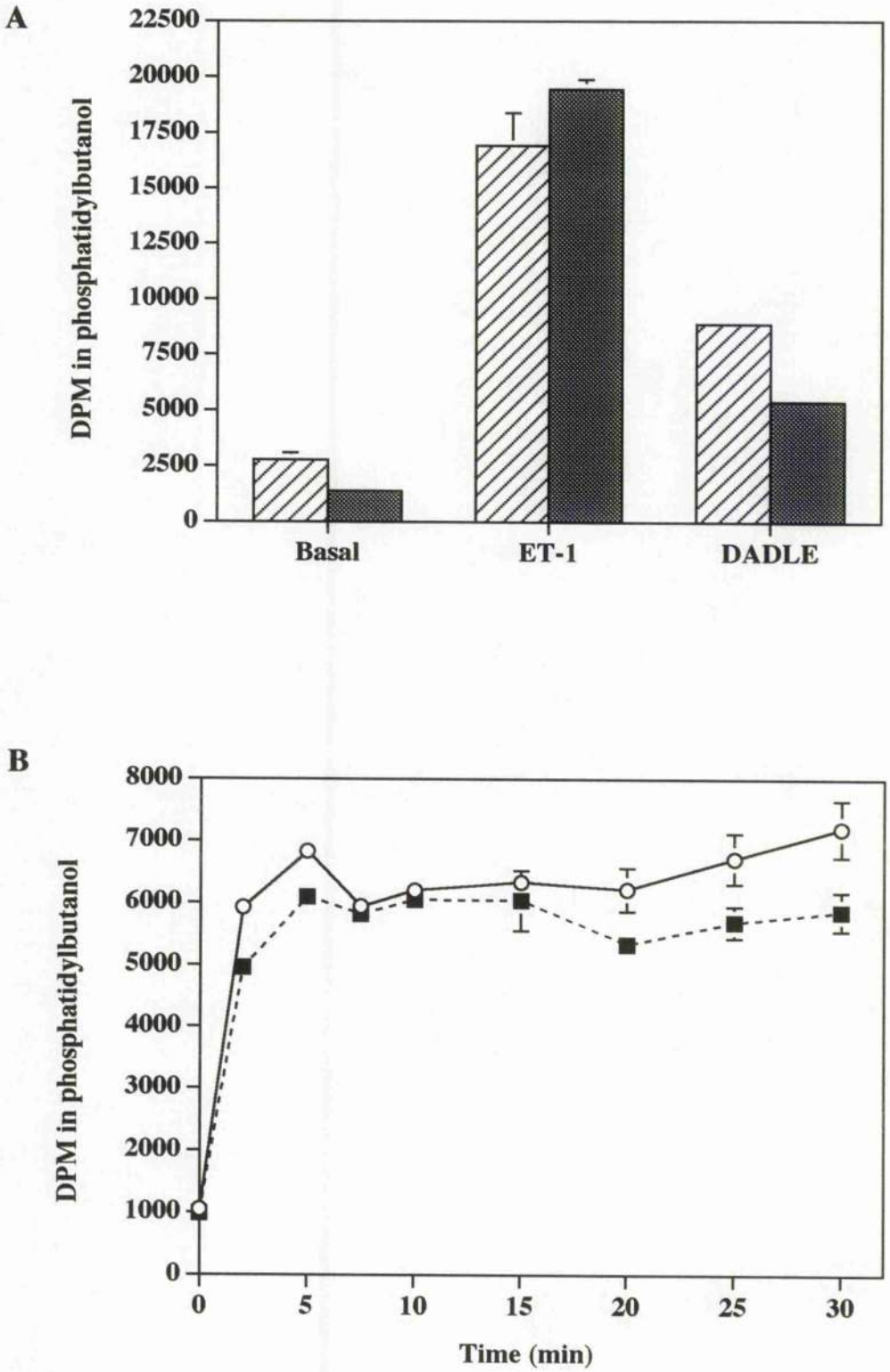
A
22500
20000
17500
15000
12500
10000
7500
5000
2500
0
DPM in phosphatidylbutanol
Basal
ET-1
DADLE
B
8000
7000
6000
5000
4000
3000
2000
1000
0
DPM in phosphatidylbutanol
0
5
10
15
20
25
30
Time (min)

Tyrphostin AG1478, at the lowest concentration used (2.5×10^{-8} M), attenuated the phosphorylation of $p44^{MAPK}$ in response to 5 min DADLE to almost half of the control level in cells of clone DOE (Figure 5.9B). Slightly more inhibition was produced by higher concentrations of this inhibitor, but it was never complete. This was in contrast to the lack of effect of tyrphostin AG1478 (at up to 2.5×10^{-7} M) on the stimulation of phosphorylation of $p44^{MAPK}$ by 5 min of DADLE treatment in cells of clone D2 (Figure 5.9A). The attenuation of δ opioid receptor-mediated phosphorylation of $p44^{MAPK}$ by tyrphostin AG1478 is consistent with its previously reported inhibitory effects on GPCR-mediated activation of $p42/44^{MAPK}$ in Rat1 fibroblasts (Daub *et al.*, 1996). However, the attenuation was never complete in clone DOE and was not detected in clone D2. This, presumably, reflects the greater receptor expression level in clone D2 and would suggest that the tyrphostin AG1478-mediated inhibition can be overcome by a greater stimulation of the MAPK cascade. A loss of sensitivity of insulin-mediated phosphorylation of $p44^{MAPK}$ to pertussis toxin and βARKct was reported following overexpression of the insulin receptor in Rat1 fibroblasts (Luttrell *et al.*, 1995b). The suggestion was made that this indicated that the insulin receptor at high density could utilise a $G_{\beta\gamma}$-independent pathway or that $G_{\beta\gamma}$ was only required at low receptor expression when efficient signalling was essential. Another interpretation of the response for the δ opioid receptor-mediated effect could be that the tyrphostin AG1478-sensitive step can similarly be by-passed, but only in clone D2 can this alternative pathway be sufficiently stimulated to produce maximal phosphorylation of $p44^{MAPK}$.

In both clones, tyrphostin AG1478 inhibited EGF-mediated phosphorylation of $p44^{MAPK}$ in a dose-dependent manner (Figure 5.9). It was reported that the G-protein coupled activation of $p44^{MAPK}$ was more sensitive to inhibition by tyrphostin AG1478 than was the stimulation by EGF (Daub *et al.*, 1996). The results presented here demonstrated that this conclusion depends on the GPCR expression level. These results therefore implicate the EGFR kinase in the $p44^{MAPK}$ cascade activated by the δ

opioid receptor. However, this conclusion depends on the specificity of tyrphostin AG1478 for the EGFR kinase which may not be as exclusive as previously reported as shown by an inhibition of the PDGF-mediated $p44^{MAPK}$ activation at similar levels to that required for the inhibition of the EGF-mediated response (Wilson, Milligan and Anderson, unpublished observations).

Some tyrphostins have been reported to display inhibitory effects on GTPase activities. However, tyrphostin AG1478 did not display any ability to interfere with the δ opioid receptor-mediated activation of G-proteins in clone D2 or DOE as demonstrated by the lack of effect of this compound on DADLE-mediated stimulation of high affinity GTPase activity in membranes prepared from either clone (data not shown). Therefore tyrphostin AG1478 must act at a point downstream of the G-protein machinery in order to inhibit the activation of the $p42/44^{MAPK}$ cascade.

Pretreatment of cells of clone DOE with 2.5×10^{-8} M tyrphostin AG1478 did not significantly alter the time course of DADLE-mediated phosphorylation of $p44^{MAPK}$ (Figure 5.10). Although the magnitude of the inhibition was not always identical, consistently a reduction in the maximal phosphorylation was detected without any drastic alteration to the time course. Therefore the effect of tyrphostin AG1478 in clone DOE was a true inhibition and not just a delay of the time course of phosphorylation.

Figure 5.9 The effect of various concentrations of tyrphostin AG1478 on DADLE and EGF-mediated phosphorylation of $p44^{MAPK}$ in cells of clone D2 and DOE. Serum starved cells of clone D2 (**A**) and clone DOE (**B**) were pretreated for 10 min with serum free DMEM containing 10^{-3}% (v/v) DMSO (control - hatched bars) or tyrphostin AG1478 at the following concentrations: 2.5 x 10^{-8} M (shaded bars), 1.25 x 10^{-7} M (striped bars) or 2.5 x 10^{-7} M (speckled bars). Cells were then treated for a further 5 min with no agonist (basal), 10^{-8} M EGF or 10^{-6} M DADLE and the phosphorylation status of $p44^{MAPK}$ was assessed by the electrophoretic mobility shift assay (Section 2.2.9.1). Data is presented as the percentage of the total detectable $p44^{MAPK}$ which was present in its phosphorylated form, mean ± range, from two independent experiments for each clone.

Figure 5.9

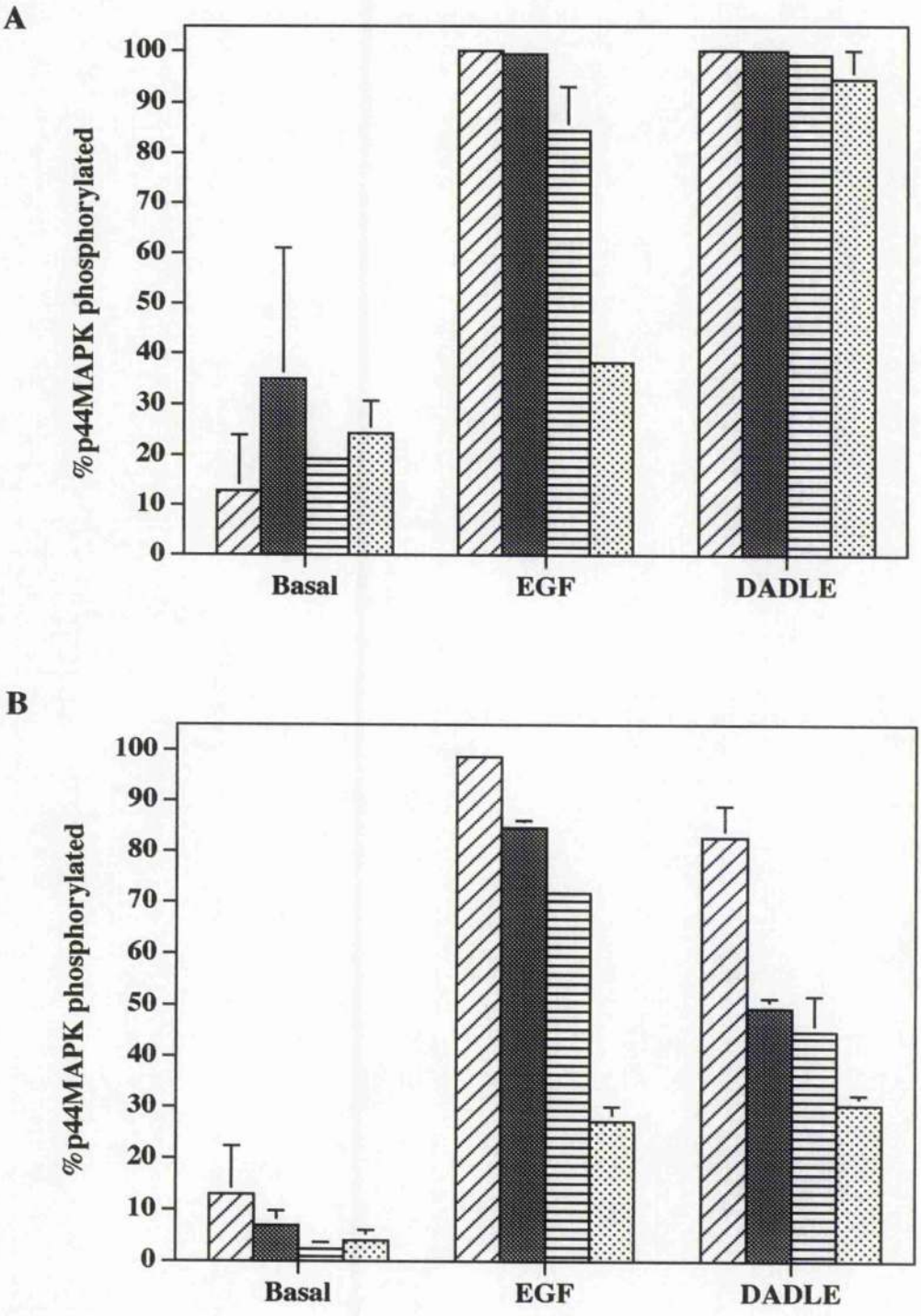
A
%p44MAPK phosphorylated
100
90
80
70
60
50
40
30
20
10
0
Basal
EGF
DADLE
B
%p44MAPK phosphorylated
100
90
80
70
60
50
40
30
20
10
0
Basal
EGF
DADLE

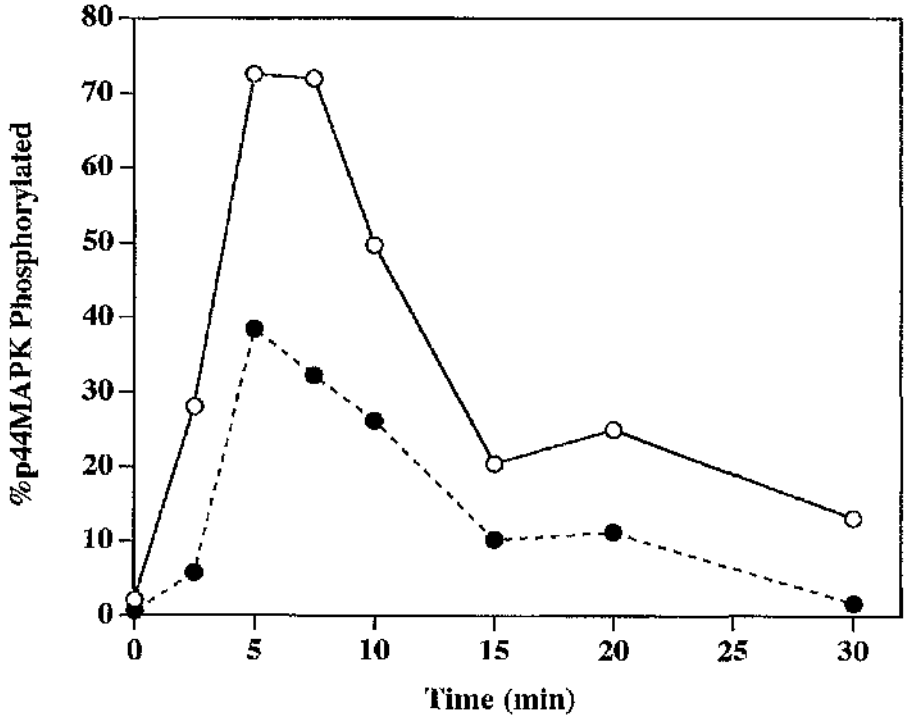

Figure 5.10 The effect of tyrphostin AG1478 on the time course of phosphorylation of p44^{MAPK} by DADLE in cells of clone DOE.

Serum starved cells of clone DOE were pretreated for 10 min with serum free DMEM containing 10^{-4}% (v/v) DMSO (control - open circles, full line) or 2.5 x 10^{-8} M tyrphostin AG1478 (filled circles, broken line). Cells were then treated with 10^{-6} M DADLE for various times and the phosphorylation status of p44^{MAPK} was assessed by the electrophoretic mobility shift assay (Section 2.2.9.1). Data is presented as the percentage of the total detectable p44^{MAPK} which was present in its phosphorylated form, and is from one of three experiments performed.

The concentration-response curve of DADLE-mediated phosphorylation of $p44^{MAPK}$ in cells of clone D2 was basically unaffected by pretreatment with 2.5×10^{-8} M tyrphostin AG1478 (Figure 5.11A). There was, however, a consistent, slight increase in the required concentration of DADLE for half-maximal effect in these cells and so there may have been some inhibition which could be easily overcome. This shift to the right in the concentration-response curves of DADLE-mediated phosphorylation of $p44^{MAPK}$ was also demonstrated in cells of clone DOE, although this was not as striking as the reduction in the maximum effect (Figure 5.11B). The magnitude of the inhibition was rather variable over different experiments, however, in each experiment with clone DOE, an obvious reduction in the maximum phosphorylation of $p44^{MAPK}$ and an increase in the EC_{50} value was observed after pretreatment with tyrphostin AG1478.

Pretreatment with 2.5×10^{-8} M tyrphostin AG1478 also produced a rightward shift in the concentration response curves of EGF-mediated phosphorylation of $p44^{MAPK}$ in both clone D2 and clone DOE (Figure 5.12). The EC_{50} values were increased between 1.5 and 4.5 fold. Therefore, although this concentration of inhibitor was unable to prevent 100% phosphorylation of $p44^{MAPK}$, the concentration of EGF which was required in order to produce this effect was consistently increased. It is of interest that these concentration-response curves also displayed a large Hill coefficient as was calculated for the DADLE-mediated phosphorylation of $p44^{MAPK}$ (see Chapter 4). Tyrphostin AG1478, therefore, appears to have a similar effect on the phosphorylation of $p44^{MAPK}$ mediated by the δ opioid receptor and by the EGFR which may imply the involvement of a common kinase in the cascades induced by either receptor.

Figure 5.11 Effect of tyrphostin AG1478 on the concentration-response curves for DADLE-mediated phosphorylation of $p44^{MAPK}$ in cells of clone D2 and DOE. Serum starved cells of clone D2 (**A**) or clone DOE (**B**) were pretreated for 10 min with serum free DMEM containing 10^{-4}% (v/v) DMSO (control - open circles, full line) or 2.5×10^{-8} M tyrphostin AG1478 (filled circles, broken line). Cells were then treated for 5 min with various concentrations of DADLE and the phosphorylation status of $p44^{MAPK}$ was assessed as described in Section 2.2.9.1 by the electrophoretic mobility shift assay. Data is presented as the percentage of the total detectable $p44^{MAPK}$ which was present in its phosphorylated form, and is from one of two (D2) and three (DOE) experiments performed.

Figure 5.11

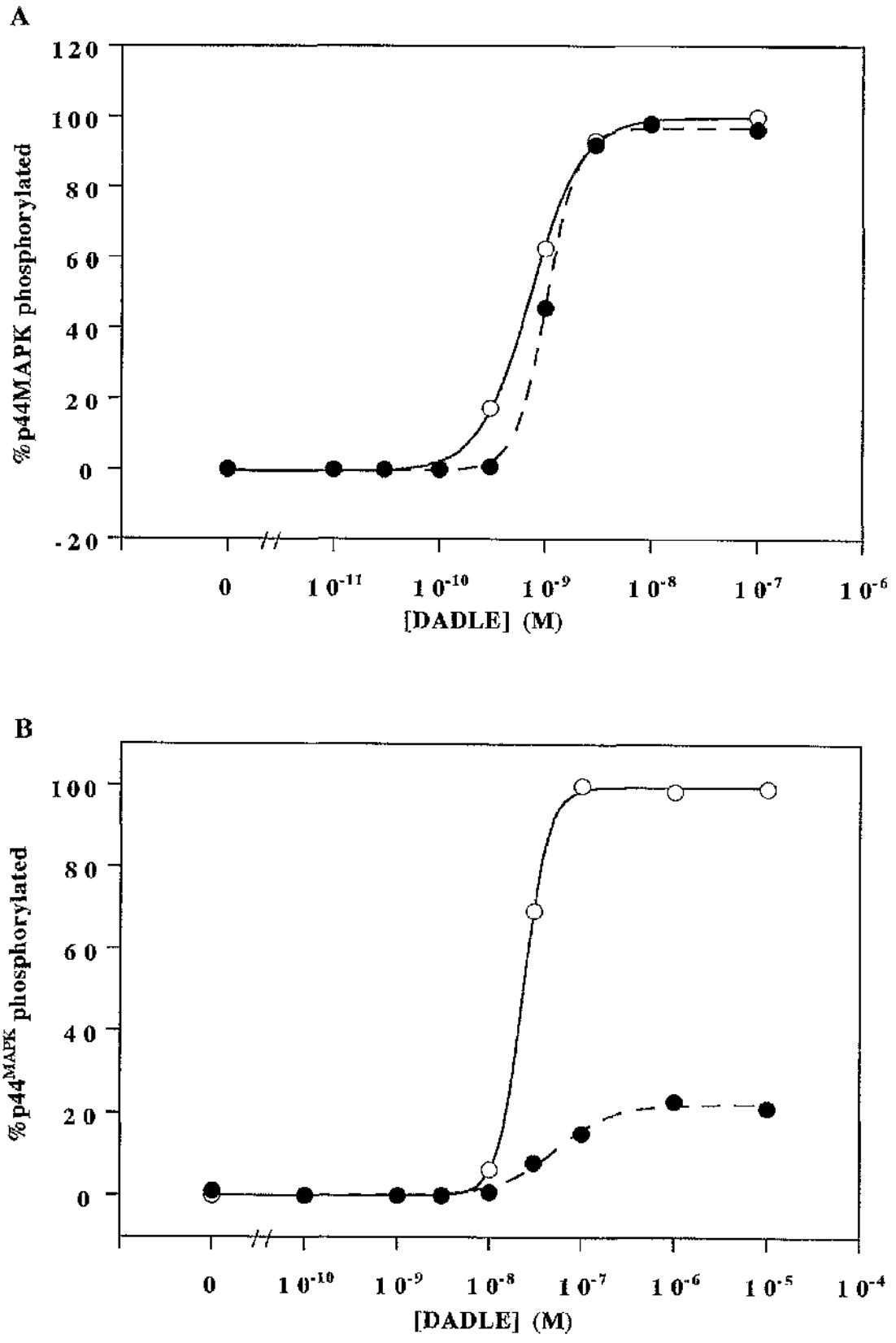
A
120
100
80
60
40
20
0
-20
% p44MAPK phosphorylated
0
10-11
10-10
10-9
10-8
10-7
10-6
[DADLE] (M)
B
100
80
60
40
20
0
% p44MAPK phosphorylated
0
10-10
10-9
10-8
10-7
10-6
10-5
10-4
[DADLE] (M)

Figure 5.12 Effect of tyrphostin AG1478 on the concentration-response curves for EGF-mediated phosphorylation of $p44^{MAPK}$ in cells of clone D2 and DOE.

Serum starved cells of clone D2 (**A**) or clone DOE (**B**) were pretreated for 10 min with serum free DMEM containing 10^{-4}% (v/v) DMSO (control - open circles, full line) or 2.5×10^{-8} M tyrphostin AG1478 (filled circles, broken line). Cells were then treated for 5 min with various concentrations of EGF and the phosphorylation status of $p44^{MAPK}$ was assessed as described in Section 2.2.9.1 by the electrophoretic mobility shift assay. Data is presented as the percentage of the total detectable $p44^{MAPK}$ which was present in its phosphorylated form, and is from one of two experiments performed.

Figure 5.12

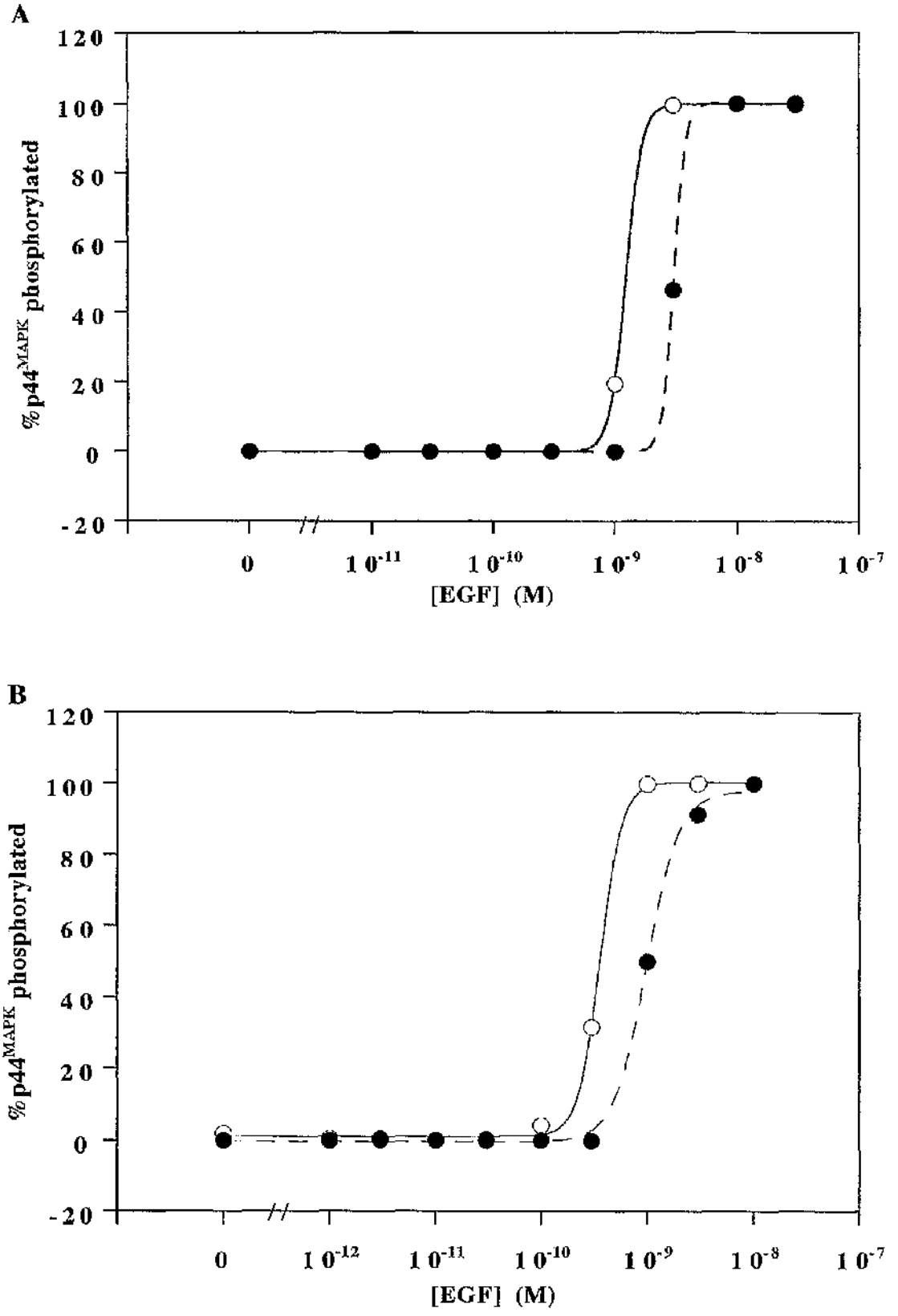
A
120
100
80
60
40
20
0
-20
% p44MAPK phosphorylated
0
10-11
10-10
10-9
10-8
10-7
[EGF] (M)
B
120
100
80
60
40
20
0
-20
% p44MAPK phosphorylated
0
10-12
10-11
10-10
10-9
10-8
10-7
[EGF] (M)

Genistein (a tyrosine kinase specific inhibitor) has been reported to attenuate the activation of $p42/44^{MAPK}$ by some, but not all, G_i-coupled receptors (see Section 1.4.13.3.3). As discussed in Chapter 3, genistein failed to display any inhibitory effect on the α_{2A} adrenoceptor-mediated activation of $p44^{MAPK}$ (see Figure 3.3). Similarly, in cells of both clone D2 and clone DOE, 5×10^{-5} M genistein pretreatment failed to affect the stimulation of phosphorylation of $p44^{MAPK}$ by a 5 min treatment with 10^{-6} M DADLE (Figure 5.13). This was observed even although, in these experiments, the DADLE-mediated phosphorylation of $p44^{MAPK}$ in clone DOE was much less than maximal. This concentration of genistein did consistently reduce the phosphorylation of $p44^{MAPK}$ by EGF to a small extent in cells of clone D2, but not (for some unknown reason) in cells of clone DOE. The data, however, would demonstrate that the δ opioid receptor-mediated phosphorylation of $p44^{MAPK}$ is insensitive to genistein.

Pretreatment of cells with 10^{-7} M wortmannin significantly ($p < 0.05$) attenuated the phosphorylation of $p44^{MAPK}$ in response to 5 min treatment of maximally effective concentrations of DADLE in cells of clone DOE (Figure 5.14B). In a similar observation to the effect of tyrphostin AG1478, only a limited attenuation of the DADLE-mediated phosphorylation of $p44^{MAPK}$ was observed in clone D2 (Figure 5.14A). The phosphorylation in response to 5 min treatment of EGF in either clone was unaffected. This would implicate a wortmannin-sensitive PI3-kinase activity in the cascade leading to phosphorylation of $p44^{MAPK}$ by the δ opioid receptor in these cells as has been reported for other GPCRs (see Section 1.4.14.1). A different explanation could be that wortmannin acted at a different target which is involved in this MAPK cascade. Wortmannin-sensitivity has been reported for the activation of $p70^{s6k}$ by the δ opioid receptor (Wilson *et al.*, submitted) and the α_{2A} adrenoceptor (Wilson *et al.*, 1996) expressed in Rat1 fibroblasts and so there is a possibility that wortmannin acts at a step which is common to the G_i-protein coupled receptor-mediated activation of $p42/44^{MAPK}$ and $p70^{s6k}$.

Figure 5.13 Effect of pretreatment with genistein on the phosphorylation of $p44^{MAPK}$ by DADLE and EGF in cells of clone D2 and DOE.

Serum starved cells of clone D2 (A) and clone DOE (B) were pretreated with serum free DMEM containing 1% (v/v) DMSO (control - hatched bars) or 5×10^{-5} M genistein (shaded bars) for 10 min. Cells were then stimulated with no agonist (basal), 10^{-8} M EGF or 10^{-6} M DADLE for a further 5 min and the phosphorylation level of $p44^{MAPK}$ was assessed by the electrophoretic mobility shift assay (Section 2.2.9.1). The percentage of the total detectable $p44^{MAPK}$ which was in its phosphorylated form is represented as mean ± range from two independent experiments performed for each clone .

Figure 5.13

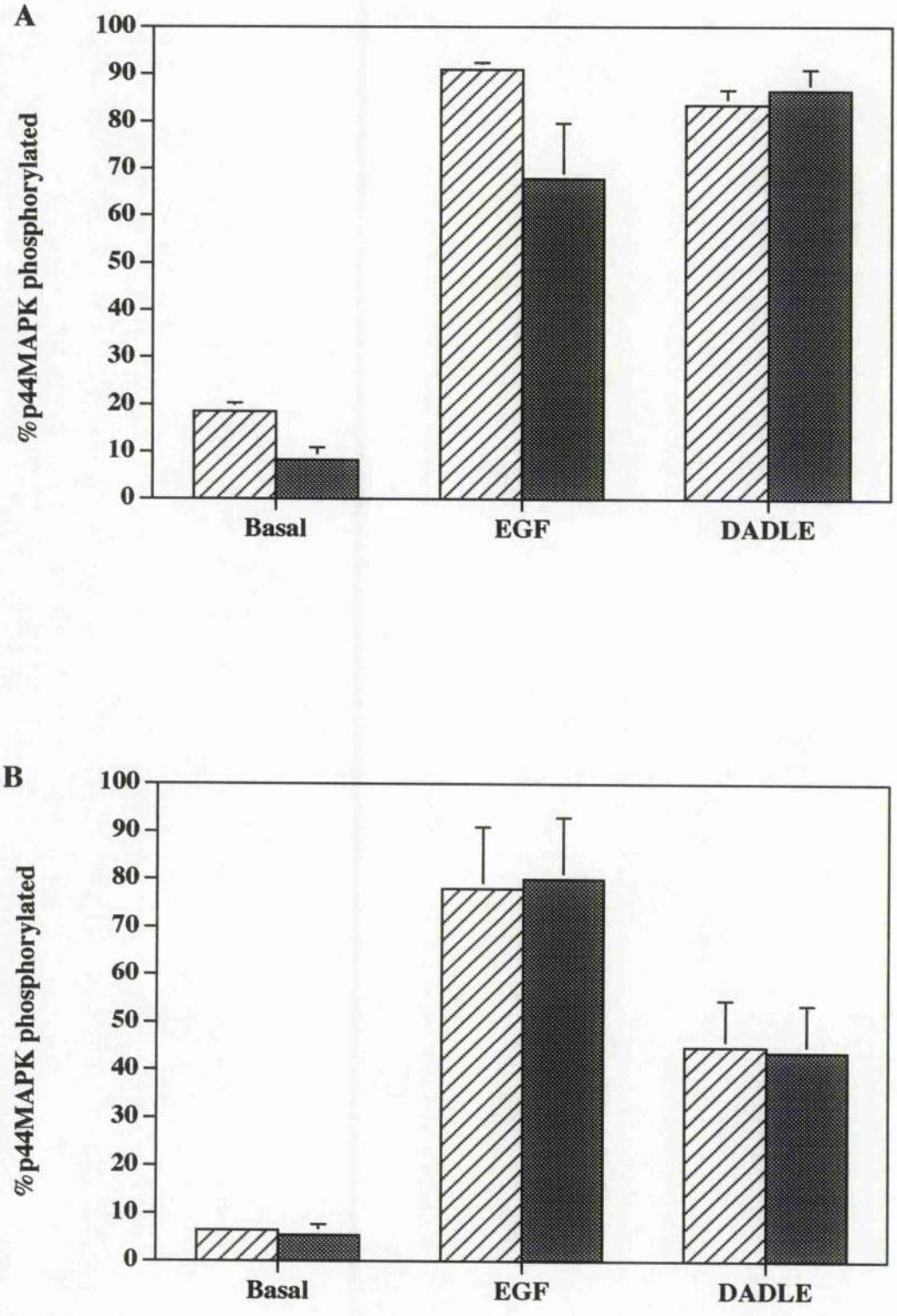
A
%p44MAPK phosphorylated
100
90
80
70
60
50
40
30
20
10
0
Basal
EGF
DADLE
B
%p44MAPK phosphorylated
100
90
80
70
60
50
40
30
20
10
0
Basal
EGF
DADLE

Figure 5.14 The effect of wortmannin on the $p44^{MAPK}$ phosphorylation stimulated by DADLE and EGF in cells of clone D2 and clone DOE.

Serum starved cells of clone D2 (A) and clone DOE (B) were pretreated in serum free DMEM containing 10^{-3}% (v/v) DMSO (control - hatched bars) or 10^{-7} M wortmannin (shaded bars) for 5 min. Cells were treated for a further 5 min in the presence of no agonist (basal), 10^{-8} M EGF or 10^{-6} M DADLE and the electrophoretic mobility shift assay was performed to determine the phosphorylation status of $p44^{MAPK}$ in each of the samples according to Section 2.2.9.1. Results are presented as the percentage of the total detectable $p44^{MAPK}$ which is present in its phosphorylated form, mean ± SEM from three (D2) or four (DOE) observations.

Figure 5.14

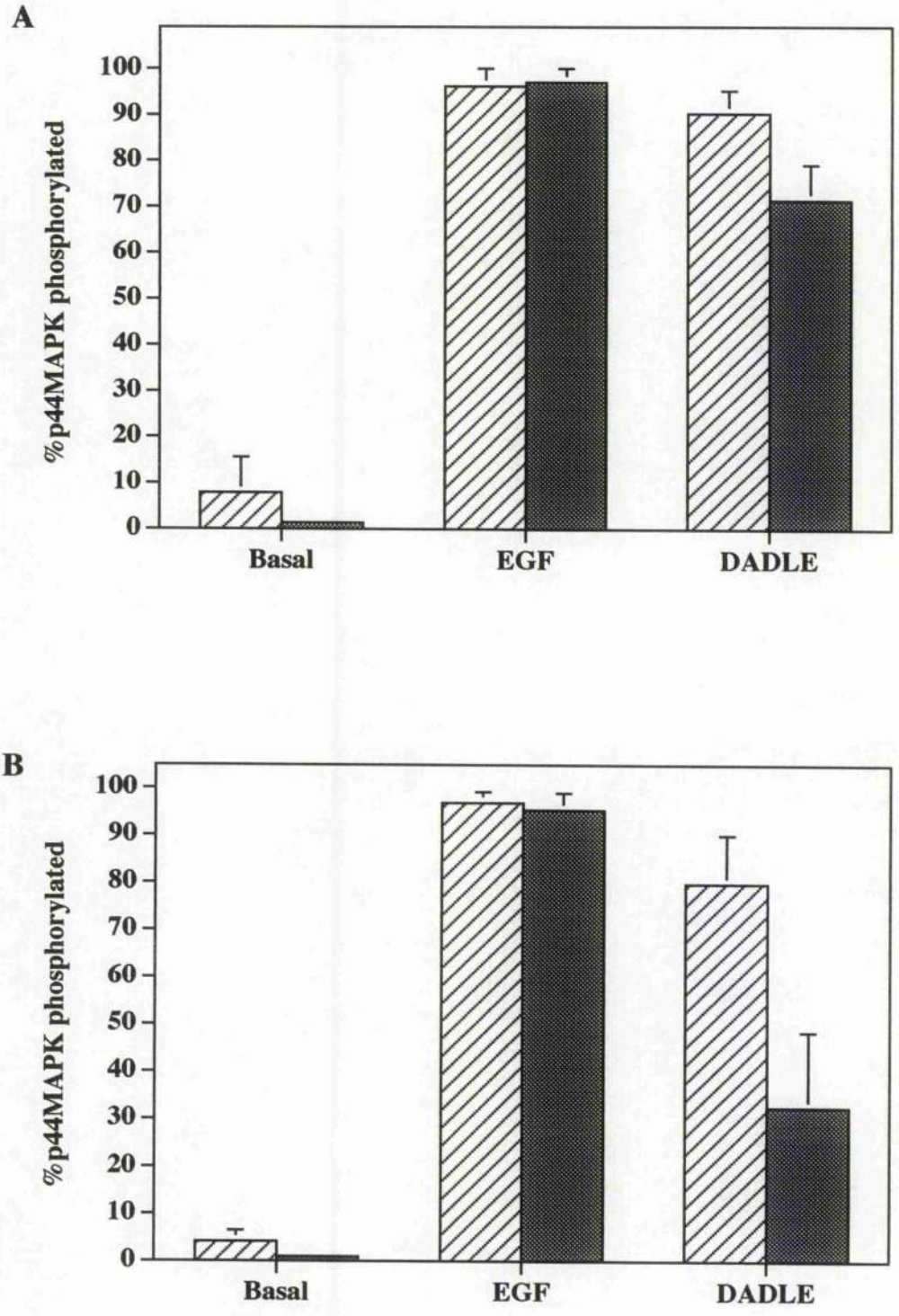
A
%p44MAPK phosphorylated
100
90
80
70
60
50
40
30
20
10
0
Basal
EGF
DADLE
B
%p44MAPK phosphorylated
100
90
80
70
60
50
40
30
20
10
0
Basal
EGF
DADLE

5.3 Conclusions

The work described in this chapter continued the study of the regulation of $p42/44^{MAPK}$ by the δ opioid receptor following its expression into Rat1 fibroblasts as described in Chapter 4. Specifically, the first section of this chapter provided evidence in support of the conclusions made regarding the quantitative relationship between the activation of $p42/44^{MAPK}$ and the stimulation of G-proteins. Opioid ligands with various intrinsic activities at this receptor demonstrated a much greater ability to stimulate $p44^{MAPK}$ phosphorylation in cells of clone D2 than in cells of clone DOE. Ligands which displayed partial agonism at the level of G-protein activation displayed activities at the level of $p44^{MAPK}$ phosphorylation which could permit their description as full agonists in that they induced maximal phosphorylation by 5 min treatment in D2 cells. However, in cells of clone DOE, these ligands struggled to stimulate phosphorylation over the basal level. This can be explained in the light of the large receptor and activated G-protein reserve present for the activation of $p44^{MAPK}$ in clone D2 (described in Chapter 4), which would enable a ligand which can stimulate only a limited G-protein coupling to significantly activate the $p42/44^{MAPK}$ cascade. A surprising and unexplainable observation, however, was the stimulation of phosphorylation in cells of clone D2 produced by previously described neutral antagonists and inverse agonists.

This work also supported the conclusion that the time course of activation was closely regulated by the extent to which the G-protein machinery was stimulated. Therefore, in clone D2, the opioid ligands which had a lower efficacy produced a delayed and more transient activation of $p44^{MAPK}$, the difference seen with the time courses corresponding to the differences measured at the level of G-protein stimulation. In clone DOE, although the efficacies of the ligands were insufficient to maximally phosphorylate $p44^{MAPK}$, two of the partial agonists were able to stimulate a limited phosphorylation of $p44^{MAPK}$ which displayed a more delayed and transient time course in comparison to that produced by DADLE.

The second section of work considered the involvement of other signalling pathways and kinases in the δ opioid receptor-mediated phosphorylation of $p44^{MAPK}$. Data was presented which indicated that PLD and PKC activity was not sufficient for, and probably not involved in, the regulation of $p44^{MAPK}$ by this receptor. In contrast, elevated cAMP displayed a definite inhibitory effect on the stimulation of $p44^{MAPK}$ phosphorylation which was consistent with the results with the α_{2A} adrenoceptor (Chapter 3). Elevated levels of cAMP did not completely eliminate the δ opioid receptor-mediated phosphorylation of $p44^{MAPK}$ in cells of clone D2 and DOE, but rather produced a delayed and more transient time course coupled with the reduction in maximal output. These effects were more substantial in the lower receptor expressing cell line and so raised the possibility of an alternative PKA-insensitive pathway which could be stimulated to a greater extent by a greater receptor density. This data also proposed a reduction in cAMP levels as a possible secondary input by the opioid receptor into the MAPK cascade. Elevated levels of cAMP also displayed very limited ability to attenuate the DADLE-mediated activation of PLD in clone D2 which was considered as evidence to indicate that the effect of elevated cAMP on the activation of $p42/44^{MAPK}$ did not occur at the level of the receptor.

The final part of this chapter made use of inhibitors which had been previously reported as having inhibitory effects on selective kinases. The data in general supported the conclusion that the δ opioid receptor-mediated phosphorylation of $p44^{MAPK}$ was achieved through a genistein-insensitive, but wortmannin and tyrphostin AG1478-sensitive pathway. This implicates both a PI3-kinase and an EGFR kinase in the cascade leading to the activation of $p44^{MAPK}$. It was also clear that the overexpression of the receptor in clone D2 allowed DADLE to activate the MAPK cascade even in the presence of these inhibitors. This would either suggest that the inhibitory effects can be overcome or that alternative pathways are possible.

Chapter 6: Final Discussion

Chapter 6: Final Discussion

Understanding of GPCR-mediated stimulation of the p42/44^{MAPK} cascade has progressed rapidly in the last few years. However, there was only a limited amount of quantitative information available on this regulation and it was this deficit that my thesis initially aimed to meet. It had been proposed that G_i-protein coupled p42/44^{MAPK} activation occurred as a result of receptor overexpression which forced unphysiological, or at least inefficient, coupling to the pathway to give a detectable response (e.g. Malarkey *et al.*, 1995). This was conclusively shown to be incorrect as low level expression of the α_{2A} adrenoceptor or the δ opioid receptor in Rat1 fibroblasts permitted significant (maximal at 5 min time point) activation of p42/44^{MAPK}. The coupling of these receptors to the MAPK cascade would thus appear to be highly efficient, because the coupling to other effectors and to G-protein activation was severely limited in these lower receptor expressing cells. This conclusion was reinforced by the ability of opioid ligands with little intrinsic activity in GTPase activity measurements to significantly phosphorylate p44^{MAPK} in clone D2.

The presence of a large receptor and activated G-protein reserve for the stimulation of p42/44^{MAPK} by the δ opioid receptor was further demonstrated by comparison of the concentration-response curves for DADLE-mediated phosphorylation/activation of p42/44^{MAPK} and high affinity GTPase activity (Figure 4.24). EC_{50} values for the activation of GTPase activity in clones D2 and DOE were 5.7×10^{-9} M and 4.2×10^{-8} M, respectively, which are in a similar range as the K_d for DADLE binding to the δ opioid receptor (approximately 2 to 5×10^{-9} M). This would possibly indicate the absence of a receptor reserve for the coupling to the G-protein population in these cells. However, the difference in EC_{50} values between clone D2 and DOE would perhaps suggest that in clone D2, such a receptor reserve does exist because in a situation of no receptor reserve, it might be expected to only see a reduction in the maximal output with no change to EC_{50} value when comparing a high and low receptor expressing cell line. This could be

investigated further by means of increasing concentrations of an irreversible antagonist which would increasingly 'knock out' proportions of the receptor population. Determination of the ability of these various functional receptor populations to stimulate high affinity GTPase activity (or another measure of G-protein activation) would determine whether a receptor reserve is present in clone D2. A receptor reserve would be seen as a shift in the concentration-response curves to the right with no reduction in the maximum output with increasing concentrations of irreversible antagonist, until the receptor reserve was abolished (Figure 6.1). Further increases in irreversible antagonist concentrations would reduce the maximum output without further affecting the EC_{50}, as might be anticipated to be observed if clone D2 contained no receptor reserve for G-protein activation. It is of interest to notice that earlier work (MacNulty *et al.*, 1992) with Rat1 fibroblast clonal cell lines expressing the α_{2A} adrenoceptor to various levels, demonstrated the absence of a receptor reserve for the activation of high affinity GTPase activity by the high correlation between receptor expression level and maximal agonist-stimulated high affinity GTPase activity, although the receptor expression levels observed in clone D2 were never produced in those experiments.

Although it is difficult to interpret the results from the concentration-response curves to DADLE for the stimulation of transphosphatidylation (PLD) activity for DOE cells, it would appear that there is no receptor reserve for this effector in the D2 cell line. This was concluded because the EC_{50} value for DADLE in clone DOE was not greater than for clone D2 but rather there was a significant reduction in the maximum output (Figure 4.9). Once again the the EC_{50} value for clone D2 was very similar to the K_d for this receptor (Figure 4.9).

Even if some degree of receptor reserve for the activation of the G-protein population in clone D2 does exist, it is dramatically smaller than that which exists for the activation of $p42/44^{MAPK}$ in these cells. This was clearly demonstrated by the significantly smaller EC_{50} value (7.3×10^{-11} M), and so for this effect there exists a large receptor and

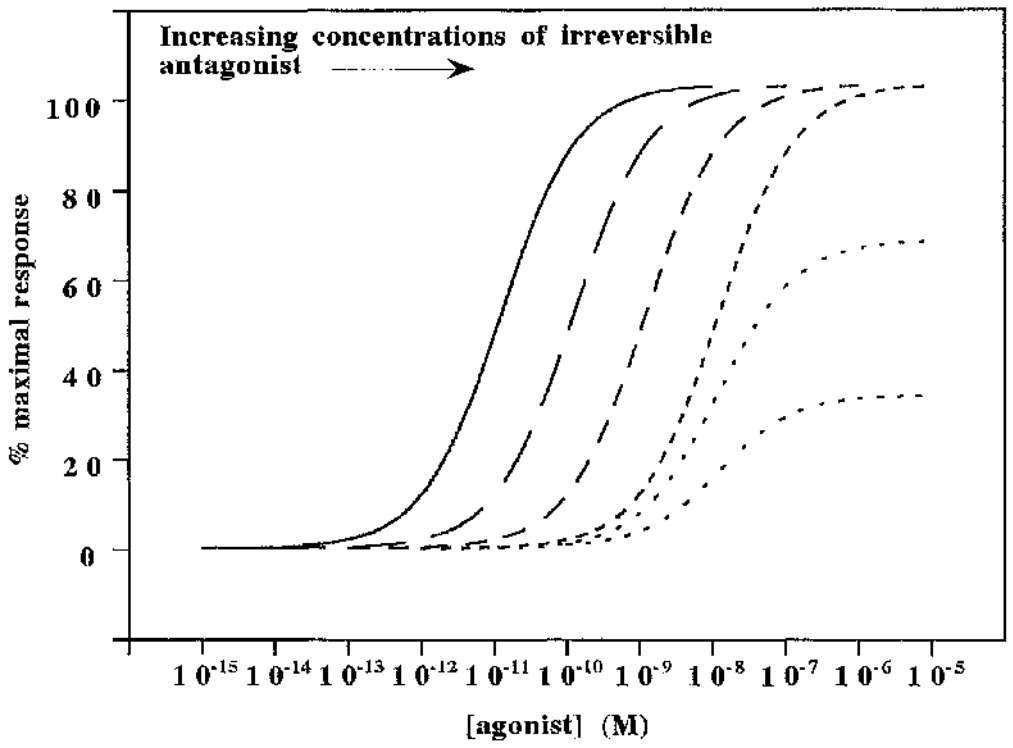

Figure 6.1 Illustration of receptor reserve

Hypothetical results from an experiment proposed in the main text to investigate the effect of treatment with increasing concentrations of an irreversible antagonist prior to concentration-response determinations for an agonist in a situation where a large receptor reserve exists in the control state.

activated G-protein reserve (Figure 4.21 and 4.22). In clone DOE, such a reserve was also obvious, although it was significantly smaller as is consistent with the lower level of receptor expression in this clone. Thus, there would appear to be a very low receptor expression requirement in order for the δ opioid receptor to maximally activate (at 5 min) the p42/44^{MAPK} cascade. The use of an irreversible antagonist acting on the δ opioid receptor in clone DOE which would further reduce the level of functional receptors in the cells, or an inducible receptor expression system to control the level of receptor expresssion would facilitate further study of the receptor reserve and may allow a determination of the minimum receptor expression level which is required to maximally activate p42/44^{MAPK}. It would then be of interest to compare this required level of receptor expression with other GPCRs expressed in Rat1 fibroblasts and various other cellular backgrounds, to investigate the generality of these observations and the possibility of receptor/cell specificity in the coupling efficiency to the p42/44^{MAPK} cascade. As the coupling to the p42/44^{MAPK} cascade is assumed to be mediated by the $G_{\beta\gamma}$ subunits, the large activated G-protein reserve for p42/44^{MAPK} activation in both clone D2 and DOE would appear to contradict the previous ideas that effectors which use such a coupling mechanism display a requirement for greater stoichiometry of G-protein and effector activation (higher receptor occupancy) than do G_{α}-coupled responses.

The situation is not as clear for the α_{2A} adrenoceptor expressed in Rat1 fibroblasts. A receptor reserve for the agonist-stimulated, high affinity GTPase response (Figure 3.6) could possibly exist based on the same reasons noted above for the δ opioid receptor. The ability of the lower expressing clone TAGWT 3 to maximally stimulate p42/44^{MAPK} on treatment with UK14304, and the ability of the ASN79 clones to stimulate the phosphorylation of p44^{MAPK} (Figure 3.10), when they displayed a much reduced signalling capacity to G-proteins and effectors (Figures 3.5, 3.7 and 3.8), would suggest that a receptor and activated G-protein reserve did exist for this effect. However, the concentration-response curves appeared to contadict such a conclusion. Unfortunately this inconsistency was not resolved in these experiments and so further work is still

required to determine if highly efficient coupling to the p42/44^{MAPK} cascade is a selective property of the δ opioid receptor.

Another difference between the GPCRs studied in this thesis was that the δ opioid receptor-mediated p42/44^{MAPK} activation/phosphorylation was co-operative in nature (Figure 4.21), whereas this was not observed for the α_{2A} adrenoceptor (Figure 3.12) or LPA receptor (Figure 4.23). This suggests that there may be additional input sites into the MAPK pathway for the δ opioid receptor which are not available for the other GPCRs. The ability of the δ opioid receptor to inhibit adenylyl cyclase activity (Figure 4.5) and the inhibitory effect of elevated cAMP levels on p42/44^{MAPK} activation in these cells (Figure 5.6) could suggest that a secondary input into the MAPK pathway may occur at this level. However, this suggestion is unable to explain the selective nature of this regulation because co-operativity has only been recorded for the δ opioid receptor, whereas the other GPCRs studied also displayed agonist-mediated inhibition of adenylyl cyclase (Figure 3.8). It would be of interest to know to what extent the co-operativity can be observed for other receptor/cell systems. This might help explain the exclusive ability of the δ opioid receptor as well as suggest what signalling component is responsible for the proposed secondary input into the MAPK cascade. In addition, the level in the cascade at which co-operativity can still be observed could also focus the investigation into possible secondary input points.

The time course of activation of p42/44^{MAPK} appeared to be closely regulated by the level of G-protein activation produced by the receptor. Therefore, a greater G-protein coupling produced a more rapid and sustained stimulation. The time course varied greatly with the GPCR expression levels, the coupling efficiency of the receptor (wild type versus Asn^{79} mutant), and the concentration and intrinsic activity of ligands used (see Figures 3.10, 4.16, 4.20, 5.3 and 5.4). As discussed previously (Section 1.4.15.1), the functional outcome of the MAPK cascade is closely dependent on the duration of activation and so in this way the outcome of the GPCR-mediated

p42/44^{MAPK} activation in each cell could possibly be modified and controlled by all of the above factors as well as by cross-talk from other signalling pathways (such as the cAMP pathway).

Understanding the involvement of various kinases and other signalling pathways in the regulation of p42/44^{MAPK} by GPCRs was the final objective of this thesis. Agents with reported inhibitory activity at selective kinases were used to address some of these issues and the conclusions from such experiments necessarily depend heavily upon the selectivity of these agents. The influence of the cAMP signalling pathway on the GPCR-mediated p42/44^{MAPK} cascade has been discussed above. It would appear, however, that PLD or PKC activity does not influence the MAPK pathway initiated by the δ opioid receptor (Figure 5.5) as expected for G_i-protein coupled receptors (see Section 1.4.13.3), although the results presented in Chapter 5 do not exclude the possibility of the δ opioid receptor using a PKC activity to provide an additional or alternative mechanism for stimulating the p42/44^{MAPK} pathway. The data does support the view that δ opioid-mediated stimulation of PLD activity was not sufficient for the observed level of activation of p42/44^{MAPK} but further study would be required in order to conclude that these pathways are completely independent.

The sensitivity to wortmannin may imply the involvement of a PI3-kinase γ-like (G-protein activated) PI3-kinase isotype (Stoyanov *et al.*, 1995) in the regulation of δ opioid-induced p42/44^{MAPK} activation (Figure 5.14), although the experiments performed made no attempt at identifying the wortmannin-sensitive species in the pathway. A role for a PI3-kinase γ-like enzyme would be consistent with a recent report of agonist-mediated activation of p42/44^{MAPK} by the muscarinic m2 acetylcholine receptor expressed in COS-7 cells which appeared to signal via PI3-kinase γ in a $G_{\beta\gamma}$-dependent manner (Lopez-Ilasaca *et al.*, 1997). In this cell system, PI3-kinase γ was placed directly downstream of $G_{\beta\gamma}$ leading to a pathway involving a tyrosine kinase, Shc, Grb2, mSos,

Ras and Raf. However, the mechanism connecting the activation of the PI3-kinase to the tyrosine phosphorylation of Shc was not investigated.

The EGFR tyrosine kinase was implicated by the inhibitory effect of tyrphostin AG1478 on DADLE-mediated phosphorylation of $p44^{MAPK}$ in clone DOE (Figure 5.9). This could imply that the δ opioid receptor can activate the $p42/44^{MAPK}$ pathway through activation of the EGFR tyrosine kinase in the absence of EGF as concluded previously for other GPCRs (Daub *et al.*, 1996). The majority of the data in this thesis would not be inconsistent with this role for EGFR kinase in the δ opioid receptor-stimulated MAPK pathway, apart from possibly the lack of effect of forskolin on DADLE-mediated $p44^{MAPK}$ phosphorylation when EGF-mediated activation was significantly attenuated (see Figure 5.6). However, this might perhaps be explained by the ability of the δ opioid receptor to mediate inhibition of adenylyl cyclase (Figure 4.5). The wortmannin-sensitive step would appear to be upstream of the EGFR kinase (or on a parallel pathway) as shown by the insensitivity of EGF-mediated phosphorylation of $p42/44^{MAPK}$ to wortmannin at concentrations which inhibit DADLE-mediated phosphorylation of $p44^{MAPK}$.

The ability of DADLE to stimulate apparently maximal phosphorylation of $p44^{MAPK}$ in clone D2 in the presence of a concentration of tyrphostin AG1478 which significantly attenuates the EGF-mediated phosphorylation of $p44^{MAPK}$ would perhaps suggest that the greater receptor expression level achieved in clone D2 permitted activation of a pathway distinct from the EGFR kinase to such an extent that full $p44^{MAPK}$ phosphorylation could be induced. Alternative kinases could be provided from the Src family of tyrosine kinases and/or by a PYK2-like kinase which have been implicated in the activation of $p42/44^{MAPK}$ by some GPCRs (see Section 1.4.13.3 and 1.4.13.5). The majority of the literature has implicated a genistein-sensitive kinase in the GPCR-mediated activation of $p42/44^{MAPK}$ and although genistein was apparently without effect in clone D2 and DOE (Figure 5.13) there could be a role for such a kinase under

conditions in which the EGFR kinase is inhibited. The EGFR kinase is thought to mediate the signal from GPCRs to $p42/44^{MAPK}$ via Shc tyrosine phosphorylation and Grb2.mSos association (Daub *et al.*, 1996) and these other kinases could also perform such a role. It would therefore be of some interest to determine whether a similar level of DADLE-stimulated Shc tyrosine phosphorylation is achieved in tyrphostin AG1478-treated cells as was observed in uninhibited D2 cells (Mullaney *et al.*, 1997) which might indicate if the tyrphostin insensitivity is the result of the direct substitution of another tyrosine kinase into the role of the EGFR or whether a distinct input into the pathway at a different level in the pathway is possible for the δ opioid receptor.

These results would therefore again raise the possibility of multiple inputs into the MAPK pathway by the δ opioid receptor as was discussed in relation to the observed co-operative nature of $p42/44^{MAPK}$ activation. Investigating the effect of tyrphostin AG1478 (and wortmannin) on the α_{2A} adrenoceptor agonist and LPA-mediated activation of $p44^{MAPK}$, to determine if this apparent choice of pathways is available for these receptors, may suggest whether a lack of such alternative pathways explain the lack of co-operativity in the responses seen with these ligands.

The above conclusions suggest a possible model pathway of agonist-mediated activation of $p42/44^{MAPK}$ by the δ opioid receptor when expressed in Rat1 fibroblasts as shown in Figure 6.2. The data discussed here does not address the question of whether the wortmannin-sensitive step and the EGFR kinase lie on the same pathway or represent alternative/parallel pathways which are both required for full activation (at least in the absence of a large receptor overexpression) and have been drawn as they are for the sake of simplicity. It is not inconsistent with the data presented for the wortmannin-sensitive step to lie on the alternative pathway which was speculated to permit full stimulation of $p44^{MAPK}$ in the presence of tyrphostin AG1478 in the D2 clone. These aspects of this model could be tested from a more thorough study of the maximum inhibition possible by

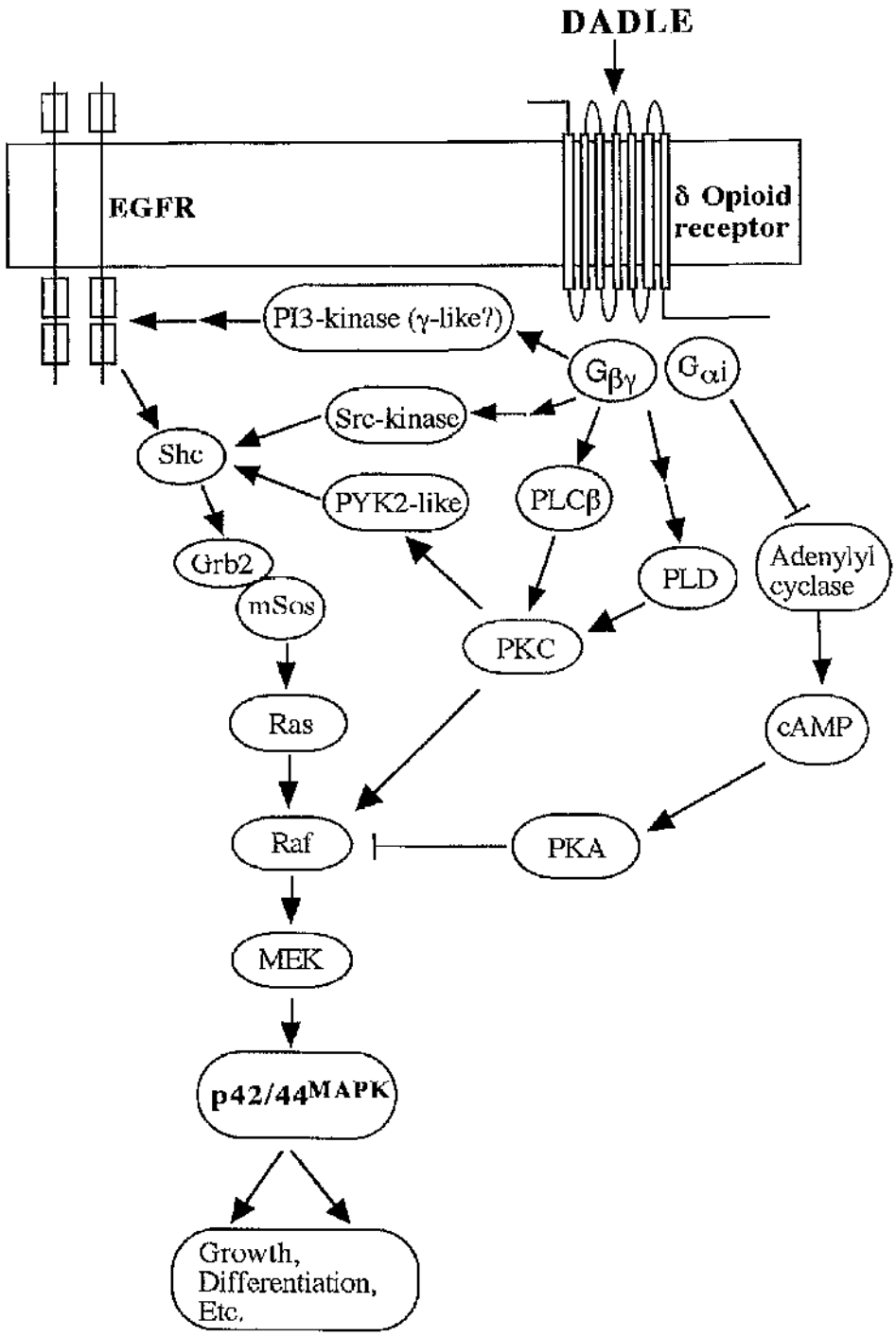

Figure 6.2 Model of p42/44^{MAPK} regulation by the agonist-activated δ opioid receptor when expressed in Rat1 fibroblasts.

Possible model of activation of p42/44^{MAPK} by the agonist activated δ opioid receptor after heterologous expression in Rat1 fibroblasts in order to explain the effects of tyrphostin AG1478 and wortmannin on this pathway. See main text for details.

tyrphostin AG1478 and wortmannin and the effect of both compounds when they are allowed to act together. Src and PYK2-like kinases and PKC are included in this model only to demonstrate possible secondary inputs and their involvement in this regulation in these cells is purely speculative at present.

This thesis has described the regulation of $p42/44^{MAPK}$ in terms of receptor expression level and G-protein activation required for coupling, the relation between G-protein activation and duration of MAPK response, the possible involvement of multiple input points into the pathway and the cross-regulation and involvement of kinases of other signal transduction pathways. Although many of these observations could possibly be described as general for G_i-protein coupled receptors, there is certainly a degree of receptor (and possibly cell) specificity, the extent of which will require further investigation.

List of Publications

List of Publications

Wilson, M., **Burt, A. R.**, Milligan, G., and Anderson, N. G. (1996) Wortmannin-sensitive activation of $p70^{s6k}$ by endogenous and heterologously expressed G_i-coupled receptors. J. Biol. Chem. **271**, 8537-8540

Burt, A. R., Carr, I. C., Mullaney, I., Anderson, N. G., and Milligan, G. (1996) Agonist activation of p42 and p44 mitogen-activated protein kinases following expression of the mouse δ opioid receptor in Rat1 fibroblasts: effects of receptor expression levels and comparison with G-protein activation. Biochem. J. **320**, 227-235

Milligan, G., **Burt, A. R.**, Wilson, M., and Anderson, N. G. (1996) The interface between α_2- adrenoceptors and tyrosine kinase signalling pathways. In alpha$_2$-adrenergic receptors: Structure, function and therapeutic implications p95-101. (Lanier, S. M., and Limbird, L. E., eds). Harwood Academic Publishers, Reading.

Milligan, G., **Burt, A. R.**, Carr, I. C., Mullaney, I. (1996) Signalling functions and G-protein specificity of the mouse δ opioid receptor following expression in Rat1 fibroblasts. Anaesthesia (in press).

Mullaney, I., Carr, I. C., **Burt, A. R.**, Wilson, M., Anderson, N. G., and Milligan, G. (1997) Agonist-mediated tyrosine phosphorylation of isoforms of Shc adapter proteins by the δ opioid receptor. Cell Signalling (in press).

Wilson, M., **Burt, A. R.**, Milligan, G., and Anderson, N. G. Mitogenic signalling by the δ opioid receptor expressed in Rat1 fibroblasts involves the activation of p70/p85 S6 kinase. (submitted)

References

References

Aitken, A. (1995) 14-3-3 proteins on the MAP. Trends Biochem. Sci. **20**, 95-97

Akiyama, T., Ishida, J., Nakagawa, S., Ogwawara, H., Watanabe, S., Itoh, N., Shibuya, M., and Fukame, Y. (1987) Genistein, a selective inhibitor of tyrosine-specific protein kinases. J. Biol. Chem. **262**, 5592-5595

Alblas, J., van Corven, E. J., Hordijk, P. L., Milligan, G., and Moolenaar, W. H. (1993) G_i-mediated activation of the $p21^{ras}$-mitogen-activated protein kinase pathway by α_2-adrenergic receptors expressed in fibroblasts. J. Biol. Chem. **268**, 22235-22238

Alessandrini, A., Crews, C. M., and Erikson, R. L. (1992) Phorbol ester stimulates a protein-tyrosine/threonine kinase that phosphorylates and activates the *ERK-1* gene product. Proc. Natl. Acad. Sci. USA **89**, 8200-8204

Alessi, D. R., Saito, Y., Campbell, D. G., Cohen, P., Sithanandam, G., Rapp, U., Ashworth, A., Marshall, C. J., and Cowley, S. (1994) Identification of the sites in MAP kinase kinase-1 phosphorylated by $p74^{raf-1}$. EMBO J. **13**, 1610-1619

Alessi, D. R., Smythe, C., and Keyse, S. M. (1993) The human CL100 gene encodes a Tyr/Thr -protein phosphatase which potently and specifically inactivates MAP kinase and suppresses its activation by oncogenic ras in Xenopus oocyte extracts. Oncogene **8**, 2015-2020

Anderson, N. G., Maller, J. L., Tonks, N. K., and Sturgill, T. W. (1990) Requirement for integration of signals from two distinct phosphorylation pathways for activation of MAP kinase. Nature **343**, 651-653

Aronheim, A., Engelberg, D., Li, N., Al-Alawi, N., Schlessinger, J., and Karin, M. (1994) Membrane targetting of the nucleotide exchange factor Sos is sufficient for activating the Ras signalling pathway. Cell **78**, 949-961

Ashkenazi, A., Winslow, J. W., Peralta, E. G., Peterson, G. L., Schimerlik, M. I., Capon, D. J., and Ramachandran, J. (1987) An M2 muscarinic receptor subtype coupled to both adenylyl cyclase and phosphoinositide turnover. Science **238**, 672-675

Avruch, J., Zhang, X., and Kyriakis, J. M. (1994) Raf meets Ras: completing the framework of a signal transduction pathway. Trends Biochem. Sci. **19**, 279-283

Blenis, J. (1993) Signal transduction via the MAP kinase: proceed at your own RSK. Proc. Natl. Acad. Sci. USA **90**, 5889-5892

Blumer, K. J., and Johnson, G. L. (1994) Diversity in function and regulation of MAP kinase pathways. Trends Biochem. Sci. **19**, 236-240

Boarder, M. R. (1994) A role for phospholipase D in control of mitogenesis. Trends Pharmacol. Sci. **15**, 57-62

Bogoyevitch, M. A., Glennon, P. E., Andersson, M. B., Clerk, A., Lazou, A., Marshall, C. J., Parker, P. J., and Sugden, P. H. (1994) Endothelin-1 and fibroblast growth factors stimulate the mitogen-activated protein kinase signalling cascade in cardiac myocytes. J. Biol. Chem. **269**, 1110-1119

Boguski, M. S., and McCormick, F. (1993) Proteins regulating Ras and its relatives. Nature **366**, 642-654

Bonfini, L., Migliaccio, E., Pelicci, G., Lanfrancone, L., and Pelicci, P. G. (1996) Not all Shc's roads lead to Ras. Trends Biochem. Sci. **21**, 257-261

Bos, J. L. (1995) A target for phosphoinositide 3-kinase: Akt/PKB. Trends Biochem. Sci. **20**, 441-442

Boulton, T. G., Nye, S. H., Robbins, D. J., Ip, N. Y., Radziejewska, E., Morgenbesser, S. D., DePinho, R. A., Panayotatos, N., Cobb, M. H., and Yancopoulos, G. D. (1991) ERKs: a family of protein-serine/threonine kinases that are activated and tyrosine phosphorylated in response to insulin and NGF. Cell **65**, 663-675

Boulton, T. G., Yancopoulos, G. D., Gregory, J. S., Slaughter, C., Moomaw, C., Hsu, J., and Cobb, M. H. (1990) An insulin-stimulated protein kinase similar to yeast kinase involved in cell cycle control. Science **249**, 64-67

Burgering, B. M., and Bos, J. L. (1995) Regulation of Ras-mediated signalling: more than one way to skin a cat. Trends Biochem. Sci. **20**, 18-22

Burgering, B. M. Th., Pronk, G. J., van Weeren, P. C., Chardin, P., and Bos, J. L. (1993) cAMP antagonizes $p21^{ras}$-directed activation of extracellular signal-regulated kinase 2 and phosphorylation of mSos nucleotide exchange factor. EMBO J. **12**, 4211-4220

Cano, E., and Mahadevan, L. C. (1995) Parallel signal processing among mammalian MAPKs. Trends Biochem. Sci. **20**, 117-121

Carr, C., Grassie, M., and Milligan, G. (1994) Stimulation of high-affinity GTPase-activity and cholera toxin-catalysed [^{32}P]ADP-ribosylation of G_i by lysophosphatidic acid (LPA) in wild-type and α2C10 adrenoceptor-transfected Rat1 fibroblasts. Biochem. J. **298**, 493-497

Cazaubon, S., Parker, P. J., Strosberg, A. D., and Couraud, P-O. (1993) Endothelins stimulate tyrosine phosphorylation and activity of p42/mitogen-activated protein kinase in astocytes. Biochem. J. **293**, 381-386

Ceresa, B. P., and Limbird, L. E. (1994) Mutation of an aspartate residue highly conserved among G-protein-coupled receptors results in nonreciprocal disruption of α_2-adrenergic receptor-G-protein interactions. J. Biol. Chem. **269**, 29557-29564

Chabre, O., Conklin, B. R., Brandon, S., Bourne, H. R., and Limbird, L. E. (1994) Coupling of the α_{2A}- adrenergic receptor to multiple G-proteins. J. Biol. Chem. **269**, 5730-5734

Chao, T-S. O., Foster, D. A., Rapp, U. R., and Rosner, M. R. (1994) Differential Raf requirements for activation of mitogen-activated protein kinase by growth factors, phorbol esters, and calcium. J. Biol. Chem. **269**, 7337-7341

Charles, C. H., Abler, A. S., and Lau, L. F. (1992) cDNA sequence of a growth factor-inducible immediate early gene and characterization of its encoded protein. Oncogene **7**, 187-190

Charles, C. H., Sun, H., Lau, L. F., and Tonks, N. K. (1993) The growth factor-inducible immediate early gene *3CH134* encodes a protein-tyrosine-phosphatase. Proc. Natl. Acad. Sci. USA **90**, 5292-5296

Chen, J., and Iyengar, R. (1994) Suppression of Ras-induced transformation of NIH 3T3 cells by activated $G\alpha_s$. Science **263**, 1278-1281

Chen, R-H., Sarnecki, C., and Blenis, J. (1992) Nuclear localization and regulation of *erk*- and *rsk*-encoded protein kinases. Mol. Cell. Biol. **12**, 915-927

Chen, Y-h., Grall, D., Salcini, A. E., Pelicci, P. G., Pouyességur, J., and Van Obberghen-Schilling, E. (1996) Shc adaptor proteins are key transducers of mitogenic signalling mediated by the G protein-coupled thrombin receptor. EMBO J. **15**, 1037-1044

Chen, Y-h., Pouyssegur, J., Courtneidge, S. A., and Van Obberghen-Schilling, E. (1994) Activation of Src family kinase activity by the G protein-coupled thrombin receptor in growth-responsive fibroblasts. J. Biol. Chem. **269**, 27372-27377

Clapham, D. E., and Neer, E. J. (1993) New roles for G protein βγ-dimers in transmembrane signalling. Nature **365**, 403-406

Cook, S. J., and McCormick, F. (1993) Inhibition by cAMP of Ras-dependent activation of Raf. Science **262**, 1069-1072

Cook, S. J., and Wakelam, M. J. O. (1991) Hydrolysis of phosphatidylcholine by phospholipase D is a common response to mitogens which stimulate inositol lipid hydrolysis in Swiss 3T3 fibroblasts. Biochem. Biophys. Acta **1092**, 265-272

Cook, S. J., Rubinfeld, B., Albert, I., and McCormick, F. (1993) RapV12 antagonizes Ras-dependent activation of ERK1 and ERK2 by LPA and EGF in Rat-1 fibroblasts. EMBO J. **12**, 3475-3485

Cooper, J. A., and Howell, B. (1993) The when and how of Src regulation. Cell **73**, 1051-1054

Cooper, J. A., Sefton, B. M., and Hunter, T. (1984) Diverse mitogenic agents induce the phosphorylation of two related 42,000-Dalton proteins on tyrosine in quiescent chick cells. Mol. Cell. Biol. **4**, 30-37

Coso, O. A., Chiariello, M., Kalinec, G., Kyriakis, J. M., Woodgett, J., and Gutkind, J. S. (1995) Transforming G protein-coupled receptors potently activate JNK (SAPK). J. Biol. Chem. **270**, 5620-5624

Cotecchia, S., Kobilka, B. K., Daniel, K. W., Nolan, R. D., Lapetina, E. Y., Caron, M. G., Lefkowitz, R. J., and Regan, J. W. (1990) Multiple second messenger pathways of α-adrenergic receptor subtypes expressed in eukaryotic cells. J. Biol. Chem. **265**, 63-69

Cowley, S., Paterson, H., Kemp, P., and Marshall, C. J. (1994) Activation of MAP kinase kinase is necessary and sufficient for PC12 differentiation and for transformation of NIH 3T3 cells. Cell **77**, 841-852

Crespo, P., Cachero, T. G., Xu, N., and Gutkind, J. S. (1995) Dual effect of β-adrenergic receptors on mitogen-activated protein kinase. J. Biol. Chem. **270**, 25259-25265

Crespo, P., Xu, N., Simonds, W. F., and Gutkind, J. S. (1994) Ras-dependent activation of MAP kinase pathway mediated by G-protein βγ subunits. J. Biol. Chem. **269**, 418-420

Crews, C. M., and Erikson, R. L. (1992) Purification of a murine protein-tyrosine/threonine kinase that phosphorylates and activates the *ERK-1* gene product: Relationship to the fission yeast *byr1* gene product. Proc. Natl. Acad. Sci. USA **89**, 8205-8209

Crews, C. M., and Erikson, R. L. (1993) Extracellular signals and reversible protein phosphorylation: what to MEK of it all. Cell **74**, 215-217

Cross, D. A. E., Alessi, D. R., Vandenheede, J. R., McDowell, H. E., Hundall, H. S., and Cohen, P. (1994) The inhibition of glycogen synthase kinase-3 by insulin or insulin-like growth factor in the rat skeletal cell line L6 is blocked by wortmannin, but not by rapamycin: evidence that wortmannin blocks activation of the mitogen-activated protein kinase pathway in L6 cells between Ras and Raf. Biochem. J. **303**, 21-26

Cross, M. J., Stewart, A., Hodgkin, M. N., Kerr, D. J., and Wakelam, M. J. O. (1995) Wortmannin and its structural analogue demethoxyviridin inhibit stimulated phospholipase A_2 activity in Swiss 3T3 cells. J. Biol. Chem. **270**, 25352-25355

Cruciani, R. A., Dvorkin, B., Morris, S. A., Crain, S. A., and Makman, M. H. (1993) Direct coupling of opioid receptors to both stimulatory and inhibitory guanine nucleotide-binding proteins in F-11 neuroblastoma-sensory neuron hybrid cells. Proc. Natl. Acad. Sci. USA **90**, 3019-3023

Daub, H., Weiss, F. U., Wallasch, C., and Ullrich, A. (1996) Role of transactivation of the EGF receptor in signalling by G-protein-coupled receptors. Nature **379**, 557-560

Daum, G., Eisenmann-Tappe, I., Fries, H-W., Troppmair, J., and Rapp, U. R. (1994) The ins and outs of Raf kinases. Trends Biochem. Sci. **19**, 474-480

Davis, R. J. (1993) The mitogen-activated protein kinase signal transduction pathway. J. Biol. Chem. **268**, 14553-14556

Davis, R. J. (1994) MAPKs: new JNK expands the group. Trends Biochem. Sci. **19**, 470-473

Deng, T., and Karin, M. (1994) c-Fos transcriptional activity stimulated by H-Ras-activated protein kinase distinct from JNK and ERK. Nature **371**, 171-175

Dent, P., Chow, Y-H., Wu, J., Morrison, D. K., Jove, R., and Sturgill, T. W. (1994) Expression, purification and characterisation of recombinant mitogen activated protein kinase kinases. Biochem.J. **303**, 105-112

Dent, P., Haser, W., Haystead, T. A. J., Vincent, L. A., Roberts, T. M., and Sturgill, T. W. (1992) Activation of mitogen-activated protein kinase by v-Raf in NIH 3T3 cells and in vitro. Science **257**, 1404-1407

De Vivo, M., and Iyengar, R. (1994a) Activated $G_{q}\alpha$ potentiates platelet-derived growth factor-stimulated mitogenesis in confluent cell cultures. J. Biol. Chem. **269**, 19671-19674

De Vivo, M., and Iyengar, R. (1994b) G protein pathways: signal processing by effectors. Mol. Cell. Endocrin. **100**, 65-70

Dikic, I., Tokiwa, G., Lev, S., Courtneidge, S. A., and Schlessinger, J. (1996) A role for Pyk2 and Src in linking G-protein-coupled receptors with MAP kinase activation. Nature **383**, 547-550

Dohlman, H. G., Thorner, J., Caron, M. G., and Lefkowitz, R. J. (1991) Model systems for the study of seven-transmembrane-segment receptors. Annu. Rev. Biochem. **60**, 653-688

Duff, J. L., Marrero, M. B., Paxton, W. G., Charles, C. H., Lau, L. E., Bernstein, K. E., and Berk, B. C. (1993) Angiotensin II induces 3CH134, a protein-tyrosine phosphatase, in vascular smooth muscle cells. J. Biol. Chem. **268**, 26037-26040

Eason, M. G., Kurose, H., Holt, B. D., Raymond, J. R., and Liggett, S. B. (1992) Simultaneous coupling of α_2-adrenergic receptors to two G-proteins with opposing effects. J. Biol. Chem. 267, 15795-15801

Edwards, D. R. (1994) Cell signalling and the control of gene transcription. Trends Pharmacol. Sci. **15**, 239-244

Egan, S. E., Giddings, B. W., Brooks, M. W., Buday, L., Sizeland, A. M., and Weinberg, R. A. (1993) Association of Sos Ras exchange protein with Grb2 is implicated in tyrosine kinase signal transduction and transformation. Nature **363**, 45-51

Erpel, T., and Courtneidge, S. A. (1995) Src family protein tyrosine kinases and cellular signal transduction pathways. Curr. Opin. Cell Biol. **7**, 176-182

Exton, J. H. (1996) Regulation of phosphoinositide phospholipases by hormones, neurotransmitters, and other agonists linked to G proteins. Annu. Rev. Pharamcol. Toxicol. **36**, 481-509

Fabian, J. R., Daar, I. O., and Morrison, D. K. (1993) Critical tyrosine residues regulate the enzymatic and biological activity of Raf-1 kinase. Mol. Cell. Biol. **13**, 7170-7179

Faure, M., and Bourne, H. R. (1995) Differential effects of cAMP on the MAP kinase cascade: Evidence for a cAMP-insensitive step that can bypasss Raf-1. Mol. Biol. Cell **6**, 1025-1035

Faure, M., Voyno-Yasenetskaya, T. A., and Bourne, H. R. (1994) cAMP and βγ subunits of heterotrimeric G proteins stimulate the mitogen-activated protein kinase pathway in COS-7 cells. J. Biol. Chem. **269**, 7851-7854

Feller, S. M., Ren, R., Hanafusa, H., and Baltimore, D. (1994) SH2 and SH3 domains as molecular adhesives: the interactions of Crk and Abl. Trends Biochem. Sci. **19**, 453-458

Feng, G-S., and Pawson, T. (1994) Phosphotyrosine phosphatases with SH2 domains: regulators of signal transduction. Trends Genetics **10**, 54-58

Ferby, I. M., Waga, I., Hoshino, M., Kume, K., and Shimizu, T. (1996) Wortmannin inhibits mitogen-activated protein kinase activation by platelet-activating factor through a mechanism independent of p85/p110 phosphatidylinositol 3-kinase. J. Biol. Chem. **271**, 11684-11688

Ferby, I. M., Waga, I., Sakanaka, C., Kume, K., and Shimizu, T. (1994) Wortmannin inhibits mitogen-activated protein kinase activation induced by the platelet-activating factor in guinea pig neutrophils. J. Biol. Chem. **269**, 30485-30488

Frödin, M., Peraldi, P., and Van Obberghens, E. (1994) Cyclic AMP activates the mitogen-activated protein kinase cascade in PC12 cells. J. Biol. Chem. **269**, 6207-6214

Frost, J. A., Geppert, T. D., Cobb, M. H., Feramisco, J. R. (1994) A requirement for extracellular signal-regulated kinase (ERK) function in the activation of AP-1 by Ha-Ras, phorbol 12-myristate 13-acetate, and serum. Proc. Natl. Acad. Sci. USA **91**, 3844-3848

Gale, N. W., Kaplan, S., Lowenstein, E. J., Schlessinger, J., and Bar-Sagi, D. (1993) Grb2 mediates the EGF-dependent activation of guanine nucleotide exchange on Ras. Nature **363**, 88-92

Gallego, C., Gupta, S. K., Heasley, L. E., Qian, N-X., and Johnson, G. L. (1992) Mitogen-activated protein kinase activation resulting from selective oncogene expression in NIH3T3 and Rat1a cells. Proc. Natl. Acad. Sci. USA **89**, 7355-7359

Gardner, A. M., Vaillancourt, R. R., and Johnson, G. L. (1993) Activation of mitogen-activated protein kinase/extracellular signal-regulated kinase kinase by G-protein and tyrosine kinase oncoproteins. J. Biol. Chem. **268**, 17896-17901

Gardner, A. M., Vaillancourt, R. R., Lange-Carter, C. A., and Johnson, G. L. (1994) MEK-1 phosphorylation by MEK kinase, Raf, and mitogen-activated protein kinase: analysis of phosphopeptides and regulation of activity. Mol. Biol. Cell **5**, 193-201

Gilmore, T., and Martin, G. S. (1983) Phorbol ester and diacylglycerol induce protein phosphorylation at tyrosine. Nature **306**, 487-490

Gómez, N., and Cohen, P. (1991) Dissection of the protein kinase cascade by which nerve growth factor activates MAP kinase. Nature **353**, 170-173

Granot, Y., Erikson, E., Fridman, H., Putten, V. V., Williams, B., Schrier, R. W., and Maller, J. L. (1993) Direct evidence for tyrosine and threonine phosphorylation activation of mitogen-activated protein kinase by vasopressin in cultured rat vascular smooth muscle cells. J. Biol. Chem. **268**, 9564-9569

Groom, L. A., Sneddon, A. A., Alessi, D. R., Dowd, S., and Keyse, S. M. (1996) Differential regulation of the MAP, SAP and RK/p38 kinase by Pyst1, a novel cytosolic dual-specificity phosphatase. EMBO J. **15**, 3621-3632

Gudermann, T., Kalkbrenner, F., and Schultz, G. (1996) Diversity and selectivity of receptor-G protein interaction. Annu. Rev. Pharamcol. Toxicol. **36**, 429-459

Gupta, S. K., Gallego, C., Johnson, G. L., and Heasley, L. E. (1992) MAP kinase is constitutively activated in *gip2* and *src* transformed Rat 1a fibroblasts. J. Biol. Chem. **267**, 7987-7990

Guyer, C. A., Horstman, D. A., Wilson, A. L., Clark, J. D., Cragoe, Jr, E. J., and Limbird, L. E. (1990) Cloning, sequencing, and expression of the gene encoding the porcine α_2-adrenergic receptor. J. Biol. Chem. **265**, 17307-17317

Haga, K., Kameyama, K., and Haga, T. (1994) Synergistic activation of a G-protein coupled receptor kinase by G-protein $\beta\gamma$ subunits and mastoparan or related peptides. J. Biol. Chem. **269**, 12594-12599

Hallberg, B., Rayter, S. I., and Downward, J. (1994) Interaction of Ras and Raf in intact mammalian cells upon extracellular stimulation. J. Biol. Chem. **269**, 3913-3916

Han, J., Lee, J-D., Bibbs, L., Ulevitch, R. J. (1994) A MAP kinase targeted by endotoxin and hyperosmolarity in mammalian cells. Science **265**, 808-811

Hawes, B. E., Luttrell, L. M., van Biesen, T., and Lefkowitz, R. J. (1996) Phosphatidylinositol 3-kinase is an early intermediate in the Gβγ-mediated mitogen-activated protein kinase signalling pathway. J. Biol. Chem. **271**, 12133-12136

Hawes, B. E., van Biesen, T., Koch, W. J., Luttrell, L. M., and Lefkowitz, R. J. (1995) Distinct pathways of G_i- and G_q-mediated mitogen-activated protein kinase activation. J. Biol. Chem. **270**, 17148-17153

Haystead, C. M. M., Gregory, P., Shirazi, A., Fadden, P., Mosse, C., Dent, P., and Haystead, T. A. J. (1994) Insulin activates a novel adipocyte mitogen-activated protein kinase kinase kinase that shows rapid phasic kinetics and is distinct from c-Raf. J. Biol. Chem. **269**, 12804-12808

Hepler, J. R., and Gilman, A. G. (1992) G proteins. Trends Biochem. Sci. **17**, 383-387

Herbert, J. M., Augereau, J. M., Gleye, J., and Maffrand, J. P. (1990) Chelerythrine is a potent and specific inhibitor of protein kinase C. Biochem. Biophys. Res. Comm. **172**, 993-999

Her, J-H., Lakhani, S., Zu, K., Vila, J., Dent, P., Sturgill, T. W., and Weber, M. (1993) Dual phosphorylation and autophosphorylation in mitogen-activated protein (MAP) kinase activation. Biochem. J. **296**, 25-31

Hill, C. S., and Treisman, R. (1995) Transcriptional regulation by extracellular signals: mechanisms and specificity. Cell **80**, 199-211

Honda, Z-i., Takano, T., Gotoh, Y., Nishida, E., Ito, K., and Shimizu, T. (1994) Transfected platelet-activating factor receptor activates mitogen-activated protein (MAP) kinase and MAP kinase kinase in Chinese hamster ovary cells. J. Biol. Chem. **269**, 2307-2315

Hordijk, P. L., Verlaan, I., Jalink, K., van Corven, E. J., and Moolenaar, W. H. (1994a) cAMP abrogates the $p21^{ras}$-mitogen-activated protein kinase pathway in fibroblasts. J. Biol. Chem. **269**, 3534-3538

Hordijk, P. L., Verlaan, I., van Corven, E. J., and Moolenaar, W. H., (1994b) Protein tyrosine phosphorylation induced by lysophosphatidic acid in Rat-1 fibroblasts. J. Biol. Chem. **269**, 645-651

Horstman, D. A., Brandon, S., Wilson, A. L., Guyer, C. A., Cragoe, E. J. Jr., and Limbird, L. E. (1990) An aspartate conserved among G-protein receptors confers allosteric regulation of α_2-adrenergic receptors by sodium. J. Biol. Chem. **265**, 21590-21595

Howe, L. R., and Marshall, C. J. (1993) Lysophosphatidic acid stimulates mitogen-activated protein kinase activation via a G-protein-coupled pathway requiring $p21^{ras}$ and $p74^{raf-1}$. J. Biol. Chem. **268**, 20717-20720

Howe, L. R., Leevers, S. J., Gómez, N., Nakielny, S., Cohen, P., and Marshall, C. J. (1992) Activation of the MAP kinase pathway by the protein kinase raf. Cell **71**, 335-342

Hoyer, D., and Boddeke, H. W. G. M. (1993) Partial agonists, full agonists, antagonists: dilemmas of definition. Trends Pharmacol. Sci. **14**, 270-275

Huwiler A., Stabel, S., Fabbro, D., and Pfeilschifter, J. (1995) Platelet-derived growth factor and angiotensin II stimulate the mitogen-activated protein kinase cascade in renal mesangial cells: comparison of hypertrophic and hyperplastic agonists. Biochem. J. **305**, 777-784

Hu, Z-W., Shi, X-Y., Lin, R. Z., and Hoffman, B. B. (1996) α_1 adrenergic receptors activate phosphatidylinositol 3-kinase in human vascular smooth muscle cells. J. Biol. Chem. **271**, 8977-8982

Inglese, J., Koch, W. J., Touhara, K., and Lefkowitz, R. J. (1995) $G\beta\gamma$ interactions with PH domains and the Ras-MAPK signalling pathways. Trends Biochem. Sci. **20**, 151-156

Ito, A., Satoh, T., Kaziro, Y., and Itoh, H. (1995) G protein $\beta\gamma$ subunit activate Ras, Raf, and MAP kinase in HEK 293 cells. FEBS Letters **368**, 183-187

Jin, W., Lee, N. M., Loh, H. H., and Thayer, S. A. (1992) Dual excitatory and inhibitory effects of opioids on intracellular calcium neuroblastoma x glioma hybrid NG108-15 cells. Mol. Pharmacol. **42**, 1083-1089

Johnson, R. A., and Salomon, Y. (1991) Assay of adenylyl cyclase catalytic activity. Methods Enzymol. **195**, 3-21

Jones, D. A., Benjamin, C. W., and Linseman, D. A. (1995) Activation of thromboxane and prostacyclin receptors elicits opposing effects on vascular smooth muscle cell growth and mitogen-activated protein kinase signalling cascades. Mol. Pharm. **48**, 890-896

Jones, L. G., Ella, K. M., Bradshaw, C. D., Gause, K. C., Dey, M., Wisehart-Johnson, A. E., Spivey, E. C., and Meier, K. E. (1994) Activations of mitogen-activated protein kinases and phospholipase D in A7r5 vascular smooth muscle cells. J. Biol. Chem. **269**, 23790-23799

Kahan, C., Seuwen, K., Meloche, S., and Pouysségur, J. (1992) Coordinate, biphasic activation of p44 mitogen-activated protein kinase and S6 kinase by growth factors in hamster fibroblasts. J. Biol. Chem. **267**, 13369-13375

Keyse, S. M., and Emslie, E. A. (1992) Oxidative stress and heat shock induce a human gene encoding a protein-tyrosine phosphatase. Nature **359**, 644-647

Kim, G-D., and Milligan, G. (1994) Concurrent specific immunological detection of both primate and rodent forms of the guanine nucleotide binding protein $G_{11}\alpha$ following their coexpression. Biochim. Biophys. Acta **1222**, 369-374

Klee, W. A., Milligan, G., Simonds, W. F., and Tocque, B. (1984) The role of adenyl cyclase in opiate tolerance and dependence. N. I. D. A. Research Monograph **54**, 109-118

Knapp, R. J., Malatynska, E., Collins, N., Fang, L., Wang, J. Y., Hruby, V. J., Roeske, W. R., and Yamamura, H. I. (1995) Molecular biology and pharmacology of cloned opioid receptors. FASEB J. **9**, 516-525

Kobilka, B. K., Matsui, H., Kobilka, T. S., Yang-Feng, T. L., Francke, U., Caron, M. G., Lefkowitz, R. J., and Regan, J. W. (1987) Cloning, sequencing, and expression of the genes coding for the human platelet α_2-adrenergic receptor. Science **238**, 650-656

Koch, W. J., Hawes, B. E., Allen, L. F., and Lefkowitz, R. J. (1994) Direct evidence that G_i-coupled receptor stimulation of mitogen-activated protein kinase is mediated by $G\beta\gamma$ activation of $p21^{ras}$. Proc. Natl. Acad. Sci. USA **91**, 12706-12710

Kolch, W., Heidecker, G., Kochs, G., Hummel, R., Vahidi, H., Mischak, H., Finkenzeller, G., Marmé, D., and Rapp, U. R. (1993) Protein kinase Cα activates RAF-1 by direct phosphorylation. Nature **364**, 249-252

Koski, G., and Klee, W. A. (1981) Opiates inhibit adenylate cyclase by stimulating GTP hydrolysis. Proc. Natl. Acad. Sci. USA **78**, 4185-4189

Kramer, R. M., Roberts, E. F., Manetta, J. V., Hyslop, P. A., and Jakubowski, J. A. (1993) Thrombin-induced phosphorylation and activation of Ca^{2+}-sensitive cytosolic phospholipase A_2 in human platelets. J. Biol. Chem. **268**, 26796-26804

Kumagai, N., Morii, N., Fujisawa, K., Nemoto, Y., and Narumiya, S. (1993) ADP-ribosylation of rho p21 inhibits lysophosphatidic acid-induced protein tyrosine phosphorylation and phosphatidylinositol3-kinase activation in cultured Swiss 3T3 cells. J. Biol. Chem. **268**, 24535-24538

Kyriakis, J. M., App, H., Zhang, X-F., Banerjee, P., Brautigan, D. L., Rapp, U. R., and Avruch, J. (1992) Raf-1 activates MAP kinase-kinase. Nature **358**, 417-421

Lambright, D. G., Sondek, J., Bohm, A., Skiba, N. P., Hamm, H. E., and Sigler, P. B. (1996) The 2.0 Å crystal structure of a heterotrimeric G protein. Nature **379**, 311-319

Lange-Carter, C. A., and Johnson, G. L. (1994) Ras-dependent growth factor regulation of MEK kinase in PC12 cells. Science **265**, 1458-1461

Lange-Carter, C. A., Pleiman, C. M., Gardner, A. M., Blumer, K. J., and Johnson, G. L. (1993) A divergence in the MAP kinase regulatory network defined by MEK kinase and Raf. Science **260**, 315-319

Lau, L. F., and Nathans, D. (1985) Identification of a set of genes expressed during the G0/G1 transition of cultured mouse cells. EMBO J. **4**, 3145-3151

Law, P. Y., and Loh, H. H. (1993) δ-opioid receptor activates cAMP phosphodiesterase activities in neuroblastoma x glioma NG108-15 hybrid cells. Mol. Pharmacol. **43**, 684-693

Leevers, S. J., and Marshall, C. J. (1992) Activation of extracellular signal-regulated kinase, ERK2, by p21*ras* oncoprotein. EMBO J. **11**, 569-574

Leevers, A. S., Paterson, H. F., and Marshall, C. J. (1994) Requirement for Ras in Raf activation is overcome by targeting Raf to the plasma membrane. Nature **369**, 411-414

Lenormand, P., McMahon, M., and Pouysségur, J. (1996) Oncogenic Raf-1 activates p70 S6 kinase via a mitogen-activated protein kinase-independent pathway. J. Biol. Chem. **271**, 15762-15768

Levitzki, A., and Gazit, A. (1995) Tyrosine kinase inhibition: an approach to drug development. Science **267**, 1782-1788

Lev, S., Moreno, H., Martinez, R., Canoll, P., Peles, E., Musacchio, J. M., Plowman, G. D., Rudy, B., and Schlessinger, J. (1995) Protein tyrosine kinase PYK2 involved in Ca^{2+}-induced regulation of ion channel and MAP kinase functions. Nature **376**, 737-745

Li, N., Batzer, A., Daly, R., Yajink, V., Skolnik, E., Chardin, P., Bar-Sagi, D., Margolis, B., and Schlessinger, J. (1993) Gunaine-nucleotide-releasing factor hSos1 binds to Grb2 and links receptor tyrosine kinases to Ras signalling. Nature **363**, 85-88

Lin, L-L., Wartmann, M., Lin, A. L., Knopf, J. L., Seth, A., and Davis, R. J. (1993) $cPLA_2$ is phosphorylated and activated by MAP kinase. Cell **72**, 269-278

Linseman, D. A., Benjamin, C. W., and Jones, D. A. (1995) Convergence of angiotensin II and platelet-derived growth factor receptor signalling cascades in vascular smooth muscle cells. J. Biol. Chem. **270**, 12563-12568

Lopez-Ilasaca, M., Crespo, P., Pellici, P. G., Gutkind, J. S., and Wetzker, R. (1997) Linkage of G protein-coupled receptors to the MAPK signalling pathway through PI 3-kinase γ. Science **275**, 394-397

Lowry, O. H., Rosebrough, N. J., Farr, A. L., and Randall, R. J. (1951) Protein measurement with the Folin phenol reagent. J. Biol. Chem. **193**, 265-275

Luttrell, L. M., Hawes, B. E., Touhara, K., van Biesen, T., Koch, W. J., and Lefkowitz, R. J. (1995a) Effect of cellular expression of pleckstrin homology domains on G_i-coupled receptor signalling. J. Biol. Chem. **270**, 12984-12989

Luttrell, L. M., van Biesen, T., Hawes, B. E., Koch, W. J., Touhara, K., and Lefkowitz, R. J. (1995b) $G_{\beta\gamma}$ subunits mediate mitogen-activated protein kinase activation by the tyrosine kinase insulin-like growth factor 1 receptor. J. Biol. Chem. **270**, 16495-16498

MacDonald, S. G., Crews, C. M., Wu, L., Driller, J., Clark, R., Erikson, R. L., and McCormick, F. (1993) Reconstitution of the Raf-1–MEK–ERK signal transduction pathway in vitro. Mol. Cell. Biol. **13**, 6615-6620

MacEwan, D. J., Kim, G. D., Milligan, G. (1995) Analysis of the role of receptor number in defining the intrinsic activity and potency of partial agonists in neuroblastoma x glioma hybrid NG108-15 cells transfected to express differing levels of the human β_2-adrenoceptor. Mol. Pharmacol. **48**, 316-325

MacKinnon, A. C., Spedding, M., and Brown, C. M. (1994) α_2-Adrenoceptors: more subtypes but fewer functional differences. Trends Pharmacol. Sci. **15**, 119-123

MacKintosh, C., and MacKintosh, R. W. (1994) Inhibitors of protein kinases and phosphatases. Trends Biochem. Sci. **19**, 444-448

MacNulty, E. E., McClue, S. J., Carr, I. C., Jess, T., Wakelam, M. J. O., and Milligan, G. (1992) α_2-C10 adrenergic receptors expressed in Rat 1 fibroblasts can regulate both adenylylcyclase and phospholipase D-mediated hydrolysis of phosphatidylcholine by interacting with pertussis toxin-sensitive guanine nucleotide-binding proteins. J. Biol. Chem. **267**, 2149-2156

McClue, S. J., Selzer, E., Freissmuth, M., and Milligan, G. (1992) G_i3 does not contribute to the inhibition of adenylyl cyclase when stimulation of an α2-adrenergic receptor causes activation of both G_i2 and G_i3. Biochem. J. **284**, 565-568

McCormick, F. (1993) How receptors turn Ras on. Nature **363**, 15-16

McKenzie, F. R., and Milligan, G. (1990) δ-Opioid-receptor-mediated inhibition of adenylate cyclase is transduced specifically by the guanine-nucleotide-binding protein G_i2. Biochem. J. **267**, 391-8

McKenzie, F. R., Seuwen, K., and Pouyességur, J. (1992) Stimulation of phosphatidylcholine breakdown by thrombin and carbachol but not by tyrosine kinase receptor ligands in cells transfected with M1 muscarinic receptors. J. Biol. Chem. **267**, 22759-22769

Malarkey, K., Belham, C. M., Paul, A., Graham, A., McLees, A., Scott, P. H., and Plevin, R. (1995) The regulation of tyrosine kinase signalling pathways by growth factor and G-protein-couled receptors. Biochem. J. **309**, 361-375

Mangoura, D., and Dawson, G. (1993) Opioid peptides activate phospholipase D and protein kinase C-ε in chicken embryo neuron cultures. Proc. Natl. Acad. Sci. USA **90**, 2915-2919

Mansour, S. J., Matten, W. T., Hermann, A. S., Candia, J. M., Rong, S., Fukasawa, K., Vande Woude, G. F., and Ahn, N. G. (1994) Transformation of mammalian cells by constitutively active MAP kinase kinase. Science **265**, 966-970

Marrero, M. B., Schieffer, B., Paxton, W. G., Heerdt, L., Berk, B. C., Delafontaine, P., and Bernstein, K. E. (1995) Direct stimulation of Jak/STAT pathway by the angiotensin II AT_1 receptor. Nature **375**, 247-250

Marshall, C. J. (1995) Specificity of receptor tyrosine kinase signalling: transient versus sustained extracellular signal-regulated kinase activation. Cell **80**, 179-185

Meloche, S., Seuwen, K., Pagès, G., and Pouysségur, J. (1992) Biphasic and synergistic activation of $p44^{MAPK}$ (ERK1) by growth factors: correlation between late phase activation and mitogenicity. Mol. Endocrin. **6**, 845-854

Milligan, G. (1993) Mechanisms of multifunctional signalling by G protein-linked receptors. Trends Pharmacol. Sci. **14**, 239-244

Milligan, G., Carr, C., Gould, G. W., Mullaney, I., and Lavan, B. E. (1991) Agonist-dependent, cholera toxin-catalyzed ADP-ribosylation of pertussis toxin-sensitive G-proteins following transfection of the human α_2-C10 adrenergic receptor into Rat 1 fibroblasts. J. Biol. Chem. **266**, 6447-6455

Milligan, G., Parenti, M., and Magee, A. I. (1995) The dynamic role of palmitoylation in signal transduction. Trends Biochem. Sci. **20**, 181-186

Minden, A., Lin, A., McMahon, M., Lange-Carter, C., Dérijard, B., Davis, R. J., Johnson, G. L., and Karin, M. (1994) Differential activation of ERK and JNK mitogen-activated protein kinases by Raf-1 and MEKK. Science **266**, 1719-1723

Mitchell, F. M., Russell, M., and Johnson, G. L. (1995) Differential calcium dependence in the activation of c-Jun kinase and mitogen-activated protein kinase by muscarinic acetylcholine receptors in rat 1a cells. Biochem. J. **309**, 381-384

Moolenaar, W. H. (1995) Lysophosphatidic acid signalling. Curr. Opin. Cell Biol. **7**, 203-210

Morrison, D. K., Heidecker, G., Rapp, U. R., and Copeland, T. D. (1993) Identification of the major phosphorylation sites of the Raf-1 kinase. J. Biol. Chem. **268**, 17309-17316

Mullaney, I., Carr, I. C., Burt, A. R., Wilson, M., Anderson, N. G., and Milligan, G. (1997) Agonist-mediated tyrosine phosphorylation of isoforms of Shc adapter proteins by the δ opioid receptor. Cell Signalling (in press).

Mullaney, I., Carr, I. C., and Milligan, G. (1996) Analysis of inverse agonsim at the δ opioid receptor after expression in Rat1 fibroblasts. Biochem. J. **315**, 227-234

Nakielny, S., Cohen, P., Wu, J., and Sturgill, T. (1992) MAP kinase activator from insulin-stimulated skeletal muscle is a protein threonine/tyrosine kinase. EMBO J. **11**, 2123-2129

Nebreda, A. R. (1994) Inactivation of MAP kinases. Trends Biochem. Sci. **19**, 1-2

Nebreda, A. R., and Hunt, T. (1993) The c-*mos* proto-oncogene protein kinase turns on and maintains the activity of MAP kinase, but not MPF, in cell-free extracts of *Xenopus* oocytes and eggs. EMBO J. **12**, 1979-1986

Neer, E. J. (1995) Heterotrimeric G proteins: Organizers of transmembrane signals. Cell **80**, 249-257

Nishida, E., and Gotoh, Y. (1993) The MAP kinase cascade is essential for signal transduction pathways. Trends Biochem. Sci. **18**, 128-131

Pace, A. M., Wong, Y. H., and Bourne, H. R. (1991) A mutant α subunit of G_{i2} induces neoplastic transformation of Rat-1 cells. Proc. Natl. Acad. Sci. USA **88**, 7031-7035

Pagès, G., Lenormand, P., L'Allemain, G., Chambard, J-C., Meloche, S., and Pouysségur, J. (1993) Mitogen-activated protein kinases $p42^{MAPK}$ and $p44^{MAPK}$ are required for fibroblast proliferation. Proc. Natl. Acad. Sci. USA **90**, 8319-8323

Papkoff, J., Chen, R-H., Blenis, J., and Forsman, J. (1994) p42 mitogen-activated protein kinase and p90 ribosomal S6 kinase are selectively phosphorylated and activated during thrombin-induced platelet activation and aggregation. Mol. Cell. Biol. **14**, 463-472

Pawson, T. (1995) Protein modules and signalling networks. Nature **373**, 573-580

Pelech, S. L. (1993) Networking with protein kinases. Curr. Biol. **3**, 513-515

Pelech, S. L., and Sanghera, J. (1992) Mitogen-activated protein kinases: versatile, transducers for cell signalling. Trends Biochem. Sci. **17**, 233-238

Pelicci, G., Lanfrancone, L., Grignani, F., McGlade, J., Cavallo, F., Forni, G., Nicoletti, I., Grignani, F., Pawson, T., and Pelicci, P. G. (1992) A novel transforming protein (SHC) with an SH2 domain is implicated in mitogenic signal transduction. Cell, **70**, 93-104

Pitcher, J. A., Inglese, J., Higgins, J. B., Arriza, J. L., Casey, P. J., Kim, C., Benovic, J. L., Kwatra, M. M., Caron, M. G., and Lefkowitz, R. J. (1992) Role of βγ subunits of G-protein in targeting the β-adrenergic receptor kinase to membrane bound receptors. Science **257**, 1264-1267

Porras, A., Muszynski, K., Rapp, U. R., and Santos, E. (1994) Dissociation between activation of Raf-1 kinase and the 42-kDa mitogen-activated protein kinase/90-kDa S6 kinase (MAPK/RSK) cascade in the Insulin/Ras pathway of adipocyte differentiation of 3T3 L1 cells. J. Biol. Chem. **269**, 12741-12748

Post, G. R., and Brown, J. H. (1996) G protein-coupled receptors and signalling pathways regulating growth responses. FASEB J. **10**, 741-749

Post, G. R., Goldstein, D., Thuerauf, D. J., Glembotski, C. C., and Brown, J. H. (1996) Dissociation of p44 and p42 mitogen-activated protein kinase activation from receptor-induced hypertrophy in neonatal rat ventricular myocytes. J. Biol. Chem. **271**, 8452-8457

Prather, P. L., McGinn, T. M., Erickson, L. J., Evans, C. J., Loh, H. H., and Law, P-Y. (1994) Ability of δ-opioid receptors to interact with multiple G-proteins is independent of receptor density. J. Biol. Chem. **269**, 21293-21302

Proud, C. G. (1996) p70 S6 kinase: an enigma with variations. Trends Biochem. Sci. **21**, 181-185

Pumiglia, K. M., LeVine, H., Haske, T., Habib, T., Jove, R., and Decker, S. J. (1995) A direct interaction between G-protein βγ subunits and the Raf-1 protein kinase. J. Biol. Chem. **270**, 14251-14254

Ray, L. B., and Sturgill, T.W. (1987) Rapid stimulation by insulin of a serine/threonine kinase in 3T3-L1 adipocytes that phosphorylates microtubule-associated protein 2 *in vitro*. Proc. Natl. Acad. Sci. USA **84**, 1502-1506

Raymond, J. R., Arthur, J. M., Casañas, S. J., Olsen, C. L., Gettys, T. W., and Mortensen, R. M. (1994) α_{2A} adrenergic receptors inhibit cAMP accumulation in embryonic stem cells which lack $G_{i\alpha 2}$. J. Biol. Chem. **269**, 13073-13075

Rens-Domiano, S., and Hamm, H. E. (1995) Structural and functional relationships of heterotrimeric G-protcins. FASEB J. **9**, 1059-1066

Robbins, D. J., Cheng, M., Zhen, E., Vanderbilt, C. A., Feig, L. A., and Cobb, M. H. (1992) Evidence for a Ras-dependent extracellular signal-regulated protein kinase (ERK) cascade. Proc. Natl. Acad. Sci. USA **89**, 6924-6928

Roche S., Koegl, M., Barone, V. M., Roussel, M., Courtneidge, S. A. (1995) DNA synthesis induced by some, but not all, growth factors requires Src family protein kinases. Mol. Cell. Biol. **15**, 1102-1109

Rohan, P. J., Davis, P., Moskaluk, C. A., Kearns, M., Krutzsch, H., Siebenlist, U., and Kelly, K. (1993) PAC-1: A mitogen-induced nuclear protein tyrosine phosphatase. Science **259**, 1763-1766

Rossomando, A. J., Payne, D. M., Weber, M. J., and Sturgill, T. W. (1989) Evidence that the pp42, a major tyrosine kinase target protein, is a mitogen-activated serine/threonine protein kinase. Proc. Natl. Acad. Sci. USA **86**, 6940-6943

Rozakis-Adcock, M., McGlade, J., Mbamalu, G., Pelicci, G., Daly, R., Li, W., Batzer, A., Thomas, S., Brugge, J., Pelicci, P. G., Schlessinger, J., and Pawson, T. (1992) Association of the Shc and Grb2/Sem5 SH2-containing proteins is implicated in the activation of the Ras pathways by tyrosine kinases. Nature **360**, 689-692

Saad, M. J., Velloso, L. A., and Carvalho, C. R. O. (1995) Angiotensin II induces tyrosine phosphorylation of insulin receptor substrate 1 and its association with phosphatidylinositol 3-kinase in rat heart. Biochem. J. **310**, 741-744

Salomon, Y., Londos, C., and Rodbell, M. (1974) A highly sensitive adenylate cyclase assay. Anal. Biochem. **58**, 541-548

Sambook, J., Fritsch, E. F., and Maniatis, T. (1989) Molecular Cloning, Second Edition, Cold Spring Harbour Laboratory Press.

Sasaoka, T., Langlois, W. J., Leitner, J. W., Draznin, B., and Olefsky, J. M. (1994a) The signalling pathway coupling epidermal growth factor receptors to activation of $p21^{ras}$. J. Biol. Chem. **269**, 32621-32625

Sasaoka, T., Rose, D. W., Jhun, B. H., Saltiel, A. R., Draznin, B., and Olefsky, J. M. (1994b) Evidence for a functional role of Shc proteins in mitogenic signalling induced by insulin, insulin-like growth factor-1, and epidermal growth factor. J. Biol. Chem. **269**, 13689-13694

Scatchard, G. (1949) N. Y. Acad. Sci. **51**, 660-672

Schaap, D., van der Wal, J., Howe, L. R., Marshall, C. J., and van Blitterswijk, W. J. (1993) A dominant-negative mutant of *raf* blocks mitogen-activated protein kinase activation by growth factors and oncogenic $p21^{ras}$. J. Biol. Chem. **268**, 20232-20236

Schieffer, B., Paxton, W. G., Chai, Q., Marrero, M. B., and Bernstein, K. E. (1996) Angiotensin II controls $p21^{ras}$ activity via $pp60^{c\text{-}src}$. J. Biol. Chem. **271**, 10329-10333

Schlessinger, J., and Bar-Sagi, D. (1994) Activation of Ras and other signalling pathways by receptor tyrosine kinases. Cold Spring Harbour Symp. Quant. Biol. **59**, 173-179

Schorb, W., Peeler, T. C., Madigan, N. N., Conrad, K. M., and Baker, K. M. (1994) Angiotensin II-induced protein tyrosine phosphorylation in neonatal rat cardiac fibroblasts. J. Biol. Chem. **269**, 19626-19632

Seger, R., Seger, D., Lozeman, F. J., Ahn, N. G., Graves, L. M., Campbell, J. S., Ericsson, L., Harrylock, M., Jensen, A. M., and Krebs, E. G. (1992) Human T-cell mitogen-activated protein kinase kinases are related to yeast signal transduction kinases. J. Biol. Chem. **267**, 25628-25631

Servant, M. J., Giasson, E., and Meloche, S. (1996) Inhibition of growth factor-induced protein synthesis by a selective MEK inhibitor in aortic smooth muscle cells. J. Biol. Chem. **271**, 16047-16052

Seufferlein, T., and Rozengurt, E. (1994) Lysophosphatidic acid stimulates tyrosine phosphorylation of focal adhesion kinase, paxillin, and p130. J. Biol. Chem. **269**, 9345-9351

Seuwen, K., Magnaldo, I., Kobilka, B. K., Caron, M. G., Regan, J. W., Lefkowitz, R. J., and Pouyssegur, J. (1990) α_2-adrenergic agonists stimulate DNA synthesis in Chinese hamster lung fibroblasts transfected with a human α_2-adrenergic receptor gene. Cell Reg. **1**, 445-451

Seva, C., Kowalski-Chauvel, A., Blanchet, J-S., Vaysse, N., and Pradayrol, L. (1996) Gastrin induces tyrosine phosphorylation of Shc proteins and their association with the Grb2/Sos complex. FEBS Letters **378**, 74-78

Skolnik, E. Y., Lee, C-H., Batzer, A., Vicentini, L. M., Zhou, M., Daly, R., Myers, M. J., Backer, J. M., Ullrich, A., White, M. F., and Schlessinger, J. (1993) The SH2/SH3 domain-containing protein GRB2 interacts with tyrosine-phosphorylated IRS1 and Shc: implications for insulin control of *ras* signalling. EMBO J. **12**, 1929-1936

Songyang, Z., and Cantley, L. C. (1995) Recognition and specificity in protein tyrosine-mediated signalling. Trends Biochem. Sci. **20**, 470-475

Sontag, E., Fedorov, S., Kamibayashi, C., Robbins, D., Cobb, M., and Mumby, M. (1993) The interaction of SV40 small tumour antigen with protein phosphatase 2A stimulates the MAP kinase pathway and unduces cell proliferation. Cell **75**, 887-897

Sternweis, P. C. (1994) The active role of βγ in signal transduction. Curr. Opin. Cell. Biol. **6**, 198-203

Stokoe, D., Macdonald, S. G., Cadwallader, K., Symons, M., Hancock, J. F. (1994) Activation of Raf as a result of recruitment to the plasma membrane. Science **264**, 1463-1467

Stoyanov, B., Volinia, S., Hanck, T., Rubio, I., Loubtchenkov, M., Malek, D., Stoyanova, S., Vanhaesebroeck, B., Dhand, R., Nürnberg, B., Gierschik, P., Seedorf, K., Hsuan, J. J., Waterfield, M. D., and Wetzker, R. (1995) Cloning and characterization of a G protein-activated human phosphoinositide-3 kinase. Science **269**, 690-693

Sun, H., and Tonks, N. K. (1994) The coordinated action of protein tyrosine phosphatases and kinases in cell signalling. Trends Biochem. Sci. **19**, 480-485

Sun, H., Charles, C. H., Lau, L. F., and Tonks, N. K. (1993) MKP-1 (3CH134), an intermediate early gene product is a dual specificity phosphatase that dephosphorylates MAP kinase in vivo. Cell **75**, 487-493

Sunahara, R. K., Dessauer, C. W., and Gilman, A. G. (1996) Complexity and diversity of mammalian adenylyl cyclase. Annu. Rev. Pharmacol. Toxicol. **36**, 461-480

Surprenant, A., Horstman, D. A., Akbarali, H., and Limbird, L. E. (1992) A point mutation of the α_2-adrenoceptor that blocks coupling to potassium but not calcium currents. Science **257**, 977-980

Symons, M. (1996) Rho family GTPases: the cytoskeleton and beyond. Trends Biochem. Sci. **21**, 178-181

Takai, Y., Sasaki, T., Tanaka, K., and Nakanishi, H. (1995) Rho as a regulator of the cytoskeleton. Trends Biochem. Sci. **20**, 227-230

Touhara, K., Hawes, B. E., van Biesen, T., and Lefkowitz, R. J. (1995) G protein $\beta\gamma$ subunits stimulate phosphorylation of Shc adaptor protein. Proc. Natl. Acad. Sci. USA **92**, 9284-9287

Traverse, S., Gomez, N., Paterson, H., Marshall, C., and Cohen, P. (1992) Sustained activation of the mitogen-activated protein (MAP) kinase cascade may be required for differentiation of PC12 cells. Biochem. J. **288**, 351-355

Traverse, S., Seedorf, K., Paterson, H., Marshall, C. J., Cohen, P., and Ullrich, A. (1994) EGF triggers neuronal differentiation of PC12 cells that overexpress the EGF receptor. Curr. Biol. **4**, 694-701

Troppmair, J., Bruder, J. T., Munoz, H., Lloyd, P. A., Kyriakis, J., Banerjee, P., Avruch, J., and Rapp, U. R. (1994) Mitogen-activated protein kinase/extracellular signal-regulated protein kinase activation by oncogenes, serum, and 12-O-Tetradecanoylphorbol-13-acetate requires Raf and is necessary for transformation. J. Biol. Chem. **269**, 7030-7035

Tsu, R. C., Chan, J. S. C., and Wong, Y. H. (1995) Regulation of multiple effectors by the cloned δ-opioid receptor: stimulation of phospholiplase C and type II adenylyl cyclase. J. Neurochem. **64**, 2700-2707

Turner, B. C., Tonks, N. K., Rapp, U. R., and Reed, J. C. (1993) Interleukin 2 regulates Raf-1 kinase activity through a tyrosine phosphorylation-dependent mechanism in a T-cell line. Proc. Natl. Acad. Sci. USA **90**, 5544-5548

Tutton, P. J. M., and Barkla, D. H. (1987) Biogenic amines as regulators of the proliferative activity of normal and neoplastic intestinal epithelial cells. Anticancer Res. **7**, 1-12

Twamley-Stein, G. M., Pepperkok, R., Ansorge, W., and Courtneidge, S. A. (1993) The Src family tyrosine kinases are required for platelet-derived growth factor-mediated signal transduction in NIH 3T3 cells. Proc. Natl. Acad. Sci. USA **90**, 7696-7700

Ui, M., Okada, T., Hazeki, K., and Hazeki, O. (1995) Wortmannin as a unique probe for an intracellular signalling protein, phosphoinositide 3-kinase. Trends Biochem. Sci. **20**, 303-307

Vaillancourt, R. R., Gardner, A. M., and Johnson, G. L. (1994) B-Raf-dependent regulation of the MEK-1/mitogen-activated protein kinase pathway in PC12 cells and regulation by cyclic AMP. Mol. Cell. Biol. **14**, 6522-6530

van Biesen, T., Hawes, B. E., Luttrell, D. K., Krueger, K. M., Touhara, K., Porfiri, E., Sakaue, M., Luttrel, L. M., and Lefkowitz, R. J. (1995) Receptor-tyrosine-kinase- and Gβγ-mediated MAP kinase activation by a common signalling pathway. Nature **376**, 781-784

van Biesen, T., Hawes, B. E., Raymond, J. R., Luttrell, L. M., Koch, W. J., and Lefkowitz, R. J. (1996) G_o-protein α-subunits activate mitogen-activated protein kinase via a novel protein kinase C-dependent mechanism. J. Biol. Chem. **271**, 1266-1269

van Corven, E. J., Groenink, A., Jalink, K., Eichholtz, T., and Moolenaar, W. H. (1989) Lysophosphatidate-induced cell proliferation: identification and dissection of signalling pathways mediated by G proteins. Cell **59**, 45-54.

van Corven, E. J., Hordijk, P. L., Medema, R. H., Bos, J. L., and Moolenaar, W. (1993) Pertussis toxin-sensitive activation of $p21^{ras}$ by G-protein-coupled receptor agonists in fibroblasts. Proc. Natl. Acad. Sci. USA **90**, 1257-1261

VanRenterghem, B., Gibbs, J. B., and Maller, J. L. (1993) Reconstitution of $p21^{ras}$-dependent and -independent mitogen-activated protein kinase activation in a cell-free system. J. Biol. Chem. **268**, 19935-19938

Wall, M. A., Coleman, D. E., Lee, E., Iñiguez-Lluhi, J. A., Posner, B. A., Gilman, A. G., and Sprang, S. R. (1995) The structure of the G protein heterotrimer $G_{i\alpha 1}\beta_1\gamma_1$. Cell **83**, 1047-1058

Wang, C-D., Buck, M. A., and Fraser, C. M. (1991) Site-directed mutagenesis of α_{2A}-adrenergic receptors: identification of amino acids involved in ligand binding and receptor activation by agonists. Mol. Pharmacol. **40**, 168-179

Wan, Y., Kurosaki, T., and Huang, X-Y. (1996) Tyrosine kinases in activation of the MAP kinase cascade by G-protein-coupled receptors. Nature **380**, 541-544

Ward, Y., Gupta, S., Jensen, P., Wartmann, M., Davis, R. J., and Kelly, K. (1994) Control of MAP kinase activation by the mitogen-induced threonine/tyrosine phosphatase PAC1. Nature **367**, 651-654

Warne, P. H., Viciana, P. R., and Downward, J. (1993) Direct interaction of Ras and the amino-terminal region of Raf-1 *in vitro*. Nature **364**, 352-355

Wartmann, M., and Davis, R. J. (1994) The native structure of the activated Raf protein kinase is a membrane-bound multi-subunit complex. J. Biol. Chem. **269**, 6695-6701

Watanabe, T., Waga, I., Honda, Z., Kurokawa, K., and Shimizu, T. (1995) Prostaglandin $F_{2\alpha}$ stimulates formation of $p21^{ras}$- GTP complex and mitogen-activated protein kinase in NIH-3T3 cells via G_q-protein-coupled pathway. J. Biol. Chem. **270**, 8984-8990

Welsh, G. I., Foulstone, E. J., Young, S. W., Tavare, J. M., and Proud, C. G. (1994) Wortmannin inhibits the effects of insulin and serum on the activities of glycogen synthase kinase-3 and mitogen-activated protein kinase. Biochem. J. **303**, 15-20

Wieland, T., and Jakobs, K. H. (1994) Measurement of receptor-stimulated guanosine 5'-*O*-(γ-thio)triphosphate binding by G proteins. Methods Enzymol. **237**, 3-13

Wilkes, L. C., Patel, V., Purkiss, J. R., and Boarder, M. R. (1993) Endothelin-1 stimulated phospholipase D in A10 vascular smooth muscle derived cells is dependent on tyrosine kinase. FEBS Lett. **322**, 147-150

Wilkie, N., Morton, C., Ng, L. L., Boarder, M. R. (1996) Stimulated mitogen-activated protein-kinase is necessary but not sufficient for the mitogenic response to angiotensin II. J. Biol. Chem. **271**, 32447-32453

Williams, N. G., Roberts, T. M., and Li, P. (1992) Both $p21^{ras}$ and $pp60^{v\text{-}src}$ are required, but neither alone is sufficient, to activate the Raf-1 kinase. Proc. Natl. Acad. Sci. USA **89**, 2922-2926

Wilson, M., Burt, A. R., Milligan, G., and Anderson, N. G. (1996) Wortmannin-sensitive activation of $p70^{s6k}$ by endogenous and heterologously expressed G_i-coupled receptors. J. Biol. Chem. **271**, 8537-8540

Wilson, M., Burt, A. R., Milligan, G., and Anderson, N. G. Mitogenic signalling by the δ opioid receptor expressed in Rat1 fibroblasts involves the activation of p70/p85 S6 kinase. (submitted)

Winitz, S., Gupta, S. K., Qian, N-X., Heasley, L. E., Nemenoff, R. A., and Johnson, G. L. (1994) Expression of a mutant G_{i2} α subunit inhibits ATP and thrombin stimulation of cytoplasmic phospholipase A_2-mediated arachidonic acid release independent of Ca^{2+} and mitogen-activated protein kinase regulation. J. Biol. Chem. **269**, 1889-1895

Winitz, S., Russell, M., Qian, N-X., Gardner, A., Dwyers, L., and Johnson, G. L. (1993) Involvement of Ras and Raf in the G_i-coupled acetylcholine muscarinic m2 receptor activation of mitogen-activated protein (MAP) kinase kinase and MAP kinase. J. Biol. Chem. **268**, 19196-19199

Wu, J., Dent, P., Jelinek, T., Wolfman, A., Weber, M. J., Sturgill, T. W. (1993) Inhibition of the EGF-activated MAP kinase signalling pathway by adenosine 3',5'-monophosphate. Science **262**, 1065-1069

Xu, S., Robbins, D., Frost, J., Dang, A., Lange-Carter, C., and Cobb, M. H. (1995) MEKK1 phosphorylates MEK1 and MEK2 but does not cause activation of mitogen-activated protein kinase. Proc. Natl. Acad. Sci. USA **92**, 6808-6812

Yan, M., Dai, T., Deak, J. C., Kyriakis, J. M., Zon, L. I., Woodget, J. R., and Templeton, D. J. (1994) Activation of stress-activated protein kinase by MEKK1 phosphorylation of its activator SEK1. Nature **372**, 798-800

Yasuda, K., Raynor, K., Kong, H., Breder, C. D., Takeda, J., Reisine, T., and Bell, G. I. (1993) Cloning and functional comparison of κ and δ opioid receptors from mouse brain. Proc. Natl. Acad. Sci. USA **90**, 6736-6740

Zaki, P. A., Bisky, E. J., Vanderah, T. W., Lai, J., Evans, C. J., Porreca, F. (1996) Opioid receptor types and subtypes: the δ receptor as a model. Annu. Rev. Pharmacol. Toxicol. **36**, 379-401

Zhang, F., Strand, A., Robbins, D., Cobb, M. H., and Goldsmith, E. J. (1994) Atomic structure of the MAP kinase ERK2 at 2.3 Å resolution. Nature **367**, 704-711

Zhang, J., Zhang, J., Benovic, J. L., Sugai, M., Wetzker, R., Gout, I., and Rittenhouse, S. E. (1995) Sequestration of a G-protein βγ subunit or ADP-ribosylation of Rho can inhibit thrombin-induced activation of platelet phosphoinositide 3-kinases. J. Biol. Chem. **270**, 6589-6594

Zheng, C-F., and Guan, K-L. (1993a) Cloning and characterization of two distinct human extracellular signal-regulated kinase activator kinases, MEK1 and MEK2. J. Biol. Chem. **268**, 11435-11439

Zheng, C-F., and Guan, K-L. (1993b) Dephosphorylation and inactivation of the mitogen-activated protein kinase by a mitogen-induced Thr/Tyr protein phosphatase. J. Biol. Chem. **268**, 16116-16119

Zheng, C-F., Guan, K-L. (1994) Activation of MEK family kinases requires phosphorylation of two conserved Ser/Thr residues. EMBO J. **13**, 1123-1131